THE PROBLEM OF ACID MINE DRAINAGE IN THE IBERIAN PYRITE BELT (IPB)

Diagnosis and Treatment Measures






Manuel Olías Álvarez
Carlos Ruiz Cánovas
M. Dolores Basallote Sánchez
Francisco Macías Suárez
José Miguel Nieto Liñan
Rafael Pérez López
Aguasanta Miguel Sarmiento

Editorial Universidad de Huelva
EUHU

THE PROBLEM OF ACID MINE DRAINAGE IN THE IBERIAN PYRITIC BELT (IPB)

Diagnosis and Treatment Measures

Manuel Olías Álvarez
Carlos Ruiz Cánovas
M. Dolores Basallote Sánchez
Francisco Macías Suárez
José Miguel Nieto Liñán
Rafael Pérez López
Aguasanta Miguel Sarmiento

Editorial Universidad de Huelva
EUHU

Editorial Universidad de Huelva EUHU
ALONSO BARBA
22

DATOS EDICIÓN

Primera edicion en formato ebook: noviembre 2024
Primera edición en formato papel: noviembre 2024

© Editorial de la Universidad de Huelva
© Manuel Olías Álvarez (Ed.)
© Carlos Ruiz Cánovas (Ed.)

I.S.B.N. (papel): 978-84-10326-48-4
EI.S.B.N. (pdf): 978-84-10326-49-1

Depósito legal: H 694-2024

PAPEL

Papel
Estucado mate de 125 g/m²
Impreso en papel de bosque certificado

Encuadernación
Rústica, cola PUR

Printed in Spain. Impreso en España.

Maquetación y composición EBOOK
MAQUETACCIÓN

CEP

The Problem of Acid Mine Drainage in the Iberian Pyritic Belt (IPB) / [editado por] Manuel Olías Álvarez, Carlos Ruiz Cánovas, M. Dolores Basallote Sánchez, Francisco Macías, José Miguel Nieto, Rafael Pérez López, Aguasanta Miguel Sarmiento. – Huelva : Universidad de Huelva, 2024

200 páginas : ilustraciones a color ; 24 cm. – (Alonso Barba (Universidad de Huelva) ; 22)

I.S.B.N. (papel): 978-84-10326-48-4
EI.S.B.N. (pdf): 978-84-10326-49-1

1. Hidrogeology 2. Water – Pollution I. Olías Álvarez, Manuel, editor literario II. Ruiz Cánovas, editor literario III. Basallote Sánchez, M. Dolores, editora literaria IV. Macías Francisco, editor literario V. Nieto, José Miguel, editor literario VI. Pérez López, Rafael, editor literario VII. Miguel Sarmiento, Aguasanta, editora literaria VIII Universidad de Huelva III. Serie

Obra sometida al proceso de evaluación de calidad editorial por el sistema de revisión por pares.

Editorial de la Univesidad de Huelva es miembro de UNE

Reservados todos los derechos. Ni la totalidad ni parte de este libro puede reproducirse o transmitirse por ningún procedimiento electrónico o mecánico, incluyendo fotocopia, grabación magnética o cualquier almacenamiento de información y sistema de recuperación, sin permiso escrito del editor. La infracción de los derechos mencionados puede ser constitutivo de delito contra la propiedad intelectual.

Clique para mayor información

La publicación de este libro ha sido financiada por la Consejería de Universidad, Investigación e Innovación de la Junta de Andalucía y cofinanciado en un 80% por fondos del programa operativo FEDER de Andalucía 2014-2020, Convocatoria 2020 de ayudas para la realización de proyectos de interés colaborativo, en el ámbito de los Ecosistemas de Innovación de los Centros de Excelencia Internacional, medida A1123060E0., dentro de las actividades propuestas en el proyecto AIHODIEL (PYC20 RE 032 UHU; Adquisición de información hidrológica para la mejora del estado del Río Odiel).

Los autores del libro: M. Dolores Basallote Sánchez, Francisco Macías Suárez, José Miguel Nieto Liñan, Rafael Pérez López, Aguasanta Miguel Sarmiento, Manuel Olías Álvarez, y Carlos Ruiz Cánovas.

UNIÓN EUROPEA
Fondo Europeo de Desarrollo Regional
Junta de Andalucía
Consejería de Transformación Económica, Industria, Conocimiento y Universidades
Andalucía se mueve con Europa

EL EBOOK LE PERMITE

Citar el libro
Navegar por marcadores e hipervínculos
Realizar notas y búsquedas internas
Volver al índice pulsando el pie de la página

Comparte #LibrosUHU
Únete y comenta
Novedades a golpe de clik
Nuestras publicaciones en movimiento
Suscribete a nuestras novedades

INDEX

PREFACE

The Iberian Pyrite Belt (IPB) is one of the most truly remarkable ore deposits in the world. It is composed of a series of massive sulfides, banded and stockwork ores, disseminated porphyries, and gold/silver gossans stretching from southern Portugal into southwestern Spain. Estimated reserves exceed 1000 million tons.

Among all the different types of ore deposits, massive sulfides can be the most detrimental to the environment when opened to mining. “Massive sulfides” means large bodies of nearly pure sulfide minerals that are usually dominated by pyrite. When pyrite begins to weather in the presence of water and oxygen, it produces strongly acidic mine drainage. At Iron Mountain mines, northern California, Dr. Charles Alpers and I have documented underground pH values less than zero with thousands of milligrams per liter of dissolved metals. Dr. Alpers and Prof. Ken Verosub and I have estimated that mining the massive sulfide deposit at Iron Mountain increased the weathering rate and the production of acid mine drainage by 2-3 orders of magnitude compared to the natural weathering rate. There are other smaller massive sulfides near the Iron Mountain deposits that were formed in the same geological time period (Devonian) which also discharged acid metal-rich waters into Lake Shasta and the Sacramento River, arguably the single largest and most important river in California. At substantial costs, remediation and litigation have alleviated the contamination for now, but permanent long-term treatment is still unresolved.

After Dr. Alpers and I had a chance to visit the IPB we agreed that it was very much like Iron Mountain mines times a thousand. Both mineral zones had been exposed to long periods of natural erosion that had converted some of the sulfide ore into gossan and both had seen substantial periods of mining. The difference is the amount of sulfides in the IPB is enormously greater than Iron Mountain, the weathering and erosion was longer, and the mining period was much longer. When Tartessians, Iberians, Phoenicians and earlier civilizations were mining the IPB thousands of years ago, Iron Mountain was only known to a few indigenous tribes and serious mining did not start until the very end of the 19th century. Weathering and erosion at Iron Mountain are estimated to have begun about 1 million years ago, whereas estimates of weathering in the IPB probably began about 24 million years ago. Although the Romans left there mining mark on the IPB, it was not until the industrial age of the 18th century when the British developed steam engines and companies such as Rio Tinto formed in the 19th century that large-scale mining was possible. These periods of change in mining activity are found in the sedimentary record in estuaries where calm waters allow metal-rich sediments to accumulate.

The city of Huelva is rather well situated on the estuary where the two rivers, Rio Odiel and Rio Tinto, run blood-red from high concentrations of dissolved and oxidized iron come together. Consequently, an opportunity existed for scholars at the University of Huelva to investigate the origins of mined and natural drainage in these rivers and to document their history. Several geologists, chemists, mineralogists, geochemists, and hydrologists at the university rose to the occasion and with governmental support and funding began a series of studies that were presented at national and international meetings. The possible subjects of study seemed unlimited. I was very pleased to see that subjects I considered to be of high priority were the same as those of this group and I eagerly looked forward to hearing

the latest work when I was able to attend international geochemistry meetings. There was always something new and astonishing to learn from these research results.

The fundamental geochemistry of sulfide oxidation sets the stage for what follows. The geology and mining history of a rather complex area is described in straight-forward terms with maps and photos that illustrate the text quite well. The greater portion of the book describes the characteristics of the pollution, first in the Tinto and Odiel Rivers followed by the quality of several reservoirs and pit lakes and then the geochemistry of the estuary. Remediation and treatment bring this book to a close along with a summary of highlights and conclusions. There are at least three important aspects that make this book valuable, one is the synthesis of many years of hard work that it took to make the field measurements, compile data, interpret the results, and understand the tributary mixing, along with seasonal and climatic factors that affect the water chemistry. Another aspect is the outstanding collections of photographs, old and new, that illustrate the geology, mineralogy, mining history, and water quality conditions in two adjacent basins of the Odiel and the Tinto. The third aspect is having the summary of a most extraordinarily large mining region, with its geologic and mining history, its pollution quantified, and an overview of treatment procedures with references all in one book. Anyone who either does research on acid mine drainage or who works on remediation of acid mine drainage can learn much from reading this book.

D. Kirk Nordstrom
U. S. GEOLOGICAL SURVEY

PROLOGUE

The geology of Spain contains the world's largest massive sulfide deposit: the Iberian Pyrite Belt. By the end of the Carboniferous Period, the influx of metal-laden fluids from magmatic depths to the seafloor of the Rheic Ocean caused the emergence of hydrothermal vents. In the orifices of these vents, the precipitation of myriad small crystals of polymetallic sulfides occurred, with pyrite being the most abundant among them. Over millions of years, the sulfide veins were deformed by the Variscan orogeny and later reached the surface through the dismantling of the mountain range due to surface erosion processes. Subsequently, sulfides began interacting with surface waters, transforming into sulfates and releasing metals into river channels in a process known as acid rock drainage.

Human arrival on the Earth's stage and the development of the first civilizations immediately led to the exploitation of metals from the Iberian Pyrite Belt. There is evidence that metals began to be exploited in this region at least from the third millennium BC, marking the Copper or Chalcolithic Age, expanding during the Bronze Age, and reaching a peak during the Roman Empire. Mining activities during these ancient times were developed mainly by open-pit operations, significantly increasing the surface area of metals in contact with surface waters, both in abandoned mineral veins and in the waste heaps generated by this mining. This marked the beginning of mine acid drainage processes in the area, representing a magnitude increase compared to natural drainage from outcropping rock.

The Industrial Revolution reached the Iberian Pyrite Belt in the form of large-scale operations developed by foreign companies, especially British. These companies initially exploited areas with historical mining indications but later expanded to the entire region, reaching an unprecedented scale. The magnitude of acid mine drainage increased to such an extent that almost no watercourses in the area remained unaffected by this process. The water in these watercourses turned acidic due to high metal content and the release of sulfates, which turned into sulfuric acid upon contact with water. The Rio Tinto is globally known for its red color and acidic character, but the Odiel, despite having a slightly higher pH, carries a much higher metal load due to its four times greater flow. The end of the Industrial Revolution led to the abandonment of most mines and the accumulation of extensive waste heaps, resulting in uncontrolled mine acid drainage processes for decades, posing an environmental problem not only for the river catchments but also for the estuaries where these rivers flowed into and the nearest coast.

The last decades of the 20th century saw the initiation of research plans, both at the regional, national, and European levels. This was when the first research groups emerged to study the environmental problems caused by acid mine drainage. At the University of Huelva, researchers from the Faculty of Experimental Sciences and the School of Engineering (now ETSI) led the TOROS project, in which I had the privilege to participate. It was a project funded by the EU's ELOISE program and a pioneer in studying the interactions of river waters affected by acid drainage with the Ria de Huelva and the adjacent coast. Other projects from the same period, such as ESTURION, attempted to determine whether metals were part of compounds that could enter the food chain. The information provided by these projects was useful in initiating remediation plans promoted by regional authorities in the last years of the previous century.

In this context, the group of Mineralogy and Environmental Geochemistry comes into play, whose current members are the authors of the book you now have in your hands. It is a multidisciplinary group composed of geologists, environmentalists, and chemists, capable of approaching this complex issue from different perspectives. They have been successful in attracting abundant funding to the University of Huelva. It is worth mentioning that in the last 10 years, they have developed 6 international projects, 10 national projects, 5 regional projects, and 8 knowledge transfer contracts with companies and institutions. From the research conducted in these projects, over 200 publications, including articles and book chapters, have emerged, along with countless presentations at national and international conferences. As indicators of their prolific nature, almost 25% of the bibliographic references included in this book belong to the book's authors. Furthermore, their contributions are widely cited by other professionals, with the 62 contributions cited in this book accumulating more than 3100 citations.

These numbers would be mere statistics if not for highlighting the achievements of this group. It can be said that among all, the most significant milestones of their contributions are threefold: 1) the development of the first pollution map of the Tinto and Odiel river basins, 2) understanding the temporal variability of this pollution and determining its causes, and 3) the development of a passive treatment for neutralizing this type of water. Precisely from this last milestone, two patents have emerged, one national and one international. However, what is more interesting is that these patents are already being effectively applied in remediating river pollution in various countries on different continents.

This book not only includes the knowledge from the scientific contributions of this research group but also, throughout its chapters, presents in easily understandable language for any non-specialist reader the characteristics that make this phenomenon possible in our territory, the historical development of this pollution, the level of impact on different river networks, the characteristics of the reservoir waters that intersect some of these rivers and the flooded mining pits, the influence on the waters, sediments, and organisms of the Ria de Huelva, and the possibilities of remediating this pollution.

I am absolutely convinced that this book will be a reference not only for scientists but also for citizens interested in delving into one of the main environmental problems that directly affect us.

Dr. Juan A. Morales González
PRESIDENT OF THE SPANISH
GEOLOGICAL SOCIETY

1

INTRODUCTION

Sulfides, among which pyrite (FeS_2) is the most abundant, are stable minerals when kept underground in the absence of oxygen. However, under oxidizing conditions and in the presence of water, they undergo different reactions (detailed in the following chapter) that generate acidic leachates with extremely high concentrations of metals, metalloids, and sulfates. This process, known as Acid Mine Drainage (AMD), also occurs in coal mining, as these deposits contain small amounts of sulfides.

This problem arises in numerous regions where sulfide and coal deposits have been exploited, and it represents one of the main causes of degradation of water resources globally. For instance, in the United States alone, it is estimated that around 20,000 km of river courses are affected (Skousen et al., 2019). Although less frequently, it can also be generated due to civil works, such as the acidification that occurred in the Eume River (Galicia) in 2008. This was caused by the exposure of rocks with small concentrations of sulfides to the atmosphere during the construction of the Cantabrian Highway, leading to a severe environmental problem (Alvarez-Campana et al., 2009).

Modern mining has resources and methods to reduce the generation of acid leachates and neutralize them, preventing significant impacts on the environment. However, the large amount of sulfide-rich waste in numerous abandoned mines in the Iberian Pyrite Belt (IPB), coupled with the limited neutralization capacity of the rocks constituting the substrate of the area, results in unparalleled contamination levels in the Odiel and Tinto rivers on a global scale.

The Tinto River is internationally known for its acidic conditions and high concentrations of dissolved iron (and other metals). However, the length of the affected watercourses and the quantity of toxic elements transported by the Odiel River are much greater because, despite having lower contaminant concentrations, its flow is higher than that of the Tinto. Segments affected by mine acid waters are profoundly degraded and present severe pollution, with no invertebrates, amphibians, fish, plants, etc., typical of regular river ecosystems. This does not imply that the rivers are devoid of life; there is an abundance of microorganisms and certain algae species adapted to these unique conditions, known as extremophilic species, which have also attracted significant scientific interest (e.g., López-Archilla and Amils, 1999; Amils et al., 2007).

The pollutants transported by both rivers also have a significant impact on the estuary of the Ría de Huelva (e.g., Palanques et al., 1995; Elbaz-Poulichet et al., 1999; Davis et al., 2000; Borrego et al., 2002; López-González et al., 2006). Most toxic elements precipitate when acidic waters from rivers mix along the estuary with seawater, improving the estuarine water quality. However, these toxic elements are stored in sediments and, depending on environmental conditions (e.g., pH, salinity, redox potential, etc.), can become bioavailable and enter the food chain (e.g., Usero et al., 2005; Morillo et al., 2005; Nieto et al., 2007; Vicente-Martorell et al., 2009; Madejón et al., 2009). Moreover, more mobile toxic elements under neutral pH conditions, such as zinc, reach the Gulf of Cádiz in significant concentrations, also causing contamination of coastal sediments (Ruiz, 2001; Morillo et al., 2004; Sainz and Ruiz, 2006; Besada et al., 2021); and even reaching the Mediterranean Sea in certain seasons (van Geen et al., 1988; Elbaz-Poulichet et al., 2001).

In addition to these environmental impacts, AMD pollution has a profound socio-economic impact, as contaminated water cannot be used for any human activity without expensive prior treatment.

This book presents, in an accessible way, the main results obtained by a group of researchers from the Department of Earth Sciences at the University of Huelva (Spain) since the early 2000s, through numerous European, national, and regional projects. Throughout this journey, we collaborated with researchers from other institutions, especially with Professor Carlos Áyora´s group at the Institute of Environmental Assessment and Water Research of the Spanish Council of Scientific Research (IDAEA-CSIC). This intense and fruitful line of research is evidenced by more than 200 scientific articles in international journals and 19 Doctoral Theses on this topic.

The book is structured into 7 different chapters, each concluding with its most relevant findings. Following this introduction, the second chapter provides basic concepts about the processes that lead to acid mine drainage, necessary to understand the characteristics of this type of contamination.

The third chapter offers a brief description of the main physical characteristics of the Tinto and Odiel river basins and a compilation of the mining history in the IPB, parallel to AMD contamination. This section presents numerous pieces of evidence demonstrating that the current state of these rivers is fundamentally due to mining activities from 1850 to the late 20th century. In other words, the conditions of the Tinto and Odiel rivers are by no means natural, as some people believe.

The fourth chapter shows how acid mine waters affect the basins of these rivers, the contamination levels in different river courses, their seasonal variations, long-term trends, the pollutant load carried by the rivers, and the effects of the accidental spill that affected the Odiel River in May 2017 due to the release of acid waters from La Zarza mine.

The fifth chapter is dedicated to the impact of AMD on the reservoirs of the Spanish part of the IPB. It explains the processes occurring in reservoirs that receive acid waters and how, depending on the balance between acid inputs and the flow of waters unaffected by AMD, the Andévalo and Chanza reservoirs have good-quality waters. The Olivargas reservoir stores neutral pH waters with small but significant concentrations of some contaminants, while the Sancho reservoir conditions are acidic with high concentrations of toxic elements. It is also concluded that at least a 70% reduction in acid water inputs is necessary for the Alcolea reservoir, currently under construction, to have good-quality waters.

The behavior of various contaminants transported by the Tinto and Odiel rivers when acidic river waters mix with seawater in the estuary of the Ría de Huelva, as well as their impact on the biota of transitional waters, is the focus of the sixth chapter.

Finally, the seventh chapter describes the treatment techniques commonly used to prevent the generation of AMD and its treatment in sulfide mining. Special emphasis is placed on the technology developed by our research group for highly contaminated acid waters generated in the IPB. Based on all the above, strategies and measures are recommended that could be applied in the Odiel basin to improve its current degraded condition. Although the magnitude of the problem is enormous and many challenges remain to be addressed, investments in scientifically sound actions must be made progressively to achieve the recovery of these aquatic ecosystems.

It is important not to forget that historical mining in the IPB, while environmentally damaging, has also left spectacular landscapes with a variety of colors and a rich archaeological and cultural heritage. Many installations and areas have been designated as Sites of Cultural Interest (SCI) in the General Catalogue of Andalusian Historical Heritage. Additionally, the headwaters and much of the course of the Rio Tinto were declared a Protected Natural Landscape in 2004, and the Gossan “Montera de Peña de Hierro” was designated a Natural Monument of Andalusia in 2010.

The publication of this book has been made thanks to the funding from the research project ‘Acquisition of Hydrological Information for the Improvement of the State of the Odiel River (AIHODIEL, reference PYC20-RE-032 UHU)’ financed by the Ministry of Economic Transformation, Industry, Knowledge, and Universities of the Junta de Andalucía.”

2

ACID MINE DRAINAGE

2.1 Sulfide oxidation

Sulfides are rare minerals in the Earth's crust, but under certain geological conditions, they can become predominant and form significant deposits (Fig. 2.1). They also appear in minor concentrations in coal deposits. The high content of Cu, Zn, and Pb in sulfides, or the possibility of obtaining sulfuric acid, has led to their exploitation throughout history. Additionally, the enrichment in Au and Ag occurring in the oxidation caps (*gossans*) of sulfide deposits has also been exploited.

Pyrite (FeS_2) is the most common sulfide in nature, found in hydrothermal formations, igneous rocks, and sedimentary deposits. However, along with pyrite, other metallic sulfides such as marcasite (FeS_2), pyrrhotite (Fe(1-x)S), chalcopyrite ($CuFeS_2$), arsenopyrite (FeAsS), galena (PbS), sphalerite (ZnS), covellite (CuS), etc., are often found.

Sulfides are stable and highly insoluble under reducing conditions that exist in the subsurface. However, exposure of these minerals to atmospheric conditions destabilizes their structure through oxidation reactions. The following summarizes the oxidation process of pyrite, necessary to understand the mechanisms that cause the extremely high levels of contamination in rivers affected by AMD and the possible prevention and treatment methods discussed in other chapters of this book.

Figure 2.1: Massive sulfides (grey colour) in La Zarza mine pit walls.

The oxidizing agent for this process can be either oxygen (O_2) or ferric iron (Fe^{3+}). Additionally, depending on the absence or presence of microorganisms that catalyze weathering reactions, it is referred to as abiotic or biotic oxidation, respectively.

2.1.1 Abiotic oxidation of pyrite

In contact with the atmosphere and in the presence of water, direct oxidation of pyrite occurs (reaction 2.1). In this reaction, for each mole of pyrite, 1 mole of ferrous iron (Fe^{2+}), 2 moles of sulfate ions (SO_4^{2-}), and 2 moles of protons (H^+) are produced. In other words, acidity is generated, and sulfate and iron, along with other accessory elements (As, Cd, Co, Ni, Pb, etc.) forming part of the pyrite in varying proportions, are released.

$$FeS_2 + 7/2\ O_2 + H_2O \rightarrow Fe^{2+} + 2\ SO_4^{2-} + 2\ H^+ \qquad (2.1)$$

The availability of oxygen is, therefore, essential for the oxidation of sulfides. Ritchie (1994) considers the primary limiting factor in sulfide oxidation processes in mine tailings to be the transport of oxygen in the subsurface. If oxidation occurs in a water-saturated environment (below the water table), oxygen availability is a limiting factor. The amount of oxygen in the water depends on the temperature, and to a lesser extent, on the altitude and salinity of the water. Thus, its concentration varies approximately between about 13 mg/L at 10 ºC and 8 mg/L at 25 ºC, considerably lower values than the nearly 290 mg/L of oxygen present in the atmosphere. Therefore, the rate of pyrite oxidation processes in a water-saturated environment is slower than in contact with the atmosphere.

The ferrous iron (Fe^{2+}), released in reaction 2.1, in the presence of oxygen converts to ferric iron (Fe^{3+}), consuming one proton per mole of Fe^{2+}.

$$Fe^{2+} + ¼\ O_2 + H^+ \rightarrow\ Fe^{3+} + ½\ H_2O \qquad (2.2)$$

The direct oxidation of pyrite is often followed by indirect oxidation (reaction 2.3), which involves the action of ferric iron (Fe^{3+}) as oxidizing agent. Fe^{3+} has the ability to oxidize pyrite approximately 20 to 200 times faster than atmospheric oxygen (Nordstrom and Alpers, 1999a).

$$FeS_2 + 14Fe^{3+} + 8H_2O \rightarrow\ 15Fe^{2+} + 2SO_4^{2-} + 16H^+ \qquad (2.3)$$

In this reaction, 16 protons are generated for each mole of pyrite, however, 14 moles of Fe^{3+} are needed, which in turn consume 14 protons according to reaction 2.2. Therefore, the final acidity production balance for reactions 2.1 and 2.3 is the same: two moles of protons are released for each mole of oxidized pyrite. This reaction involves the reduction of Fe^{3+} to Fe^{2+}, so for it to occur, there must be a reoxidation of Fe^{2+} to Fe^{3+} by oxygen (reaction 2.2). In other words, although oxygen is not directly involved in the indirect oxidation reaction of pyrite (reaction 2.3), it is necessary to occur.

Reaction 2.3 depends on the availability of dissolved Fe^{3+} in water, which, in turn, is controlled by the pH of the solution. The solubility of Fe^{3+} is very low in neutral and alkaline solutions, so under those conditions, direct oxidation of pyrite predominates. This is due to the precipitation of Fe as ferric hydroxide (actually more complex minerals are formed, see section 2.3.3) that occurs at pH values around 3 (reaction 2.4):

$$Fe^{3+}\ +\ 3H_2O \rightarrow\ Fe(OH)_3\ +\ 3H^+ \qquad (2.4)$$

At pH values below 4, the oxidation of pyrite by Fe^{3+} is much faster than by O_2, but reaction 2.2, which controls the availability of Fe^{3+}, is extremely slow (Fig. 2.2). For this reason, the oxidation of Fe^{2+} to Fe^{3+} is the limiting process in the abiotic oxidation of pyrite and cau-

ses these reactions to be very slow without the intervention of microorganisms (Singer and Stumm, 1970)

2.1.2 Biotic oxidation of pyrite

It has been demonstrated from laboratory experiments that the abiotic oxidation of pyrite is a very slow process and, therefore, would not pose a serious environmental problem. However, in nature, the speed of these reactions is much higher due to the intervention of certain aerobic chemolithotrophic bacteria (those that 'feed' on inorganic substrates). These microorganisms thrive in acidic pH conditions, catalyzing oxidation reactions and obtaining energy from this process. The most abundant is *Acidithiobacillus ferrooxidans*, followed by *Leptospirillum ferrooxidans* and *Acidithiobacillus sp.* (Córdoba, 2022).

Particularly important is the increase in the rate of Fe^{2+} to Fe^{3+} oxidation mediated by these bacteria, which was the limiting factor in the entire abiotic process. Bacteria like *Acidithiobacillus ferrooxidans* can accelerate the speed of this reaction up to 100,000 times (Nordstrom and Alpers, 1999a). By increasing the concentration of Fe^{3+} in solution, there is an increase in the indirect oxidation of pyrite (reaction 2.3), generating more Fe^{2+} that is again oxidized to Fe^{3+}, so these reactions feedback into an endless cycle.

The leachates formed in the subsurface often have a high content of ferrous iron (Fe^{2+}) due to the limited supply of oxygen under these conditions, giving the water a greenish color (Fig. 2.3). When these leachates circulate on the surface, Fe^{2+} quickly oxidizes to Fe^{3+}, producing precipitates that give the water a reddish color, typical of environments affected by AMD (Fig. 2.3).

The bacteria catalyzing these reactions are extremophiles and only thrive upon acidic conditions (Langmuir, 1997). If oxidation is slow, not enough protons are produced to acidify the environment, so the ideal conditions for the growth of these bacteria are not achieved, and the reactions occur at a very slow rate. However, if acidic conditions are reached, the bacteria develop rapidly, and the oxidation of sulfides increases dramatically, triggering a process that is practically unstoppable and will continue until the sulfides are completely oxidized.

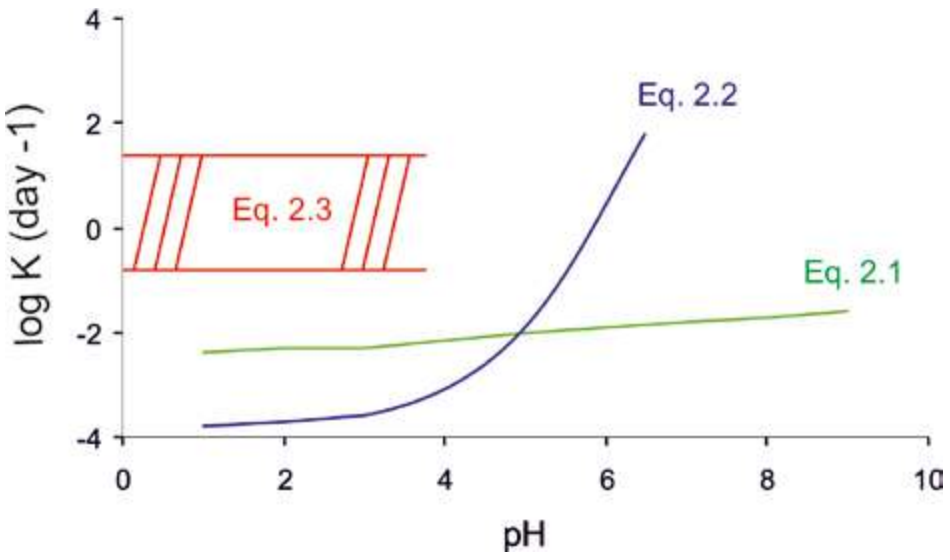

Figure 2.2: Comparison of speed reaction with pH for pyrite oxidation by O_2 (reaction 2.1), Fe^{2+} oxidation to Fe^{3+} (reaction 2.2) and pyrite oxidation by Fe^{3+} (reaction 2.3). Modified from Nordstrom (1982a).

Figure 2.3: Photos of acidic drainages outflowing from Esperanza Mine, with high concentrations of Fe^{2+} (left) and drainages from Poderosa mine, with more oxidizing conditions and high concentration of Fe^{3+} (right).

The reactions mentioned above are simplifications of the actual mechanisms and have certain limitations. A more detailed description of pyrite oxidation processes can be found in, among others, Evangelou (1995), Keith and Vaughan (2000), and Rimstidt and Vaughan (2003).

2.1.3 Oxidation of other sulfides

As mentioned before, in sulfide deposits, there are other accessory minerals apart from pyrite (usually those with economic value) such as chalcopyrite ($CuFeS_2$), sphalerite (ZnS), and galena (PbS). Pinedo Vara (1963) notes that 91% wt of pyrite in the IPB consists of Fe and S, which combined with the sterile part accompanying the mineral (mainly Si), constitutes 95% of the total. The remaining 5% includes various elements (metals and metalloids), including Cu, Pb, Zn, As, Au, Ag, Co, Ni, Se, Cd, Ti, etc.

Additionally, other sulfides (sphalerite, galena, chalcopyrite, arsenopyrite, etc.) also undergo oxidation reactions that, while generally not generating acidity, lead to the release of significant amounts of Zn, Pb, Cu, Cd, As, and other trace elements. The following reactions illustrate the oxidation reactions of sphalerite, galena, and chalcopyrite as examples.

$$ZnS + 2O_2 \rightarrow Zn^{2+} + SO_4^{2-} \quad (2.5)$$

$$PbS + 2O_2 \rightarrow Pb^{2+} + SO_4^{2-} \quad (2.6)$$

$$CuFeS_2 + 4O_2 \rightarrow Cu^{2+} + Fe^{2+} + 2SO_4^{2-} \quad (2.7)$$

Most of the released metals are insoluble under neutral and alkaline pH conditions, but at low pH values and under oxidizing conditions, their mobility is significantly increased, and they can persist in water at very high concentrations.

2.2 Natural processes or anthropic contamination?

The oxidation process of pyrite and other sulfides occurs naturally in the exposed parts of surface deposits, in this case referred to as Acid Rock Drainage (ARD). On the other hand, mining activity begins with the extraction of the ore, which must then be separated from the gangue and concentrated for commercial use through metallurgical processes. Significant amounts of waste are generated during each of these phases, classified as extraction waste, ore processing waste, and metallurgical waste (Lottermoser, 2003).

Extraction waste consists of materials that either do not contain the target ore or contain it in such low concentrations that its beneficiation is not profitable. Typically, these materials, extracted to reach the ore deposit, are highly heterogeneous and can be composed of metamorphic, sedimentary, or igneous rocks, with a wide range of particle sizes. These waste materials, which may contain some sulfides, are deposited in the vicinity of the mine in large waste dumps.

After ore extraction, ore processing or beneficiation takes place to concentrate the ore. This process begins with the crushing of the rock containing the ore to reduce its size and separate the ore from the gangue. Rocks of large size are reduced to fragments of a few millimeters or even microns. Common methods of concentration include various physical processes, such as ore washing, gravity separation, magnetic separation, etc., or chemical processes, such as the addition of substances to adjust particle size and separate the valuable ore from the gangue through flotation. The waste generated from ore processing or beneficiation, known as tailings, is deposited in tailings ponds or waste dumps. These waste materials mainly consist of sludges with high water content formed by pyrite and other sulfides, silicates, oxides, hydroxides, and other minerals.

Ore processing generates an intermediate product known as concentrate, which serves as the raw material for extractive metallurgy. Extractive metallurgical processes are divided into hydrometallurgy, pyrometallurgy, and electrometallurgy, depending on whether they use solvents, heat, or electricity to break down the crystalline structure of the ore. In ancient mines, pyrometallurgical processes were carried out by placing smelting furnaces at the mine site, making it common to find smelting slags in derelict mines.

Figure 2.4: Sulfide dumps at Filón Sur (Tharsis mines). Rainfall waters infiltrate into the dump, leading to the oxidative dissolution of sulfides (note the small dissolution sinkholes) and the generation of highly pollutant drainages.

All these processes greatly enhance the oxidation processes of pyrite, referred to in this case as Acid Mine Drainage (AMD). Acid Mine Drainage produces the same results as Acid Rock Drainage: acidity, sulfates, and toxic metals and metalloids, but in much larger quantities due to:

- The creation of large waste dumps with extraction waste, which occurs to a greater extent with open-pit mining. These wastes exhibit high heterogeneity, composed of different types of rocks with a wide variety of particle sizes and usually contain sulfides in varying proportions (Fig. 2.4). Moreover, the problem is aggravated because the rock is fragmented into small pieces, increasing the surface area exposed to weathering.
- The creation of kilometers of tunnels and galleries through which atmospheric oxygen penetrates, distributing through cracks, fissures, etc., coming into contact with large amounts of sulfides that undergo oxidation. Once mining activity ceases and the tunnels are flooded, the large conduits create an artificial aquifer in which recharge water circulates, supplying oxygen and allowing oxidation to continue.
- The excavation of large open-pit mines (Fig. 2.5). To reach great depths, the water table must be depressed by pumping, causing enormous volumes of sulfide-rich materials to come into contact with atmospheric oxygen, initiating oxidation processes (in addition to generating large waste dumps).
- Historical mining methods and treatments (Fig. 2.6), such as burning heaps that smoldered for months, and their ashes were washed to extract copper. On other occasions, the mining method involved exposing the ore to atmospheric action and irrigating it with water to oxidize and solubilize the metals; subsequently, the leachate was used to recover copper and silver, and the rest was discharged directly into rivers (Sainz et al., 2003).
- Smelting plants, which generate slags and numerous wastes containing sulfides.
- Tailings ponds from hydrometallurgical activity, where pyritic sludge from fine ore grinding accumulates, and therefore, is highly susceptible to oxidation (Fig. 2.7).

To sum up, as a result of mining activity, large amounts of pyrite and other sulfides come into contact with the atmosphere, greatly enhancing oxidation processes and, consequently, the release of acidity, sulfates, metals, and metalloids into water bodies. Nordstrom (2015) estimates that mining multiplies the natural oxidation of sulfides, and therefore the release of contaminants, between 10 and 1000 times. Modern mining is subject to strict environmental requirements and has the technology to prevent the generation of acid leachates. However, in abandoned mines or when these measures are not adopted, severe problems are caused.

Figure 2.5: Confesionarios open pit flooded by AMD, forming a pit lake.

2.3 Natural attenuation processes of pollution

2.3.1 Hydrolysis reactions of carbonates and silicates

The initial composition of waters affected by AMD is conditioned by the oxidation of sulfides, leading to the acidification of the environment. However, its composition can vary due to the disso-

lution of other minerals, such as carbonates and aluminosilicates, contained in gangue minerals or in riverbed materials of streams affected by AMD. The high acidity of mining leachates promotes the dissolution of these minerals through hydrolysis reactions, mobilizing a large number of elements into solution. Thus, the concentration of Mn, Al, Si, Ca, and Mg in AMD can become very high, even though none of these elements are part of sulfides.

The dissolution of these minerals consumes acidity. In the case of the presence carbonate materials in host rocks, the protons released during sulfide oxidation are rapidly neutralized, constituting a very effective mechanism for the natural attenuation of pollution. The abundance of these minerals in the vicinity of sulfides and their neutralization capacity will determine whether the resulting leachate is acidic or neutral. For example, in the Linares area (Jaén province, Spain), where there has been significant sulfide mining (mainly galena), there are no acidification problems due to the presence of carbonate gangue minerals. On the contrary, the neutralization capacity of materials in the IPB is very low due to the absence of carbonate materials.

Figure 2.6: Mineral processing wastes and abandoned mining infrastructures by the Tinto River (Zarandas-Naya zone).

Calcite ($CaCO_3$) is the main acidity neutralizer, as it is the most common carbonate within a wide range of geological environments and has a high reaction rate under acidic conditions. Calcite neutralizes acidity by releasing Ca^{2+} and bicarbonate (reaction 2.8) or carbonic acid under acidic conditions (reaction 2.9). Dolomite ($CaMg(CO_3)_2$), although less abundant in nature than calcite, is also very effective in acidity neutralization (reaction 2.10).

$$CaCO_{3(s)} + H^+ \rightarrow Ca^{2+} + HCO_3^- \quad (2.8)$$

$$CaCO_{3(s)} + 2H^+ \rightarrow Ca^{2+} + H_2CO_3 \quad (2.9)$$

$$CaMg(CO_3)_{2(s)} + 2H^+ \rightarrow Mg^{2+} + Ca^{2+} + 2HCO_3 \quad (2.10)$$

Silicates have lower neutralization capacity because the reaction rates are much slower. Here are two reactions as examples: the incongruent hydrolysis (uncompleted dissolution) of potassium feldspar (reaction 2.11) and the congruent hydrolysis of albite (reaction 2.12). Although the hydrolysis of silicates initially consumes acidity, the dissolution of Al^{3+} causes an increase in the potential acidity of the leachate (see the next section).

$$KAlSi_3O_{8(s)} + H^+ + 9/2H_2O \rightarrow K^+ + 2H_4SiO_4 + 1/2Al_2Si_2O_5(OH)_{4(s)} \quad (2.11)$$

$$NaAlSiO_{4(s)} + H^+ + 3H_2O \rightarrow Na^+ + Al^{3+} + H_4SiO_4 + 3OH^- \quad (2.12)$$

Figure 2.7: Tailings dam in Cueva de la Mora mine, where an experimental station to investigate sulfide oxidation processes was installed in 2008. This dam was subsequently restored and is currently sealed with impermeable materials.

2.3.2 Dilution and mixing processes

As the produced acidic leachates moves away from the mining area, they may receive contributions from groundwater and other streams not affected by AMD, leading to a dilution process that causes a decrease in pollution levels. The final outcome of these processes will depend not only on the relative flow rates of freshwater and AMD-affected water during the mixing, but also on their composition, especially acidity and alkalinity.

Alkalinity is defined as the capacity of water to neutralize acids. The alkalinity of water depends primarily on the amount of dissolved bicarbonate (HCO_3^-) and carbonate (CO_3^{2-}). Alkalinity is usually expressed as mg/L of $CaCO_3$. The reactions established between CO_2, carbonates, and bicarbonates can be exemplified as:

$$H_2O + CO_{2(g)} \leftrightarrow H_2CO_3 \quad (2.13)$$

$$H_2CO_3 \leftrightarrow HCO_3^- + H^+ \quad (2.14)$$

$$HCO_3^- \leftrightarrow CO_3^{2-} + H^+ \quad (2.15)$$

In the presence of an acid discharge, these reactions shift to the left, releasing CO_2. If carbonate and bicarbonate ions are not depleted, the pH of the medium hardly changes. Therefore, in natural waters pH is buffered by the carbonate system, which keeps pH values close to neutral conditions, usually between 6 and 9. However, if the acidity from the discharge exceeds the alkalinity contained in water, the pH rapidly drops to acidic values.

As discussed in Chapter 3, the Tinto and Odiel watersheds have scarce carbonate materials, resulting in freshwaters with very low alkalinity. As a result, streams have little capacity to neutralize the acidity generated by the intense sulfide oxidation processes.

On the other hand, it is crucial to differentiate between the concepts of pH, free acidity, and mineral acidity of water. Acidity is defined as the water capacity to neutralize bases (i.e., the opposite of alkalinity). Free acidity is caused by dissolved protons (H^+) in water, essentially what is measured by pH. The mineral or potential acidity of water also depends on the dissolved concentration of Fe and Al and, to a lesser extent, other metals, as these elements can undergo hydrolysis processes that generate protons (reactions 2.4, 2.16, and 2.17). In the IPB, the potential or mineral acidity is generally much higher than the value of free acidity (Sánchez-España et al., 2007)

$$Al^{3+} + 3H_2O \rightarrow Al(OH)_3 + 3H^+ \quad (2.16)$$

$$Mn^{2+} + 2H_2O \rightarrow Mn(OH)_2 + 2H^+ \quad (2.17)$$

To determine the acidity of waters affected by AMD, the total acidity, resulting from the sum of free acidity and potential acidity, must be considered. Total acidity can be determined for waters with pH values below 4.5 using the following expression (Hedin et al., 1994; Kirby and Cravotta, 2005).

$$\text{Total Acidity } (mg/L \text{ of } CaCO_3) = 50\left[\frac{2Fe(II)}{56} + \frac{3Fe(III)}{23} + \frac{3Al}{27} + \frac{2Mn}{55} + 1000 * 10^{-pH}\right] \quad (2.18)$$

For example, a common leachate of the IPB with a pH of 2.5 and dissolved concentrations of 2000 mg/L of Fe (50% ferric iron and 50% ferrous iron), 500 mg/L of Al, and 200 mg/L of Mn would have a free acidity of 158 mg/L of $CaCO_3$, a mineral acidity of 7606 mg/L of $CaCO_3$, and a total acidity of 7764 mg/L of $CaCO_3$. Considering that the alkalinity of a stream in the IPB can be around 50 mg/L of $CaCO_3$, it can be deduced that to neutralize 1 liter of AMD, a flow of freshwater of 155 liters is required (the result of dividing 7764 by 50). This implies that a low-flow mining leachate can lead to the acidification of a significant freshwater stream.

As discussed in the following sections, when an acidic leachate joins a freshwater stream, not only a dilution process occurs, but some elements, especially Fe and Al, may precipitate, buffering the pH, while others undergo coprecipitation and/or adsorption onto these minerals.

2.3.3 Secondary minerals precipitation

Mining activities increase the accessibility of oxygen in sulfide deposits, accelerating oxidation processes and hydrolysis reactions of gangue minerals, thereby generating acidic leachates with high contents in dissolved elements (primarily dissolved sulfates and metals). Under these conditions, the solubility product of several compounds is often exceeded, leading to the formation of secondary minerals, causing a transfer of elements from water to the solid phase. The formation of these minerals can occur on the surface of pyrite itself or away from the mineral mass, in response to oxidation, dilution and mixing, neutralization, evaporation, etc.

Two major groups of secondary minerals may precipitate from acidic leachates:

- Iron precipitates in the form of insoluble (or more accurately, sparingly soluble) oxides, hydroxides, hydroxysulfates, and oxyhydroxysulfates. These precipitates, which typically occur at pH values around 3, cover the riverbed and margins of watercourses affected by AMD, giving them typical yellowish and reddish colorations. At pH values between 4 and 5, aluminum precipitation also occurs, producing a colloidal precipitate with a milky appearance. At higher pH values, minerals such as Cu, Zn, Mn, etc., may also precipitate.

- Sulfate-rich evaporitic salts that precipitate during dry periods as efflorescence salts due to the effect of the high concentration of dissolved elements and intense evaporation. These salts generally have high solubility and are redissolved, generally during autumn, with the arrival of the first significant rains.

2.3.3.1 Oxides, hydroxides and hydroxysulfates

- *Fe(III) minerals*

The precipitation of these ferric minerals can occur due to various causes, such as the oxidation of Fe(II) to Fe(III) when acidic leachates with reducing conditions emerge at the surface, or through mixing and dilution with waters unaffected by AMD.

The precipitation of Fe(III) has been represented in reaction 2.4 in the form of ferric hydroxide ($Fe(OH)_3$). However, this is a simplification, and in reality, the phases that typically precipitate in these environments are minerals such as potassium jarosite (reaction 2.19) and schwertmannite (reaction 2.20).

$$K^+ + 3Fe^{3+} + 2SO_4^{2-} + 6H_2O \rightarrow KFe_3(SO_4)_2(OH)_6 + 6H^+ \quad (2.19)$$

$$8Fe^{3+} + SO_4^{2-} + 14H_2O \rightarrow Fe_8O_8(OH)_6(SO_4) + 22H^+ \quad (2.20)$$

The precipitation of these mineral phases buffers the pH to values around 2.5 to 3.0. For example, when an acidic leachate joins a natural stream, as long as dissolved Fe(III) is present, the precipitation of Fe(III) occurs, and the pH remains approximately constant. Thus, the concentration of Fe decreases downstream of mining areas, but the pH barely changes (as long as dissolved Fe(III) continues to exist). This precipitation is catalyzed by the action of acidophilic bacteria, often giving rise to spectacular stromatolitic structures (Fig. 2.8).

The main oxides, hydroxides, and hydroxysulfates of Fe (along with those of Al) that precipitate from acidic waters are listed in Table 2.1. In AMD-affected watercourses and mining areas, minerals such as goethite and hematite are common. However, these phases usually do not precipitate directly but transform from metastable phases like schwertmannite or jarosite (Bigham et al., 1996). During this transformation, certain compounds such as iron, sulfate, or arsenic are released (Bigham et al., 1996; Schroth and Parnell, 2005; Acero et al., 2006).

Figure 2.8: Stromatolitic structures formed by Fe precipitates in the Tinto River, close to the mining area (left) detailed stromatolitic structure (right).

Mineral	Type	Formula
Hematite	Oxide	Fe_2O_3
Ferrihydrite	Hydroxide	$Fe_5OH_8\ 4H_2O$
Goethite	Oxyhidroxide	α-FeOOH
Akaganeite	Oxyhidroxide	β-FeO(OH, Cl)
Lepidocrocite	Oxyhidroxide	γ-FeOOH
Boehmite	Oxyhidroxide	AlO(OH)
Jarosite-K	Hydroxysulfate	$KFe_3(SO_4)_2(OH)_6$
Jarosite-Na	Hydroxysulfate	$NaFe_3(SO_4)_2(OH)_6$
Jarosite-H	Hydroxysulfate	$(H_3O)Fe_3(SO_4)_2(OH)_6$
Jarosite-Pb	Hydroxysulfate	$Pb_{0,5}Fe_3(SO_4)_2(OH)_6$
Gibbsite	Hydroxide	$Al(OH)_3$
Alunite	Hydroxysulfate	$KFe_3(SO_4)_2(OH)_6$
Basaluminite	Hydroxysulfate	$Al_4(SO_4)(OH)_{10}\cdot 5H_2O$
Schwertmannite	Oxyhydroxysulfate	$Fe_8O_8(OH)_6(SO_4)$

Table 2.1: Main secondary minerals (i.e., oxides, hydroxides, oxyhydroxides and hydroxysulfates) commonly found in AMD environments. From Alpers et al. (1994).

Whether Fe(III) precipitates as jarosite, schwertmannite, or ferrihydrite will depend on the pH conditions of the solution and the concentration of ions involved in these reactions. Figure 2.9 illustrates the stability fields of these minerals as a function of pH and redox potential (expressed as pe). The precipitation of these minerals also induces coprecipitation and/or adsorption processes, which are explained in Section 2.3.4.

- *Al minerals*

When the amount of dissolved iron is low in an acidic leachate (for example, due to intense Fe precipitation), the pH rises to values between 4 and 5 because aluminum takes on the buffering role. The main aluminum phases that can precipitate in acidic waters are: alunite ($KAl_3(SO_4)_2(OH)_6$), basaluminite ($Al_4(SO_4)(OH)_{10}\cdot 5H_2O$), and microcrystalline gibbsite or amorphous Al hydroxides ($Al(OH)_3$). Jurbanite ($Al(SO_4)(OH)\cdot 5H_2O$) is another aluminum phase frequently mentioned but, despite its apparent thermodynamic stability, it does not play a significant role in controlling the solubility of Al and has not been found in environments affected by AMD (Nordstrom and Alpers, 1999a; Bigham and Nordstrom, 2000, and Blowes et al., 2004). Alunite is a stable aluminum hydroxysulfate in the pH range of 3.3 – 5.7, with an SO_4^{2-} activity of 10^{-4} to 10^{-2} M (Nordstrom, 1982b). The precipitation reaction of alunite is defined by the following expression

$$3Al^{3+} + K^+ + 2SO_4^{2-} + 6H_2O \rightarrow KAl_3(SO_4)_2(OH)_6 + 6H^+ \qquad (2.21)$$

Basaluminite is a common aluminum hydroxysulfate in environments affected by AMD, and its stability is very sensitive to pH values, precipitating at values around 4.5 according to the following reaction:

$$4Al^{3+} + SO_4^{2-} + 15H_2O \rightarrow Al_4(SO_4)(OH)_{10}\ 5H_2O + 10H^+ \qquad (2.22)$$

Finally, microcrystalline gibbsite or amorphous aluminum hydroxide would precipitate at pH values around 5:

$$Al^{3+} + 3H_2O \rightarrow Al(OH)_3 + 3H^+ \qquad (2.23)$$

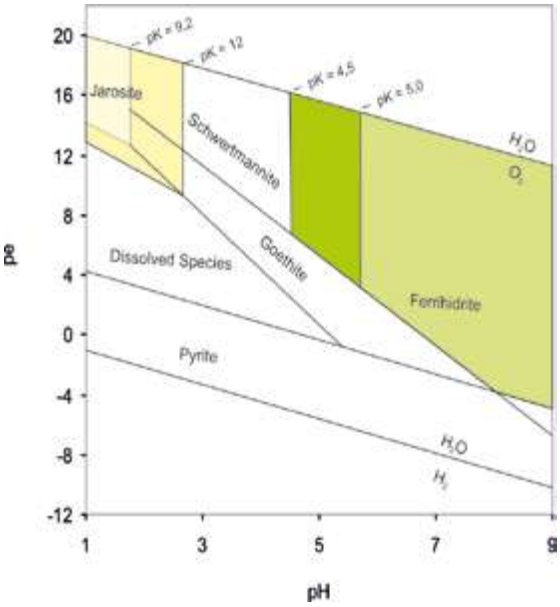

Figure 2.9: Stability fields for different Fe minerals according to pH and redox potential (pe) values. Areas with more intense color represents the extension of stability fields for jarosite-K and ferrihidrite at lower solubility constants. Activity values of log SO_4 = -2,32; log K =-3,78; log Fe^{2+} = -3,47 and log Fe^{3+}= -3,36 o -2,27.

The precipitation of one phase or another depends, in addition to pH, on the concentration of aluminum, sulfates, and other ions that are part of these minerals, such as potassium. Aluminum precipitates are very different from those of iron, as they form whitish or greenish-colored colloidal particles that accumulate in stagnant water areas or remain in suspension and are carried away by the river current (Fig. 2.10).

- *Other metals*

Other metals such as Cu, Mn, Zn can precipitate as oxides or hydroxides. Figure 2.11 shows the concentration of some elements in equilibrium with their corresponding metal hydroxide. Each of these metals precipitates at certain pH values; thus, Fe^{3+} precipitates at values close to 3, Al^{3+} at pH values close to 4, and Zn^{2+} and Mn^{2+} at neutral or slightly alkaline pH values, respectively. However, except for Fe and Al, the importance of these minerals in controlling the hydrochemistry of acid leachates is very limited.

Figure 2.10: Left: turquoise-colored aluminum precipitates in the Villar stream (a tributary of the Odiel) after receiving AMD from the Gloria mine. Right: River Tinto passing through Niebla in October 2022, showing the same turquoise color instead of its usual red one; this exceptional circumstance occurred due to its low flow during the drought and the mixing with waters unaffected by mining, causing the pH to rise to values close to 5 and all dissolved iron to precipitate.

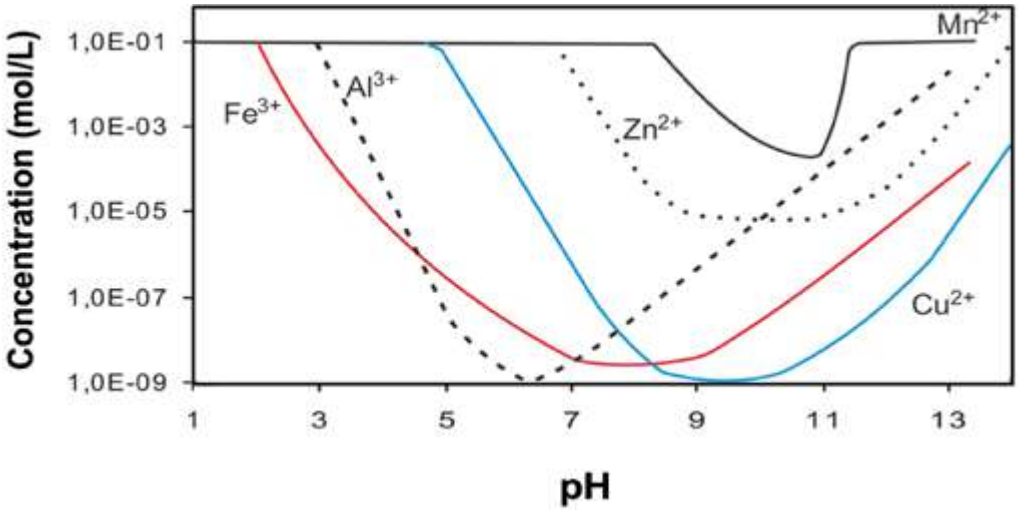

Figure 2.11: Variation in the concentration of some metals in equilibrium with their corresponding metal hydroxide. A maximum concentration of 0.1 mol/L is assumed in the absence of hydroxides (modified from Cortina et al., 2003).

2.3.3.2 Evaporitic soluble salts

The precipitation of these salts occurs when very high concentrations of sulfates, iron, and other elements are reached, especially during spring and summer due to the intense water evaporation (Fig. 2.12). However, they also precipitate inside waste heaps or in the subsurface, near where the oxidation of sulfides occurs.

The nature of evaporitic salts depends on the composition of the water from which they form (Buckby et al., 2003). Thus, sulfate-rich water with a high content of Fe^{2+} will lead to the precipitation of ferrous salts (melanterite, rozenite, szomolnokite, etc.), while waters with high Fe^{3+} contents will cause the precipitation of ferric salts (coquimbite, kornelite, rhomboclase, etc.). However, initially, soluble divalent salts can also form and subsequently undergo processes of dehydration and oxidation to form trivalent soluble salts (Jambor et al., 2000). The most common salts in areas affected by AMD are shown in Table 2.2. Reactions 2.24 to 2.26 show the stoichiometry of the precipitation/dissolution of some of these salts. This phenomenon is particularly intense in warm and semiarid climates, such as that of the IPB, and involves the temporary retention of acidity, sulfates, and metals (Fig. 2.12). However, with the arrival of the first rains after the dry period, their rapid redissolution occurs, causing the highest pollution levels of the year in watercourses (Bayless and Olyphant, 1993; Alpers et al., 1994; Cravotta, 1994; Keith et al., 2001; Hammarstrom et al., 2005; etc.)

Melanterite $Fe^{2+} + SO_4^{2-} + 7H_2O \leftrightarrow Fe_2SO_4 \cdot 7H_2O$ (2.24)

Coquimbite $2Fe^{3+} + 3SO_4^{2-} + 9H_2O \leftrightarrow Fe_2(SO_4)_3 \cdot 9H_2O$ (2.25)

Römerite $2Fe(OH)_3 + Fe^{2+} + 4SO_4^{2-} + 6H^+ + 9H_2O \leftrightarrow Fe^{2+}Fe_2^{3+}(SO_4)_4\ 14H_2O$ (2.26)

Apart from these salts, other sulfates may precipitate from AMD, some of them highly soluble like gypsum ($CaSO_4 \cdot 2H_2O$, Fig. 2.13) and chalcanthite ($CuSO_4 \cdot 5H_2O$), but others with a low solubility such as barite ($BaSO_4$), anglesite ($PbSO_4$), etc.

Mineral	Formula	Mineral	Formula
Melanterite	$Fe^{2+}SO_4\ 7H_2O$	Epsomite	$MgSO_4\ 7H_2O$
Rozenite	$Fe^{2+}SO_4\ 4H_2O$	Hexahydrite	$MgSO_4\ 6H_2O$
Szomolnokite	$Fe^{2+}SO_4\ H_2O$	Gypsum	$CaSO_4\ 2H_2O$
Halotriquite	$Fe^{2+}Al_2(SO_4)_4\ 22H_2O$	Anhydrite	$CaSO_4\ H_2O$
Aluminocopiapite	$Mg^{2+}Fe_4^{3+}(SO_4)_6(OH)_2\ 20H_2O$	Goslarite	$ZnSO_4\ 7H_2O$
Magnesocopiapite	$Fe^{2+}Fe_4^{3+}(SO_4)_6(OH)_2\ 20H_2O$	Bianchite	$ZnSO_4\ 6H_2O$
Römerite	$Fe^{2+}Fe_2^{3+}(SO_4)_4\ 14H_2O$	Chalcanthite	$CuSO_4\ 5H_2O$
Voltaite	$K_2Fe_5^{2+}Fe_4^{3+}(SO_4)_{12}\ 18H_2O$	Barite	$BaSO_4$
Coquimbite	$Fe_2^{3+}(SO_4)_3\ 9H_2O$	Mallardite	$MnSO_4\ 7H_2O$
Ferricopiapite	$Fe_5^{3+}(SO_4)_6\ O(OH)\ 9H_2O$	Alunogen	$Al_2(SO_4)_3\ 17H_2O$
Rhomboclase	$HFe^{3+}(SO_4)_2\ 4H_2O$	Copiapite	$Al_{2/3}\ Fe_4^{3+}(SO_4)_6(OH)_2\ 20H_2O$

Table 2.2. Main evaporitic soluble salts commonly found in AMD environments. From Alpers et al. (1994) and Buckby et al. (2003).

Figure 2.12: Photos of bluish evaporitic salts (mainly melanterite) on the margins of a leachate from the Riotinto mines (left) and a detail of the efflorescences (right).

Figure 2.13: Precipitation of gypsum on roots in the Batán stream (Odiel River basin). The water has a high concentration of calcium due to the neutralization treatment of acid leachates carried out in Almagrera mines.

2.3.4 Coprecipitation and adsorption processes

The surface of minerals is electrically charged, allowing them to retain chemical species from solution. Besides that, when a mineral precipitates, some dissolved ions can enter its crystalline structure. Secondary minerals formed by the oxidation of sulfides exhibit high reactivity on their surface, providing them with a high capacity to retain adsorbed or coprecipitated metals (Webster et al., 1998; Lee et al., 2002; Zänker et al., 2002; etc.).

The adsorption of metallic ions on the mineral surface strongly depends on pH (Dzombak and Morel, 1990). The pH value determines whether the functional groups on the mineral surface carry a positive or negative charge and the intensity of that charge. The pH at which the mineral surface changes from being positively charged to negatively charged is called the zero point of charge (ZPC).

Figure 2.14 shows the adsorption curves of oxyanions and cations on iron oxihydroxides as a function of pH. In waters affected by AMD, the surface of different minerals is positively charged due to the excess of protons in solution, leading to preferential adsorption of oxyanions at acidic pH values (Figure 2.14). The adsorption of cations is very low unless they form sulfate complexes (Smith, 1999; Lee et al., 2002). However, as pH increases, the positive charge on the surface of iron hydroxides decreases until it reaches the ZPC. From this point onwards, the mineral surface acquires a negative charge, causing the desorption of oxyanions and adsorption of cations. The degree of adsorption/desorption also depends on each compound and the type of retention process.

On the other hand, as mentioned above, coprecipitation involves the incorporation of metal ions into the crystal structure of a mineral during its formation. It refers to the transfer of a metal from the dissolved to the solid phase when a secondary mineral precipitates, incorporating it as an impurity in the crystal structure (Lottermoser, 2003). Unlike adsorption processes, coprecipitation can impact the concentration of cations under acidic conditions. For instance, the precipitation of jarosite causes the removal of Pb from the water, resulting in relatively low concentrations of lead (Cánovas et al., 2010). Similarly, arsenic is strongly adsorbed/coprecipitated by schwertmanite (Acero et al., 2006), so that, even though there are high concentrations in mining areas, as the precipitation of Fe occurs in river courses, the concentration of dissolved arsenic rapidly decreases. To a lesser extent, Cu, Zn, Co, and many other elements are also coprecipitated with the secondary minerals discussed earlier.

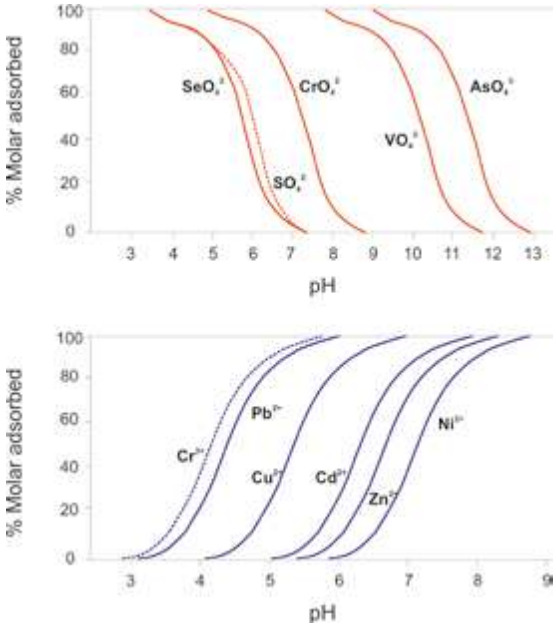

Figure 2.14: Adsorption curves of the main oxyanions and cations in AMD on the surface of iron(III) hydroxides. This information is based on the work of Dzombak and Morel (1990) and Stumm and Morgan (1996).

2.3.5 Sulfate reduction processes

Another process, typically less important in terms of the natural attenuation of AMD pollution, is sulfate reduction and subsequent precipitation of metal sulfides. It is the reverse reaction to the oxidation of sulfides, and requires the absence of oxygen and strongly reducing conditions in the environment to occur, which usually happens when there is a

high content of organic matter. The reduction of sulfates can be schematically represented by reaction 2.27:

$$SO_4^{2-} + CH_2O \leftrightarrow H_2S^- + HCO_3^- \quad (2.27)$$

This reaction produces alkalinity (HCO_3^-) and, in the presence of divalent metals (Fe^{2+}, Zn^{2+}, etc.), the generated sulfides would precipitate in the form of pyrite, sphalerite, etc. This reaction, like pyrite oxidation, occurs abiotically at a very slow rate but can be catalyzed by specific microorganisms (sulfate-reducing bacteria) that oxidize organic compounds using sulfate ions as the final electron acceptor.

In surface waters, the necessary reducing conditions for this process typically do not occur, except in the bottom of mining pit lakes, natural lakes, and reservoirs where a thermal stratification process develops, creating horizontal layers in the water column that do not mix. Thus, the upper layer (epilimnion) has oxic conditions as it is in contact with the atmosphere, while the lower layer (hypolimnion) may have conditions that are sufficiently reducing to allow sulfate reduction to occur.

2.4. Persistence of acid mine drainage

As mentioned earlier, in addition to its high capacity for degrading aquatic ecosystems, another very dangerous characteristic of AMD is its persistence over time. Once acidic conditions are reached in sulfide-rich residues, populations of acidophilic bacteria develop and catalyze oxidation reactions, and if appropriate measures are not taken, the problem will persist after the cessation of mining activity as long as sulfides remain.

Typically, to extract minerals at depth, groundwater needs to be pumped to facilitate mining operations. In the unsaturated zone, when the water occupying the pores is removed, atmospheric oxygen causes the oxidation of sulfides and the subsequent precipitation of soluble sulfate salts. When mining activity ends, drainage ceases, and the groundwater level begins to rise. This recovery can take decades to reach equilibrium and stabilize. For example, the water level in Sierra Bullones and Filón Norte pit lakes in the Tharsis mines has not stabilized and continues to rise today, even though drainage operations ceased in the late 1990s (Moreno-González et al., 2018). As the water table rises, soluble secondary minerals dissolve, enriching the groundwater with sulfates, iron, and metals that are subsequently transported to nearby rivers and streams. Paradoxically, there is an increase in contaminants when mining activity ceases, referred to as the ‘rebound effect’ (Fig. 2.15).

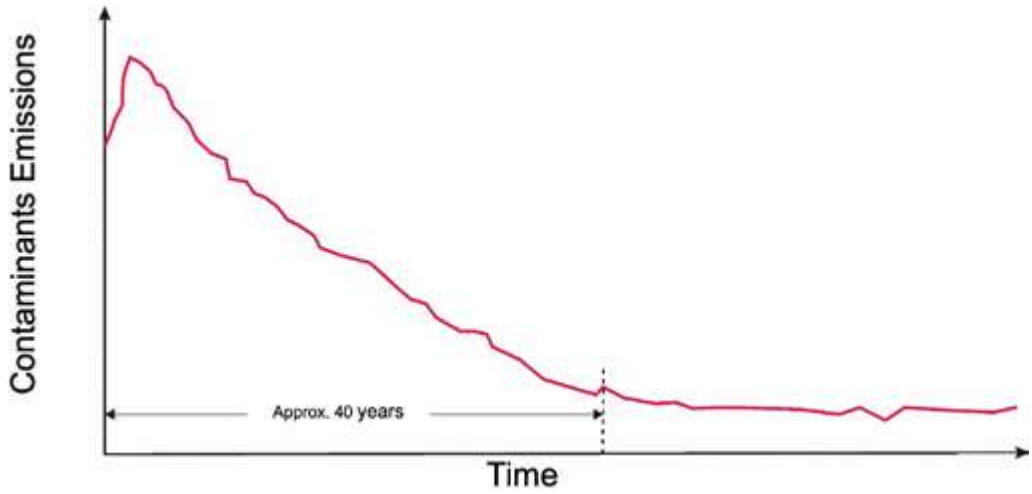

Figure 2.15: Persistence of pollution by AMD (adapted from Younger et al., 2002).

After the 'rebound effect,' contaminant concentrations begin to decrease slowly. It has been observed in many abandoned mines that contaminant reductions are relatively rapid between 10 to 40 years after the cessation of activity (Fig. 2.15), but then they slow down following an exponential law. Eventually, contaminant concentrations stabilize and can persist at these levels, which are still high, for hundreds or even thousands of years (Fig. 2.16; Younger et al., 2002).

Figure 2.16: The continued production of contaminating AMD in the Confesionarios mine, despite its closure at the end of the 19th century, more than 120 years ago, highlights the persistent and enduring nature of the environmental impacts caused by AMD.

2.5. Main conclusions

The oxidation of pyrite occurs when it comes into contact with the atmosphere in the presence of water, releasing acidity, sulfates, and iron. This process can occur naturally, referred to as Acid Rock Drainage (ARD), or anthropogenically, resulting in Acid Mine Drainage (AMD). The latter multiplies the production of contaminants up to 1000 times compared to natural processes, posing a severe global environmental problem.

Associated with iron sulfides like pyrite, there are other metallic sulfides in smaller quantities that also oxidize, releasing other metals and metalloids such as Cu, Pb, Zn, As, Au, Ag, Co, Ni, Se, Cd, Tl, etc. This acidic leachate may dissolve the minerals in the surrounding rocks, incorporating additional elements such as Ca, Mn, Mg, Al, etc.

The chemical reactions governing AMD production are slow when occurring abiotically. However, the process is significantly accelerated in the presence of certain bacteria, such as *Acidithiobacillus ferrooxidans*. The contamination produced by AMD can be naturally attenuated through various mechanisms, including carbonate and silicate hydrolysis reactions, mixing and dilution processes with freshwaters, precipitation of secondary minerals, coprecipitation and/or adsorption processes, sulfate reduction, etc. The dissolution of carbonates such as calcite and dolomite is very effective in neutralizing acidity due to their high reaction rates. However, these minerals are scarce in the IPB, exacerbating acidification issues from sulfide mining.

Mixing and dilution processes with freshwaters can raise the pH of AMD, leading to the precipitation of insoluble secondary minerals such as iron oxides, hydroxides, hydroxysulfates, and oxyhydroxysulfates, if the pH is around 3, or aluminum if the pH rises above 4. The formation of these minerals reduces the concentration of toxic elements in water through processes of precipitation, coprecipitation, and/or adsorption. However, pH increase through mixing or dilution requires a significant amount of unaffected water, also depending on its alkalinity.

Other secondary minerals that decrease metal concentrations in AMD are evaporitic salts, which precipitate in streambeds during low-flow periods due to intense evaporation processes, resulting in extremely high dissolved concentrations. These salts are highly soluble and redissolve with the first rains after the dry season.

Under anaerobic conditions, such as the deeper zones of reservoirs or lakes where atmospheric oxygen is depleted, sulfate reduction can occur, leading to the precipitation of metal sulfides and generating alkalinity.

Once acidic conditions are established, and bacteria catalyzing oxidation reactions develop, it becomes challenging to halt the generation of AMD, which will persist for hundreds or even thousands of years, even after mining activities cease.

3

THE IBERIAN PYRITE BELT

MINING HISTORY AND POLLUTION

3.1 Geology

The province of Huelva is divided into three major geological zones: 1) The Ossa Morena Zone, located to the north, approximately coinciding with the Sierra de Huelva, 2) The South Portuguese Zone, which encompasses approximately the Andévalo region and includes the IPB, and 3) The Cenozoic sedimentary materials filling the Guadalquivir Basin in the southern part of the province (Fig. 3.1). The Ossa Morena and South Portuguese zones belong to the Iberian Massif, formed during the Variscan orogeny, with ancient rocks from Precambrian to Carboniferous ages (older than approximately 300 million years), while the materials in the Guadalquivir Basin are of Neogene age, much more recent (less than about 20 million years). The following provides a brief description of these major zones, with particular emphasis on the IPB, which is the region with the highest concentration of polymetallic massive sulfide deposits globally, with original reserves exceeding 2000 million tons (Almodóvar et al., 2019). The exploitation of these deposits since the mid-19th century has led to severe pollution problems due to AMD, which is the focus of this book.

3.1.1 Ossa Morena Zone

The Ossa Morena Zone exhibits a great diversity of materials and structural complexity. It is bounded by significant tectonic features resulting from the later stages of deformation during the Variscan orogeny. The materials in this zone, which include numerous magmatic bodies, range in age from Precambrian to Carboniferous. The area is compartmentalized by a dense network of fractures and shear zones, forming elongated bands in the ESE-WNW direction, where materials affected by variable degrees of metamorphism are exposed.

Among the major tectonic zones differentiated in the Ossa Morena Zone, the most important in the province of Huelva is the Aracena Metamorphic Belt. The contact between the Ossa Morena and South Portuguese zones is considered a tectonic suture, signifying the boundary between two large continental blocks that were initially separated but eventually collided during the Variscan orogeny (Fernández Rodríguez and Díaz Aspiroz, 2008). The predominant rocks include shales, graywackes, and schists, with some outcrops of limestones, dolomites, and marbles. Additionally, there are volcanic and volcaniclastic rocks, as well as intrusions of plutonic rocks such as gabbros, diorites, and granites. A continental domain is recognized, with rocks affected by varying degrees of metamorphism, and an oceanic domain, primarily composed of metabasites, representing a fragment of ancient oceanic crust.

3.1.2 South-Portuguese Zone and Iberian Pyrite Belt (IPB)

The South-Portuguese Zone is the outermost region in the southern part of the Iberian Massif. It consists of Paleozoic rocks ranging in age from the mid-Devonian to the Permian. It is bounded to the north by the Ossa Morena Zone and to the south by the more recent materials of the Guadalquivir Basin filling. The South-Portuguese Zone is divided into several domains, among which the most significant in the province of Huelva are Pulo do Lobo and, especially, the IPB (Fig. 3.1).

The IPB forms a band approximately 230 km long and 40 km wide, extending from the province of Seville to the Portuguese coast. Three major tectonostratigraphic units are differentiated from bottom to top in the following order: Phyllite and Quartzite Group (or PQ Group), Volcano-sedimentary Complex (VSC), and Culm Group. The PQ Group, ranging from the mid to upper Devonian, consists mainly of shales or phyllites intercalated with quartzite levels (Moreno and González, 2004). The thickness of these materials is estimated to be around 2000 m.

The Volcano-sedimentary Complex (VSC), ranging in age from the upper Devonian to the lower Carboniferous, exhibits greater heterogeneity compared to the PQ Group, both in thickness (ranging from 0 to over 1000 m) and lithology. Variations in its materials result from intense magmatic activity in the area and the compartmentalization of the ancient marine basin, which influenced the distribution of different sedimentary material contributions. The stratigraphic column of the VSC consists of sedimentary rocks, primarily shales, interspersed with various types of igneous rocks, mainly acidic volcanic and subvolcanic rocks (riolites and dacites) and volcanic basic rocks (basalts). The column is completed with discontinuous levels of flint and massive polymetallic sulfide masses. The top of the VSC is marked by manganese oxide mineralizations, purple shales, and jaspers.

Numerous massive polymetallic sulfide deposits are associated with acidic magmatic sequences (Fig. 3.1), making the IPB globally renowned. There are several deposits referred to as 'supergiants' (over 100 million tons): Las Cruces, Aznalcóllar-Los Frailes, Riotinto (the world's largest of its kind), Sotiel-Migollas, La Zarza, Masa Valverde, Tharsis, and, in the Portuguese part, Neves Corvo and Aljustrel. Additionally, there are many other deposits scattered throughout the IPB. These deposits formed due to submarine volcanism. Pyrite is the most abundant mineral, with lesser amounts of sphalerite, galena, chalcopyrite, arsenopyrite, etc.

In addition to sulfides, other important mineral deposits in the IPB are gossans (iron caps) and supergene enrichment zones (García Palomero, 2004). Gossans form slowly due to natural oxidation processes of sulfides exposed to atmospheric oxygen (ARD). Sulfates and other metals are leached away, while iron primarily remains in the gossan in the form of oxides and hydroxides, giving rise to reddish crests, which typically indicate the presence of an underlying sulfide deposit. The more soluble elements (Cu, Zn, etc.) are transported

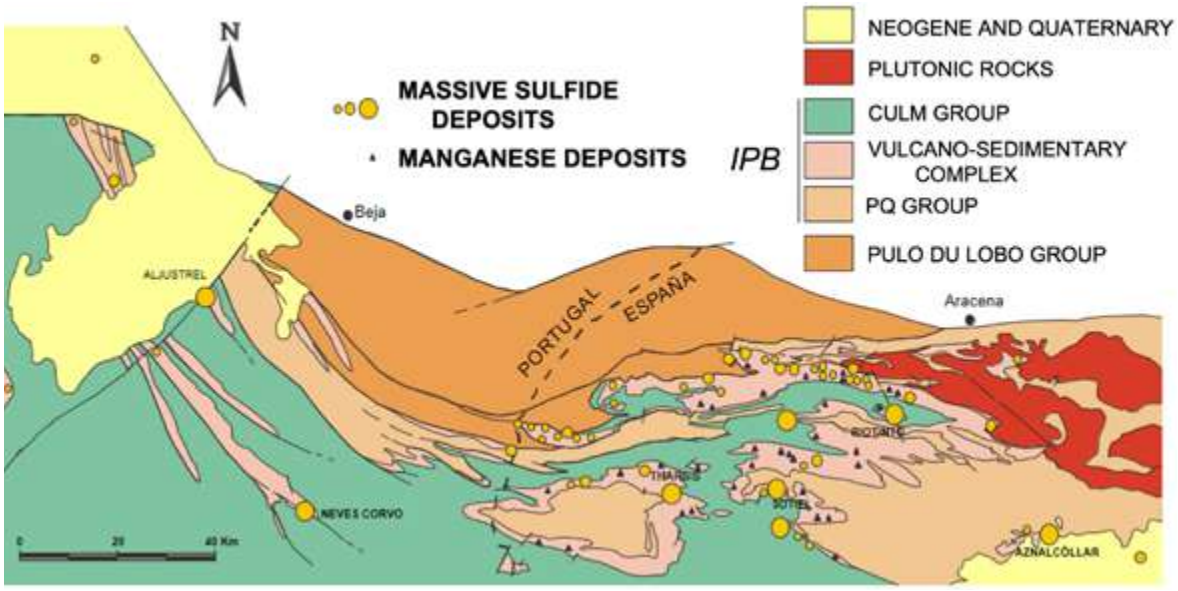

Figure 3.1: Location map of the IPB, indicating the main sulfide deposits and their size.

along with sulfates by water to other areas where they may precipitate again, often forming interesting secondary and supergene deposits. Other less soluble metals (such as gold and silver) concentrate residually. For example, in the Riotinto gossan, a gold concentration five times higher than the average value of the original sulfide mass has been estimated (García Palomero, 2004).

The Culm Group comprises sedimentary rocks deposited after the magmatic phase. Three units are differentiated (Moreno and González, 2004): the basal shale series, the turbiditic formation of Culm facies, and the sandy unit of shallow platform. The basal shale series is a mixed vulcanodetritic and shale sequence composed of shales with a thickness not exceeding 50 m, and it may even be absent. The turbiditic formation of Culm facies is the most characteristic of this group and extensively outcrops in the province of Huelva (Fig. 3.1). It is a sequence that includes shales, sandstones, and scarce conglomerates, with a maximum known thickness of about 3000 meters. Finally, the sandy unit of shallow platform consists of an alternation of shales and quartzose sandstones arranged in a grain and stratocrescent sequence.

3.1.3 Guadalquivir Depression

The Guadalquivir Basin, an elongated depression running in ENE-WSW direction, is primarily filled with marine sedimentary materials that extend from the eastern part of Andalusia (at about 800 meters in altitude) to sea level in the provinces of Huelva and Cadiz. These materials are of Neogene age, much more recent than the Paleozoic rocks on which they overly. They are generally subdivided into four lithostratigraphic units, which, from bottom to top, are the “Calcarenitas de Niebla” Formation, the “Arcillas de Gibraleón” Formation, the “Arenas de Huelva” Formation, and the “Arenas de Bonares” Formation. Across the entire western sector, these four formations together have a thickness of 400 meters and are unconformably overlain by Quaternary materials.

The “Calcarenitas de Niebla” Formation, of upper Tortonian age, is composed of sands and conglomerates that vertically evolve into calcarenites and bioclastic limestones, and subsequently into glauconite-rich silts (Baceta and Pendón, 1999). The “Arcillas de Gibraleón” Formation, ranging from upper Tortonian to lower Pliocene age, consists of a sequence of clays and marls, occasionally with silts and sands, featuring abundant planktonic and benthic microfauna. The Arenas de Huelva Formation, of lower Pliocene age, is made up of fine-grained sands and silts, and is characterized by several fossiliferous levels with large accumulations of shells and mollusks. Lastly, the Arenas de Bonares Formation, of Pliocene age, consists of coarsening-upward sands with intercalations of small conglomerate levels, all of which have a coastal character and abundant ichnofossils (Mayoral, 2008).

3.2 Characteristics of the Tinto and Odiel Rivers

Most of the drainage basins of the Tinto and Odiel rivers are located over IPB materials. However, the northern part of the Odiel River drains materials belonging to the Ossa Morena Zone, and in their lower reaches, before flowing into the Atlantic Ocean, both rivers cross materials belonging to the Guadalquivir Basin.

3.2.1 Relief

The Tinto and Odiel rivers have drainage basins of 1646 and 2333 km^2, respectively, which represent approximately 40% of the surface area of the province of Huelva (Fig. 3.2). The Tinto River originates in the Sierra del Padre Caro and has a length of 101 km. On the other hand, the Odiel River originates in the Sierra de Aracena and has a length close to

Figure 3.2: Location of the Tinto, Odiel and Piedras river basins in the province of Huelva, indicating the occurrence of main aquifers, rivercourses and reservoirs.

140 km. In their final sections, both rivers lose their riverine character and form a common estuary, the Ría de Huelva.

In the Odiel River basin, four well-defined geographical areas are distinguished: the Sierra de Huelva, the Andévalo (a transitional area between the Sierra and the plains of the southern part of the province), the Condado, and the Huelva Coast. The Tinto River basin is restricted to the latter three: Andévalo, Condado, and Coast. The maximum altitude in the Odiel River basin is 926 m, while in the Tinto River basin, it is 680 m (Fig. 3.3). The steepest slopes are found in the northern part. However, the high-altitude areas constitute only a small part of their basins; the area above 500 m represents only 5% in the Odiel basin and 1.5% in the Tinto basin. The average altitude is 202 m in the Odiel basin and 159 m in the Tinto basin.

The Tinto, Odiel, and Piedras rivers were historically managed by the Guadiana River Basin Authority. However, in January 2005, their management was transferred to the Andalusian Regional Government. Currently, they form the Hydrographic Demarcation of the Tinto, Odiel, and Piedras Rivers, under the administration of the regional government of Andalusia.

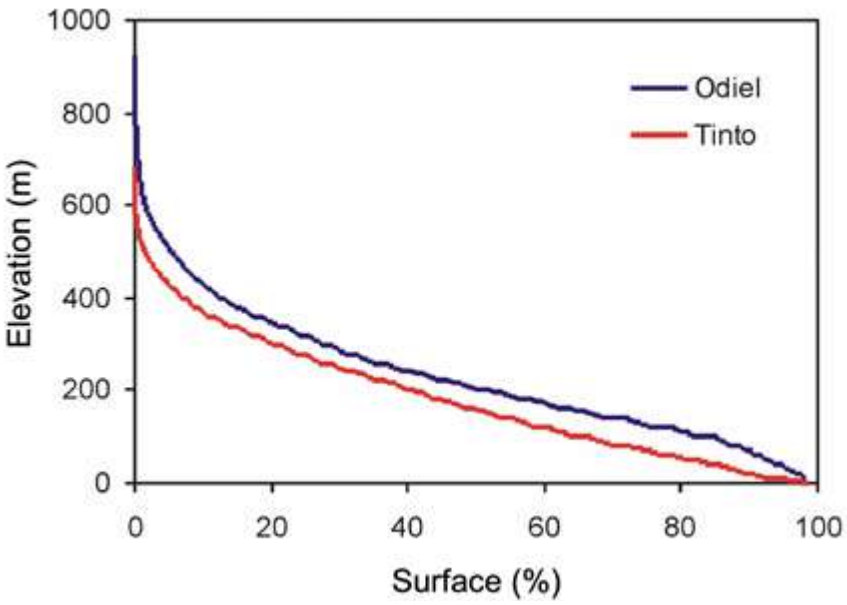

Figure 3.3: Hypsometric curves for the Tinto and Odiel River basins

3.2.2 Climate

The climate in the Huelva province is of Mediterranean type. However, temperature and rainfall characteristics vary widely in the southwest to northeast direction. In the southern sector of the province, where the lower reaches of the Tinto and Odiel river basins are located, the average temperature is 18 ºC, and annual precipitation is around 500 mm. In the northern sector of the province, where the headwaters of the Odiel River are situated, the annual average temperature is 15 ºC, and annual precipitation reaches about 1000 mm.

Minimum temperature values, and consequently evapotranspiration (Fig. 3.4), occur during the months of November to January, while the maximum values are reached during summer (June-August). Precipitation is concentrated in the wet period, generally between October and April (Fig. 3.4), preceded by a dry period between May and September. However, rainfall is highly irregular, showing high seasonal and interannual variability, with cycles of drought and periods of heavy rain observed over time.

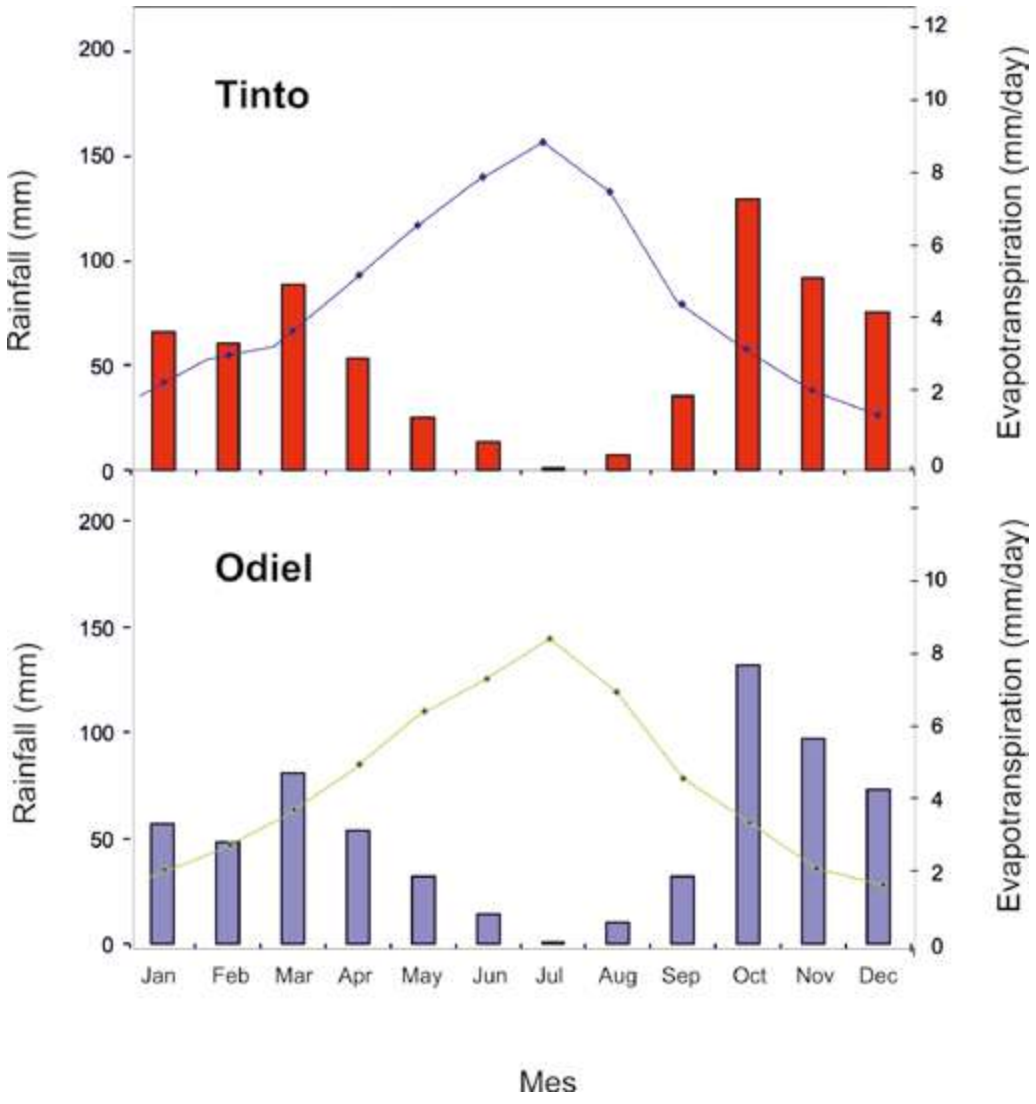

Figure 3.4: Intra-annual distribution of monthly rainfalls (columns) and daily potential evapotranspiration (lines) in the Tinto and Odiel river basins (Cánovas, 2008).

3.2.3 Hidrology

As mentioned before, the Odiel River basin has a total area of 2333 km^2, and it can be divided into three main sub-basins (Fig. 3.5): the Oraque, Meca, and the Odiel sub-basins. The Oraque River sub-basin covers an area of 612 km^2, with its major tributaries being the Fresnera, Aguas Agrias, Pelada, and Tamujoso streams (Fig. 3.5). The Meca River sub-basin has an extension of 317 km^2, with the Agustanos, Aserrador, Dehesa-Boyal, and Multas streams as its most important tributaries. Finally, the Odiel River sub-basin has an area of 1404 km^2, with its main tributaries being the Santa Eulalia, Seca, Escalada, and Olivargas streams on its right bank, and the Villar stream and Agrio stream on its left bank (Fig. 3.5).

The Odiel River maintains its fluvial character until Gibraleón, from where a complex estuary is formed, hosting the Marismas del Odiel Natural Site. This area was declared a UNESCO Biosphere Reserve in 1983 and are considered the most important tidal marshes in the Iberian Peninsula, strategically located in the migratory routes of numerous bird species. The Odiel joins the Tinto River near the city of Huelva, forming a common estuary known as the Ría de Huelva.

With the onset of mining operations in the Odiel River basin in the 19th century and their consolidation during the 20th century, numerous small reservoirs, dams, and hydraulic structures were built to ensure water supply for these operations and for the human consumption of the populations settled in the basin. The Odiel sub-basin is the most regulated, with the Olivargas reservoir (29 hm^3) being the most important. The Meca River is regulated just before its confluence with the Odiel through the Sancho reservoir (58 hm^3), the largest in the Odiel River basin, intended for industrial use. The Oraque River currently has the least regulation; however, at its confluence with the Odiel, the Alcolea dam (246 hm^3) is located, whose construction is currently halted and is discussed in section 5.1.5.

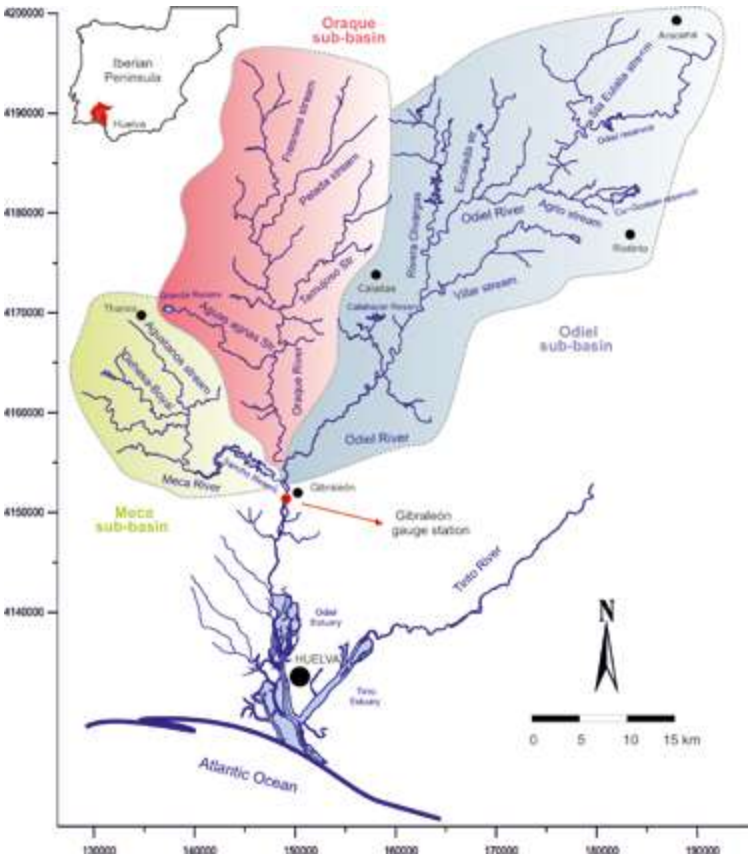

Figure 3.5: Main Odiel River sub-basins.

On the other hand, the Tinto River has a basin with a surface area of 1646 km^2. Along its course towards the Atlantic Ocean, it receives contributions from the Jarrama and the Corumbel rivers on its left bank, and from the Nicoba River and the Candón stream on its right bank (Fig. 3.6). Additionally, there are numerous streams in its basin that only carry water during the rainy season, such as the Gallego stream, Hornueca, Giraldo, and Casa Valverde rivers. Near the town of San Juan del Puerto, the Tinto River loses its fluvial character and reaches the marshes of the Tinto estuary. Finally, it joins its waters with those of the Odiel in the Ría de Huelva.

The two most important reservoirs in the Tinto River basin are the Jarrama and Corumbel reservoirs. The Corumbel reservoir, located 1 km from the confluence of the Corumbel River with the Tinto River, has an approx-

imate capacity of 18 hm^3 and supplies water to the Condado area. The Jarrama reservoir, with a capacity of 39 hm^3, was completed in 2000 and is used to supply water to the population of 8 municipalities in the mining basin. Additionally, there are numerous small reservoirs distributed throughout the basin, such as the Tumbanales reservoirs that regulate the Tinto River near its source, the Beas reservoir (3.2 hm^3 capacity) that regulates the Candón stream, the Candoncillo reservoir (1.3 hm^3), and the Zumajo and Silillos reservoirs (2.0 hm^3).

As mentioned in the previous section, the predominant materials in the Tinto and Odiel basins are primarily igneous and metamorphic rocks, especially shales and quartzites. These materials have low permeability, so they do not constitute significant aquifers. Therefore, the Tinto and Odiel rivers have low natural regulation, and their flow is closely dependent on precipitation patterns (Fig. 3.7). Only the superficial alteration zone, several meters thick, may contain water, with limited resources and very small reserves, but they do not have sufficient magnitude to be considered as aquifers. The only exception occurs in the north of the Odiel River basin due to the presence of some karstified carbonate outcrops in Sierra Morena, which have high permeability. The materials giving rise to this aquifer correspond to the calcareous formations of the Precambrian and Cambrian and form the main mountain ranges in the province. In the lower part of both basins, located in the southern part of the province, there are large detrital aquifers such as Almonte-Marismas, Ayamonte-Huelva, and Niebla-Gerena (Fig. 3.2).

The average contribution of the Tinto and Odiel rivers during the period 1980-2006 is about 46 and 336 hm^3/year, representing an average flow of 1.5 and 11 m^3/s, respectively. There is a high variability due to the irregularity of precipitations. The contribution of the Tinto River in the years 1987/88 and 1989/90 exceeded 100 hm^3, while during 1994/95

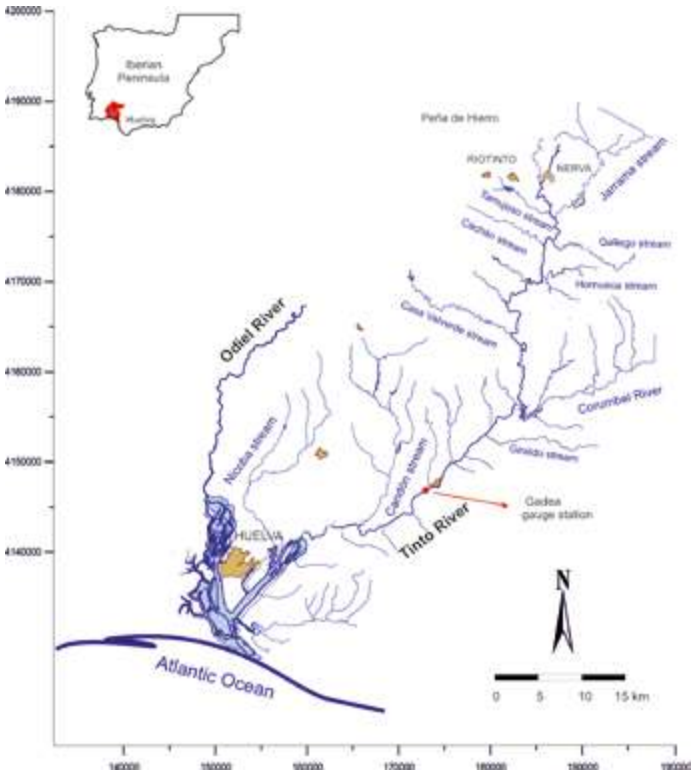

Figure 3.6: Hydrographyc network of the Tinto River

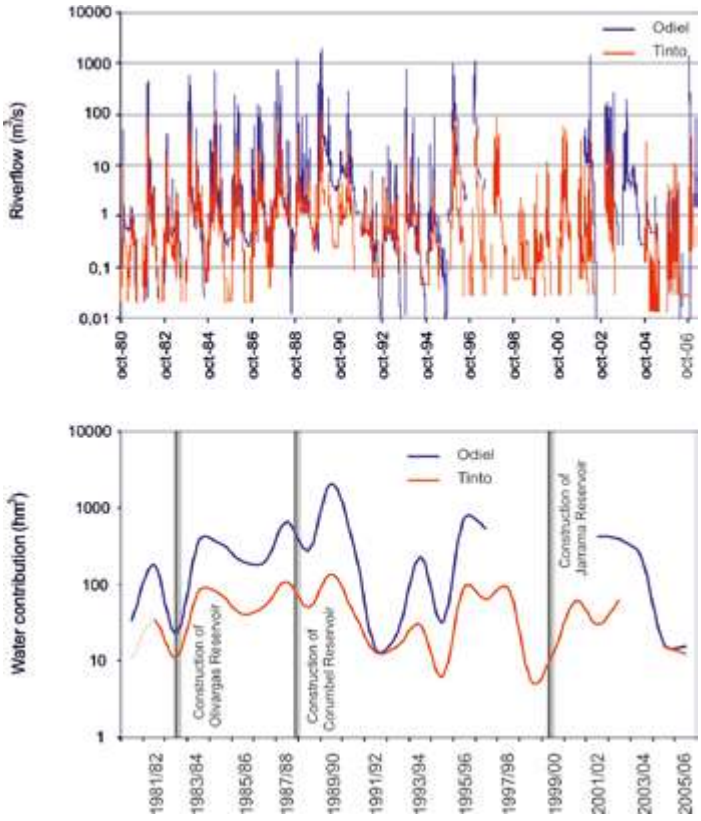

Figure 3.7: Evolution of average daily riverflow (above) and the contribution (below) of the Tinto and Odiel rivers during 1980-2006, showing the occurrence of hydraulic infrastructures in the basins (Cánovas, 2008).

and 1998/99, the contribution did not reach 10 hm^3. Similarly, in the Odiel River, there are some years with contributions exceeding 1000 hm^3, while in others, it is less than 20 hm^3.

This variability can be observed in Figure 3.7, where the daily average flow during the period from October 1980 to September 2006 in the Tinto and Odiel rivers at the Gadea and Gibraleón gauging stations is depicted. It is evident that the contribution of both rivers varies widely depending on precipitation, although other factors such as the regulation of different watercourses through hydraulic structures also influence it.

3.3 Mining History and Pollution in the IPB

3.3.1 Brief mining history in the IPB

The IPB is one of the most exploited metallogenic regions by humans since ancient times. Archaeological evidences indicate that metal production began sometime in the third millennium BC, which means almost 5000 years of mining in this area. The following summarizes the history of mining in the region, primarily based on the compilation made by Olías and Nieto (2012).

The first mining and metallurgical activities date back to the Chalcolithic period (third millennium BC). During this time, specialized populations engaged in mining produced copper from carbonate minerals (azurite and malachite), oxides (cuprite and tenorite), and even some sulfides like chalcocite and covellite (Nocete et al., 2008). For example, in the mining settlement of Cabezo Juré (Alosno, Huelva), from the third millennium BC, numerous installations for metallurgical production have been discovered, including furnaces and crucibles (Nocete, 2006) (Fig. 3.8).

In the Bronze Age (2000 BC), the use of copper became widespread in manufacturing tools. Between the Early Bronze Age and the Middle Bronze Age (1800 – 1200 BC), silver was first melted in the Iberian Peninsula (Pérez Macías, 1996; Pérez Macías and Delgado Domínguez, 2011). As production increased, mining activities sought minerals in lead and silver-rich gossans, formed by the oxidation of complex sulfides. The Late Bronze Age (1200 – 900 BC) witnessed a significant flourishing of mining and metallurgical activities, accompanied by the establishment of a robust trade gradually controlled by Phoenician merchants (Salkield, 1987). This technological and cultural peak materialized into a native civilization that based its economy on metal production, reaching high levels of power. This civilization was known by the mythical name of Tartessos (Carrasco Martiañez, 2000).

With the advent of the Iron Age, new mining tools allowed miners to reach greater depths. Evidence of underground mining in Riotinto dates back to the 7th century BC (Pérez Macías and Delgado Domínguez, 2011). Toward the first half of the 6th century BC, signs of decline appeared in Riotinto, lasting until the early 5th century BC (Carrasco Martiañez, 2000). The Carthaginian civilization became the first power in the Western Mediterranean, establishing itself in the southeastern Iberian Peninsula and developing a significant mining and metallurgical industry that marked the end of Tartessos (Pinedo Vara, 1963).

Roman technology greatly boosted mining in the IPB (Fortes-Garrido et al., 2023), enabling the exploitation of deposits on an unprecedented scale. Almost all mines exploited during the last two centuries showed signs of Roman workings (Pinedo Vara, 1963). Mining was primarily underground, with silver being the main metal beneficiated from jarositic materials located at the contact between the gossan and secondary minerals. In some mines, Roman workings reached depths of even a hundred meters (Pinedo Vara, 1963), necessitating the lowering of the water table through drainage galleries (adits) and water wheels or other pumping systems. Up to 40 Roman water wheels have been found in Riotinto (Fig. 3.9), along with a complex system comprising 14 water wheels in Tharsis, accompanied by advanced drainage devices such as Archimedean screws and Ctesibius hydraulic pumps.

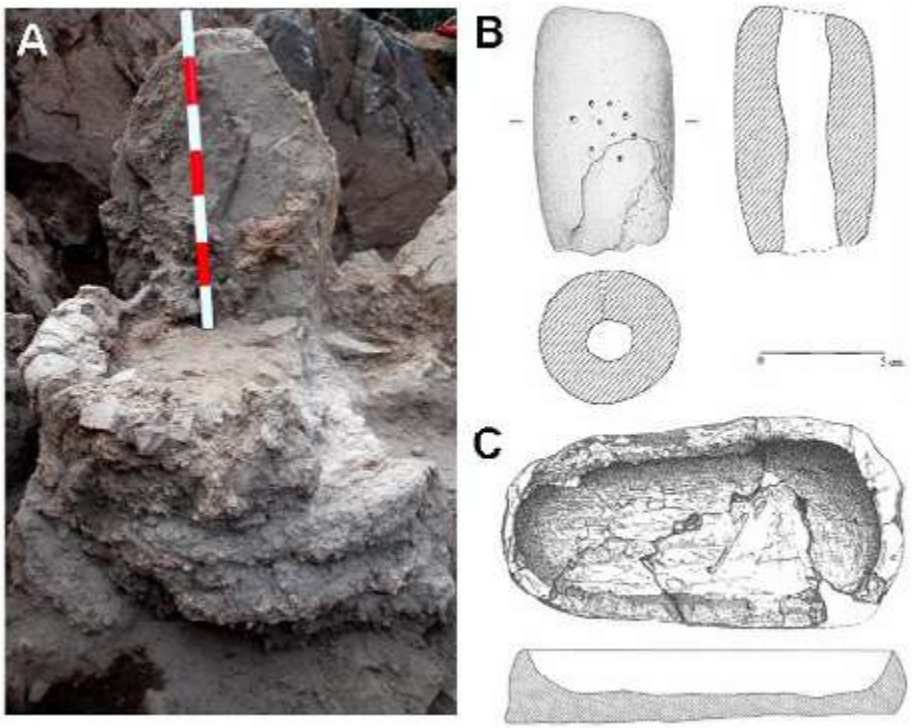

Figure 3.8: A) Copper smelter furnaces, B) Nozzle scheme and C) Crucibles recovered from the early Chalcolithic mining settlements in Huelva (Nocete, 2004).

Copper mining developed later because the average grades of the IPB deposits were probably lower than what the Romans sought. The ores exploited were those of the supergene enrichment zone and perhaps higher-grade chalcopyrites (Gonzalo y Tarín, 1888; Carrasco Martiañez, 2000). Roman mining was selective, with small waste heaps as the extraction of sterile or low-grade minerals was avoided (Pérez Macías and Delgado Domínguez, 2011). The peak activity in this period occurred in the 1st century aD; after the 2nd century aD, the mines entered a progressive decline. With the arrival of the Visigoths in the peninsula (405 aD), the period of Roman mining in the IPB ended.

It has traditionally been considered that mining activity was greatly reduced during the Middle Ages. However, Pérez Macías and Delgado Domínguez (2011) point out that many workings attributed to the Romans could be of medieval origin since the mining technology used by the Romans remained with few variations until the late 15th century. The sedimentary record of the Guadiana River estuary also suggests the existence of significant mining activity during the Middle Ages (Delgado et al., 2012). In the 16th century, numerous explorations for gold and silver were initiated in the provinces of Huelva and Seville but did not work. During this period, *caparrosa* or *aceche* (iron sulfate; Fig. 2.12) and alum (aluminum sulfate), soluble evaporitic salts deposited in mining areas during summer, were collected for medicinal, dyeing, etching, and other purposes (Ortiz Mateo and Romero Macías, 2004).

In the first half of the 18th century, mining operations in Riotinto were resumed through a lease to Liebert Wolters, of Swedish origin. Initially, copper was obtained by precipitation, placing the acidic leachates that emanated from the area in contact with iron scrap in channel systems (Fig. 3.10). The collection of *caparrosa* continued, the extraction of minerals with higher Cu grades began, and some small smelters were built. Gradually, copper production through smelting became more important compared to natural cementation processes (Ortiz Mateo and Romero Macías, 2004).

In the second half of the 18th and the early 19th century, mining exploitation remained of small scale, limited to Riotinto, with some periods of inactivity due to the French invasion and the War of Independence. By the mid-19th century, the calcination in "teleras" (Fig. 3.11) and the obtaining of copper through artificial cementation began to be used. The method involved the slow ore roasting (six to seven months) in piles of 40 to 50 tons, releasing sulfur into the atmosphere and forming copper sulfates and oxides. Once the ore was calcined, it was placed in deposits (piles) filled with acidic water to dissolve copper sulfates, and later, copper cementation occurred with iron scrap in channel systems. The use of this method resulted in lower wood consumption than smelting and grew rapidly, but it caused serious problems due to air pollution and the generation of acid rain, leading to diseases, increased mortality in the population, and damage to crops in nearby areas (Fernández Caliani, 2008).

During this time, there was a flourishing of trade and industry in Europe. England was at the height of building its empire (Checkland, 1967). Copper gained multiple applications in the new electrical industry due to its excellent conducting properties. Thus, from 1820, global copper production increased by 30% per decade (Flores Caballero, 1983), and the region became to be known as the "California of copper" (Carrasco Martiañez, 2000). Mining in the IPB received the definitive boost in the mid-19th century with the strong growth of the chemical industry to obtain sulfuric acid from pyrite, later used to manufacture fertilizers, explosives, and other products.

Thus, until the mid-19th century, the only active mine was Riotinto, but from 1850, there was a spectacular development of mining. By 1855, mines such as Castillo de las Guardas, Peña de Hierro, Concepción, Chaparrita, Poderosa, Tinto Santa Rosa, San Miguel, Sotiel-Coronada, and San Telmo were already in production. In 1873, the Spanish State sold the exploitation of the Riotinto mines to the Rio Tinto Company, a British-owned company. Many other mines also experienced significant growth due to foreign investments (Checkland, 1967). The need to transport large amounts of ore led to the rapid construction of numerous railway lines in the province. From then on, the introduction of large-scale open-pit mining accelerated, and a large number of mines in the area were put into operation.

As copper production increased through roasting methods, also did the pollution from emissions released in this process. Up to 500 tons of sulfurous and arsenical gases were daily released to the atmosphere, leading the area to be known as the 'Valley of Lucifer' (Carrasco Martiañez, 2000). Complaints from the population continued until violently erupting in 1888, known as the 'year of the shots,' when a large protest demonstration was violently suppressed, resulting in between 70 and 200 fatalities (Carrasco Martiañez, 2000).

Figure 3.9: Roman-era waterwheel for water extraction in underground mining operations found in the Riotinto mines (Riotinto Foundation).

Calcinations were gradually phased out after these events, and the method of natural cementation was developed. This method remained operational in some mines until the late 1960s (Carrasco Martiañez, 2000). The ore was stacked in large piles with chimneys for air entry, called "terreros," which were periodically wa-

tered with AMD, causing the oxidation of sulfides. The leachates were collected and cemented in channels with iron scrap. The 'washed' pyrites were sold for the production of sulfuric acid, and later, the roasting ashes were processed to obtain Cu, Pb, Zn, and other metals, utilizing 100% of the ore (Carrasco Martiañez, 2000).

During the first two decades of the 20th century, copper prices and the demand for sulfuric acid remained high, with annual Spanish pyrite production accounting for 50 to 60% of the global production (Carrasco Martiañez, 2000). Thus, between 1900 and 1930, the IPB experienced its peak period of sulfide production.

Figure 3.10: Channel system in the Riotinto mines for copper cementation in the first half of the 20th century (Riotinto Foundation).

In the early 1930s, mineral separation processes using flotation were introduced. This hydrometallurgical technique allowed the exploitation of minerals with lower grades than those previously processed, enabling the recovery of zinc and lead contained in sulfides. As a consequence of these activities, a new type of waste, stored in tailing ponds, began to be generated, such as the one responsible for the Aznalcóllar spill in 1998.

During World War II, difficulties in exporting minerals led to a significant decrease in production. In the 1950s, there was a revitalization of the international pyrite market, leading to a resurgence in mineral prices. In the 1960s, Spain experienced an "economic miracle" facilitated by the new open-door policy of the dictatorship. This period allowed for the construction of a Chemical Complex near the port of Huelva, where the copper smelting and sulfuric acid factory of Riotinto was relocated in 1970 (Carrasco Martiañez, 2000).

In the 1970s, pyrite-producing mines entered a period of decline due to issues in the sulfuric acid market. Competition from sulfur extracted through other industrial processes, along with the sulfur recovered from desulfurization of gases from metal smelters, natural gas, or petroleum, emerged due to environmental legislation requirements (Carrasco Martiañez, 2000). However, global demand for copper continued to increase, and exploration research in the IPB intensified. In 1970, the largest mining project in Spain up to that point was launched: the open-pit exploitation of copper, gold, and silver at Cerro Colorado (Carrasco Martiañez, 2000), with the construction of the Copper and Gossan ponds for the storage of generated tailings (Olías and Nieto, 2015; Fig. 3.13).

Figure 3.11: "Teleras" (mineral piles) for open-air pyrite roasting during the second half of XIX century (Riotinto Foundation).

At the beginning of the 1980s, the entry of new materials into the market, such as aluminum or fiber

Figure 3.12: Channel system for copper cementation at La Zarza mine, which was in use until the 1960s.

optics, along with recycling, led to a decrease in the demand for copper and sulfuric acid, culminating in a major crisis in 1986 (Carrasco Martiañez, 2000). Additionally, the growing environmental awareness led to the consideration of ashes produced in the roasting of pyritic minerals as a toxic waste. This initiated the closure of numerous operations, affecting mainly small and medium-sized mining operations (Lomero-Poyatos, San Telmo, Concepción, and Herrerías, etc.). To overcome the crisis, copper production was abandoned in Riotinto, and the focus shifted to gold and silver, leaving Filón Norte and La Zarza, both owned by the Tharsis Company, as the only producers of pyrite for sulfuric acid until their closure in the late 90s. Mines that resisted the crisis better were Riotinto, Sotiel-Coronada, Aguas Teñidas, and Aznalcóllar, dedicated to the production of copper, zinc, and lead concentrates, and those exploiting precious metals from the gossan (Tharsis and Riotinto). However, a new crisis in metal prices in the international market during the late 90s, along with other problems like the disaster caused by the spill from the Aznalcóllar mining pond in 1998, led to the closure of all sulfide mines of the IPB in 2001.

The mining activity throughout history has drastically transformed the landscape of the exploited areas and caused enormous environmental impacts in the surroundings. On the other hand, it has left a rich industrial and cultural heritage from different extraction periods, of great interest.

As history shows, mining is a cyclical activity, with periods of crisis followed by periods of resurgence. Thus, the increase in commodity prices from 2004, mainly due to the strong demand from Asian countries, has led to a reconsideration of the economic viability of copper mining. Currently, we are in a new period of prosperity in sulfide mining. In the Spanish

part of the IPB, there are currently five large mines in production: Cobre-Las Cruces in Seville, and Aguas Teñidas, Mina Magdalena, Sotiel, and Riotinto in Huelva. Los Frailes mine (Aznacóllar) is waiting to obtain permits to restart its operation, and there are numerous reopening projects at various stages of development.

Figure 3.13: Gossan and Copper tailing dams from the Riotinto mines built in the 1970s and currently being raised to store waste from the new operation.

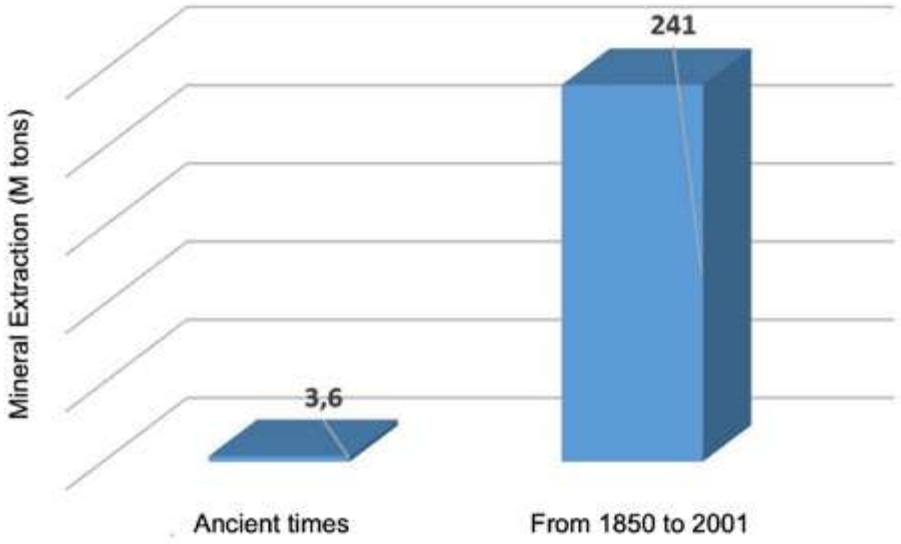

Figure 3.14: Comparison between mineral extraction from Riotinto during ancient times (pre-Roman and Roman periods) and modern mining (1850-2001)

To have a global view of what mining has meant in the IPB throughout history, Figure 3.14 shows estimates of sulfides extracted in the Riotinto mines during the Roman and pre-Roman periods and during modern large-scale mining from 1873 to 2001 (extractions before 1873 are negligible). Based on the existing ancient dumps in the area before the start of modern mining, it has been estimated that 3.6 million tons were extracted during ancient mining (Rothenberg and García Palomero, 1986; Ortiz Mateo, 2004), mostly during the centuries of Roman domination (Olías and Nieto, 2015). Extractions from 1873 to 2001 amounted to 245 million tons (Moreno Bolaños, 2011), nearly 70 times more than ancient mining. Currently, more than 10 million tons of ore are extracted in Riotinto in a single year, a figure much higher than the amount of sulfides extracted in all centuries of Roman and pre-Roman exploitation. It is important to keep in mind the magnitudes of these figures when understanding the environmental impact caused in these different periods.

3.3.2. Evolution of AMD pollution

Natural Sulfide Oxidation Processes

Before mining activity began, natural oxidation processes of sulfides were already occurring under oxidizing conditions near the surface. These natural processes release acidity, sulfates, and more mobile metals, resulting in oxidation caps or *gossans*. By studying the age of these gossans located over many sulfide deposits in the IPB, researchers can determine the age of the onset of metal release processes and acidity to the environment. Fernández Remolar et al. (2003) suggest that a natural sulfide oxidation process existed around 300,000 years ago, possibly even at the Pliocene-Pleistocene boundary (2 million years ago), creating suitable conditions for the development of acidophilic bacteria in these aquatic ecosystems. Moreno et al. (2003) provide an age of at least 6 or 7 million years for the gossan formed at the Las Cruces deposit, located about 50 km east of Riotinto. In a more recent and precise dating using paleomagnetic studies of gossans in Riotinto and other deposits, Essalhi et al. (2011) trace the beginning of their formation (and hence acid rock drainage processes) to over 24 million years ago (late Oligocene). In summary, natural sulfide oxidation processes and acidity generation in the IPB are very ancient, allowing for the development of a high biodiversity of eukaryotic organisms in these environments (Amaral Zettler et al., 2002).

However, the release of acidity and toxic elements during this long period of 'natural contamination' occurred over millions of years. Even if acidic environments existed in some areas, these must have been very restricted, and the amount of contaminants released into the environment must have been negligible compared to current levels. Therefore, these processes left no significant signs in the sedimentary record of the Huelva estuary and the Gulf of Cádiz, although locally they are evident in the form of fluvial terraces in the Riotinto area (Essalhi et al., 2011).

Early Signs of Contamination

Metal concentrations of mining origin in the sediments of the Huelva estuary show a slight increase around 4500-5000 years ago, corresponding to the beginning of mining in the IPB during the Copper Age. Leblanc et al. (2000) found an initial contamination peak around 2530 BC in materials from a survey in the estuary of the Tinto River. Data from Ruiz et al. (2020), Arroyo et al. (2021), and Romero et al. (2023), based on sediment cores from the Tinto Estuary, also place the onset of mining contamination between 4500 and 5000 years BP, while other authors obtain slightly more recent ages (Ruiz et al., 1998; Davis et al., 2000; López-González et al., 2006). These results align with archaeological studies showing an increase in Cu, Zn, and As levels in mollusk shells found at the archaeological site of Cabezo Juré (Alosno) in the third millennium BC, coinciding with the earliest

documented mining activities (Nocete et al., 2005). Concurrently, massive deforestation occurred to fuel the smelting furnaces, leading to a significant decrease in arboreal pollen quantity in the area, disappearing entirely during the phase of major mining activity around 2500 BC (Nocete et al., 2005).

Roman Period

After this initial exploitation phase in the Copper Age, mining activity slowed until its resurgence in the Roman era. As mentioned earlier, Roman mining represents a period of intense activity, involving the excavation of kilometers of tunnels and galleries. This required lowering the water table using wheels and other systems. Naturally, all this mining activity resulted in a considerable amount of sulfides coming into contact with atmospheric oxygen, increasing the levels of contaminants transported by the Tinto and Odiel rivers. The history of this contamination is recorded in the sediments of the Huelva estuary, showing an increase in metal concentrations (Ruiz et al., 1998; Davis et al., 2000; Romero et al., 2023), and even in the estuary of the Guadiana River (Delgado et al., 2012). Evidence of this contamination, transported through atmospheric circulation, has been found even in Greenland. Through the analysis of ice cores, an increase in lead, copper, and other metal concentrations coinciding with the Roman era has been detected. Comparing the isotopic ratios of lead with those of the main mining deposits existing in that period, Rosman et al. (1997) concluded that around 70% of the lead content in Greenland ice came from IPB deposits. Similar conclusions are obtained from the analysis of copper concentration in the ice (Hong et al., 1996). All of this highlights the enormous importance of southwestern Iberian mining during the Roman era.

Middle Age and Modern Age

After the Roman era, mining activity experienced a sharp decline, although it continued intermittently during the Visigothic and Arab dominations, the Middle Ages, and the Modern Age. According to this, an improvement in the ecosystem quality of the Huelva estuary between the 3rd and 19th centuries has been confirmed through the study of microfossils (Ruiz et al., 2009) and sediment geochemistry (Ruiz et al., 1998; Davis et al., 2000; Romero et al., 2023).

In a well-known report from 1556 by Diego Delgado, commissioned by the Spanish King Felipe II to conduct a mining investigation in the province of Huelva, emissions of acidic leachates from Roman galleries and shafts in the Riotinto area are described. The Tinto River originated from a large cave excavated by the Romans, called Cueva del Lago (Pinedo Vara, 1963):

> 'We also went to see another cave, which was filled with water, and from it, a river flowed, called Río-Tinto, the reason for its origin being the springs of caparrosa, also known as aceche, which is used for ink. Thus, all the banks of this river are full of aceche, especially in the month of August... and with this aceche, they pay certain tributes to the Archbishop of Seville... In this river, no kind of fish or living thing is bred, people do not drink its water, and it is not useful for anything.... It has another property that if iron is thrown into the water, it corrodes in a few days... I took a live frog and threw it into the river, and it died without being able to come out of the water...'

Diego Delgado also describes the waste heaps in the area and numerous traces of ancient mining activity, including the emergence of acidic waters from the Tintillo River (a tributary of the Odiel) in a Roman drain gallery. That is, although pollution levels were lower than in Roman times, after many centuries of mining cease (or very little activity), acidic leachates were still being produced in Riotinto (and also in other mines of the IPB) due to the persistent oxidation processes of sulfides, contaminating the Tinto and Odiel rivers near the most important mines (Olías and Nieto, 2012).

The historian Rodrigo Caro, in his 1634 book 'Antigüedades y Principado de la ilustrísima ciudad de Sevilla y Chorographia de su Convento Jurídico, o antigua Chancillería,' also notes:

> 'The other river very close to this, called Río Tinto or Azige, is born near the village of Río Tinto, from very rough terrain; and from its source, until more than a league and a half where other streams merge with it, it flows the color of azige, or the same color as topaz, solidifying the sands where it passes, turning them into very firm stone; it does not nurture any living thing, but rather kills those thrown into its water, being small, because it burns and consumes even the herbs and trees on its banks, turning everything its color; they give this water to livestock when they have worms, to kill them, and I think that because of these properties, the Romans called it Urium, from the verb Uro, that is, to burn' (p. 89)...
>
> 'It grows much azige on its banks; this nature lasts until, mixing with other rivers and streams, they make it lose its primitive property and nature; so that when it reaches Niebla, its waters already flow like those of other rivers' (p. 206).

According to Rodrigo Caro's description, the river reach where the Tinto River was acidic and had 'topaz' colored waters was limited to a league and a half from its source, not its entire course (100 km) as it is today, so that when it reached Niebla, 'its waters already flow like those of other rivers.'

These documents show that after many centuries of mining paralysis (or very little activity), acidic leachates continued to be produced in Riotinto (and also in other IPB mines) due to the persistence of sulfide oxidation processes.

Contemporary Age

De Prado (1851), based on the recovery of copper from the water flowing from Roman mine shafts, estimated that *'it can be well assured that the Tinto River has carried to the sea since the fall of the Roman Empire at least seventy or eighty thousand tons of this metal.'* Dividing this latter figure by 1450 years (from the end of the Roman period until 1850) yields an annual amount of 55 tons, which, although it may seem high, indicates pollution levels much lower than the 450 tons that the Tinto River currently transports to the Huelva estuary (see section 4.3.2). Additionally, it should be noted that the copper dissolved in the headwaters of the Tinto gradually precipitates along with iron along its course (Cánovas et al., 2007), so that only a minimal part of the estimated amount by De Prado (1851) would likely reach the Huelva estuary (Olías and Nieto, 2012).

In the Statistical-Geographical-Historical Dictionary of Madoz, comprising 16 volumes published between 1845 and 1850, several references to the Tinto River can be found. About the city of Niebla (at the lower part of the basin):

> '...the Tinto River bathes it, from whose waters the residents make use... It passes through the territory of Villarrasa about half league from the population, fertilizing on both banks a portion of farming land... It is abundant in all kinds of shellfish and very exquisite lizard fish. It is saline water up to the ford of La Luz, and good for livestock up to the Cabezo de Salomón, where the high content of vitriol it contains harms the animals.'

That is, as Rodrigo Caro speaks of a river with pollution problems in the mining area, from Cerro Salomón onwards, but in its final stretch, it seems to have good water quality as it is used by the residents of Niebla, located in the lower part of the catchment. It is interesting to note that before Cerro Salomón, where the Tinto River originates in the Cueva del Lago (Fig. 3.15), the water was not contaminated ('good for livestock'). Currently, the origin of the Tinto River is considered in the Peña de Hierro area, about 2 km north of Cerro Salomón (which has completely disappeared due to mining activity). This implies that, due to mining in Peña de Hierro that began in 1850, the reach from this point to Cerro Salomón was contaminated. That is, the birth of the Tinto River has been linked since Roman times to mining activity and has changed depending on the opening of new mines, which caused

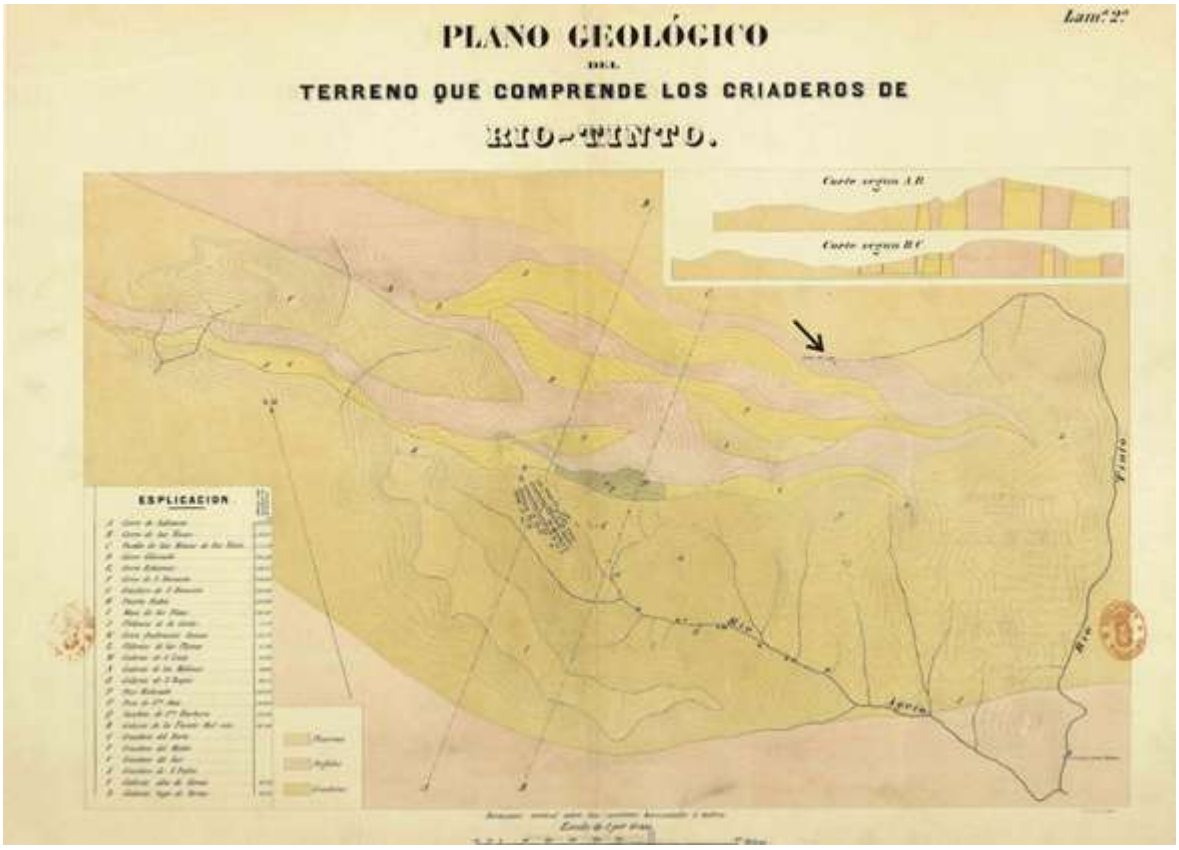

Figure 3.15: Old map of Riotinto mining area (in Spanish) in the mid-19th century (Anciola y Cossio, 1856). The origing of the Tinto River was in the Cueva del Lago (Cave of the Lake), a Roman mine (indicated by the arrow). Upstream this point, the Tinto River water had a good quality. The origin of the Tinto River is currently considered at Peña de Hierro mine, 2 km to the north of Cueva del Lago.

the initiation of acid leachate generation. All this shows that the current conditions of the Tinto River are not natural.

After about 30 years from the mining start of Peña de Hierro, Gonzalo y Tarín (1886) reported:

> "In the origin and upper portion of the river course, its waters and those of its tributaries are pure and crystalline. However, from the moment it receives those coming from the beneficiation of pyritic ores of Ríotinto and Peña de Hierro, they become not only unsuitable for domestic use but, like those of the Odiel, harmful to vegetation, unfit for the life of beings that would otherwise develop in them, and detrimental to the fish and shellfish in the Huelva estuary when, after summer, they carry, in the first floods, the metallic salts that, through evaporation and chemical precipitation, remained in the channel forming excessively ferruginous efflorescences and salts... Light green when these waters, unfortunately tributaries of the Tinto, leave the channels where the copper cementation takes place, they gradually lose this color to acquire that of wine red, corresponding to ferric salts, which they retain in the river as they pass through Niebla. In this place, they have been considered, lately, suitable for beneficial baths."

It is interesting to note that while in the comprehensive work of Madoz (1845-50), it is mentioned that the waters of the Tinto River fertilized the lands of Villarrasa and nearby municipalities, and its waters were used by the locals, Gonzalo y Tarín (1886) state that the Tinto River arrived contaminated in Niebla (wine-red in color) and that its waters began to be used for medicinal baths.

Another argument indicating that the current conditions of the Tinto River are recent is the fish populations in its tributaries. Due to its extremely acidic conditions, the main course of the Tinto River acts as an insuperable longitudinal barrier for fishes (Fig. 3.16). The observed distribution of different fish species in the tributaries of the Tinto River indicates interconnection between sub-basins until very recent times. If there had been a longitudinal barrier from ancient times, as in the current conditions of the Tinto River, the fish fauna in most tributaries should have become extinct due to the small surface area of their basins (Prenda, 2022). This implies that historically, the waters of the Tinto River must have had relatively good physicochemical characteristics to allow the interconnection of fish fauna between tributaries through its main channel (Prenda, 2022).

In relation to the Odiel River, there is also historical evidence regarding the quality of its waters: *'The waters of the Odiel River would be of exquisite quality if it were not for the circumstance that the metallurgical plants of Tharsis, La Zarza, San Telmo, Cueva de la Mora, and others discharge into it'* (Gonzalo y Tarín, 1888). *'The Odiel River is navigable up to Gibraleón, where the high tides reach; it abounds in rich flatfish, and sometimes in spring, sardines are caught as exquisite as those of the Guadalquivir'* (Madoz, 1845-50). Other historical evidence, collected by Gómez Ruiz (2003) in the book 'Molinos del Río Odiel,' speaks of a river with good-quality waters (Fig. 3.17):

> 'It had in other times... waters of exquisite quality... with fishing and... clams in its sandy bottoms.'
>
> 'In the dams of some mills, the ferryman provided his services. It bred freshwater fish that he caught with a net....'

Figure 3.16: The Tinto River acts currently as an insuperable barrier for fishes inhabiting its tributaries, which have good water quality. During floods, the force of the current sweeps some fishes from the high-quality streams into the main course of the Tinto River, where they perish due to the high level of pollution.

All this indicates a significant degradation of the Tinto and Odiel watersheds between 1850 and 1880, which continued afterward and has persisted to the present day. The pollutants transported by both rivers had a major impact on the Huelva estuary, as documented by Gonzalo y Tarín (1888). Another interesting historical document is a survey conducted in 1868 by the Permanent Fishing Commission to inquire about the state of bivalve banks on the Spanish coast (García del Hoyo, 2010). The response from the Navy Commander of Huelva was:

> "The coast used to be very abundant in oysters and other mollusks everywhere, but for some years now, the production has been reduced to the point of nullity, and the causes are unknown, but they may very well derive from the movement and shipping of copper ore, which is done in considerable quantity and contaminates the waters. Such is the opinion of knowledgeable people, confirmed by the fact that production continues on the shores and estuaries of the Piedras River, whose waters are not affected by the ore..."

The disappearance of bivalves in the Huelva estuary was probably due to the pollutant contributions from the Tinto and Odiel rivers, as noted by Gonzalo y Tarín (1888), rather than the shipment of minerals transported by train from the mines. Sediment core records from the Huelva estuary also show a significant increase in pollution levels from mining since the 19th century, much higher than those during the pre-Roman and Roman periods. Starting from around 1960, additional pollutant contributions from the Chemical Industrial Complex further exacerbated the bad conditions of the estuary (e.g., Ruiz et al. 2020; Arroyo et al., 2021).

Figure 3.17: Old mill in the Odiel River at Sotiel. The river water has currently pH values close to 3 the greater part of the year.

In summary, the most significant alteration of the waters in the Tinto and Odiel rivers began in the second half of the 19th century, coinciding with the onset of large-scale and technified exploitation of the IPB deposits. Most sulfide mines opened during this period and began to produce acid leachates. In 1886, the Mojafre stream (a tributary of Olivargas) was already contaminated by the mines of La Zarza, and the Escalada stream was polluted by discharges from the San Miguel mine (Gonzalo y Tarín, 1888). Eleven years later, pollution of the El Villar stream due to discharges from the Castillo del Buitrón mine was also reported (Gómez Ruiz, 2003).

Although there is extensive literature on the problem caused by smelting fumes, references to the degradation of river water during this period are scarce (Olías and Nieto, 2012). This may be due to the strong pressure exerted by powerful mining companies. News of this type is only found in media sympathetic to the 'Anti-smoke League.' As an example of the power of mining companies to silence those who protested against the impacts of mining, a case reported by Ferrero Blanco (1999) is summarized below. A resident of Alosno sued the Tharsis mines for damages caused by acidic waters in the watering holes on his property. Thanks to having two prestigious lawyers, Tharsis Mines was ordered to pay 100,000 *pesetas* (old Spanish currency). After this lawsuit, the two lawyers went on to work for Tharsis Mines. In other words, due to their economic strength, the mines silenced protests, acquiring the services of the best professionals and exerting enormous influence on the social and political life of the region.

Associated with this great intensification of mining from the second half of the 19th century is a significant increase in the content of toxic metals in sediments, not only in the Huelva estuary (Ruiz et al., 1998; Davis et al., 2000; Leblanc et al., 2000), but even in samplings taken along the Atlantic coast and the Gulf of Cádiz. Van Geen et al. (1997) observed a substantial increase in the concentrations of Zn and Cu between 1840 and 1890 in two sediment cores collected near the mouth of the Guadalquivir River. These cores did not show the impact of older mining (pre-Roman and Roman), whose effects were limited to the Huelva estuary due to their lower magnitude.

The process of mining pollution in the Tinto River is even reflected in the verses of Juan Ramón Jiménez, the universal Spanish poet, winner of the Nobel Prize of Literature (1956) in his master piece "Platero and I".

> Chapter XCV THE RIVER
>
> Look, Platero, how they have placed the river among the mines, the evil heart, and step-motherhood. Barely does its red water gather here and there this evening, amid the violet and yellow mud, the setting sun; and almost only small boats can navigate its course.
>
> How impoverished!
>
> Before, the large ships of the winemakers, lutes, schooners, feluccas—El Lobo, La joven Eloísa, San Cayetano, which belonged to my father and was commanded by poor Quintero; La Estrella, from my uncle, commanded by Picón—cast the joyful confusion of their masts—those main masts, wonders for the children!—over the sky of San Juan; or they went to Málaga, to Cádiz, to Gibraltar, sunk under the weight of so much wine cargo... Among them, the boats complicated the waves with their eyes, saints, and names painted in green, blue, white, yellow, carmine... And the fishermen brought sardines, oysters, eels, soles, crabs to the village... The copper from Riotinto has poisoned everything. And luckily, Platero, the poor eat the miserable catch of today with the disgust of the rich... But the felucca, the schooner, the lute, all of them are lost.

3.4 Main Conclusions

The IPB is a metallogenic zone with a massive concentration of sulfide deposits extending from the province of Seville to southern Lisbon (Portugal), covering a large area in the province of Huelva. In this zone, there are scarce carbonate materials capable of neutral-

izing the acid leachates generated by sulfide oxidation. The sulfide deposits have been exploited for about 5000 years, with a much more intense scale of exploitation, and therefore environmental impact, from the second half of the 19th century to the late 20th century. Five periods can be distinguished throughout history (Olías and Nieto, 2012 and 2015):

1. Stage of natural sulfide oxidation and formation of oxidation caps or gossans. This natural process started at least 24 million years ago, occurring on a geological scale, very slowly. Locally, near sulfide deposits, acidic conditions would occur, allowing for a high diversity of eukaryotic organisms to develop in these acidophilic environments. However, the amounts of toxic elements released should have been very small on a basin scale, as shown by the low levels of mining-related metals in the sediments of the Huelva estuary, the Guadiana estuary, and the Gulf of Cádiz.
2. Early mining activities in the third millennium BC (Copper Age) and later in the Bronze Age with the Tartessian civilization, resulting in a slight increase in background metal levels in the sedimentary record.
3. Roman period, characterized by extraordinary mining activity (considering the technology available in this time). In addition to numerous archaeological evidences, the impact of mining is recorded by a peak in concentrations of toxic elements in estuarine sediments.
4. After the Roman era, a period of low mining intensity occurs. However, due to the longevity of acid mine drainage processes, acid leachates continue to be produced in old Roman (or medieval) mines, locally contaminating the Tinto and Odiel rivers. Historical evidence suggests that the Odiel and Tinto rivers had good water quality in their middle and lower reaches. Sedimentary and historical evidence also highlights a good state of the Huelva estuary during this period.
5. With the resurgence of mining from 1850 onwards, the rivers of the IPB were degraded, especially the majority of the Odiel River network and the main course of the Tinto River. Pollution levels increased significantly, reaching a state similar to what they are today. As a result of the large amount of toxic elements reaching the Huelva estuary, pollution occurred in the estuary, and its fishery wealth was lost. An increase in toxic element levels in the sediments of the Gulf of Cádiz is also detected during this stage.

In summary, the current situation of the rivers is primarily due to mining activities since the second half of the 19th century, especially between approximately 1850 and 1880. Natural oxidation processes that produced the gossans are negligible from the point of view of contaminant emission to the water bodies compared to those generated by mining.

Since it is an ancient pollution (more than 150 years in this last phase), there has been a ‘naturalization’ of the process, that is, it has been assumed that the natural state of the rivers is as they are today. This belief has also been fueled by some researchers (e.g., Amils et al., 2014; Gómez Ortiz et al., 2014) who, without any scientifically verifiable basis, have argued for a natural origin for the pollution of the Tinto River. However, as shown by numerous geological and historical evidences presented above, the current pollution of the Tinto and Odiel rivers is clearly associated with the intense mining activity initiated in the mid-19th century. Studies conducted in other sulfide-rich deposit areas also conclude that mining activity, without proper environmental controls, multiplies natural oxidation processes, and therefore contaminant emissions, up to 1000 times (Nordstrom, 2015).

4

POLLUTION IN THE TINTO AND ODIEL RIVER CATCHMENTS

4.1 SPATIAL DISTRIBUTION OF POLLUTION

This section outlines how acid leachates generated in sulfide mines affect the drainage networks of the Tinto and Odiel rivers. While with less intensity, these processes also contaminate other rivers in the IPB:

- Guadiamar: affected by mining activities in Aznalcóllar and, to a lesser extent, in Castillo de las Guardas.
- Rivera Cobica: receives contaminants from Herrerías and Lagunazo mines.
- Rivera del Chanza: constitutes the border between Spain and Portugal in part of its course, with acidic contributions from several small mines on the Spanish side of the IPB and, especially, from the Sao Domingos mine on the Portuguese side (Grande, 2016).

The following describes contamination in the Tinto River basin first and then in the Odiel River basin

4.1.1 Tinto River catchment

Unlike the Odiel, which accumulates acid leachates from a large number of mines scattered throughout its basin, the Tinto River receives acid leachates only from its headwaters, in the so-called Riotinto Mining District, encompassing the 'small' Peña de Hierro mine and the enormous Riotinto mine. Consequently, in the first 10 km from its source, the Tinto River traverses an extensive mining landscape, receiving acid leachates from numerous dumps, galleries, tunnels, tailing dams, smelting residues, and other waste materials (Fig. 4.1).

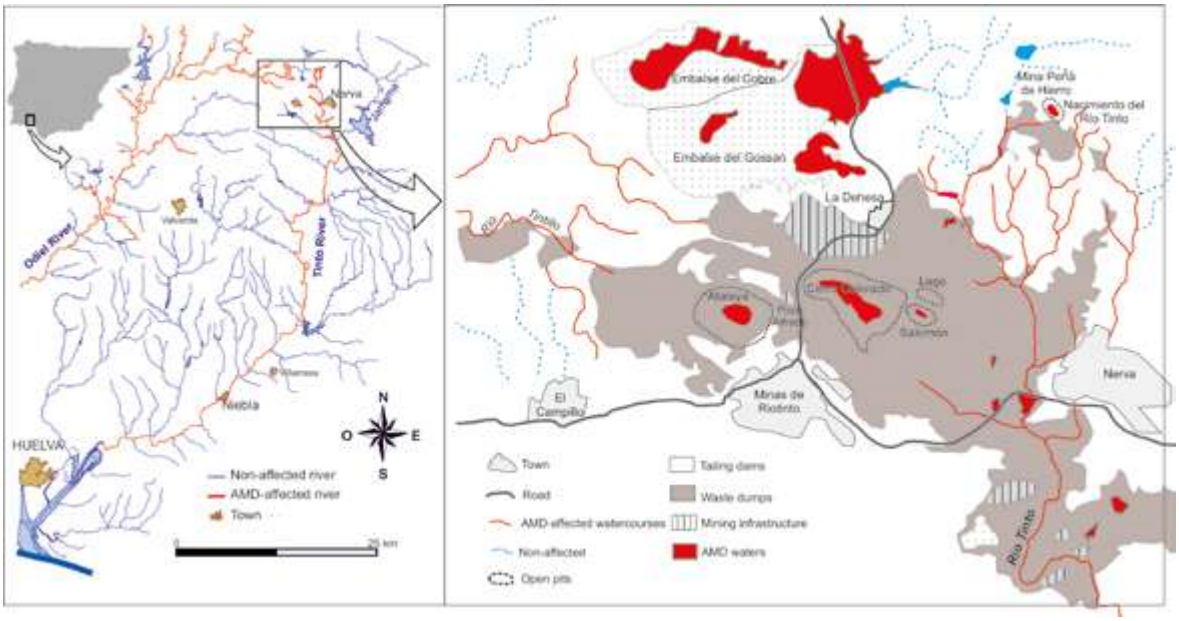

Figure 4.1: Fluvial network of the Tinto River, indicating those watercourses affected by AMD (left) and detail of headwaters area (right).

First, we will discuss the characteristics and significance of the different contributions that the Tinto River receives in the mining area. Subsequently, we will analyze the water quality evolution once it leaves the mining district.

4.1.1.1 Riotinto Mining District

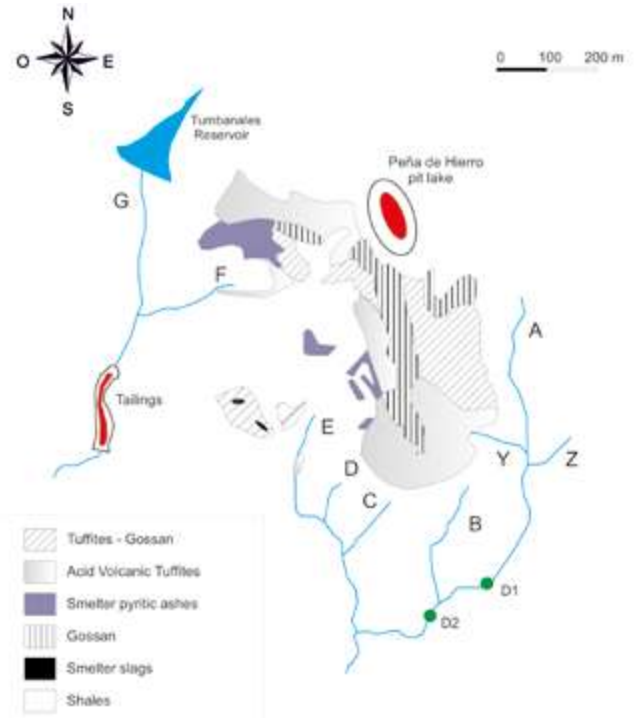

Figure 4.2: Riotinto headwaters, indicating the origin of the Tinto River in the vicinity of Peña de Hierro mine (modified from Romero et al., 2003).

The source of the Tinto River is presently considered to be located in the vicinity of the Peña de Hierro mining complex, where at the base of a waste pile containing large sulfide blocks a small continuous flow of AMD originates (stream Y; Figs. 4.2 and 4.3). These drainage waters have an average pH value close to 2.5 and very high dissolved concentrations of metals and sulfates, with approximately 8000 mg/L of sulfates, nearly 1000 mg/L of iron, and many other toxic elements (Hubbard, 2007), occasionally reaching levels exceeding 15000 mg/L of iron (Allman et al., 2021).

Subsequently, other small streams coming from waste piles and mining residues join the river, altering its pH, coloration and element concentrations. Among them, a stream that collects a natural emergence of acidic waters not associated with mining residues is observed (Figure 4.4). This stream has much less extreme conditions, with a pH value around 5 and iron concentrations usually below 100 mg/L.

Figure 4.3: Right: Photo of what is currently considered the origin of the Tinto River, at the base of a waste pile from the Peña del Hierro mine (stream Y in Figure 4.2). On the right side, the plaque indicating the source of the Tinto River can be seen. Left: Detail of sulfide blocks exposed to oxidation.

As a result of all the acidic inputs, at point D1 (Figure 4.2), the Tinto River has a pH close to 2 and concentrations of 1941 mg/L of Al, 10275 mg/L of Fe, and 40950 mg/L of sulfate (Cánovas, 2008). Due to dilution caused by stream B (Figure 4.2) and the precipitation of Fe mineral phases, there is a slight increase in pH (up to 2.1) and a decrease in metal and sulfate concentrations at point D2 (386 mg/L of Al, 1292 mg/L of Fe, and 7830 mg/L of sulfates).

About 3 km from its source, the G stream (Figure 4.2) converges with a pH value of 2.1 and a moderate content of metals and sulfate (335 mg/L of Fe and 33 mg/L of Al; Hubbard, 2007). The concentration of metals and sulfate in this stream decreases significantly during the wet season due to the input of non-AMD-affected waters (pH 6.7 and 37 mg/L of sulfate) from the Tumbanales Reservoir (Figure 4.2).

Downstream from the Peña de Hierro mining complex, numerous small leachates from dumps and other wastes from the Riotinto mines converge, reaching the vicinity of the Marismillas Reservoir (Figure 4.5). This reservoir was built to supply water to the Riotinto mine but is currently filled with mining wastes (Valente et al., 2015). Downstream, leachates from Tunnel 11 (Figure 4.6), built during the early years of English exploitation to transport ore from Filón Sur, near Cerro Colorado (Figure 4.7), to the Zarandas Naya area, join the Tinto River.

Figure 4.4: Photo of a natural emergence of acidic waters in the same area as the origin of the Tinto River (stream Z in Figure 4.2). Although it apparently has similar characteristics, the Fe concentration is more than 1000 times lower than at the origin of the Tinto River, where the exposure of sulfides to atmospheric conditions significantly enhances oxidation processes.

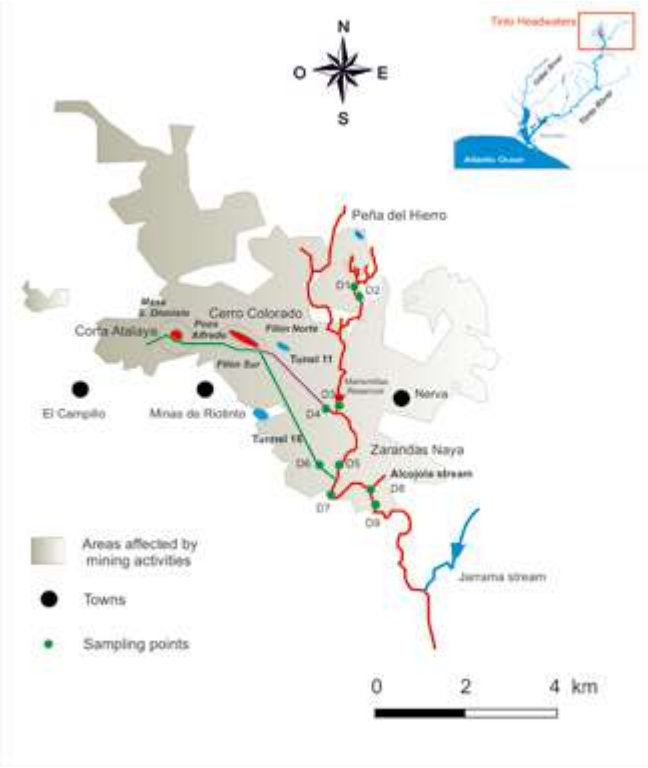

Figure 4.5: Tinto River crossing the mining area. In red the watercourses affected by AMD, in blue those unaffected (modified from Hubbard, 2007).

Figure 4.6: Photo of algae and stromatolitic structures from AMD inputs of Tunnel 11.

Figure 4.7: Cerro Colorado open pit flooded in October 2015 (above) and in October 2017 after dewatering to reopen the mine (below).

Despite the contributions of Tunnel 11, the Tinto River has a lower content of metals and sulfate at point D4 (Fig. 4.5) than at D3 (Cánovas, 2008), although there is a slight increase in the concentration of some elements, such as arsenic. After the Marismillas Reservoir, formerly used for ore washing, the Tinto receives wastewaters from the towns of Nerva and Riotinto, causing a considerable decrease in electrical conductivity and metal concentration and an increase in pH (point D5).

About 7 km from the source of the Tinto River is located the Zarandas-Naya area, where ore from Corta Atalaya and Pozo Alfredo, transported through Tunnel 16, was formerly processed by smelting, leaching and natural cementation. The leachates from Tunnel 16 (Figure 4.8) had a relatively moderate concentration of metals and sulfate; however, it was one of the major sources of AMD to the Tinto River due to its large flow (Buckby, 2003). Nevertheless, the flow and contaminant concentration at this point have undergone significant changes over time based on mining activities (Hubbard, 2007). Currently, it remains dry due to maintenance work carried out in the current mining operation which reopened in 2015 (Fig. 4.7).

One kilometer downstream from the confluence with Tunnel 16, at 8.2 km from the source, the Tinto River receives several AMD inputs from the Zarandas-Naya area (Figure 4.9), where a mineral treatment plant was located, including crushing, flotation, and cementation, as well as a railway station for ore loading. Among the contaminant inputs, the most significant is Alcojola Creek (point D8), which has high acidity (pH 1.6) and an extremely high concentration of Fe (12 g/L), sulfate (31 g/L), As (42 mg/L), and other elements (Cánovas, 2008). The flow of Alcojola Creek represents between 3% and 15% of the Tinto River flow in the mining area but contributes more than 25% of Fe, As, Cr, and Pb (Hubbard, 2007).

Figure 4.8: AMD outflows from Tunnel 16 towards the Tinto River.

Figure 4.9: Left: Tinto River in the Zarandas-Naya area, where mineral processing was formerly carried out, and trains were loaded to transport it to the port of Huelva. In this area, there are a large number of abandoned sulfide-rich residues that produce highly contaminating leachates. Right: Detail of acid leachates along with a large amount of evaporitic salts precipitated during summer.

4.1.1.2 Donwstream of mining area

After the Zarandas-Naya area, the Tinto River no longer receives acid leachates and its flow increases as various freshwater tributaries join it (Fig. 4.10). Figures 4.11 and 4.13 present some of the results obtained in 4 samplings carried out along the river under different hydrological conditions in 2005 and 2006 (Cánovas, 2008). The concentration of different elements shows a downward trend along the river, except for Pb, which behaves differently and remains approximately constant or even increases in June 2006. This general decrease in pollution levels is mainly due to dilution processes, because of contributions from streams not affected by AMD, among which the Jarrama and the Corumbel rivers stand out (both regulated by reservoirs). Thus, due to the increased flow, the concentration of Al, Co, Cu, Mn, and sulfate decreases by approximately 90% from the mining area to Niebla, although the amount transported by the river is the same. However, this figure is subject to seasonal variations (Cánovas, 2008).

Likewise, it is observed that once the Tinto River leaves the Mining District, electrical conductivity progressively decreases due to the reduction of dissolved ions. However, the pH value barely varies and remains between 2.3 and 2.8 in all four samplings, as it is buffered by the precipitation of ferric iron. For this same reason, the concentration of dissolved iron decreases more sharply than the rest of the elements. Similarly, Cr and, especially, As also decrease more strongly due to the intense precipitation of ferric iron in the form of oxyhydroxysulfates (Fig. 4.12). When these minerals precipitate, adsorption/coprecipitation processes occur, which particularly affect As, as it can replace sulfate in the structure of schwertmannite (Acero et al., 2006; Regenspurg and Peiffer, 2004). Thus, the values of As in Niebla are much lower (generally less than 3%) than those observed in the mining area.

Lead (Pb) behaves differently from the other elements as it also precipitates along with Fe but in jarositic phases (Acero et al., 2006; Cánovas et al., 2010). Additionally, the hydro-

Figure 4.10: Tinto River at the middle reach, downstream of Salomon Tunnel.

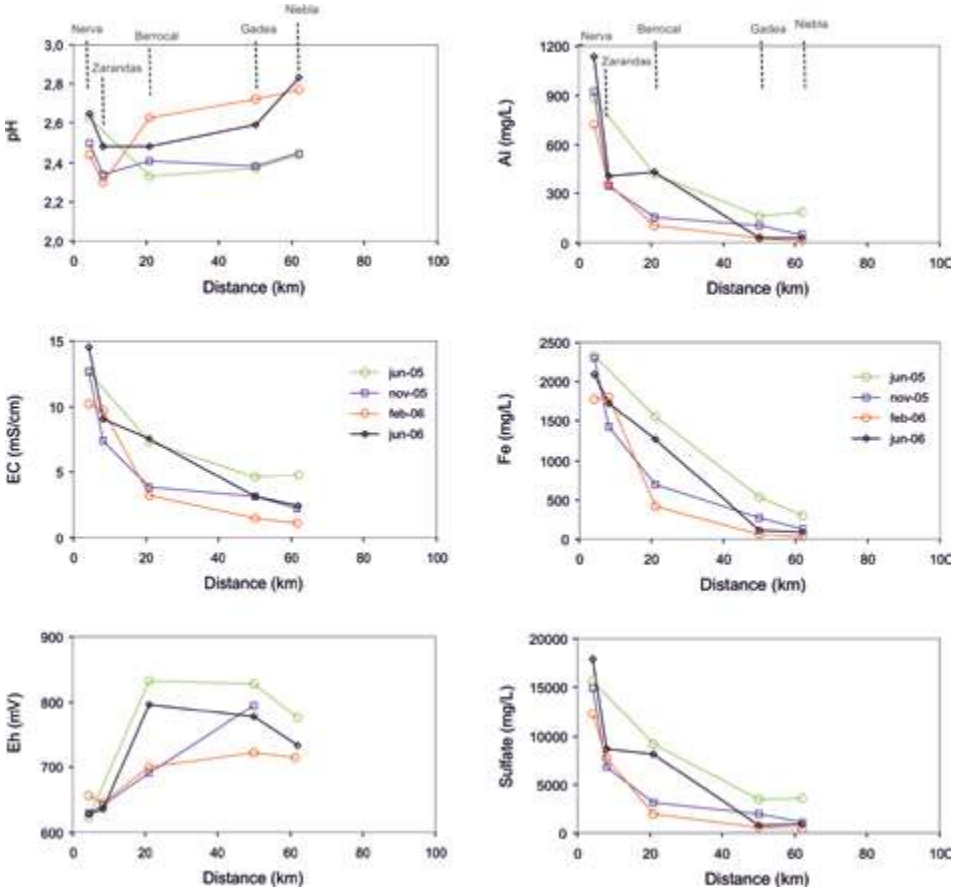

Figure 4.11: Evolution of pH, electrical conductivity (EC), redox potential (Eh) and concentration of sulfate, Al, and Fe in different points along the Tinto River.

Figure 4.12: Photo of the Tinto River at Niebla (lower reach of the river).

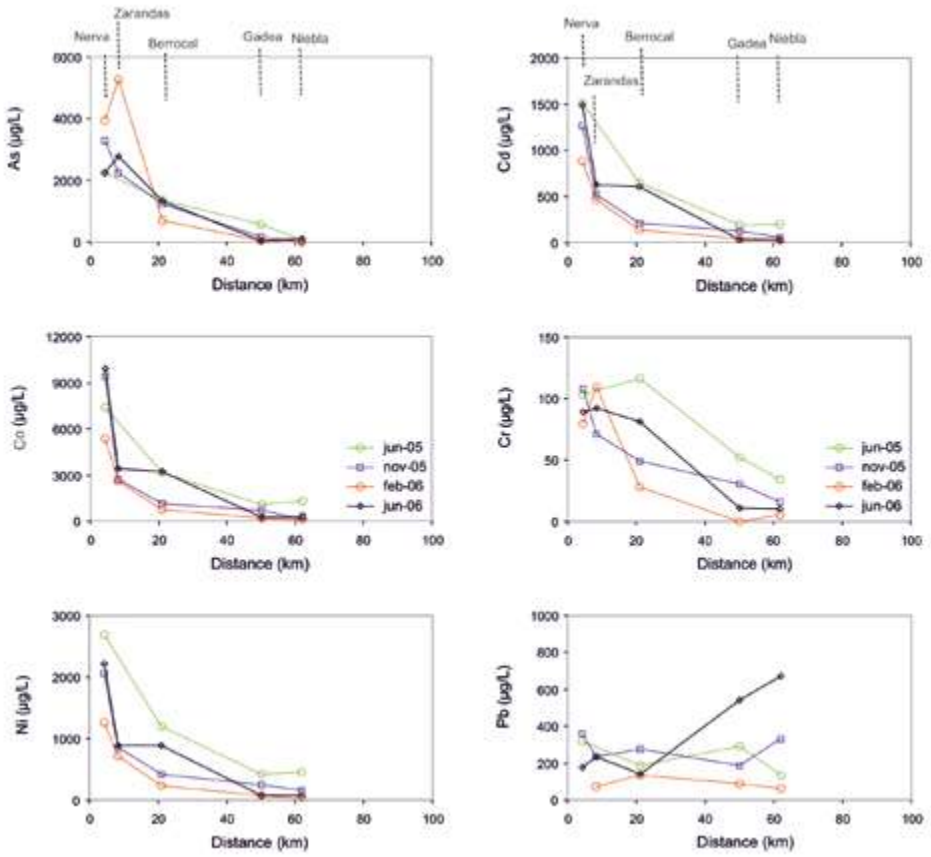

Figure 4.13: Evolution of the concentration of some trace elements along the Tinto River.

chemical behavior of Pb is more complex because its solubility in acidic waters can also be conditioned by the precipitation of anglesite; this aspect is discussed in section 4.2.1.

In summary, along its course, the Tinto River flow increases due to the incorporation of various freshwater tributaries, causing the concentration of pollutants to decrease through dilution. Thus, in Niebla (Fig. 4.13), concentrations of sulfate, Cu, Zn, and other elements are approximately 90% lower than those in the mining area. However, the total amount of these elements transported by the river remains approximately constant throughout its course. The concentration of Fe decreases more intensely due to the precipitation of this element in the form of oxyhydroxysulfates, which buffers the pH, so this parameter barely varies. Along with Fe, other elements such as Cr and, especially, As also coprecipitate.

4.1.2 Odiel River catchment

Unlike the Tinto River, where pollution is limited to the main course with extreme values from its origin in Peña del Hierro to its mouth in the Huelva estuary, the Odiel River presents a wide variety of conditions in its different sections, from levels of extreme pollution to areas with apparent good quality and low concentrations of toxic elements (Sarmiento, 2007). Obviously, a river reach with water with more than 1000 mg/L of Fe cannot be considered the same as another with less than 1 mg/L. Therefore, the following contamination levels have been differentiated (Olías et al., 2018):

- Slight affection, when pH values remain above 6 throughout the year, and concentrations of toxic metals are very low, although there are more mobile elements (mainly

Cd and Zn) at neutral pH conditions whose concentrations exceed the values of RD 817/2015 (Criteria for monitoring and assessing the state of surface waters and environmental quality standards).

- Moderate affection, when pH values are generally above 5 (in winter), and dissolved contaminant concentrations are low (less than 1 mg/L of Fe and Al), but clearly higher than values in unaffected rivers. During the dry season, pH is usually lower, and concentrations of Fe and Al can exceed 1 mg/L.
- High affection, when pH values are usually below 5 in winter, but with relatively low concentrations of dissolved contaminants (less than 10 mg/L of Fe and Al). During the dry season, pH values can be lower, and contaminant concentrations higher.
- Very high affection, pH values remain below 4 (with exceptions of short duration during periods of heavy floods), and concentrations of Fe and Al and other toxic elements are usually below 100 mg/L.
- Extreme affection, when pH values remain below 3 throughout the year, and concentrations of toxic elements are very high, with Fe and/or Al values exceeding 100 mg/L (with exceptions of short events during periods of heavy floods).

To show how AMD spatially affects the Odiel River, the area has been divided into three parts corresponding to the most important sub-basins: 1) the Odiel River sub-basin (up to its confluence with the Oraque), 2) the Oraque River sub-basin, and 3) the Meca River sub-basin. Subsequently, the state of the Odiel, along with the Tinto, before its mouth in the Huelva estuary is discussed in section 4.1.3.

4.1.2.1 Odiel sub-catchment

The Odiel River in its initial reaches in the Sierra of Aracena drains materials formed by plutonic and metamorphic rocks from the Ossa Morena region, where some lithologies of carbonate nature outcrop. Therefore, these are slightly alkaline waters with a very low concentration of toxic metals (Table 4.1). These conditions are maintained until receiving the first AMD inputs from Concepción mine (Figs. 4.14 and 4.15).

The first AMD input to the Odiel River, from the Concepcion Mine, is located 30 km downstream of its source (Fig. 4.16). These leachates have an average flow rate of about 17 L/s, although with highly variable values due to mixing with surface runoff. The pollutant contributions from this mine have decreased since the operation of a passive treatment plant based on the DAS technology in April 2016 (see section 7.3). However, there are still acid leachates emerging downstream from the treatment plant, continuing to contribute acidity and metals to the Odiel. After this initial contribution, several diffuse acid discharges also occur from areas affected by mining that are directly in contact with the course of the Odiel (Fig. 4.17).

Inmediately downstream of Concepción Mine, the Odiel receives the pollutant contributions from San Platón Mine (Fig. 4.17). There is a continuous discharge with high concentrations of toxic metals and low flow during summer (approximately 0.2 L/s), which increases significantly during rainy periods without a decrease in pollutant concentrations.

About 800 m downstream of San Platón, a small stream from the Esperanza Mine joins the Odiel. This mine has a continuous discharge from an old gallery with a flow rate of around 1 L/s, along with small diffuse contributions (Sarmiento, 2007). In December 2014, a passive treatment plant based on DAS technology was built to treat the leachates from this gallery. Currently, this plant requires maintenance (see section 7.3).

The next pollutant contribution to the Odiel is the confluence of the Palomino stream, located about 700 m downstream (Fig. 4.17). This stream carries leachates from the El Soldado and Poderosa mines, with the latter having much higher pollutant potential. The flow rates of this stream vary widely, from less than 1 L/s in summer to over 500 L/s during

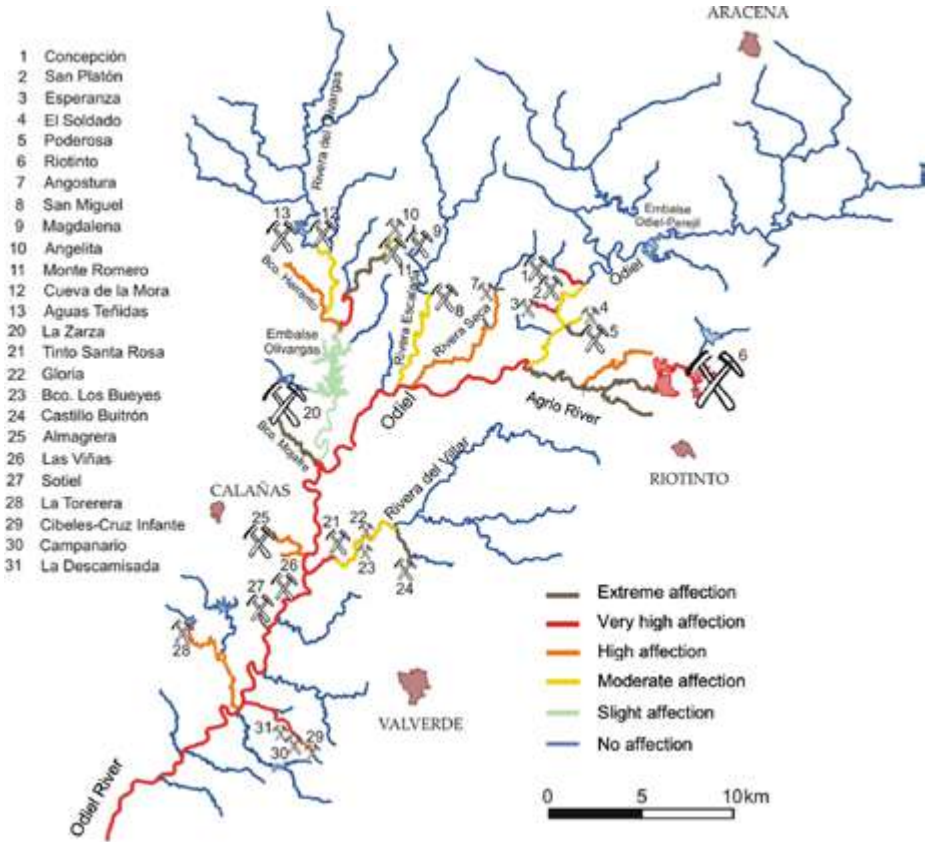

Figure 4.14: Main mines and levels of AMD pollution along the Odiel sub-basin.

Figure 4.15: Odiel River upstream of Concepción Mine.

Figure 4.16: Odiel River at the confluence of AMD from Concepción Mine. Note the vegetation disappearance from the river margins downstream the confluence.

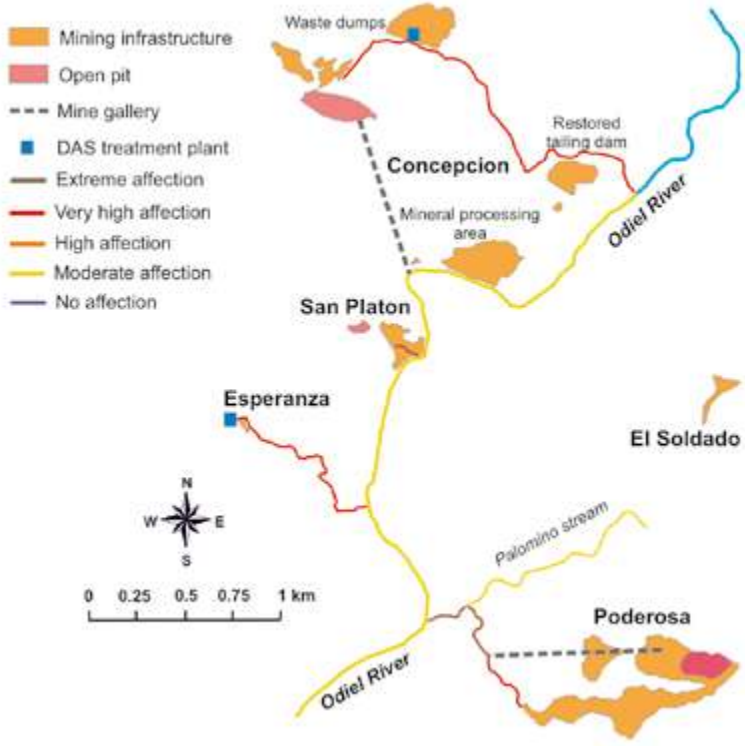

Figure 4.17: Location map of the Odiel River crossing the area of mines of Concepción, San Platón, Esperanza, El Soldado and Poderosa.

periods of heavy rainfall, although under these conditions, concentrations decrease significantly due to dilution processes. The most important source of pollution in this area is the main gallery of the Poderosa Mine (Fig. 4.18).

Despite the contributions from the aforementioned mines, under high flow conditions, the Odiel River continues to have pH values close to 7 and low levels of metals (Table 4.1). This is due to its higher flow compared to acid discharges and its neutralization capacity, with relatively high concentrations of bicarbonates. As a result, in areas where AMD mix with the alkaline waters of the Odiel, there is intense precipitation of Fe and Al, along with the coprecipitation of other toxic elements, generating high suspended particle contents that settle in areas of lower water velocity. Bicarbonates are consumed in this process, and their concentration decreases as the river receives various AMDs, while sulfate concentrations increase (Table 4.1). During low-flow periods, when extractions from the Odiel-Perejil reservoir, located upstream, cause the river flow to decrease sharply or even become completely dry before the confluence with the Concepción mine leachates, there are acidic pH values and high concentrations of toxic metals. This is because practically all the water carried by the river comes from mining contributions (Fig. 4.19 right).

Figure 4.18: Greenish AMD outflowing from the galleries of Poderosa mine, with high concentration of pollutants.

The conditions of the Odiel River change drastically after its confluence with the Agrio River (also known as Tintillo River), originating from the Riotinto mines (Fig. 4.20 and Table 4.1). This watercourse has high flows and concentrations of contaminants, contributing approximately 50% of the mining-related contaminants that the Odiel receives (Galván et al., 2016). At the confluence between the Agrio and the Odiel, there is a progressive change in pH, from typically near-neutral values of around 7 in the Odiel to values close to 2.5 of Agrio, creating a banding effect with whitish colors in the zone with pH around 5 due to aluminum precipitation and yellow-reddish colors due to iron precipitation where pH values are around 3 (Fig. 4.21).

After the confluence with the Agrio River, contaminant concentrations in the Odiel increase dramatically, accompanied by a notable decrease in pH (Fig. 4.22; Table 4.1). This is because the acidity input is much higher than the neutralization capacity of the Odiel, which is further reduced by the initial mining contributions. Despite the contaminant concentrations in the main course of the Odiel decrease slightly dowstream, these poor conditions persist until its mouth at the Huelva Estuary.

Downtream, the Odiel River receives contributions from the Rivera Seca and Rivera Escalada streams (Fig. 4.14). The Rivera Seca stream experiences a high level of impact after receiving AMD from the Angostura mine, with pH values usually close to 5 and concentrations of Fe, Al, and other toxic metals typically lower than a few mg/L. The Rivera Escalada stream is affected by the San Miguel mine, but due to its larger flow, contaminant concentrations are lower, typically reaching pH values close to 7 before its confluence with the Odiel.

Moving downstream, the Rivera del Olivargas stream receives small diffuse acid contributions generated in the Cueva de la Mora mine (Galván, 2011), which discharge into the Olivargas Reservoir. Other streams affected by AMD also join the reservoir, with the most significant acid discharge coming from the Monte Romero mine (Fig. 4.14), characterized

Figure 4.19: Odiel River in the section between San Platón and Poderosa mines during different periods of the year. The colors reflect different levels of contamination, with the most extreme values (right) corresponding to summer when the river flow decreases, and acidic contributions persist. Lower concentrations of contaminants occur during periods of higher flows (left).

		Upstream Concepción	Upstream Agrio	Downstream Agrio
pH		8.36	6.71	3.30
EC	mS/cm	0.28	0.34	1.93
Al	mg/L	< bdl	0.07	99
Cu	mg/L	< bdl	0.07	10
Fe	mg/L	< bdl	0.44	15
Mn	mg/L	0.02	0.28	15
Zn	mg/L	0.02	0.39	18
SO_4	mg/L	13	79	1305
HCO_3	mg/L	112	53	0
As	µg/L	3.2	1.6	4.1
Cd	µg/L	< bdl	8.4	90
Ni	µg/L	< bdl	3.5	245
Pb	µg/L	< bdl	29	6

Table 4.1: Median values of pH, electrical conductivity (EC) and dissolved concentrations of some elements in different points of the Odiel River upper reach: 1) Before receiving the Concepción Mine effluents, 2) Before the confluence with Agrio River, after receiving the AMD inputs from Concepción, San Platón, Esperanza, El Soldado and Poderosa and 3) downstream of the confluence with the Agrio River. (< bdl: below detection limit; Cánovas et al., 2018a).

Figure 4.20: Photo of the Agrio River (also known as Tintillo) coming from Riotinto mines. This leachates constitute the most important pollutant load in the whole Odiel catchment.

by high concentrations of Zn and Cd, among other toxic elements. Previously, this stream is slightly affected by the acid discharge from the Angelita mine, which is of minor importance. Finally, the facilities of the old Aguas Teñidas mine also contribute to the pollution of the Herrerito stream (Fig. 4.14).

All these contributions join the Olivargas Reservoir, but because the flows of the acid drainage are small compared to the total flows generated in its basin, this reservoir has pH values close to 7 (Jofre-Meléndez et al., 2017; Galván et al., 2021; see chapter 5). In these conditions, most toxic metals precipitate and settle in the sediment. However, dissolved concentrations of Mn and Zn, which are more mobile under neutral pH conditions, are slightly elevated, typically ranging between 0.1 and 0.5 mg/L (Sarmiento et al., 2009a). The concentrations of Cd, established by regulations on the state of surface water quality (RD 817/2015), are frequently exceeded.

Downstream of the reservoir, just before the confluence of the Olivargas River with the Odiel, the Mojafre stream joins, carrying a significant flow of AMD with high concentrations of contaminants from La Zarza mines (Fig.

Figure 4.21: Photo of the different color bands formed due to pH changes and subsequent precipitation of Fe (orange/reddish band) and Al (withish band) in the confluence of the Odiel and Agrio rivers.

Figure 4.22: Odiel River in the crossing with road N-435, downstream the confluence with rhe Agrio River, during the dry season.

4.23). These contributions cause significant impairment in the final stretch of the Olivargas tributary and subsequently worsen the conditions of the Odiel River.

The next acidic contributions to the Odiel River come from the Almagrera mine through the Batán stream (Fig. 4.14). These inputs are of minor importance due to the treatment and restoration actions being carried out in this area by the Andalusian Regional Government.

Very close to the previous point, the Odiel joins the Rivera del Villar stream, one of its main tributaries on the left bank. This course receives acidic inputs from the Castillo de Buitrón mine in its middle reach. However, due to its neutralization capacity, the impact on the Villar tributary in this zone is moderate (Fig. 4.14). Downstream, the tributary receives AMD from the Gloria and Barranco de los Bueyes mines, also causing no severe impact due to their minor importance. The confluence of the AMD from the Tinto Santa Rosa mine does, however, cause a significant impact in the final reach of the Rivera del Villar stream (Fig. 4.24).

About 2.5 km downstream of the confluence of the Villar stream, the Odiel flows alongside the areas affected by the cementation zone of Las Viñas, from which several acid discharges originated. However, this zone has recently been restored by the Andalusian Regional Government. Following the course of the Odiel, the leachates from the small-scale cementation area of Turmio join the river, along with those from the more significant Sotiel mine, carried through a small stream that crosses this town. After this discharge, the Odiel River exhibits pH values close to 2.9 most of the year, with concentrations of Fe, Al, and other toxic metals below 50 mg/L (Fig. 4.25 and Table 4.2). Subsequently, acidic contributions from the Torerera mine join on the right bank through the Galaperosa stream, and on the left

bank, those from the Descamisada, Cibeles/Cruz Infante, and Campanario mines, but they do not cause a significant change in the conditions of the Odiel River.

		Odiel at Sotiel	Oraque downstream Aguas Agrias	Meca upstream Sancho
pH		3.30	3.01	3.04
EC	mS/cm	1.44	1.28	1.48
Cu	mg/L	6.3	2.9	5.1
Fe	mg/L	6.7	14.6	13.0
Mn	mg/L	11.4	5.2	7.1
Zn	mg/L	14.0	11.7	12.0
SO_4	mg/L	879	571	645
As	µg/L	5	5	<1
Cd	µg/L	60	31	27
Pb	µg/L	43	23	17

Table 4.2: Median values of pH, electrical conductivity (EC) and dissolved concentrations of some elements in several points along the Odiel catchment (period 2002/2017). The concentration of Al is not shown, despite its importance in AMD processes, due to the scarce number of analisis available.

Figure 4.23: Mojafre stream during the dry season with abundance of evaporitic soluble salts in its margin and riverbed. This stream collects AMDs from La Zarza mine and constitute an important contribution of pollutants to the Odiel River.

Figure 4.24: Impact of the leachates from the Tinto Santa Rosa mine on the Villar stream, which flows from the upper left to the lower right part in the photo. It is observed how the conditions change completely, and the vegetation in the margins disappears.

Figure 4.25: Odiel River at the old bridge of Sotiel.

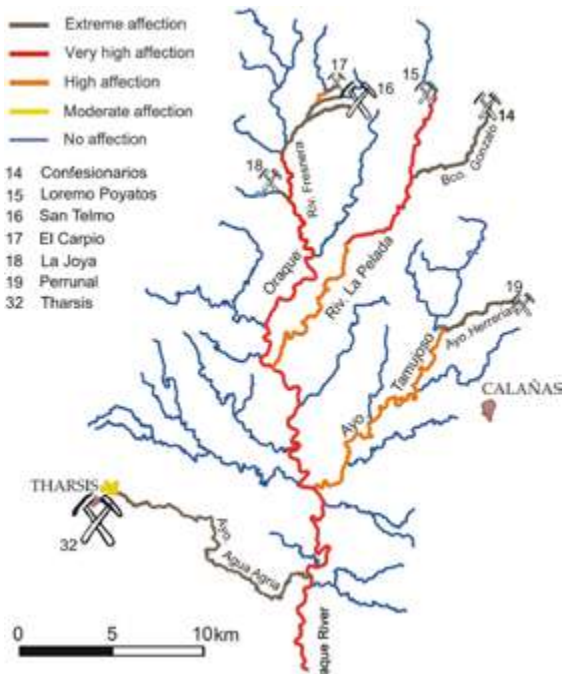

Figure 4.26: Main mines and level of AMD-pollution in the Oraque sub-basin.

4.1.2.2 Oraque sub-catchment

The Oraque River, with a basin covering 612 km^2, is the largest tributary of the Odiel River. La Joya, El Carpio, and San Telmo mines, located in headwaters, impact the Fresnera stream, while Lomero Poyatos and Confesionarios mines discharge towards La Pelada stream (Fig. 4.26). Concerning the Fresnera stream, it receives a small acidic contribution from El Carpio mine, causing a moderate impact. However, approximately 2 km downstream, it combines with the leachates from the San Telmo mine (Fig. 4.27), resulting in a significant degradation of the watercourse. Just downstream, this watercourse receives AMD from La Joya mine, which cause lower impacts than those from San Telmo.

To the east, La Pelada stream maintains a good water quality status until passing by the Lomero Poyatos mine, undergoing a noticeable impact when receiving AMD generated by these facilities (Fig. 4.28). This course also receives downstream significant AMD inputs from Confesionario mine, through the Gonzalo stream (Fig. 4.26).

Figure 4.27: Sulfide dumps in San Telmo Mine; the extreme soil conditions prevent the growth of any plants. In the background, the San Telmo pit lake can be seen.

Figure 4.28: Pollution in La Pelada stream after receiving AMD from the Lomero Poyatos mine.

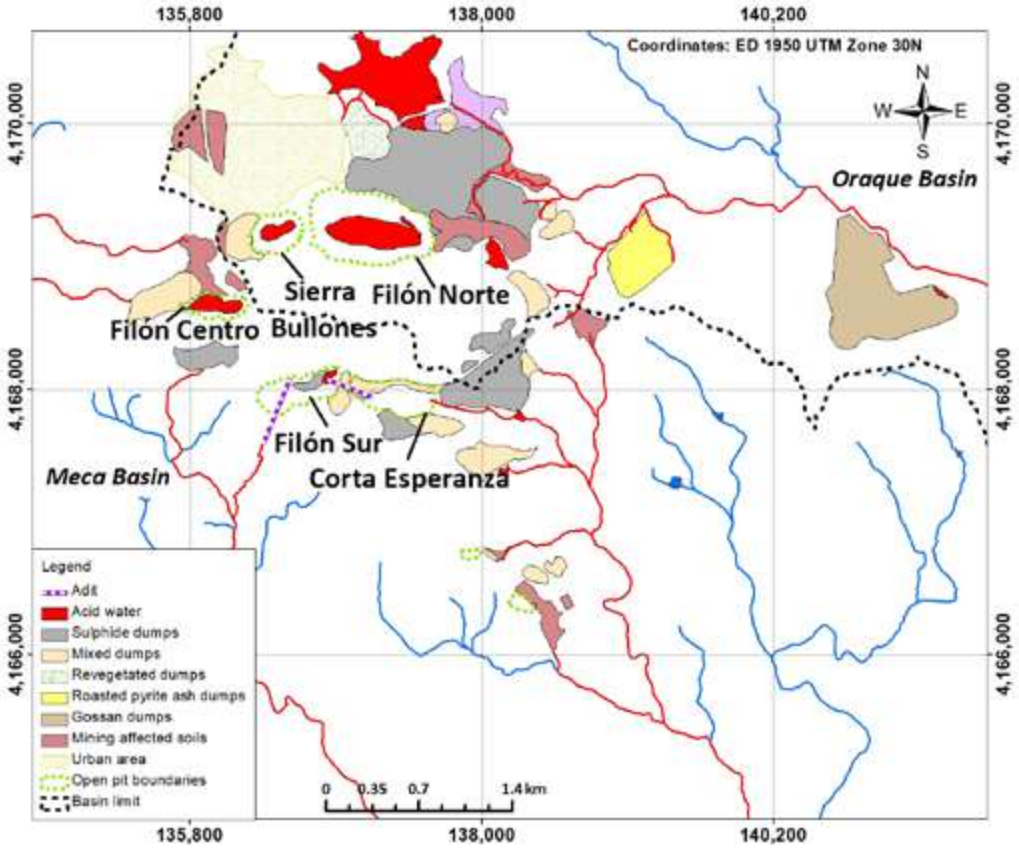

Figure 4.29: Map showing the affected áreas by effluents delivered from Tharsis mine, located between the Oraque sub-catchment (north) and Meca sub-catchment (south), impacting seriously both rivers.

Figure 4.30: Aguas Agrias stream nearby cianide leaching heaps (Tharsis mine).

Figure 4.31: Melanterite crystals in Tharsis Mine. The leachate originated from this dump reach the most extreme conditions in the whole IPB, with pH values close to 0.

In its middle section, the Oraque receives pollutant inputs from the Perrunal mine, causing a moderate impact on the Tamujoso stream. Due to the confluence of this stream and others unaffected by AMD, the water quality of the Oraque slightly improves in its middle reach. However, near its final section, it receives highly contaminating AMD from Aguas Agrias stream (Figs. 4.29 and 4.30), originating from the Tharsis mines, leading to a new increase in toxic metal concentrations. In the part of the Tharsis mines that discharge into the Oraque, the leachates exhibit the most extreme conditions in the entire IPB, with pH values

close to zero, electrical conductivity of up to 76 mS/cm, and dissolved concentrations of 408 g/L of sulfate, 194 g/L of Fe, etc. (Fig. 4.31; Moreno González et al., 2020).

In this way, the Oraque River in its final reach typically exhibits pH values close to 3 and concentrations of Fe, Zn, and other toxic elements near 5 mg/L (Table 4.2), while Al reaches values around 20 mg/L. In summary, the main course of the Oraque River is profoundly affected by AMD, particularly due to San Telmo mines in its headwaters area and the Tharsis mines in its lower reach.

4.1.2.3 Meca sub-catchment

The Meca River, with a basin covering 317 km^2, is regulated by the Sancho reservoir (58 hm^3; Fig. 4.32), the largest currently existing in the Odiel basin. The water quality of the Meca River is primarily affected by AMD from Filón Centro, Filón Sur, and Corta Esperanza areas, all belonging to the Tharsis mines (Fig. 4.29). The major pollutant contributions come from the Corta Esperanza area, where large sulfide-rich dumps exist. These leachates are transported through the San Agustín stream (Fig. 4.33), where contaminant contributions from other small mines also join the river.

Additionally, the Valdeoscuro stream receives acidic waters from a huge dump at Filón Centro, the La Sabina gallery (Fig. 4.34), and the Vulcano mine (the latter being of lesser importance). Finally, the Dehesa Boyal stream is also contaminated, albeit to a lesser extent, by leachates generated in the Filón Centro area (Fig. 4.31; Sarmiento, 2007; 2009b, and Moreno González et al., 2020).

Concentrations decrease slightly towards the south as the streams move away from the mining area due to the precipitation of iron minerals, coprecipitation processes, and dilution caused by mixing with uncontaminated streams. However, pollution levels in the Meca River before its entry into the Sancho reservoir remain high, with median concentrations of over 10 mg/L of Fe and Zn (Table 4.2). The conditions are similar to those in the Odiel at Sotiel

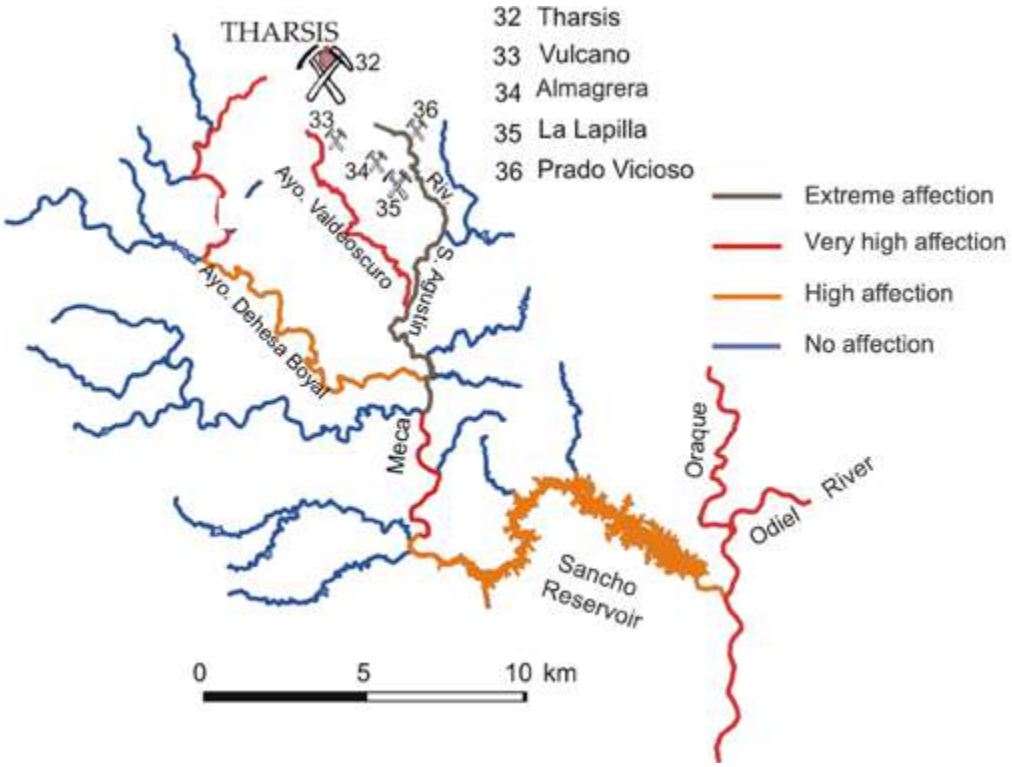

Figure 4.32: Distribution of AMD pollution in the Meca sub-basin.

Figure 4.33: Photo of San Agustín stream, main AMD contributor to the Meca River, with sulfide dumps of Filón Sur and Corta Esperanza in the background.

Figure 4.34: Greenish acidic leachates outflowing from La Sabina gallery (Tharsis mine), which are collected by the Valdeoscuro stream.

and the Oraque after the Agrio River, categorizing the main courses of the Odiel, Oraque, and Meca as having a 'very high' AMD affection.

The contaminants transported by the Meca reach the Sancho Reservoir, where acidity is partially neutralized by the flows from unaffected streams, along with dilution processes occurring during floods. As a result, precipitation and coprecipitation/adsorption processes of dissolved metals take place in the reservoir (Sarmiento et al., 2009a; Torres et al., 2016). However, elevated levels of contaminants persist in the reservoir (see Chapter 5).

4.1.3 Concentrations before the Ría de Huelva estuary

Table 4.3 shows a statistical summary of the values obtained in the official quality control network of the Tinto River at Niebla between 1968 and 2022 (graphs showing the evolution are provided in Section 4.2.2). The Tinto River at Niebla has an average pH value of 2.6, with values below 3.0 (90^{th} percentile) most of the year. This value is only exceeded during major floods (the highest recorded pH is 6.7). The water exhibits high electrical conductivity (mean of 3.4 mS/cm), sulfate (mean of 2730 mg/L), and dissolved metals and metalloids (334 mg/L of Fe, 119 mg/L of Zn, 797 µg/L of As, etc.). It is worth noting that aluminum concentrations, which are also very high and contribute to the net acidity of the water, are not measured in the official network.

		Mean	Median	Minimum	Maximum	Percentile 10	Percentile 90
pH		2.62	2.50	1.70	6.70	2.30	3.0
EC	mS/cm	3.4	2.95	0.21	12.2	1.12	6.1
Cu	mg/L	24.4	18.5	0.02	296	5.2	48.9
Fe	mg/L	334	220	0.02	4668	23.7	804
Mn	mg/L	12.8	9.1	0.09	110	2.3	26.9
SO_4	mg/L	2730	1948	85	20091	466	6316
Zn	mg/L	53.4	29.3	0.02	730	6.4	119
As	µg/L	797	81	<ld	11710	3.0	2580
Cd	µg/L	212	120	<ld	2020	30	530
Pb	µg/L	171	98	<ld	2200	44	331

Table 4.3: Statistical summary of pH, electrical conductivity and dissolved concentrations of some elements in the Tinto River at Niebla (Official Quality Control Network, 1968-2022).

The level of contamination in the Odiel River at Gibraleón is lower (Table 4.4). The mean pH value is 3.2, and fluctuates between 2.7 and 3.8 most of the year (10th and 90th percentiles). It also shows lower electrical conductivity (average of 1.56 mS/cm) and dissolved concentrations, with average values of 959 mg/L for sulfate, 20 mg/L for Zn, 17 mg/L for Fe, and 30 µg/L for As, etc. It is worth noting that the dissolved concentrations of Al, as well as those of Zn, are higher than those of Fe (Cánovas et al., 2007).

		Mean	Median	Minimum	Maximum	Percentile 10	Percentile 90
pH		3.18	3.10	2.20	6.30	2.70	3.80
EC	mS/cm	1.56	1.45	0.12	4.40	0.50	2.61
Cu	mg/L	6.2	5.3	0.01	37.6	1.85	11000
Fe	mg/L	17.2	6.3	0.03	180	0.77	48.4
Mn	mg/L	12.4	10.6	0.49	52.6	3,2	25.0
SO_4	mg/L	959	801	11.6	3960	216	1995
Zn	mg/L	20.0	15.2	0.17	86.1	4.9	42.2
As	µg/L	29.9	3.2	<ld	500	0.75	31.5
Cd	µg/L	65.3	50	<ld	270	20	130
Pb	µg/L	134	60	<ld	1180	10	454

Table 4.4: Statistical summary of pH, electrical conductivity and dissolved concentrations of some elements in the Odiel River at Gibraleón (Official Quality Control Network, 1968-2022).

Figure 4.35 displays the Ficklin diagram illustrating weekly sampling in the Tinto and Odiel rivers between 2002 and 2007, comparing them with extreme data from Iron Mountain in California (Alpers and Nordstrom, 1999) and samples taken in the Riotinto Mining District (Cánovas, 2008). In these diagrams, the horizontal axis represents pH, while the vertical axis represents the sum of base metals resulting from sulfide oxidation.

Samples from the Tinto River are characterized by being predominantly highly acidic-highly metallic, while those from the Odiel River are mainly acidic-highly metallic. Samples from the Riotinto Mining District and, especially, Iron Mountain exhibit higher acidity

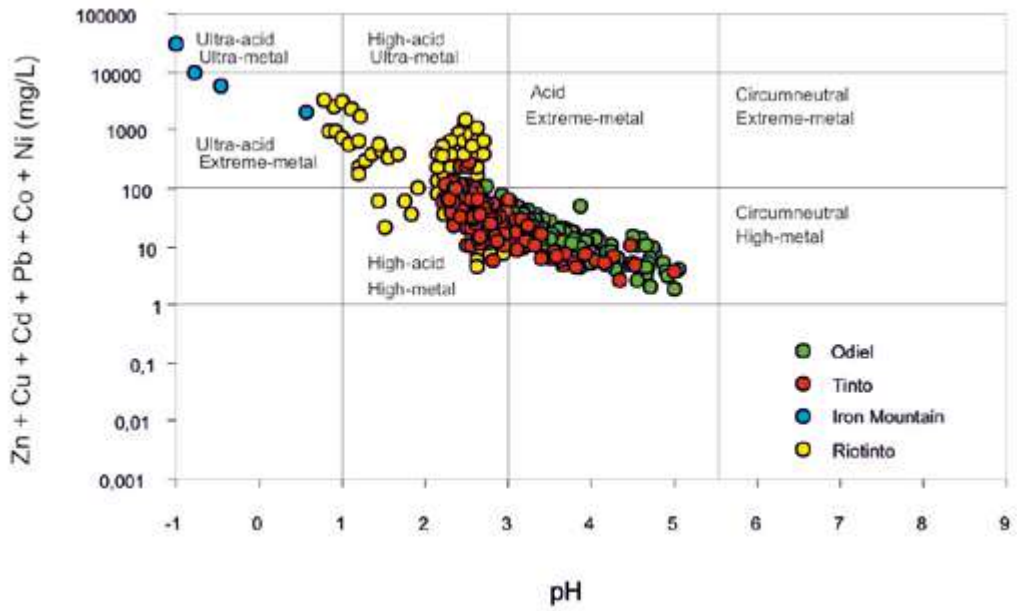

Figure 4.35: Ficklin diagram of samples collected in the Tinto and Odiel rivers, Iron Mountain and the Riotinto Mining District (Cánovas, 2008).

and metal content (the latter having the most extreme documented values of AMD contamination). It is also observed that for pH values between 3 and 5, the Odiel samples have a slightly higher concentration of base metals.

Figure 4.36 presents box plots (also known as 'box and whiskers') illustrating the dissolved concentrations analyzed by Cánovas (2008) in the Tinto River at Niebla and the Odiel River at Gibraleón (the lower reaches of both rivers). The vertical length of the box represents the interquartile range (25^{th} to 75^{th} percentiles), while the inner horizontal line indicates the median. The lines outside the box connect the minimum and maximum values, excluding extreme cases (*) and outliers (o). Extreme cases are those whose values exceed 3 times the interquartile range, while outliers are data that fall between 1.5 and 3 times this range.

Similar to other rivers affected by AMD, the highest concentration values correspond, notably, to sulfate. The most striking difference between both rivers lies in the uneven iron content. While iron is the metal with the highest concentration in the Tinto River (average of 334 mg/L), in the Odiel, its concentration is much lower (average of 17.2 mg/L).

Among the minor elements, cobalt (Co) reaches the highest concentration (Fig. 4.36). In the Odiel, nickel (Ni) is the second most abundant element, while in the Tinto, it is the third after Sr. It is also noteworthy that the concentration of As and Cr in the Odiel River is significantly lower than in the Tinto.

For comparative purposes, if we divide the mean values of each element in the Tinto River by their equivalents in the Odiel (Fig. 4.37), it can be observed that the concentration in the Tinto River is approximately three times higher in sulfate, Cd, and Zn, and slightly higher in the case of Cu. The most significant differences are observed in Fe and As, with concentrations in the Tinto being 19 and 27 times higher, respectively. On the contrary, the concentrations of Mn and Pb are similar in both rivers (Fig. 4.37).

Sulfates are a reliable indicator of AMD contamination because they are a relatively conservative compound found in high concentrations in acidic leachates and low concentrations in natural watercourses unaffected by AMD. Moreover, the chemical processes that could remove sulfates from water are negligible compared to dilution processes (Nordstrom

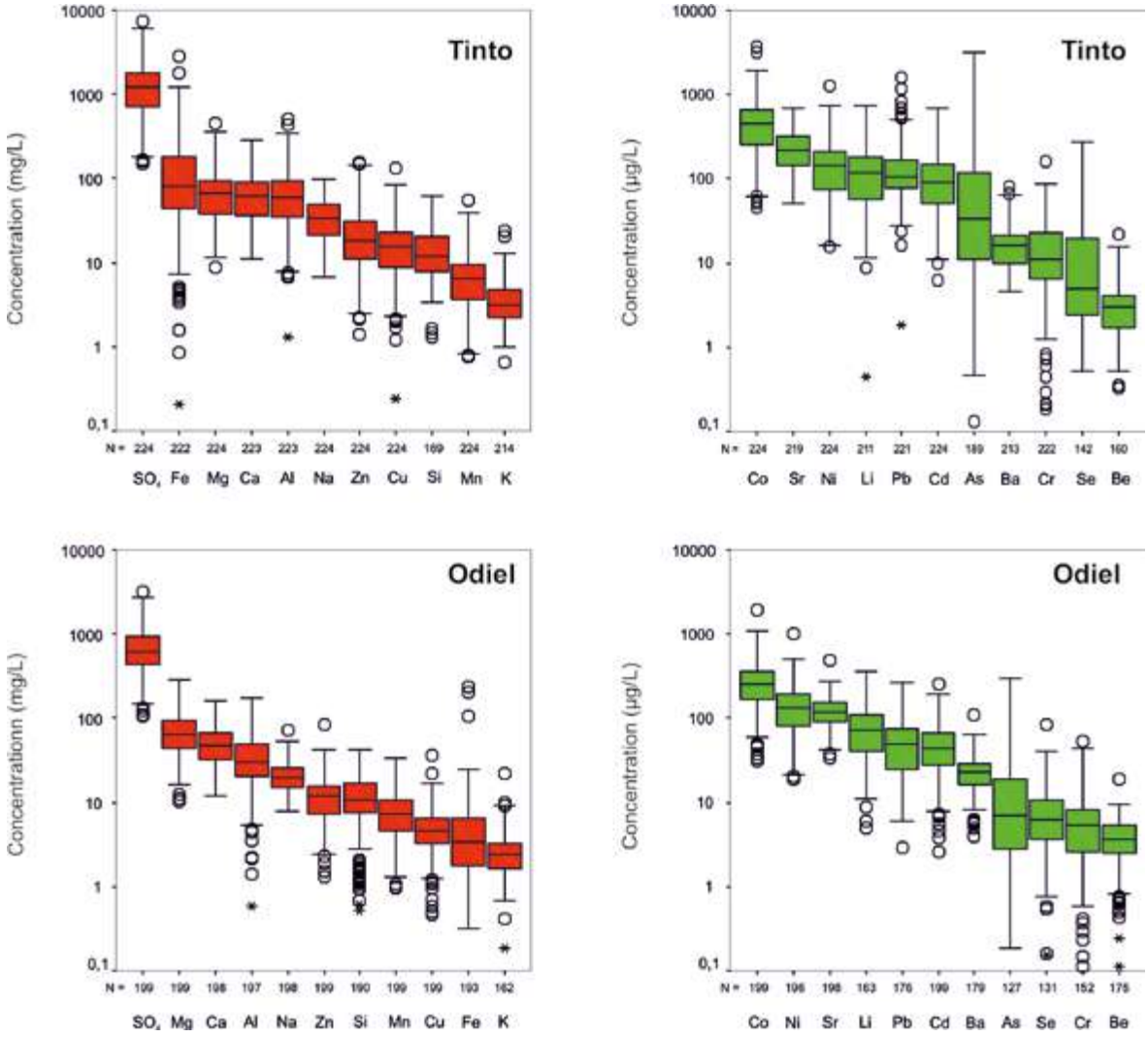

Figure 4.36: Box plots of the concentration of major (in red) and minor (in green) elements in the Tinto and Odiel rivers (Cánovas, 2008).

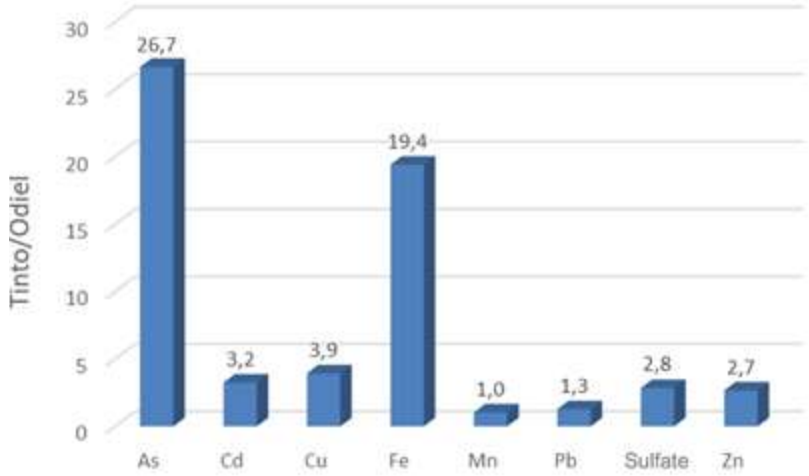

Figure 4.37: Comparison between mean values of dissolved concentration in the Tinto River (at Niebla) and the Odiel River (at Gibraleón) during 1968-2022.

and Ball, 1986; Berger et al., 2000). Considering sulfates as conservative, the Tinto River receives almost three times the amount of contaminants per unit flow compared to the Odiel River. In other words, acidic leachates in the Odiel River undergo greater dilution and neutralization. As previously mentioned, when acidic leachates mix with neutral freshwaters, dissolved Fe undergoes hydrolysis processes and precipitates as ferric oxyhydroxysulfate, buffering the pH. This process, more intense in the Odiel River due to greater dilution, causes significant differences in dissolved Fe concentrations between both rivers. Additionally, the intense precipitation of Fe in the Odiel River network results in low concentrations of As, much lower than in the Tinto River, as As is strongly adsorbed and/or coprecipitated during the precipitation of ferric oxyhydroxysulfates (e.g., Williams, 1999; Casiot et al., 2003). Although to a lesser extent, Cu also undergoes preferential precipitation in ferric oxyhydroxysulfates (Alpers et al., 1994; Gray, 1998; Olías et al., 2004), explaining the lower concentration of Cu in the Odiel River, almost 4 times lower than that in the Tinto River.

On the other hand, it is observed that the average concentration of Mn is equal to that in the Tinto River, and the same applies to Mg, Ni, and Be (Cánovas et al., 2007). This seems to be related to lithological differences between both river basins, due to a higher abundance of hydrothermal Mn and Ni mineralizations in the Odiel River basin.

In addition to the higher dissolved Fe concentration in the Tinto River, another difference from the Odiel is the form (species) in which this element is present. Figure 4.38 represents the mean values of the distribution of Fe species obtained from the PHREEQC code (Cánovas, 2008). Due to the high redox potential values in the Tinto River, Fe is primarily found in its ferric state (91% of total dissolved iron). Among the dissolved species of Fe(III), sulfate complex $FeSO_4^+$ (80% of ferric iron) predominates. In the Odiel River, the proportion of ferrous Fe is much higher (41%), predominantly in the free ionic form Fe^{2+} (Fig. 4.38).

Regarding the importance of particulate transport in the Tinto and Odiel rivers, Figure 4.39 illustrates the percentage of each element in the dissolved phase based on data from Cánovas (2008). A 100% indicates that there is no suspended transport in the form of small solid particles, while, for example, 75% indicates that 25% of that element is transported in particulate form (and 75% is dissolved). In the Tinto River, almost all elements are primarily found in the dissolved phase with values exceeding 95%, except for As, Ba, Cr, Fe, and Pb,

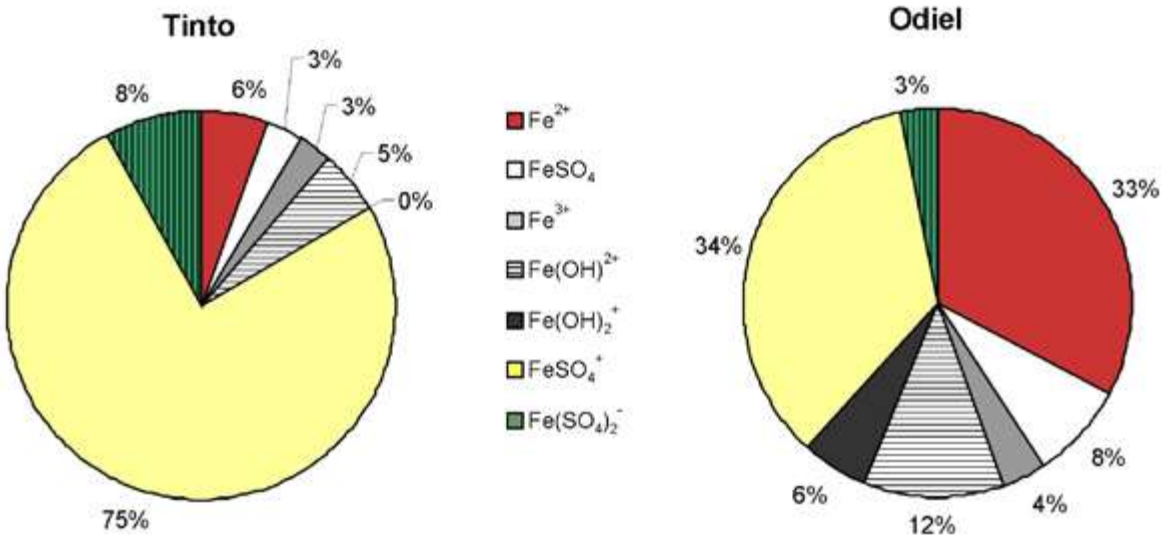

Figure 4.38: Mean values of Fe species int the Tinto (at Niebla) and Odiel (at Gibraleón) rivers (Cánovas, 2008).

which have dissolved percentages below 90%. In the Odiel River, most elements are also in the dissolved form, with only Al, As, Ba, Cr, and Fe having values below 90%. In both rivers, Cd, Co, Cu, Mn, Ni, and Zn show dissolved percentages very close to 100%. In summary, the main elements transported by the Tinto and Odiel rivers are in the dissolved phase. However, it should be noted that during floods, when suspended material transported to the estuary increases (Achterberg et al., 2003), the transport in the particulate phase for some elements may become more important.

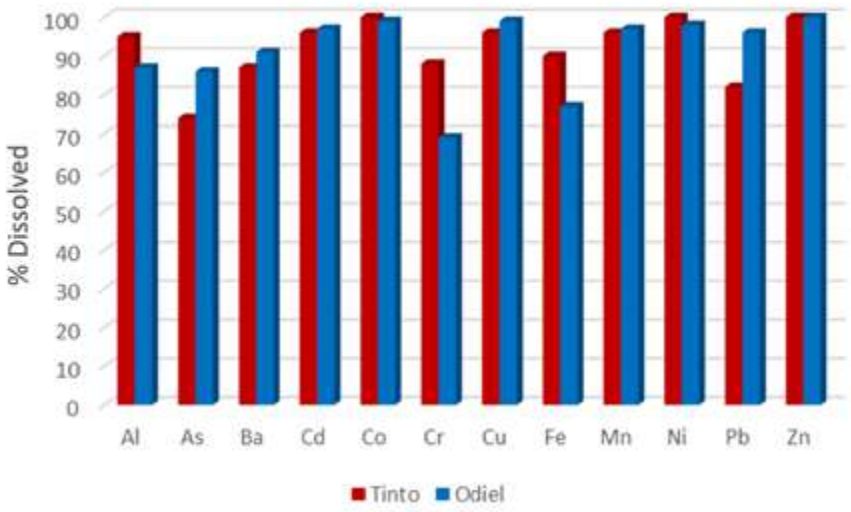

Figure 4.39: Mean values of the percentage of dissolved concentrations of elements in the lower reaches of the Tinto (at Niebla) and Odiel (at Gibraleón) rivers.

4.2. TEMPORAL EVOLUTION

As evident from Tables 4.3 and 4.4, the Tinto and Odiel rivers exhibit significant variations in the concentrations of dissolved toxic elements in the water due to:

- Seasonal fluctuations throughout the year. For instance, concentrations are much higher in summer than during winter when floods cause substantial dilution.
- Long-term trends resulting from the construction of reservoirs, opening or closing of mines, changes in environmental controls at mining sites, etc. For example, mine closures can lead to an increase in water contamination in the surrounding areas due to the abandonment of environmental control measures.
- Additionally, there can be occasional releases of large amounts of pollutants due to accidents or failures in leachate control at mining facilities. An example is the Aznalcóllar incident in 1998, which resulted in a massive disaster in the Guadiamar River. In 1988, a significant discharge of pyritic sludge occurred from the Almagrera mine facilities into the Odiel River, leaving a layer of about 10 centimeters in some floodplain areas (Álvarez Valero et al., 2009; Adánez Sanjuán et al., 2014). Several acidic water spills also occurred in 2002 from this mining area after the mining company managing the site abandoned it. The latest significant spill, detailed in this book, occurred in May 2017 in the Odiel River from the pit lake of La Zarza mine.

4.2.1. Seasonal variations

In Mediterranean-climate rivers affected by AMD, an approximate cycle of changes in the concentrations of toxic elements is repeated throughout the year. During summer, the

oxidation of sulfides reaches its highest intensity because elevated temperatures lead to increased microbiological activity and, consequently, the oxidation processes of pyrite. Additionally, under these conditions, intense evaporation in surface water bodies causes an increase in the concentration of dissolved elements and the oversaturation of various sulfate-evaporitic salts (see section 2.3.3), which precipitate onto riverbeds and mining-affected areas (Buckby et al., 2003; Olías et al., 2004; Sánchez-España et al., 2005; Cánovas et al., 2007).

These salts serve as a temporary storage for acidity, sulfates, and metals (e.g., Alpers et al., 1994; Cravotta, 1994; Nordstrom and Alpers, 1999b; Hammarström et al., 2005). Their dissolution with the first rains after summer, usually in October, results in the sudden release of the contained acidity, sulfates, and metals, with the highest pollution levels recorded throughout the year (Fig. 4.40). The pollution levels during the washing of evaporitic salts depend on the distribution and intensity of precipitation, as well as the duration of the preceding dry period and the amount of accumulated evaporitic salts. Similar episodes, although of lesser magnitude, can also occur in spring or other seasons when precipitation follows periods without rain.

In late autumn and early winter, precipitation is usually more intense, and along with decreasing temperatures, significant volumes of surface runoff reach the rivers, causing a dilution effect on pollutant concentrations. As a result, pH values increase slightly, and the concentration of dissolved elements decreases, marking the lowest values of the year (Fig. 4.40). However, even though concentrations decrease in rainy years, the amount of pollutants carried by the river increases due to the rise in flow. In spring, when precipitation is lower and temperatures rise, river flow decreases due to reduced surface runoff. Thus, pH values gradually decrease while dissolved concentrations increase due to a higher percentage of leachates from AMD emission sources and evaporation. Consequently, there is a progressive increase in the concentration of the main elements studied, continuing into summer, completing the cycle of the annual variation in water quality.

There are some exceptions to this seasonal behavior. Figures 4.41 and 4.42 depict the evolution of dissolved concentrations in the form of box plots. Concentrations of Fe, As, Cr, and Pb are shown logarithmically due to their high variability. Some differences are observed between both rivers, such as the evolution of Fe concentration. The lowest Fe content values in the Tinto River are reached at the end of the rainy period (February-April), then they increase during spring and stabilize or slightly decrease during low flow, instead of increasing like sulfates, Mn, Zn, etc. This is due to intense Fe precipitation during summer. In the Odiel River, the Fe concentration decreases at the beginning of low flow periods (Fig.

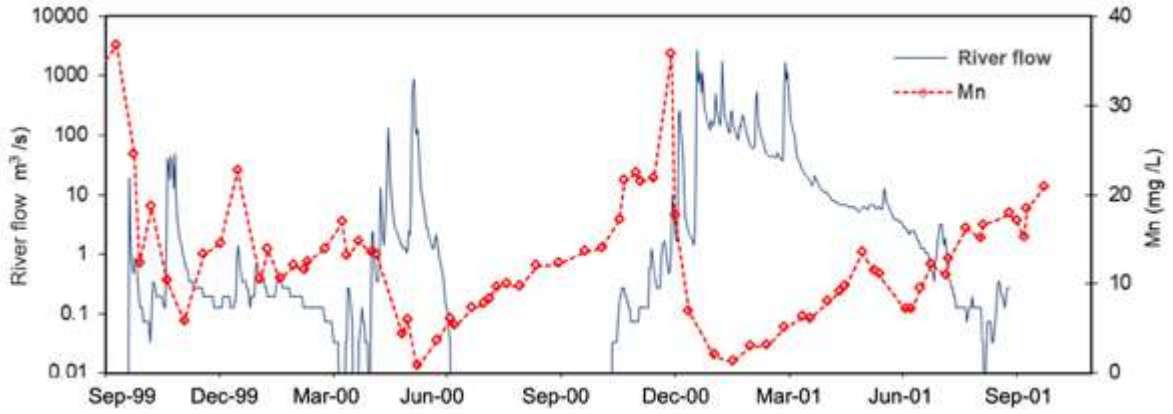

Figure 4.40: Seasonal variations of river flow and concentration of Mn in the Odiel River (at Gibraleón) during the hydrological years 1999/2000 and 2000/2001.

4.42). This is because the Fe concentration in the Odiel is very low and is mainly in the form of ferrous iron, which behaves differently than ferric iron (Cánovas, 2008).

On the other hand, in the Odiel, the concentration of Al does not increase during summer and even decreases slightly, unlike sulfates and the rest of the associated elements (Fig. 4.42). This could indicate a change in the pH buffering system in the Odiel during summer, with Al taking on this role instead of Fe. Pb also follows a different behavior in both rivers

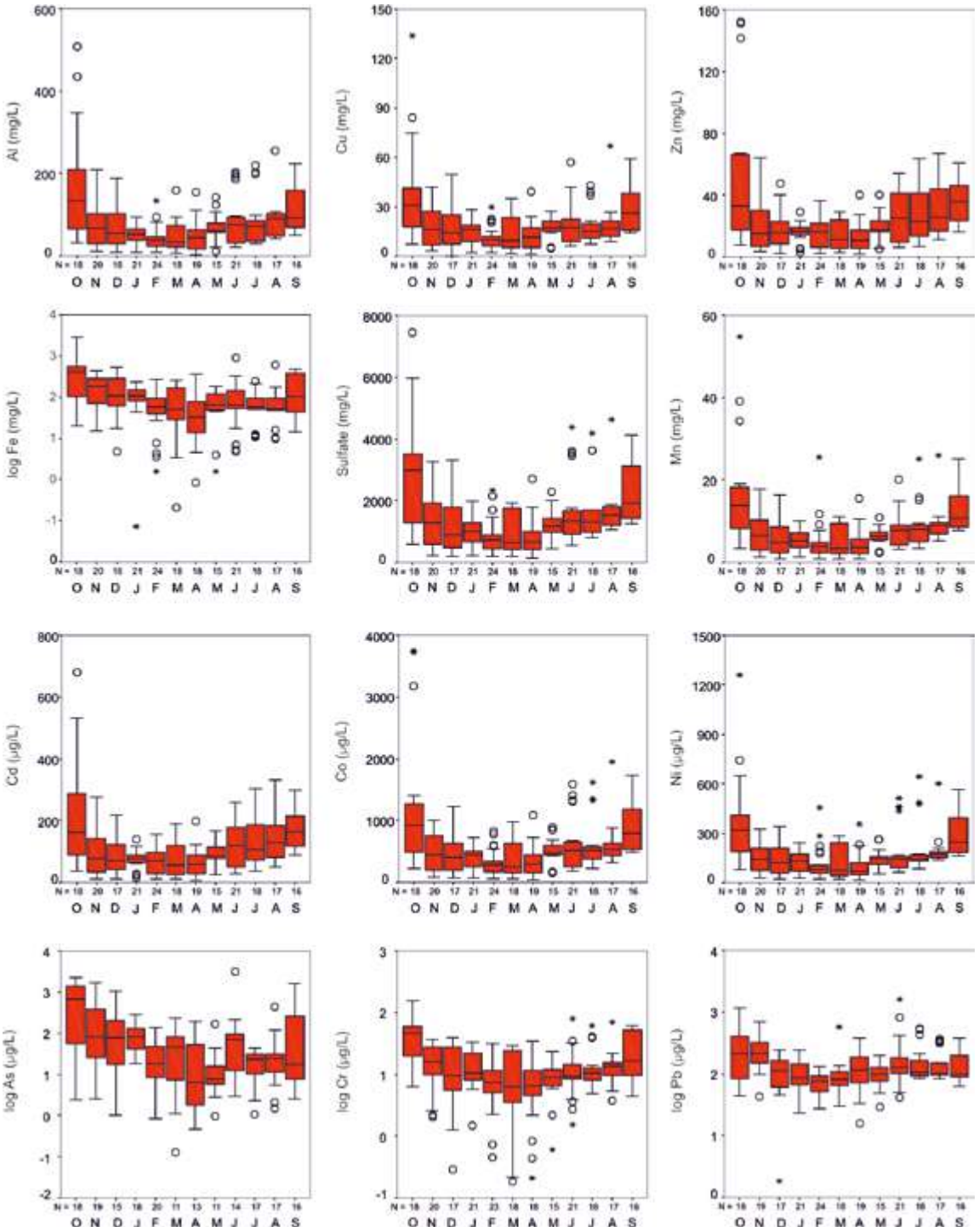

Figure 4.41: Box plots showing the seasonal evolution of dissolved concentrations in the Tinto River at Niebla (Cánovas, 2008) along hydrological years (October to September).

during low flow conditions. While its concentration considerably increases in the Odiel River, in the Tinto, it remains stable or slightly decreases. This could be due to anglesite solubility controlling Pb concentration in the Tinto River, while in the Odiel, the product of solubility of this mineral is not exceeded due to lower concentrations of sulfates and Pb.

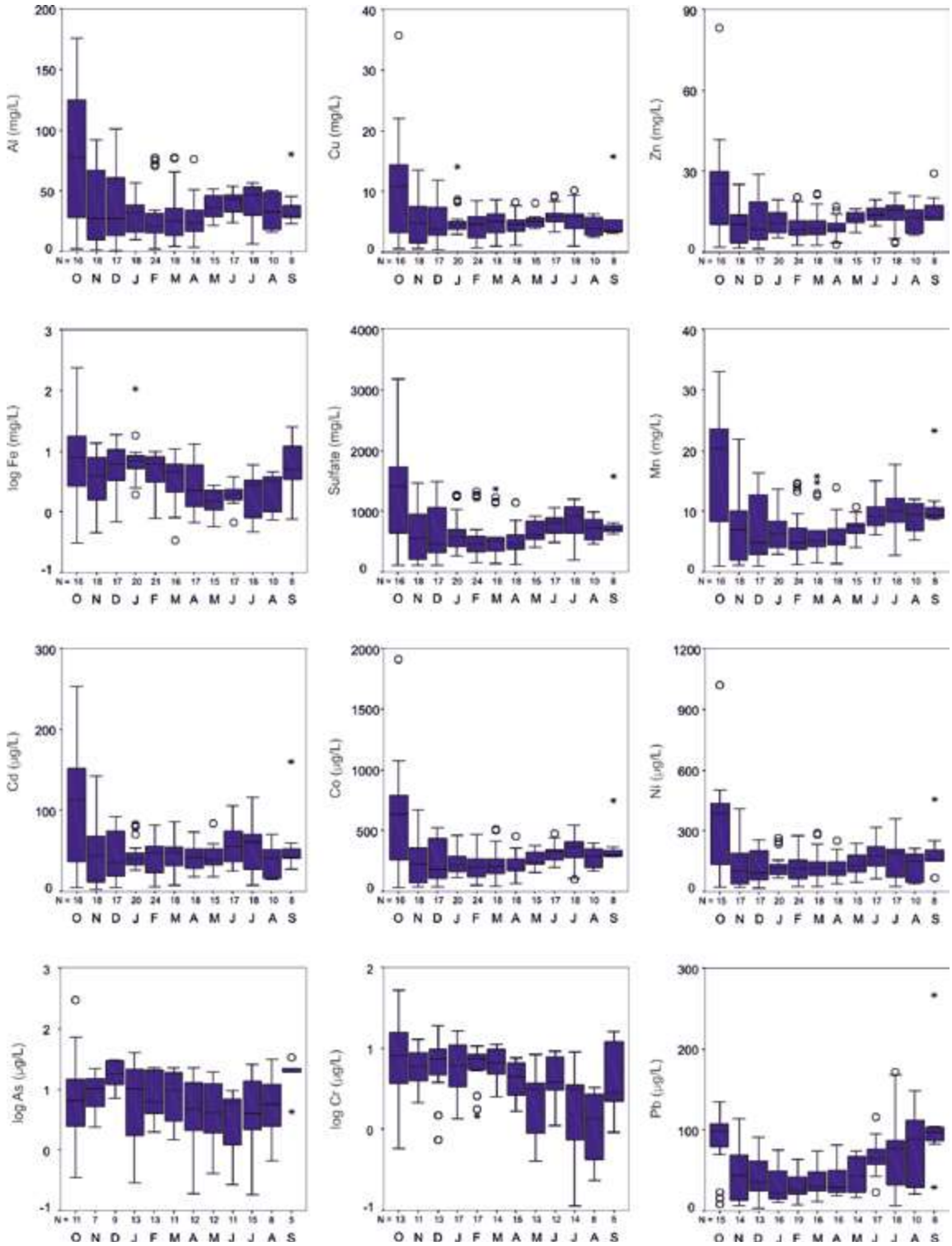

Figure 4.42: Box plots showing the seasonal evolution of dissolved concentrations in the Odiel River at Gibraleon (Cánovas, 2008) along hydrological years (October to September).

Besides that, the water quality of rivers affected by AMD not only varies throughout the year but also experiences interannual variations primarily because in wetter years, there is greater dilution of contaminants, while in drier years, concentrations of elements increase.

4.2.2 Long term evolution

To gain a more comprehensive understanding of the problem of AMD pollution in the Tinto and Odiel rivers, it is necessary to understand how pollutant concentrations have evolved beyond current values or recent years. For this purpose, official data from water quality networks obtained by the Guadiana River Basin Authority until 2007 and subsequently by the Andalusian Regional Government, after assuming management of the Tinto, Odiel, and Piedras rivers, have been compiled.

The first available data for electrical conductivity, pH, and sulfate values date back to 1968. Measurements for iron (Fe) and copper (Cu) concentrations began in 1973, but for other elements (e.g., As), regular data is not available until the late 1990s. The analysis frequency is generally monthly, although not for all determined variables (in recent years, it is monthly for pH, electrical conductivity, Cd, and Pb, and approximately quarterly for the rest of the parameters). It is also noteworthy that there are periods without information (for example, from October 2002 to March 2004 and from October 2015 to October 2016). After representing the concentrations, some anomalous data from the early sampling years, clearly erroneous, have been removed.

Figures 4.43 to 4.46 show the evolution of the Odiel and Tinto rivers, before their mouths in the estuary. Concentrations are higher in the Tinto River, as discussed in section 4.1.3. The controlled values show large oscillations depending on the flow (higher flow results in more dilution of pollutants) and the time of year (maximum concentrations occur in early autumn due to the redissolution of soluble evaporitic salts, as discussed in previous sections). Despite these large oscillations, it is observed that pH values of the Odiel River were approximately between 3 and 4 from 1968 to 1975 (Fig. 4.43). From 1975 to around 1995, minimum values decreased and approached to 2.5. From 1996 onwards, the situation improved, and pH rarely dropped below 3, with maximum values approaching 5 (there are three values above 6, which may be due to very high flows or, in some cases, measurement errors).

The electrical conductivity and sulfate concentration show a very similar evolution since sulfates are the ions with the highest concentration in AMD. Lower values of EC and sulfates are present in the early years of monitoring (between 1968 and approximately 1975), coinciding with somewhat higher pH values. From there, the values increase, reaching their peak during 1987 to 1995. Subsequently, the values decrease slightly, remaining approximately stable until now (Fig. 4.43). For Cu and Fe, a similar evolution is observed, with lower values from the start of the dataset in 1973 until 1978, higher values between 1980 and 1995, and a slight decrease thereafter until the end of the series. In the concentration of Fe (Fig. 4.44), a prominent peak is observed in May 2017, with a concentration close to 140 mg/L, due to the discharge that occurred several days earlier from La Zarza pit lake (see the next section).

In the trend lines, a progressive increase in pH and a decrease in almost all elements are observed, except for sulfate and EC (Figs. 4.43 and 4.44). In other words, for most elements a clear trend towards improvement is observed. In the case of sulfate and EC, the increasing trend seems to be due to their very low values during the first years of the series, which could be related to higher circulating flows in the Odiel before the construction of several reservoirs, such as Olivargas and Odiel-Perejil. If only the data from 1980 onwards are considered, a downward trend would be obtained.

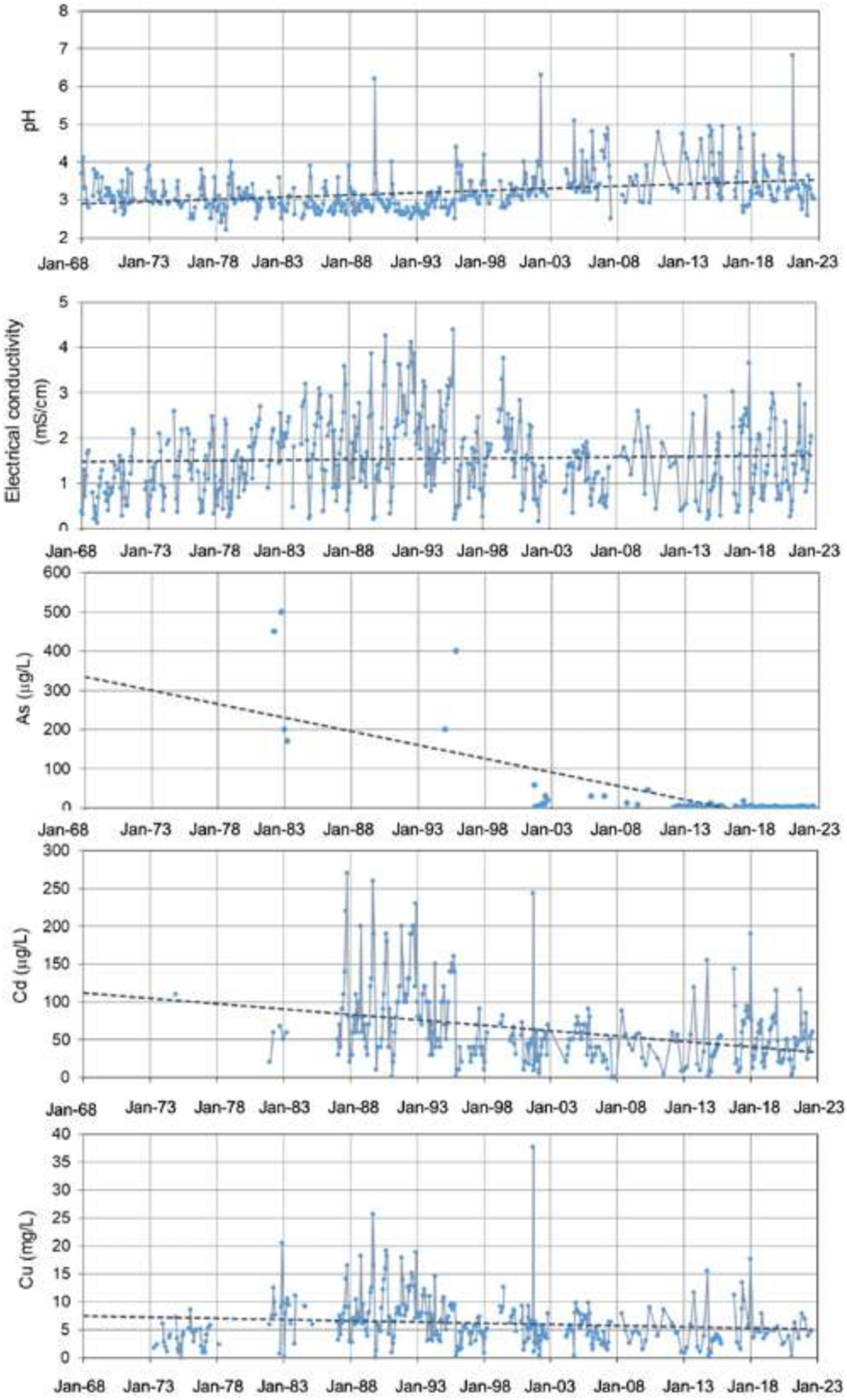

Figure 4.43: Historical data for the evolution of pH, electrical conductivity, and the concentration of As, Cd and Cu in the Odiel River at Gibraleón. Discontinuous lines represents the trend obtained following a linear fitting.

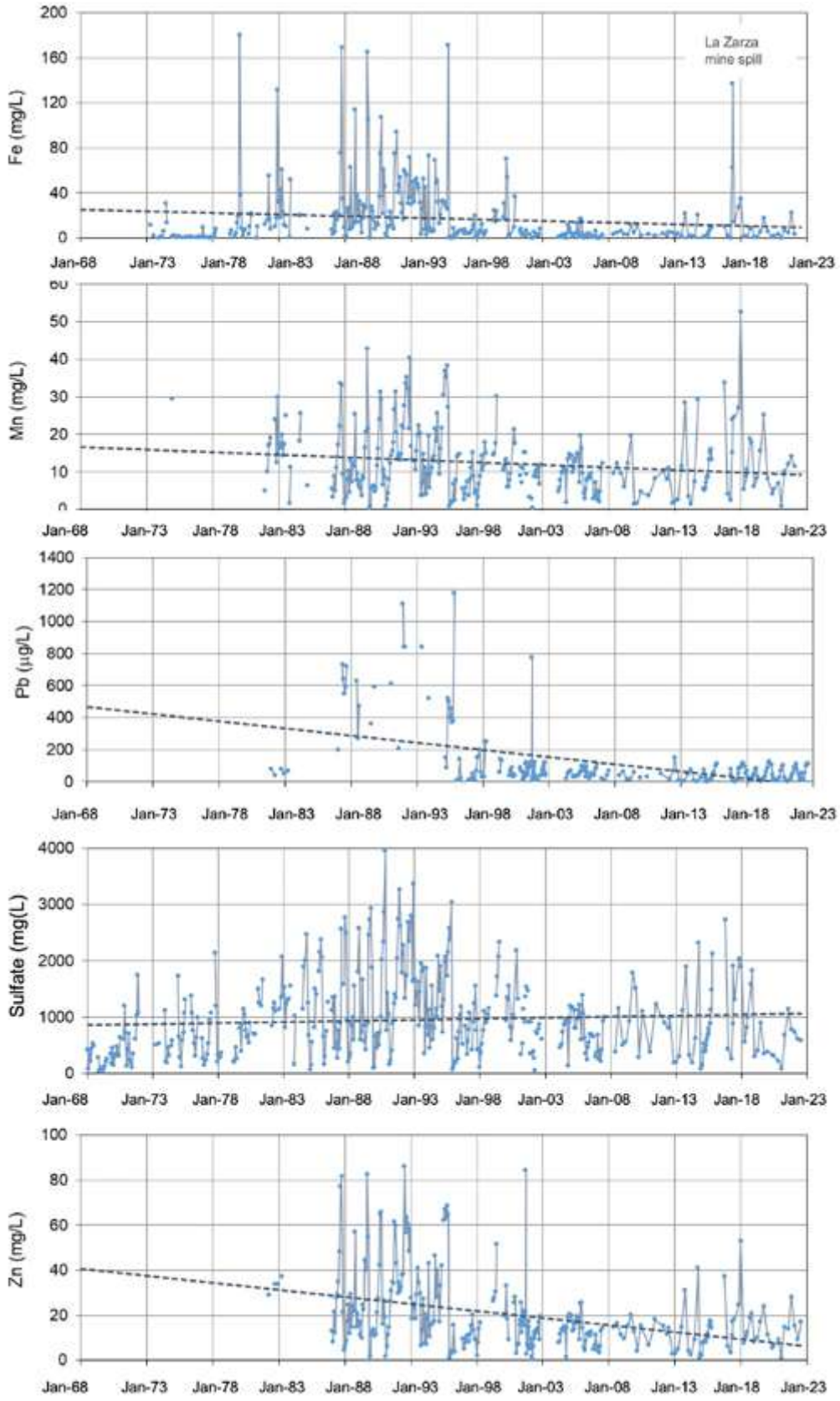

Figure 4.44: Historical data for the evolution of the concentration of Fe, Mn, Pb, sulfate and Zn in the Odiel River at Gibraleón. Discontinuous lines represents the trend obtained following a linear fitting.

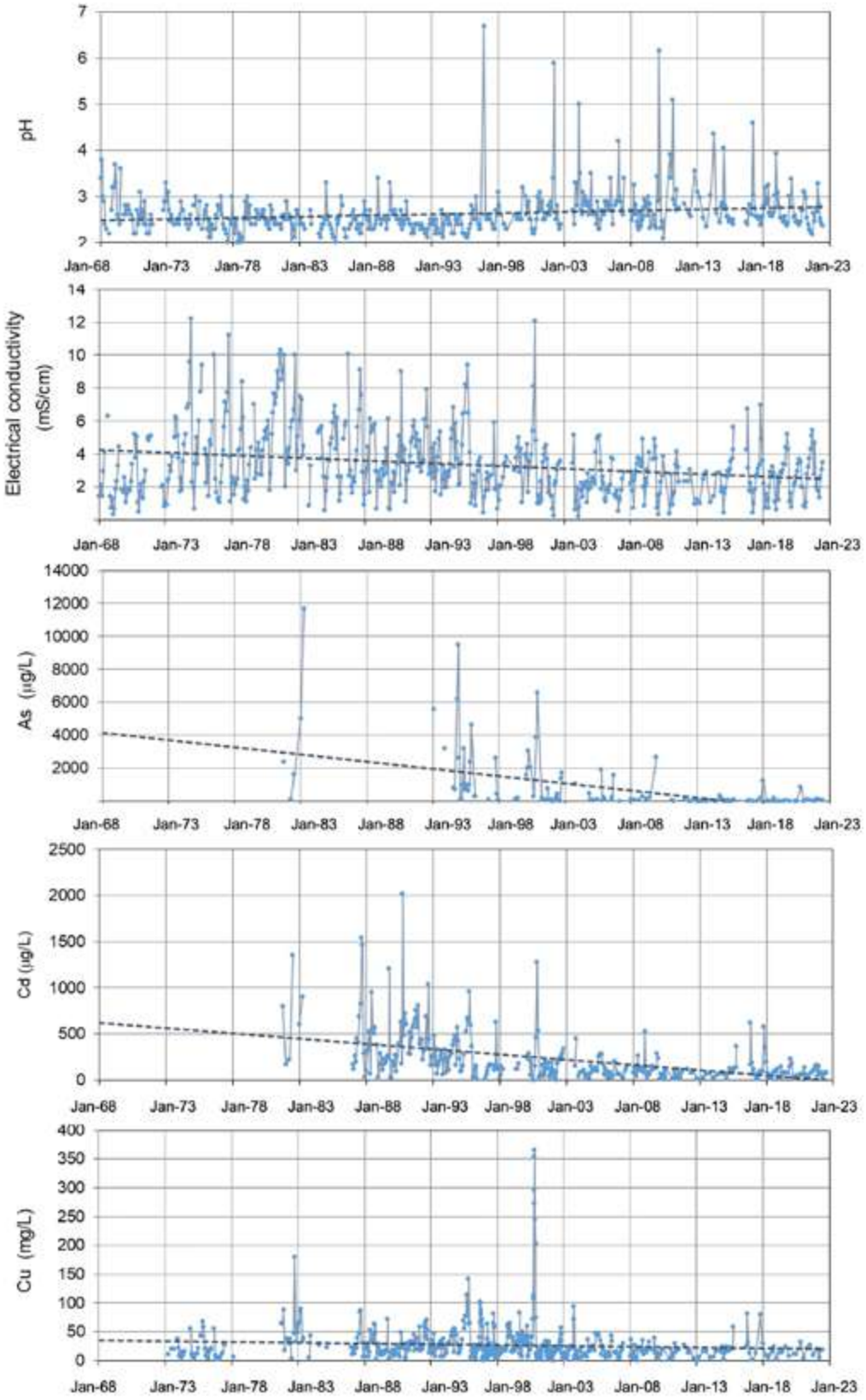

Figure 4.45: Historical data for the evolution of pH, electrical conductivity, and the concentration of As, Cd and Cu in the Tinto River at Niebla. Discontinuous lines represents the trend obtained following a linear fitting.

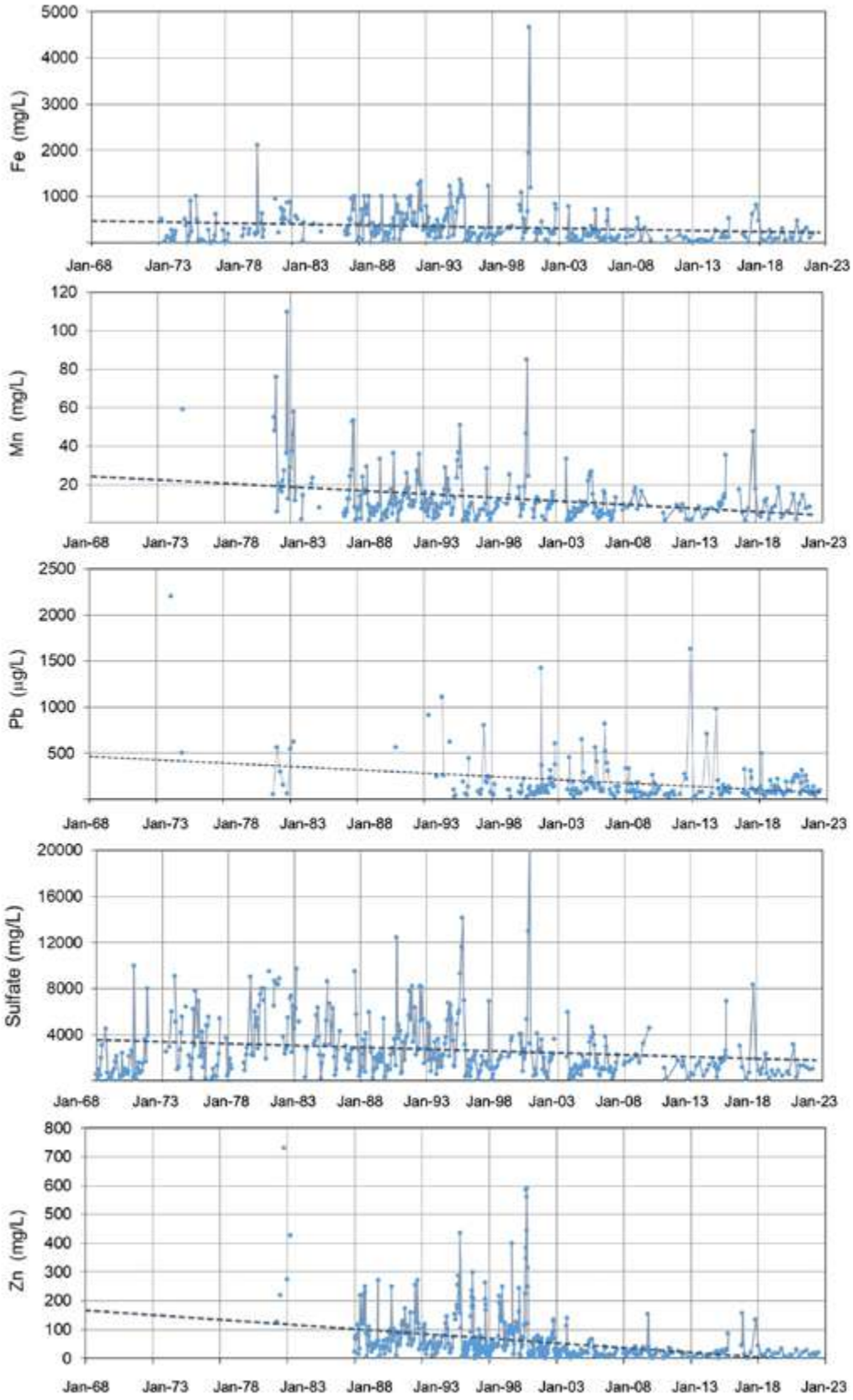

Figure 4.46: Historical data for the evolution of the concentration of Fe, Mn, Pb, sulfate and Zn in the Tinto River at Niebla. Discontinuous lines represents the trend obtained following a linear fitting.

In the Tinto River, pollutant concentrations are higher as mentioned above (Figs. 4.45 and 4.46). As in the Odiel, three periods can be distinguished: 1) lower values of EC and slightly higher pH until 1975, 2) a second period between 1975 and 1995 with lower pH values and higher EC values, and 3) an improvement in conditions in 1996 and a maintenance of values since then until now. A similar evolution can also be observed in metal and sulfate concentrations, although for most metals, there is no data prior to 1980. In addition, a significant peak in concentrations is observed in 2000, reaching maximum values for Cu, Fe, sulfate, and Zn (Figs. 4.45 and 4.46). This sharp increase in pollution is attributed to the closure of the Riotinto mine in the late 1990s and the subsequent abandonment of drainage and maintenance operations (Olías et al., 2020). However, from 2000 onwards, pollution levels are significantly lower than those recorded during the 1980s and 1990s. It is also observed that the reopening of the Riotinto mine in 2015 apparently has not had any influence on this evolution. Throughout the period, a clear trend towards increased pH and decreased concentrations and EC is observed (Figs. 4.45 and 4.46). The decrease is more pronounced for arsenic, cadmium, and zinc.

In summary, both in the Tinto and Odiel rivers, the following observations are made: 1) a first period with lower pollution levels (between the start of the data series and approximately 1975), 2) a worsening of conditions from 1976 to 1995 due to increased mining activity from 1970, which included the massive exploitation of Cerro Colorado in the Riotinto mines (Arenas Posadas, 2017), and finally, 3) a slight decrease in pollutant levels in 1996 (this year was very humid after a significant drought, which must have contributed to the observed decrease) and approximately stable conditions since then. Additionally, a pollution peak is detected in the Tinto River in 2000 due to the cessation of maintenance operations, and in the Odiel River, the effect of the spill from La Zarza pit lake in May 2017 is also evident. Due to the persistence of AMD generation processes, it is expected that current pollution levels will persist for a long time unless restoration measures are implemented.

Figure 4.47: Acidic leachates outflowing from Los Cepos gallery before the La Zarza spill (September 2011).

4.2.3. Impact of La Zarza mining spill on the Odiel River (May 2017)

On May 17, there was an accidental discharge of AMD from the La Zarza pit lake. The cause of the spill was the rupture of a concrete plug that sealed the Los Cepos gallery (Fig. 4.47), which could not withstand the pressure due to the rise in water level in the pit lake after the mine closure and the subsequent abandonment of drainage pumps in 1995 (Olías et al., 2019). Based on the flooded surface area and the observed water level drop on the pit-walls (Fig. 4.48), the discharged volume was estimated to be approximately 270,000 m^3. The acid waters rapidly moved through the Mojafre stream, the Olivargas River, and from there into the Odiel River (Fig. 4.14), eventually reaching the estuary of the Ría de Huelva.

The discharged water had a pH of 2.4 and extreme values of EC (9.1 mS/cm) and contaminant concentrations, with 2883 mg/L of Fe, 624 mg/L of Al, and 6.75 mg/L of As (Table 4.5). Approximately 800 tons of Fe, 168 tons of Al, 1.8 tons of As, etc., were released during the spill. Of the total discharge, about 50,000 m^3 were retained in an ex-

Figure 4.48: La Zarza pit lake after the AMD discharge occured on May 2017. It can be seen a yellowish band in the pit walls caused by the decrease in the water level of the pit lake as a consecuence of the spill.

isting mining dam in the area and several dams hastily constructed along the Mojafre stream, resulting in a lesser amount of contaminants reaching the Odiel River (Table 4.5)

	Spill		Load reaching the Odiel
	mg/L	tons	tons
SO_4	13602	3673	2992
Al	624	168	137
As	6.75	1.82	1.5
Cd	0.44	0.12	0.10
Co	5.83	1.6	1.3
Cu	125	34	28
Fe	2883	778	634
Mn	208	56	46
Ni	4.53	1.2	1.0
Pb	0.76	0.21	0.17
Zn	139	38	31

Table 4.5: Concentrations and pollutant loads released during the La Zarza mine spill

Immediately after the discharge was detected, remediation measures were initiated. On one hand, measures were taken to prevent AMD outflowing from the pit lake by injecting impermeabilizing agents into the Los Cepos gallery, which was successfully completed 10 days after the discharge occurred. On the other hand, the mining dam and the constructed dams to retain the acidic water were not completely impermeable, so a system was established to pump upstream the produced leakages. This system operated until the whole retained acidic waters were treated. The treatment took place during June and July by

neutralizing the water with caustic soda (NaOH) and the subsequent precipitation of metals. An attempt was also made to treat it by circulating the water through channels filled with limestone gravel (with grain diameters between 1 and 3 cm; Fig. 4.49). However, this measure proved to be ineffective because the large amounts of dissolved Fe and other metals precipitated around the limestone particles as the pH increased, preventing their dissolution due to the passivation of the limestone gravel and clogging all the voids. As a result, the water could not flow through the limestone gravels (see section 7.3).

The discharge led to the release of significant amounts of pollutants to the Odiel River, affecting 53 km of watercourses (Table 4.5). In this area, the Odiel River was already contaminated by other mines and exhibits acidic conditions, preventing the presence of fish and other typical aquatic organisms in river ecosystems. Thus, only bacteria, algae, and other microorganisms adapted to acidic conditions live in this reach of the Odiel River. Therefore, the discharge did not cause a major environmental disaster in the river, although it did result in a significant increase in toxic element concentrations and a drastic change in its usual color (Fig. 4.50).

In May 19 concentrations of some elements increased up to 450 times in the Odiel River at Sotiel (Fig. 4.51), reaching concentrations of 437 mg/L for Fe and 410 µg/L for As (there are no analyses available for May 18, so they could have been even higher). After May 19, concentrations at Sotiel rapidly decreased, and the effect of the discharge disappeared by the end of May.

The discharge spread downstream, with the same change in color also being observed at Gibraleón. However, since the Odiel River flow rates were not very high, the movement of the concentration peak along the river was relatively slow. The highest concentrations of toxic elements observed at Gibraleón, in the lower part of the catchment, occurred on May 31, two weeks after the discharge (Fig. 4.51). At this point the effect of the discharge lasted until mid-June, one month after the acidic water spill. For most elements (Al, Cd, Co, Cu, Mn, Ni, Zn,

Figure 4.49: Addition of limestone gravel to treat the AMD delivered from the La Zarza spill (May 2017).

Figure 4.50: Photo of the common color of the Odiel River Waters at Sotiel (left) and those observed on May 19 after the mine spill (right).

etc.) the maximum concentrations at Gibraleón were approximately 25% lower than those observed at Sotiel. Due to the acidic conditions, these elements were transported dissolved and exhibited a conservative behavior, with their concentration decreasing only through dilution and dispersion processes. However, the maximum Fe concentration was 60% lower, indicating significant precipitation along the river. Approximately only one-third of the Fe discharged into the Odiel reached the estuary, while the remaining two-thirds precipitated. Also, due to the strong tendency of As to coprecipitate with Fe, its dissolved concentrations rapidly decreased, and it was estimated that only 3% of the discharged As reached the Ría de Huelva. Concentrations of other elements such as Cr, Se, Pb, and Tl also significantly decreased due to coprecipitation processes (Olías et al., 2019).

Regarding the impact of the discharge on the estuary of the Ría de Huelva, episodes of mortality of aquatic organisms were not observed, but there was a significant increase in dissolved concentrations in the upper part of the Odiel estuary, ranging from 5 to 77 times higher than previous values. Like the Odiel River, unfortunately, the estuary is subject to significant chronic contamination by AMD, which was aggravated by La Zarza spill.

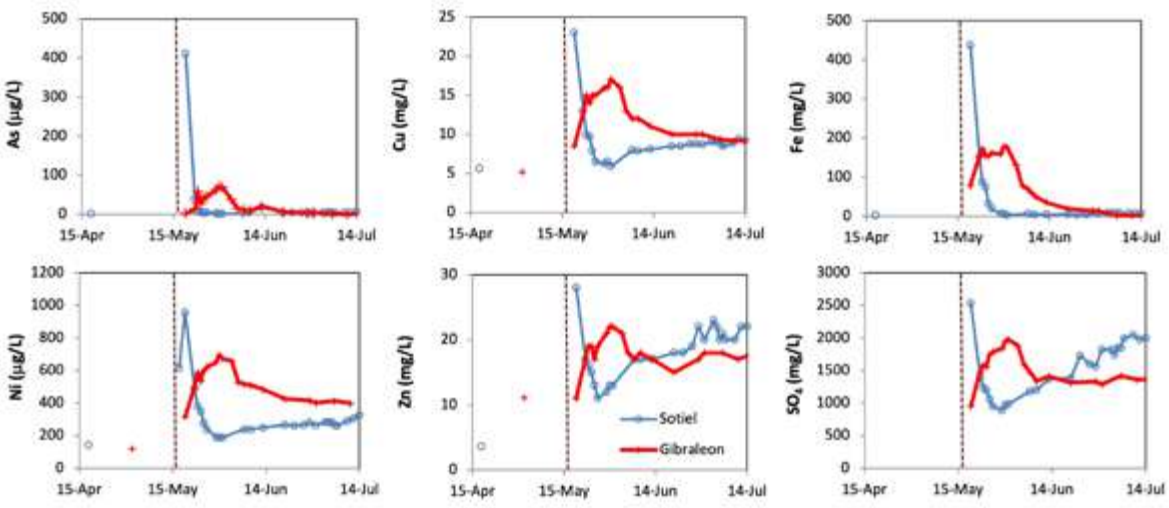

Figure 4.51: Increase in dissolved concentrations of some elements in the Odiel River at Sotiel (middle reach) and Gibraleón (lower reach) after the La Zarza spill (spring 2017).

4.3. POLLUTANT LOAD

4.3.1. Estimation methodology

The estimation of the contaminant load transported by a river is complicated because, in most cases, continuous flow measurements are available at certain points of the river (gauge stations), but contaminant concentrations are less frequently measured, usually once a month. The simplest way to calculate the amount of an element transported by a river during a specific period is to calculate the average concentration obtained from the analyses conducted during that period (C_m in equation 4.1) and multiply it by the river contribution during the same time.

$$C_m = \frac{C_1 + C_2 + \ldots\ldots + C_n}{n} \qquad (4.1)$$

This method, although very simple, involves a significant error because the concentrations of elements also vary significantly with changing flow rates. Large flow rates, which contribute a greater amount of water and dissolved elements, often have lower dissolved concentrations. These high flow rates occur for only a few days each month, making it statistically unlikely to sample them. Therefore, this methodology typically leads to an overestimation of the contaminant load.

A more precise estimation could be done by considering the flow rate (Q) on the day of sampling to weigh the importance of that concentration value within the set of analyses conducted. For example, if we have four samples in a month and three of them represent contaminant concentrations under low flow conditions, while the fourth corresponds to a flood event, we should give more weight to the latter. The weighted average concentration (C_{mp}) would be calculated as follows:

$$C_{mp} = \frac{C_1Q_1 + C_2Q_2 + \ldots\ldots\ldots + C_nQ_n}{Q_1 + Q_2 + \ldots\ldots + Q_n} \qquad (4.2)$$

Another method for estimating the transported load is based on the correlation between flow rate and element concentrations. Dissolved concentration values tend to decrease as the river flow rate increases. If we can establish a relationship between flow rate and concentration, we could calculate the element concentration on days when no samples are available based on daily flow rate measurements.

When correlations between flow rate and concentration are statistically significant, this method is much more accurate than the previous ones (Preston et al., 1989; Quilbé et al., 2006), although it is more time consuming because establishing correlations is not always straightforward. For example, as seen in the section on seasonal concentration variations, early in the hydrological year, the first rainfall washes away the leachate products from pyrite oxidation accumulated and soluble salts precipitated in the mining areas and riverbeds during the summer. Instead of dilution with increased flow rates, this leads to an increase in contaminant concentrations. Once these salts have been washed away, the concentration of elements decreases, and with the same flow rate, we can have very different values than those at the beginning of the hydrological year.

Furthermore, in the Tinto and Odiel rivers, establishing these correlations is complicated by the presence of samples that do not have a good correlation with flow rates for various reasons (e.g., uncontrolled mining discharges, reservoir releases, etc.). All of this makes the relationship between flow rate and concentration not constant throughout the year. On the other hand, there are some elements, such as As, Fe, and Pb, that do not always show

a significant correlation with flow rate, and therefore, this methodology cannot be applied to them. In the results presented below, this last method has been applied whenever possible. The procedure followed consisted of identifying, for each hydrological year, the periods in which the relationship between flow rate and dissolved concentration is maintained and calculating the corresponding regression equation.

As an example, the relationship between dissolved Cd concentration and flow rate in the 1996/97 hydrological year in the Tinto River is shown (Fig. 4.52). It can be observed that the correlation for the whole year is low (upper right part of the figure), but it increases significantly when different periods are separated. The first period (Nov 14 to Dec 5, 1996) corresponds to the first significant wash out after autumn, causing dissolved concentrations to increase with flow rate. The second period covers the entire winter and the beginning of spring (Dec 6 1996 to Apr 21 1997). This evolution is interrupted by an increase in flow rates in April (Apr 22 1997 to May 24 1997). Subsequently, flow rates are low, but in June, a new increase occurs in response to rainfall, causing an increase in contaminant concentrations (Fig. 4.52).

Once regression equations are obtained, the concentration and contaminant load are calculated based on daily flow rates. Monthly and annual contributions of each element are derived from daily contributions. In periods where the obtained correlations were not significant due to the presence of some unusual samples (high concentrations of metals or, conversely, very low concentrations), the weighted average method has been used, ensuring that the samples reasonably represent the flow rate variability.

The accuracy of contaminant load calculations depends on the representativeness of samples, the precision of chemical analyses, and the accuracy of flow rate data. Regarding analytical data, the protocol used has been evaluated by various laboratories, and the analyses have been validated with reference materials, making them highly reliable. However, the same level of certainty cannot be claimed for flow rate data. The gauge station on the Odiel River at Gibraleón does not have a weir (an artificial channel), making the information less reliable, and currently, flow rate data is not recorded. Until 2008, flow rates were calculated based on water level, recorded using a limnigraph. However, in many previous periods, this equipment experienced malfunctions, so there are no flow rate data available.

In the Tinto River, there is currently a flow rate station with a weir at Gadea (at the crossroads of La Palma del Condado and Valverde del Camino towns, Fig. 4.53). But previously, it had the same issues as the Odiel River gauge station at Gibraleón, with numerous months lacking information. In months where flow rate data is unavailable, contaminant load has been estimated based on its correlation with precipitation data in the Tinto and Odiel basins.

Finally, in the Tinto River, the gauging station is located at Gadea (Fig. 4.53), about 12 km upstream from the sampling point of Niebla. This circumstance requires applying a correction factor for calculating the pollutant load. The correction factor has been estimated based on the drainage areas of the river at Gadea (756 km^2) and Niebla (950 km^2). The flow of the Tinto River at Niebla can therefore be estimated by multiplying the flow at Gadea by a correction factor equal to the ratio of the drainage areas of both basins, which is 1.256 (950 km^2/756 km^2).

4.3.2. Pollutant load delivered to the Ria de Huelva estuary

Based mainly on the relationships between element concentrations and flow rates, the load of dissolved pollutants transported by the Tinto and Odiel rivers has been estimated. The initially period considered was between the hydrological years 1995/96 to 2002/03 (Olías et al., 2006), and it was later extended until the year 2005/06 (Cánovas, 2008).

Table 4.6 shows the total average values of the dissolved pollutant load for both rivers, along with the percentages representing the contribution of each river to the total received

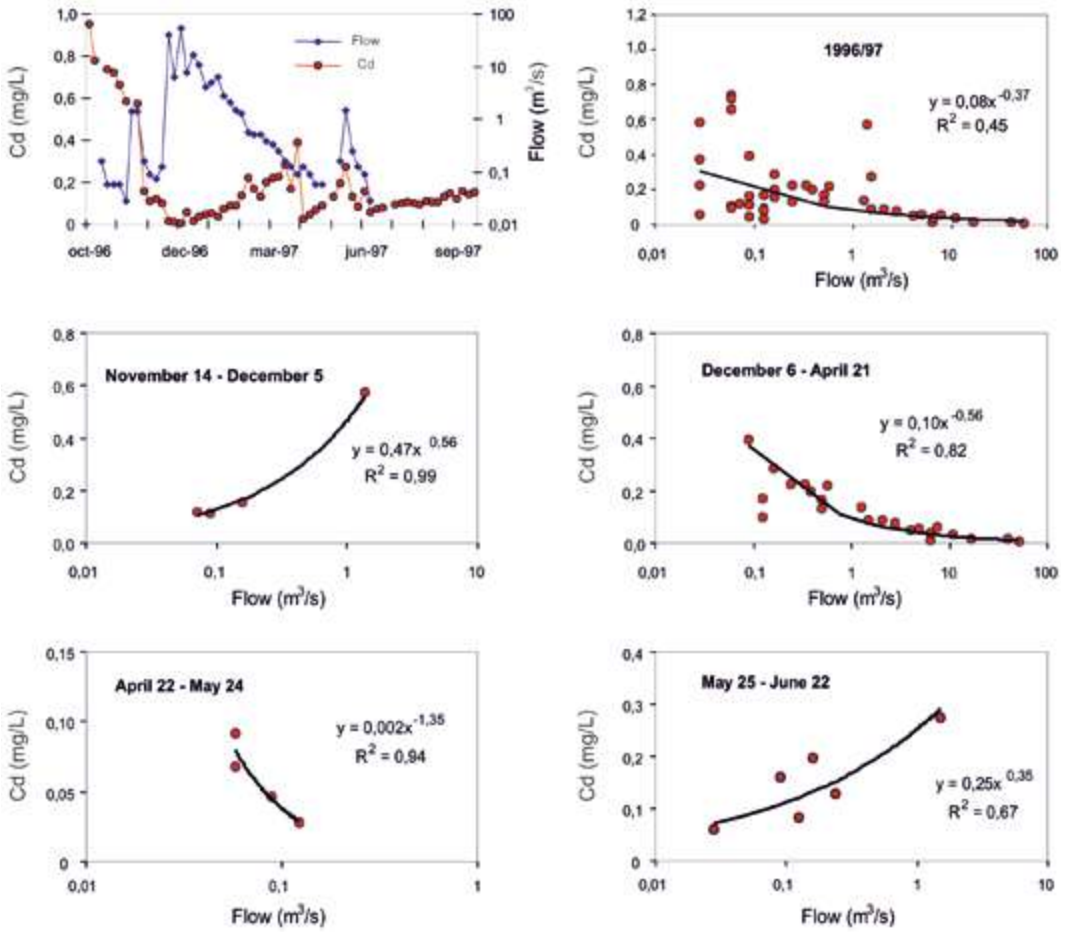

Figure 4.52: Relationship between flow rate and dissolved concentration of Cd in the Tinto River for the whole hydrological year 1996/97, and for the different periods identified.

Figure 4.53: Gauge station in the Tinto River at its lower reach (Gadea).

by the Huelva estuary. The considered period is somewhat wetter than normal, so the average pollutant load may be slightly overestimated (Olías et al., 2006). Although the conditions are more extreme, and pollutant concentrations are higher in the Tinto River, the Odiel River contributes more pollutants to the Huelva estuary due to its higher flow rate, except for Fe and Pb. The difference is most significant in the case of Ni and Mn, where the contributions from the Odiel River are six times higher than those from the Tinto River. For other pollutants, the load transported by the Odiel River is 2 to 3 times greater than that transported by the Tinto River. It should be noted that the values for Al, Co, and Ni were calculated with fewer analytical data and are subject to greater uncertainty

	Tinto		Odiel		Total
	ton/yr	%	ton/yr	%	ton/yr
SO_4	34700	23	115100	77	149800
As	10	33	21	67	31
Cd	3	36	6	64	10
Cu	450	31	1000	69	1450
Fe	4900	69	2200	31	7100
Mn	180	13	1200	87	1380
Pb	13	56	10	44	23
Zn	750	27	2000	73	2750
Al	1450	29	3600	71	5050
Co	11	23	36	77	47
Ni	3	16	18	84	21

Table 4.6: Average values of dissolved pollutant loads carried by the Tinto and Odiel rivers from 1995/96 to 2005/06.

If these values are compared with those obtained by GESAMP (1987) regarding the transfer of dissolved metals from all rivers worldwide to the seas and oceans, it is evident that the amounts contributed by the Tinto and Odiel rivers during the study period represent extremely high percentages. Thus, two small rivers in the province of Huelva transport 14% of all dissolved Cu reaching the oceans worldwide and 47% of Zn. Similarly, it is observed that the quantities transported by the Tinto and Odiel rivers are much higher than those transported by large rivers in European industrial areas such as the Elbe, the Seine, and the Rhine (Olías et al., 2010).

Figure 4.54 illustrates the dissolved pollutant load transported by the Tinto and Odiel rivers during this period. It is observed that the evolution is mainly controlled by precipitation, so that in rainier years, the rivers transport more pollutants. In recent years (2002 to 2006), there is a decrease in the pollutant load because these years were drier. In other words, although concentrations decrease during floods, the amount of pollutants transported during these periods increases significantly due to higher flow rates.

The pollutants transported by the Tinto River come exclusively from the Riotinto mines and, to a lesser extent, from Peña del Hierro. Regarding the Odiel River, using a hydrological model and the relationships between the flow rates obtained and pollutant concentrations, Galván et al. (2016) determined that, in the period 1980/2010, approximately 50% of the dissolved pollutant load reaching the Huelva estuary comes from the Riotinto mines. The average pollutant load values calculated in this way were similar to those in Table 4.6, except for aluminum (Al), for which Galván et al. (2016) obtained a much higher value (9100 ton/year), indicating that the data in Table 4.6 might be underestimated.

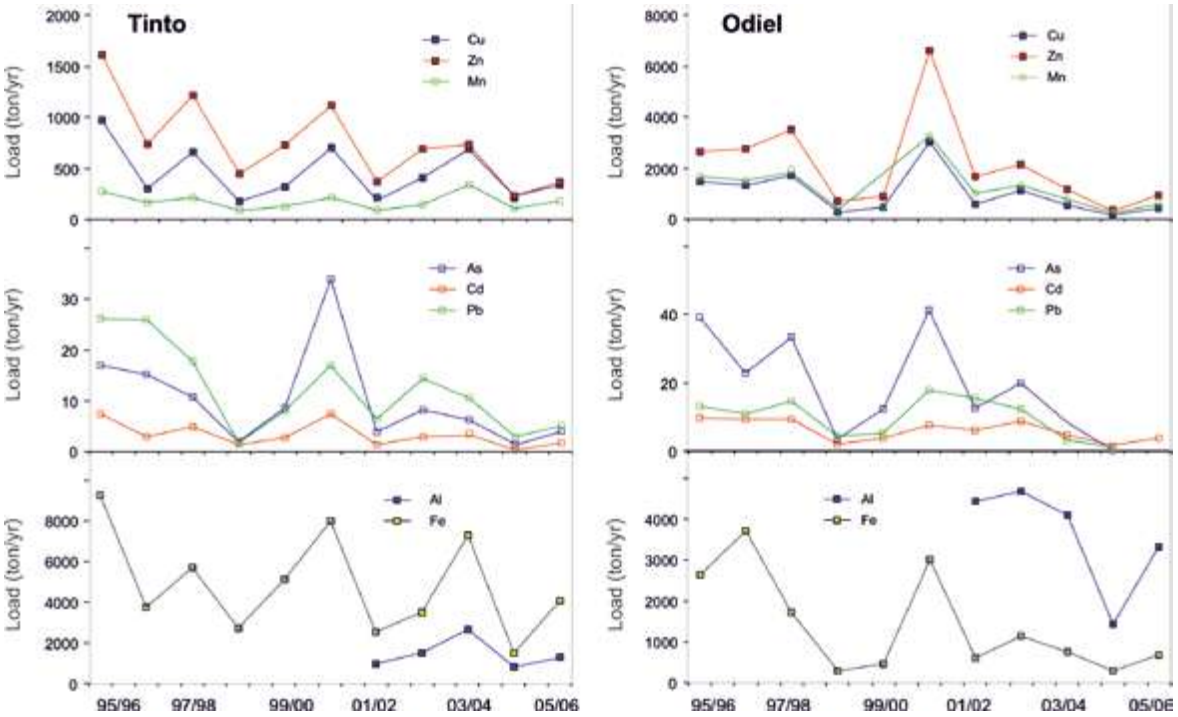

Figure 4.54: Evolution of the dissolved pollutant load carried by the Tinto and Odiel rivers to the Ría de Huelva estuary from 1995 to 2006.

During the year 2017/18, a detailed sampling was carried out at the Gadea gauge station in the Tinto River using an automatic sampler. Samples were taken at intervals ranging from 2 to 24 hours, with higher frequency during floods and lower frequency during dry periods. Out of all the samples, 143 were selected for analysis, allowing for a precise characterization of the pollutant concentration evolution for this period. The pollutant load was calculated by interpolating concentrations between two consecutive samples and multiplying them by the flow rate at each moment. The precipitation during that period (2017/18) was similar to the average, although the autumn and winter were dry, and the most intense rainfall occurred in March. The results obtained are shown in Table 4.7; the Tinto River transported nearly 5000 tons of Fe, 2600 tons of Al, 680 tons of Zn, 560 tons of Cu, etc. The values match those obtained for the period 1995/96-2005/06, except for As and Al (Olías et al., 2020)

	ton/yr		ton/yr
SO_4	49420	Cu	556
Al	2593	Fe	4963
As	3.6	Mn	234
Cd	2.1	Ni	3.0
Co	15	Pb	15
Cr	0.44	Zn	683

Table 4.7: Dissolved pollutant load carried by the Tinto River obtained from a high-resolution sampling during the hydrological year 2017/18.

The annual distribution of the pollutant load carried by the Tinto River in 2017/18 is shown in Figure 4.55. In March, the water contribution accounted for 65% of the total Tinto River

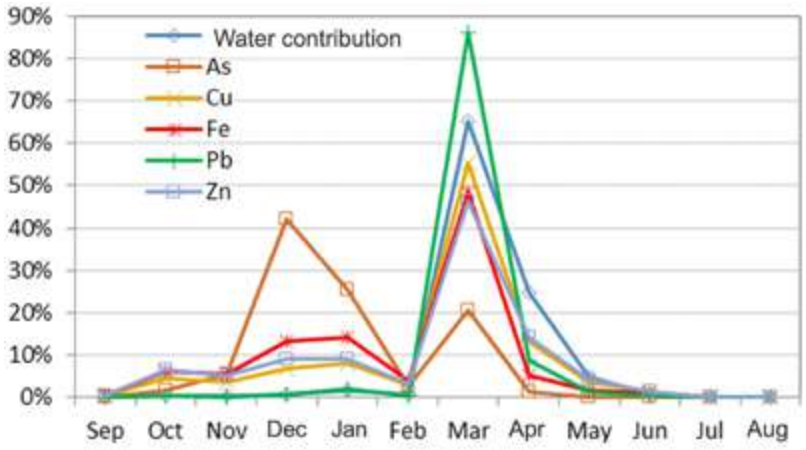

Figure 4.55: Monthly distribution of water contribution and dissolved pollutant load for some mining-related elements transported by the Tinto River in 2017/18.

annual flow, and consequently, most of the pollutants were also transported, especially Pb (86% of the total annual load), as its concentration increased during floods. Arsenic (As) exhibited a unique behavior, being predominantly transported in December and January. This is attributed to the different hydrochemical behavior of this element (Olías et al., 2020).

All figures discussed in this section refer to dissolved concentrations; however, some elements (especially As, Fe, Cr, and Pb) are primarily transported as particulate matter. For instance, in the high-resolution sampling of the Tinto River in 2017/18, it was found that the presence of Al, Cd, Co, Cu, Ni, and Zn in particulate matter was negligible (less than 2% of the total), while for Cr and Pb, it ranged between 10 and 30% of the total. For Fe, it ranged between 30 and 50%, and for As, it was highly significant, constituting more than 90% of the total (Olías et al., 2020). Similarly, in the study of a flood event in the Odiel River, it was observed that there was a significant transport of As in the particulate phase. Additionally, the particulate load of Fe was 37 times higher than the dissolved load, and that of Pb was 8 times higher (Cánovas et al., 2012).

When these acidic waters reach the Ría de Huelva, they mix with seawater, and the pH increases. As a result, many elements are not stable in solution and precipitate (e.g., Grande et al., 1999 and 2003; Hierro et al., 2014). Consequently, sediment pollution levels in the Ría de Huelva are extremely high. Some elements can enter the food chain, posing a serious environmental problem, as detailed in Chapter 6.

4.4 MAIN CONCLUSIONS

The Tinto River is affected by the Peña de Hierro mine in its headwaters and, to a much greater extent, by the Riotinto mines. In the Peña de Hierro area, there are some natural acidic springs, but their flow rates are low, and their conditions are much less extreme (contaminant concentrations about 1000 times lower than those from mining facilities). Downstream the Riotinto mines, the river no longer receives additional contaminant inputs, and concentrations progressively decrease due to dilution with unaffected streams and the precipitation of iron and co-precipitation of other elements, especially arsenic. However, before reaching the Ría de Huelva estuary, it still has extreme contaminant levels, with average values of 334 mg/L of Fe, 53 mg/L of Zn, 797 µg/L of As, etc.

The Odiel River receives contaminant inputs from numerous mines, with the most significant coming from Riotinto. Other highly contaminating mines include Tharsis, San Telmo, and La Zarza. The Odiel river courses exhibit varying levels of contamination, ranging from

very low concentrations of contaminants in some streams to extreme pollution in others. The main course of the Odiel River exhibits a 'very high' contamination level from the confluence of the Agrio River, originating from the Riotinto mines, to its mouth in the Ría de Huelva estuary. The main courses of the Oraque and Meca rivers also present a similar level of impact. Concentrations of most contaminants in the Odiel River before the Ría de Huelva are about three times lower than those in the Tinto, reflecting that the Tinto River receives almost three times the contaminants in relation to its flow. Consequently, acidic mine leachates undergo greater dilution and neutralization in the Odiel, leading to higher precipitation of iron and co-precipitation of arsenic. Therefore, concentrations of these elements are much higher in the Tinto (between 19 and 26 times).

Contaminant levels from mining activities follow a seasonal cycle. During summer, oxidation of sulfides, lower dilution with freshwaters, and evaporation lead to a progressive increase in dissolved element concentrations and the precipitation of evaporitic sulfate salts. These salts are soluble and redissolve with the first rains after summer, typically in October, causing the sudden release of acidity, sulfates, and metals they contain, resulting in the highest pollution levels of the year. Similar episodes, albeit of lesser magnitude, can occur in spring or other seasons when precipitation follows a long period of drought. Winter floods dilute contaminants, reducing concentrations. In spring, concentrations begin to rise again, closing the annual cycle.

Historical water quality data from the Tinto and Odiel rivers, available since 1968, allow differentiating three periods with different pollution levels: 1) an initial period with relatively lower pollution levels (from the start of the data series until approximately 1975), 2) a deterioration of conditions from 1976 to 1995 due to increased mining activity without environmental control measures, and finally, 3) a slight decrease in pollutant levels from 1996 to the present. However, due to the persistence of AMD processes, it is expected that current pollution levels will persist for a long time if restoration measures are not adopted.

Contaminant concentrations are also influenced by actions taken in mines, which can lead to a reduction or increase in pollutant emissions. For example, in the year 2000, a significant pollution peak was observed in the Tinto River linked to the suspension of environmental control activities. Additionally, sporadic releases of large amounts of contaminants due to accidents, such as the discharge of nearly 300,000 m^3 of extremely acidic waters from the La Zarza pit lake in May 2017, can contribute significantly to worsen the conditions in the Odiel River and the upper part of its estuary.

The Tinto and Odiel rivers annually transport an enormous amount of dissolved contaminants to the Ría de Huelva estuary, with almost 7000 tons of Fe, 2750 of Zn, or 1450 of Cu, as well as significant quantities of other highly toxic elements such as As, Cd, or Pb. To provide an idea of the magnitude of these figures, comparing these data with estimates by GESAMP (1987) of the amount of dissolved metals reaching the world's oceans and seas, the Tinto and Odiel rivers alone would contribute 47% of Zn and 14% of Cu delivered to oceans worldwide. Although contaminant concentrations are higher in the Tinto River, the Odiel represents a greater contribution of contaminants to the Ría de Huelva due to its higher flow, except for Fe and Pb, primarily contributed by the Tinto.

During flood periods, dissolved concentrations in the water decrease, but the significant increase in flow causes the contaminant load to increase markedly. Therefore, these periods represent a very important percentage of the annual quantity of pollutants transported by the Tinto and Odiel rivers.

Most mining-related contaminants (such as Al, Cd, Co, Cu, Mn, Ni, Zn, and sulfate) are transported in the dissolved phase by IPB rivers, making suspended transport negligible. However, for Cr, Fe, and Pb, particulate transport can constitute a significant percentage of the total, while it is predominant in the case of As.

5

POLLUTION IN WATER RESERVOIRS AND MINING PIT LAKES

5.1. Acidification processes in reservoir waters of the IPB

5.1.1. Introduction

The water quality of reservoirs is strongly influenced by activities developed in their watershed (Igarashi and Oyama, 1999; Cánovas et al., 2016). In areas affected by sulfide mining, the primary process leading to the degradation of water bodies is acid mine drainage (AMD). The acidity load received by the reservoir depends on the quantity of sulfide-rich mining wastes stockpiled in its watershed. Natural attenuation mechanisms, such as mineral dissolution processes in the surrounding host rocks, can neutralize this acidity, especially effective are carbonate materials (reactions 2.8 to 2.10). The precipitation of evaporitic salts (reactions 2.24 to 2.26) during dry periods in mining areas and watercourses affected by acid waters temporarily retains part of the acidity released during AMD processes. However, with the onset of the first rains, these minerals dissolve again, reintroducing acidity to the water bodies. Therefore, reservoirs susceptibility to acidification depends on the balance between the acidity load released and the neutralization capacity of rocks in its drainage basin.

Additionally, hydrological factors such as the interaction between groundwater and surface water, spatial and temporal variability in acidity sources, and runoff generation play a crucial role in reservoir acidification processes (Blodau, 2006). Among these factors, runoff generation is a critical parameter, especially in semi-arid climates characterized by long dry periods and short but intense precipitation events when river flow significantly increases (Fig. 5.1). During these events, large volumes of water and sediments are transported from the watershed to the reservoirs. For example, in a study on pollutant transport from the Meca River to the Sancho reservoir, Cánovas et al. (2017) found that during the November 2012 rains, 19% of the annual water input to the reservoir, along with 39% of the annual acidity and 43% of the dissolved Fe, As, and Pb load, were transported. The transport of particulate matter during this period was also significant, with approximately 332 tons of Fe, 49 tons of Al, about 800 kg of As, or 370 kg of Pb deposited in the reservoir bottom sediments.

Similar to lakes, in reservoirs, the dynamic of the water column is controlled by the relationship between the surface area of the reservoir and its depth, as well as the variation in temperatures in the area throughout the year (Wetzel, 2001). In the IPB climatic context, during spring and summer, the surface layer warms up, and therefore, its density decreases, preventing it from mixing with the deeper, denser layers of the reservoir. This creates a thermal stratification of the water column, divided into 3 layers with different characteristics (Fig. 5.2): i) the *epilimnion* or upper layer, characterized by lower density, because of higher temperature, and elevated concentration of dissolved oxygen, as it is in contact with the atmosphere, ii) the *metalimnion* or thermocline, characterized by a sharp temperature gradient, and iii) the *hypolimnion* or lower layer, with lower temperature and higher density, which is in contact with organic matter-rich sediments, where reducing conditions can occur if dissolved oxygen is depleted. Throughout autumn and winter, the water temperature of the epilimnion gradually decreases, reaching a point where the entire water column has the same temperature, and thus, equal density. This leads to water

Figure 5.1: Tinto river at Gadea (road from La Palma to Valverde del Camino towns) during low flow conditions (left) and flood events (right), when the pollutant load delivered by the river sharply increases.

mixing (*turnover*), eliminating thermal stratification and equalizing the concentration of dissolved oxygen throughout the column (Fig. 5.2)

These processes of stratification and mixing significantly impact the mobility of dissolved metals, primarily due to different pH and redox potential conditions. For instance, Fe(III) precipitates at pH values above 3, and Al precipitates at values above approximately 4.5, while other metals require higher values for precipitation (see Fig. 2.11). Therefore, some metals transported in the dissolved form by watercourses feeding the reservoir can precipitate if the pH increases, turning into small suspended particles that may settle and deposit in the bottom sediments. These processes lead to the formation and accumulation of metallic oxides and oxyhydroxysulfates in the reservoir sediments (Torres et al., 2013). However, if dissolved oxygen in the hypolimnion is depleted, and reducing conditions are reached, the redissolution of these metallic oxides and oxyhydroxysulfates can occur, releasing the metals back into the water column (Raiswell and Canfield, 2012).

In the Spanish part of the Iberian Pyrite Belt (IPB), there are 5 large reservoirs with a capacity greater than 10 hm^3 that receive mining leachates: Sancho and Olivargas in the Odiel River basin, Andévalo and Chanza in the Chanza River basin, and Agrio in the Guadiamar River basin (Fig. 5.3). Additionally, in 2014, the construction of the Alcolea dam began at the confluence of the Oraque and Odiel rivers, with a planned reservoir capacity of 246 hm^3. This project was halted in 2017 due to issues with building companies, with approximately 25% of the dam currently built.

The following describes the characteristics of the IPB reservoirs not contaminated by acid waters (Jarrama and Corumbel reservoirs), the Olivargas and Andévalo reservoirs, which receive acid waters but have a pH close to 7 and low dissolved concentrations of mining-related metals, and the Sancho reservoir, which receives higher inputs of acid leachates and has elevated dissolved concentrations of contaminants. The data presented below correspond to the official quality control network of the Junta de Andalucía from 2008 to 2021. The Chanza and Agrio reservoirs are not considered due to issues with available analytical data (Olías et al., 2022). Finally, estimates regarding the water quality of the controversial Alcolea reservoir in case the dam construction is completed are discussed.

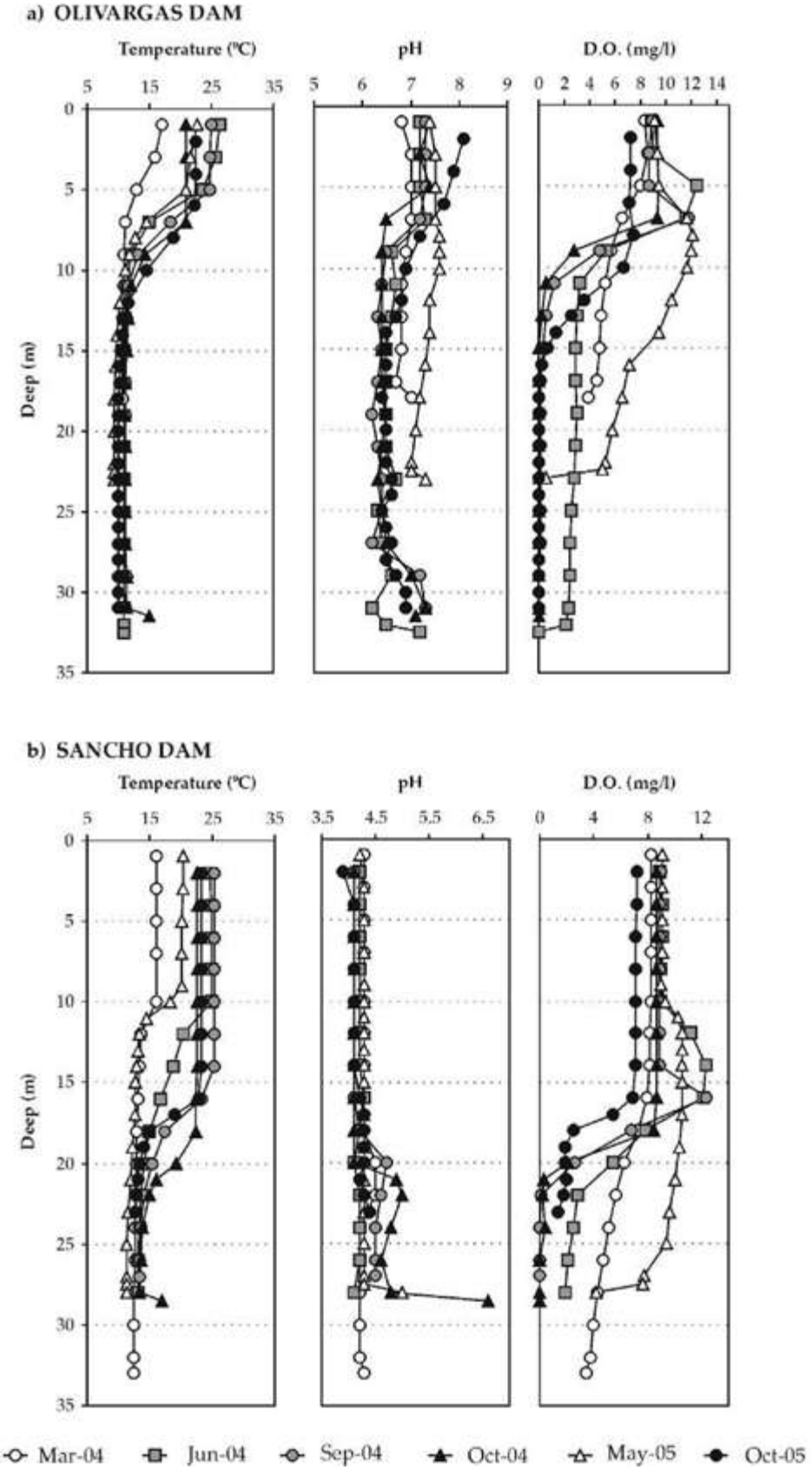

Figure 5.2: Seasonal variation of the temperature, pH and dissolved oxygen concentration (D.O.) in the water column of Olivargas (a) and Sancho (b) reservoirs due to thermal stratification processes (Sarmiento, 2009a).

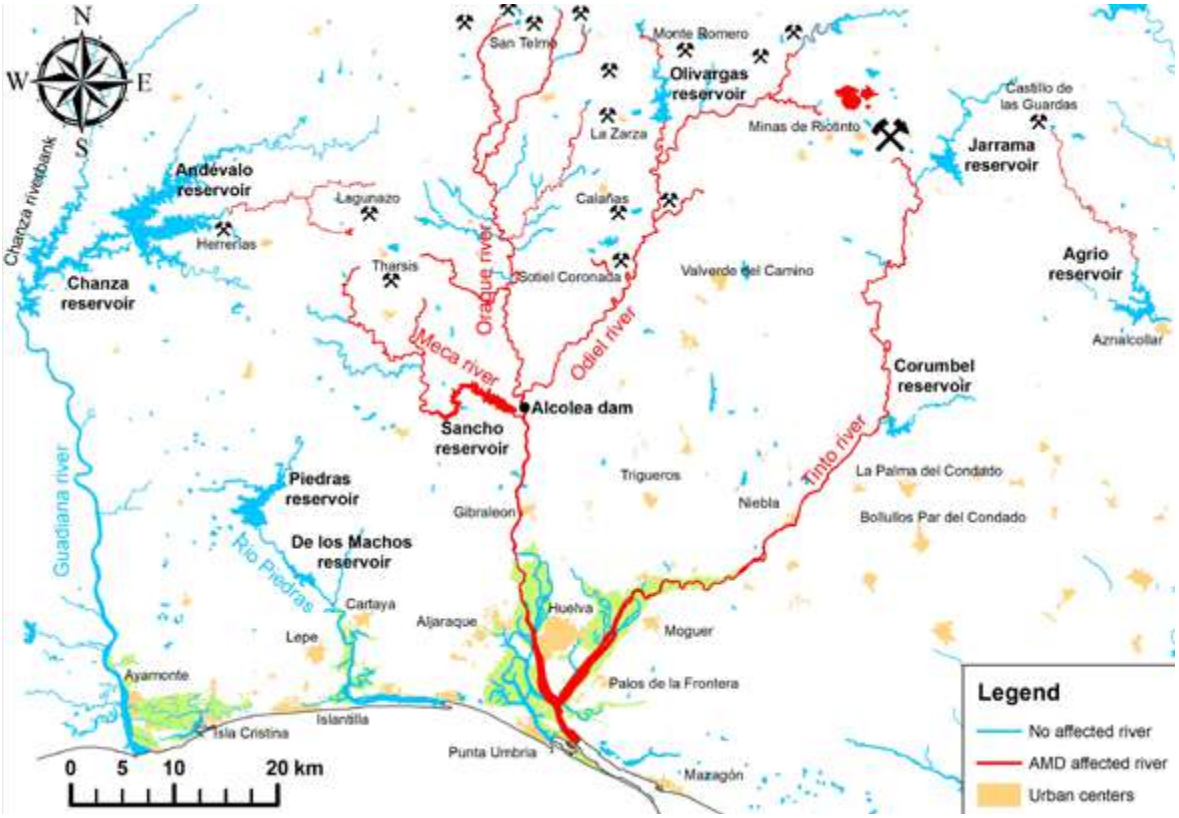

Figure 5.3: Main reservoirs existing in the Spanish part of the IPB. Main mines, AMD-affected watercourses and the location of Alcolea dam, which construction is currently stopped, are also shown.

5.1.2. Reservoirs non-affected by AMD

The Jarrama reservoir (with a capacity of 39 hm^3) is representative of the conditions of reservoirs in the Iberian Pyrite Belt (IPB) not contaminated by AMD. The Corumbel reservoir, with a capacity of 18 hm^3, is located on the boundary between the IPB and the Neogene materials filling the Guadalquivir Depression, where marly materials with high carbonate content outcrop, thus having different conditions than IPB reservoirs. Both reservoirs have pH values slightly above neutrality, with mean values of 7.7 in Jarrama and 8.0 in Corumbel (Fig. 5.4). The lower electrical conductivity (EC) value is observed in the Jarrama reservoir (mean of 125 µS/cm), while in the Corumbel reservoir, EC is higher (mean of 272 µS/cm). This significant difference is due to the higher alkalinity content in Corumbel waters (average of 88 mg/L of $CaCO_3$), as well as in Ca, Cl, and Na (Fig. 5.4), as it drains marly materials rich in carbonates.

On the contrary, alkalinity in the Jarrama reservoir is very low (average of 36 mg/L of $CaCO_3$) due to the scarcity of carbonate materials in the IPB, indicating that reservoirs located in this geological area are highly susceptible to acidification. Another interesting piece of data is the low sulfate values in both reservoirs (between 11 and 12 mg/L), clearly distinguishing them from reservoirs receiving AMD, which have high sulfate concentrations (Fig. 5.4).

The dissolved concentrations of other elements abundant in mine leachates (such as Cd, Cu, Fe, Mn, Ni, Pb, and Zn) are low in both reservoirs, with the exception of As in Corumbel (Fig. 5.5), the origin of which should be investigated.

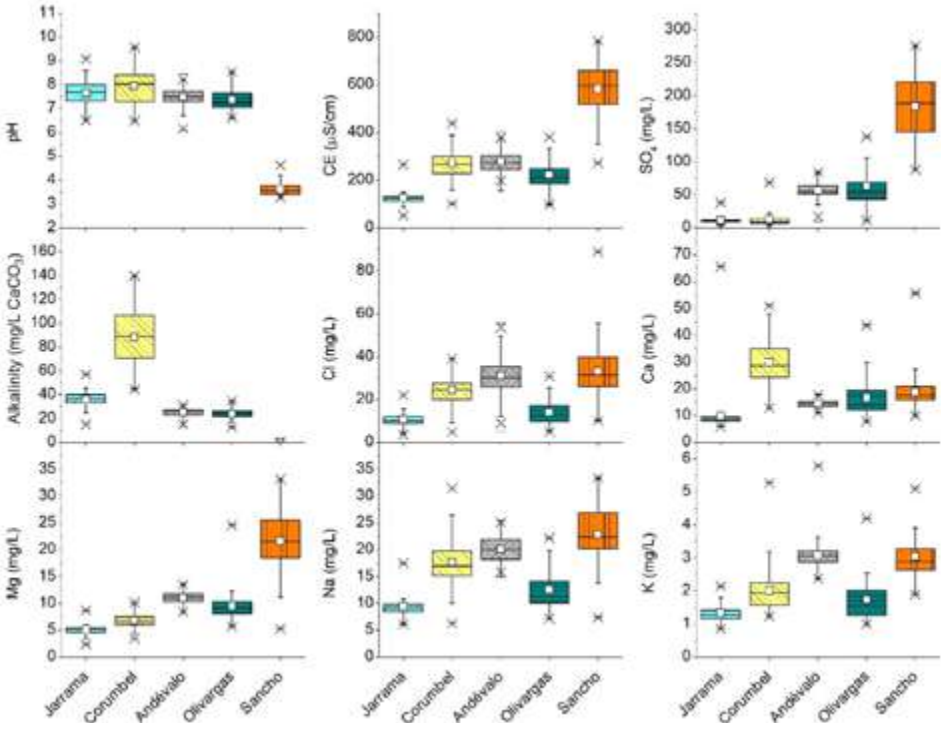

Figure 5.4: Box plots of pH, electrical conductivity (EC) and concentracions of major water components of Jarrama, Corumbel, Andévalo, Olivargas and Sancho reservoirs. The length of the box represents the interquartile range, which contains 50% of the values, and the heavy horizontal line inside the box indicates the median. The ‘‘whiskers’’ are lines that extend from the box to the highest and lowest values excluding outliers (o) and extremes (x). Outliers are defined as cases in which the values are between 1.5 and 3 times larger than the length of the box from its upper or lower border; those greater than 3 times are extremes.

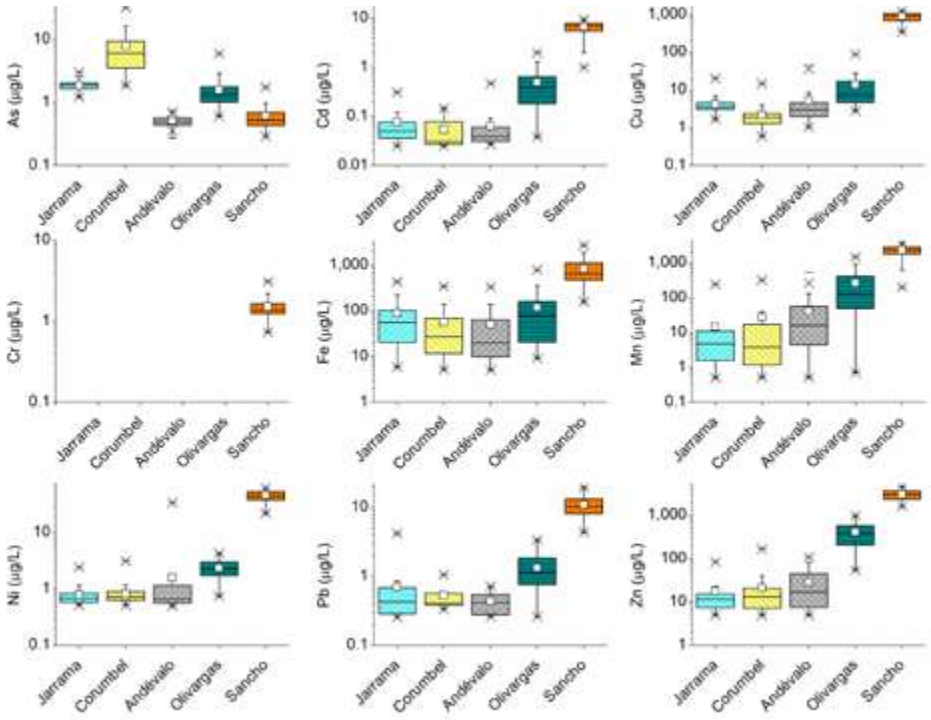

Figure 5.5: Box plots of trace element concentracions in Jarrama, Corumbel, Andévalo, Olivargas and Sancho reservoir waters (Olías et al., 2022). See figure caption of Fig. 5.4 for symbols explanation.

5.1.3. Olivargas and Andévalo reservoirs

The Olivargas reservoir was built in 1982 to supply water to the former Almagrera mine (located at Calañas). It has a capacity of 29 hm^3 and currently its waters are primarily used for agriculture and mining. The main water source for the reservoir is the Olivargas stream (67% of the total contribution), which becomes slightly contaminated as it passes through the Cueva de la Mora mine (Fig. 5.6). It also receives contributions from Los Peces stream (4% of the reservoir's contribution), which carries a significant load of acidity and metals from the Angelita and, especially, Monte Romero mines. Other contaminant contributions come from the Herrerito stream (3% of the reservoir's contribution), slightly affected by the old Aguas Teñidas mine. The remaining contribution (26%) comes from streams unaffected by AMD that flow directly into the reservoir (Galván et al., 2021).

The Andévalo reservoir was completed in 2003 and is used for irrigation, urban, and industrial supply. It is the largest reservoir in the Huelva province, with a total capacity of 634 hm^3. This reservoir receives acidic inputs from the abandoned Lagunazo and Herrerías mines (Fig. 5.3).

Despite the arrival of acid leachates, both reservoirs have pH values above 7, although slightly lower than reservoirs unaffected by AMD (Fig. 5.4). However, alkalinity values are lower (close to 25 mg/L of $CaCO_3$) and sulfate concentrations are clearly higher (approaching 60 mg/L) than those of Jarrama (Fig. 5.4).

Unlike the approximate constant values of electrical conductivity (EC) throughout the water column, redox potential and dissolved oxygen values vary associated to thermal stratification processes (Fig. 5.7). The pH values in the Olivargas and Andévalo reservoirs remain close to neutrality throughout the water column because acidic inputs are small compared to those of unaffected waters. With these pH values, the Fe and Al contained in the acidic effluents precipitate in the reservoir (reactions 2.19 to 2.23) and are deposited in particulate form in the sediments, where they can undergo further transformation. For example, pore water in the Olivargas reservoir sediments shows concentrations of up to 25 mg/L of Fe and 4 mg/L of Al, unlike the water column, where both elements are below the detection limits (Sarmiento et al., 2009a). These high concentrations of metals in sediment pore waters are due to the dissolution of Fe and Al oxides/oxyhydroxysulfates under reducing conditions.

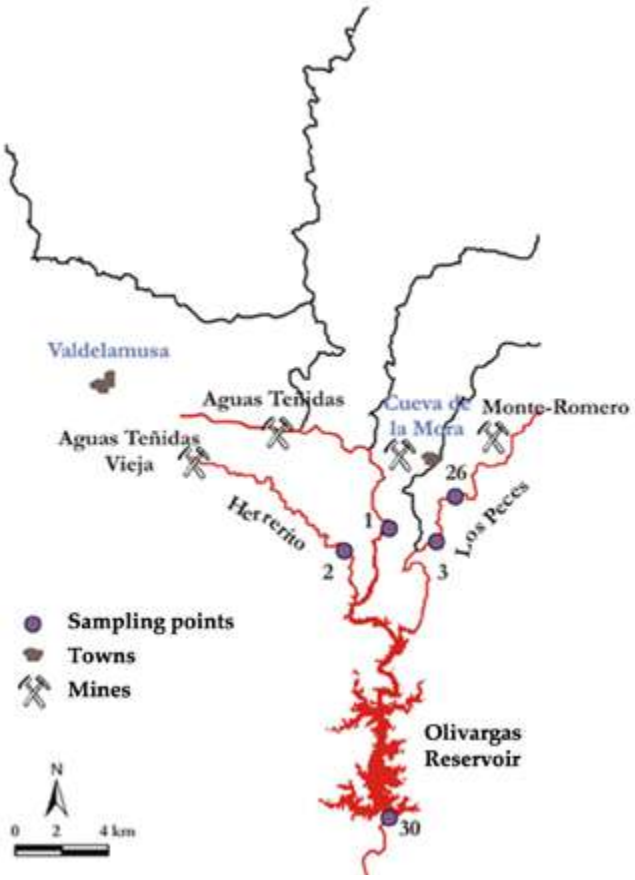

Figure 5.6: Acidic inputs to the Olivargas reservoir (Galván, 2011)

Although most metals and metalloids are retained in the sediment, they can be mobilized depending on their geochemical fractionation. In this regard, Sarmiento et al. (2009a) calculated from sequential extractions that around 97% of Zn, 95% of Cu, 91% of Co, 88% of Pb, 39% of As, and 21% of Cr could be remobilized as they are in the mobile fraction of the sediment (i.e., soluble, exchangeable, oxidizable, and reducible). This implies that these elements could return to the water column if

physicochemical conditions change. Another important factor in metal mobility in reservoirs is the accidental increase in acidity fluxes. For example, Jofre-Meléndez et al. (2017) identified anomalous pH and EC values in the hypolimnion of the reservoir in 2012 due to an accidental discharge of acid leachates. Using a mathematical model, these authors estimated that around 3000 tons of sulfate and 27 tons of Fe(II) were released in a 15-day period, altering the conditions of the hypolimnion. The reservoir conditions, however, recovered 7 months after the discharge through natural attenuation processes.

On the other hand, metals like Cd and Zn exhibit a more conservative behavior and are scarcely affected by the precipitation processes occurring in the reservoir, remaining therefore in solution. Thus, due to the high concentrations of these elements in the acidic leachates from the Monte Romero mine and their conservative behavior, their dissolved concentrations in the Olivargas reservoir (average value of 0.5 µg/L for Cd and 411 µg/L for Zn; Fig. 5.5) exceed environmental quality standards, resulting in a poor state of this reservoir according to current legislation (Galván et al., 2021)

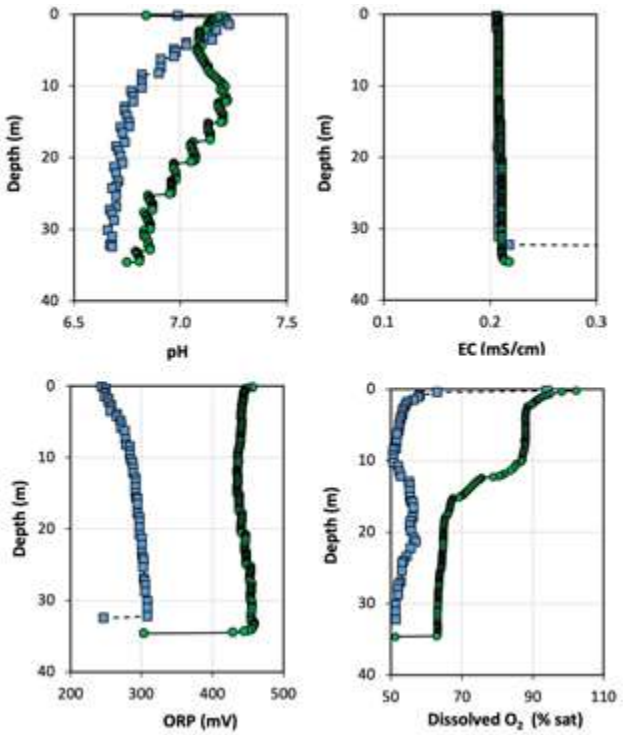

Figure 5.7: Profile of physico-chemical properties (i.e., pH, electrical conductivity (EC), redox potential (ORP) and disolved oxygen) in the Olivargas reservoir during January (blue) and February (green) 2019.

5.1.4. Sancho Reservoir

The Sancho reservoir has a capacity of 58 hm^3 and a maximum depth of 40 m (Galván et al., 2009). It was built in 1962 to supply a paper industry and was subsequently enlarged in 1972. Unlike the Olivargas and Andévalo reservoirs, the Sancho reservoir is more affected by AMD due to the input of contaminants from the Meca River, which collects acid effluents generated in the Tharsis mines. For example, in the hydrological year 2012/13, around 9200 tons of dissolved sulfates, 595 tons of Al, 255 tons of Fe, 181 tons of Zn, etc., reached the reservoir (Cánovas et al., 2017). The input of contaminants to the reservoir strongly depends on hydrological conditions. As mentioned earlier, flood events are especially important; although short-lived, they transport large quantities of dissolved contaminants (between 48 and 71% of the annual total in the year 2012/13; Fig. 5.8). The high energy of these events also increases the transport of particulate matter by the river, so that during these events, approximately 330 tons of Fe and 49 tons of Al arrived at the reservoir in the form of suspended particles, in addition to significant amounts of other metals and metalloids (Cánovas et al., 2017).

These significant contaminant inputs overcome the alkalinity supplied by uncontaminated watercourses and preclude neutralizing the acidity received by the reservoir, resulting in stored water with an average pH of 3.6 and high sulfate concentrations (average of 184 mg/L; Fig. 5.4). With this pH value, only part of the dissolved iron and other elements, such as As, coprecipitates along with Fe. Others mining-related metals exhibit a conservative behavior and remain in solution, leading to elevated concentrations of Cd, Cu, Cr, Mn, Ni,

Pb, Zn, and other elements (Fig. 5.5), much higher than those observed in the Olivargas and Andévalo reservoirs.

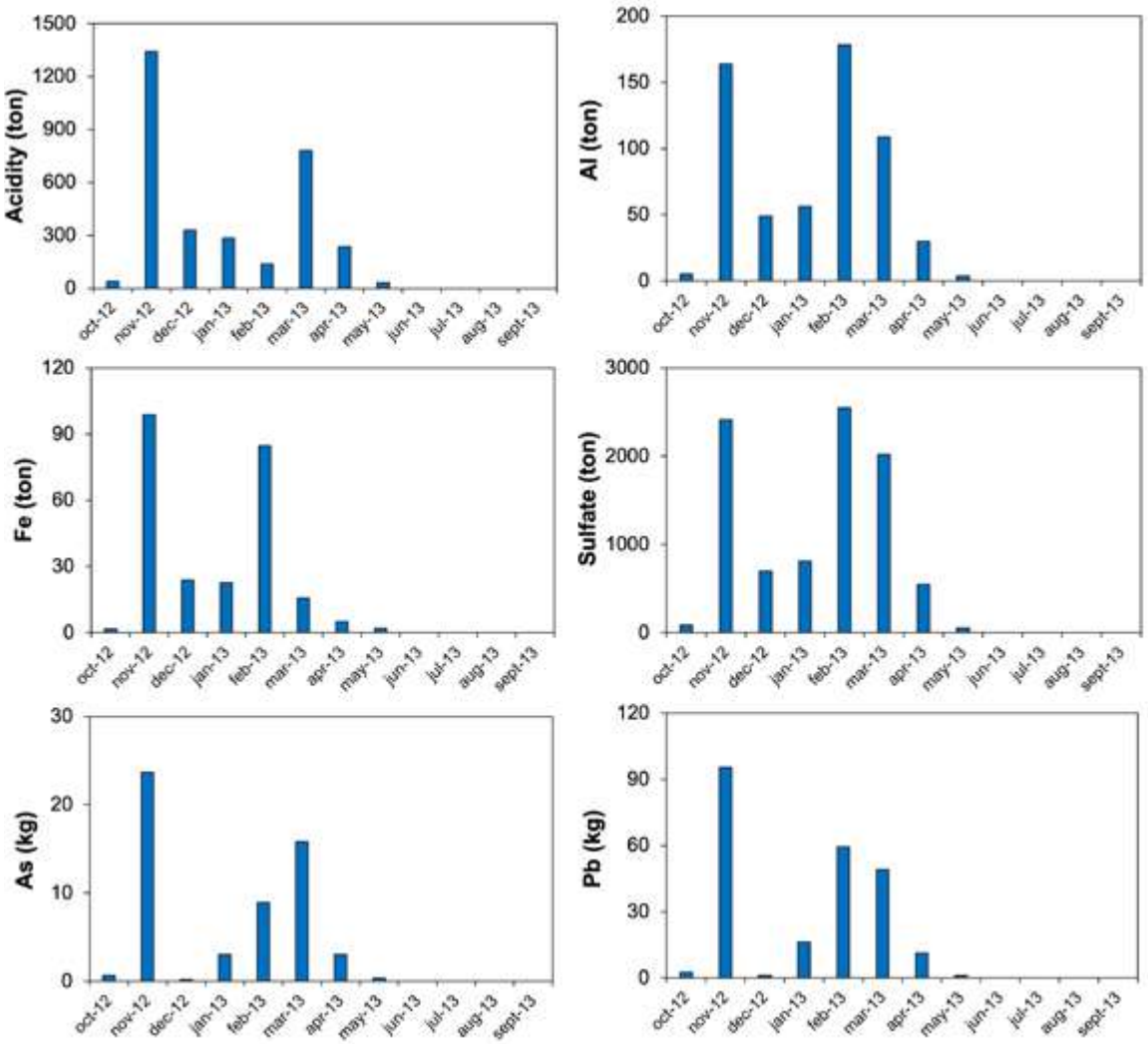

Figure 5.8: Dissolved load of pollutants delivered from the Meca River to the Sancho reservoir during 2012/13, where is clearly appreciated the importance of flood events occurred in November and February/March on the load delivery (Cánovas et al., 2017).

Figure 5.9 depicts the evolution of EC, pH, and concentrations of Fe and Zn from 1994, when data are available, until 2021. Fluctuations in the various parameters are observed due to: 1) dilution during periods of intense floods and, conversely, higher contaminant concentrations from inputs during dry periods, 2) concentration by evaporation during the low-flow period in the surface layer (epilimnion), and 3) the occurrence of thermal stratification processes during spring and summer, causing water quality differences between the epilimnion (surface layer) and hypolimnion (deep layer). These fluctuations overlay a clear trend of worsening conditions in the reservoir, especially from 2007 onwards, with a decrease in pH values from approximately 4.5 to 3.5 and a notable increase in EC, and concentrations of Fe and Zn (along with other elements of mining origin). The pH decrease indicates a shift in the pH buffering system, transitioning from being controlled by Al (pH around 4.5) to being currently buffered by Fe (pH 3.5). A study of the chemical composition

of sediments and radiometric dating identified a progressive enrichment in sulfur and metals (e.g., Fe, Zn, Cu, Ni, Co, or Cd) in the upper 20 cm of sediment, pointing to the year 2003 as the onset of worsening conditions in the reservoir (Cánovas et al., 2016). This change is attributed to the cessation of mining activity in Tharsis in the late 1990s and the lack of pumping and environmental control activities, illustrating the rebound effect commonly observed when a mine is abandoned (see section 2.4).

In this reservoir, there are no fish or any higher forms of living organisms. However, despite the observed acidity, there is a high photosynthetic activity of phytoplankton due to the

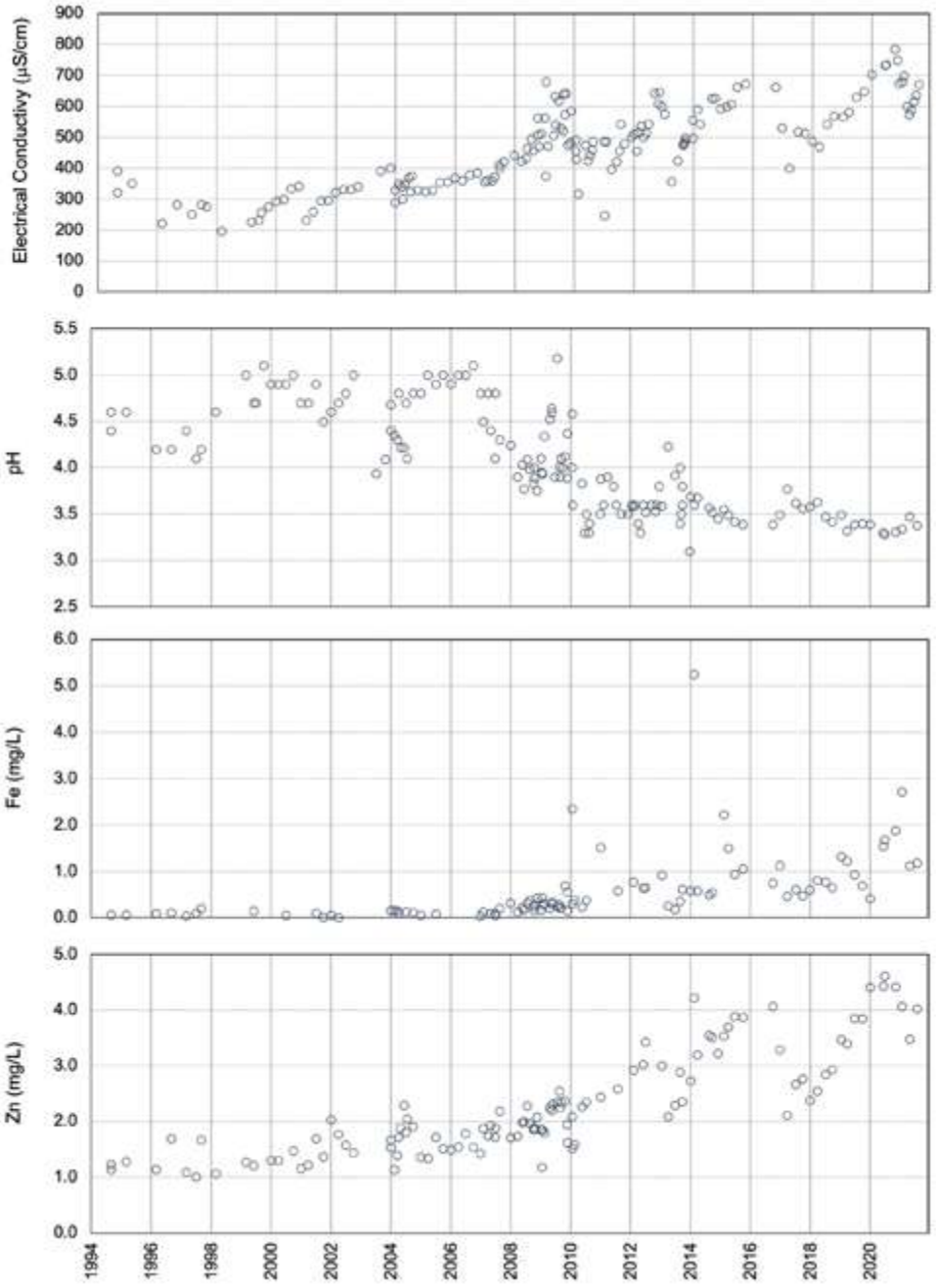

Figure 5.9: Evolution of pH and EC values, together with dissolved concentrations of Fe and Zn in the Sancho reservoir from 1994 to 2021.

availability of nutrients such as ammonium, nitrate, and phosphate (Corzo et al., 2018). The accumulation of organic matter in the bottom sediment plays a crucial role in metals mobility. Under reducing conditions, the presence of organic matter favors sulfate-reduction processes, as well as the reductive dissolution of Fe oxides/oxyhydroxysulfates and the precipitation of metallic sulfides if reducing conditions persist (Torres et al., 2014; 2016). However, when turnover occurs in the water column, dissolved oxygen reaches the hypolimnion, penetrating the most superficial layer of the sediments and causing the oxidation of organic matter and previously reduced compounds such as sulfides. This leads to a redissolution of metals into the water column. The alternation of these redox processes, therefore, controls the mobility of metals at the water-sediment interface. Nevertheless, Torres et al. (2015) confirmed that the reservoir sediments act as a net sink for metals, with an annual removal of 80% of Fe and 98% of As from the water column, around 10% for sulfate, Al, Zn, and Cu, and 2% for Co and Ni. However, if the acidification trend of the reservoir continues due to an increase in mining inputs, there could be a redissolution of metals retained in the sediments, causing a drastic increase in metal/oid concentrations in the water column (Cánovas et al., 2016). On the contrary, if AMD inputs are progressively eliminated, it is estimated that the transfer of metals and metalloids from sediments to the water column would be insignificant, due to the high sedimentation rates in the reservoir causing the burial of sulfides and preventing their re-oxidation (Torres et al., 2015).

5.1.5. Alcolea Reservoir

The Alcolea Reservoir would be located just downstream from the confluence of the Oraque and Odiel rivers (Fig. 5.3). The projected capacity of this reservoir is 246 hm^3, primarily for agricultural irrigation, including the expansion of irrigation in the Condado and Andévalo regions and the replacement of groundwater with surface water in the northern part of Doñana, to alleviate the overexploitation of this significant aquifer. To a lesser extent, urban and industrial use is also planned, along with flood prevention in Gibraleón.

The construction of the dam began in 2014 but was stopped in 2017 due to issues with the concessionaire companies, with only about 25% completion at that time. The future water quality of this reservoir has been a source of controversy since its planning in the 1990s, as both the Oraque and the Odiel rivers in this area are heavily contaminated by AMD. Recently, this controversy has increased due to a report from the Deltares Institute (Netherlands) commissioned by the Andalusian Government, stating that the water pH in the Alcolea reservoir would have a minimum pH of 6.39 (Dionisio Pires, 2021a). However, the authors later amended its conclusions in an addendum to the original report, acknowledging that their study was based on limited data, contained numerous errors, and that there is high uncertainty about the water quality in the Alcolea reservoir (Dionisio Pires, 2021b).

The dam project foresees the achievement of good water quality through the dilution of contaminants during floods and their subsequent precipitation and sedimentation in the reservoir bottom (DGOHCA, 1996). However, our studies indicate that, if acidic discharges from its watershed are not eliminated, the water will be acidic and have high concentrations of mining-derived metals such as Al, Cu, Cd, Mn, and Zn (Olías et al., 2007; 2011). On the other hand, farmers claim that the water quality in Alcolea will be suitable for irrigation, as other reservoirs in the province such as Olivargas, Chanza, and Andévalo also receive mine leachates and have neutral pH values. However, the Alcolea reservoir would receive acidic inputs from a large number of abandoned mines, including Riotinto, Poderosa, Concepción, La Zarza, Perrunal, San Telmo, Lomero Poyatos, Confesionarios, and Tharsis, so the situation of the Alcolea reservoir would be similar to that of the Sancho reservoir (Olías et al., 2022).

The dissolved concentrations of mining-related elements in the reservoir waters are primarily controlled by: 1) the balance between acidity and alkalinity received from the drainage basins, 2) dilution processes during major floods, and 3) precipitation/coprecipitation processes in the reservoir, which affect mining-related metals differently depending on the water pH.

As mentioned earlier, the water composition of the Jarrama reservoir, representative of IPB water bodies unaffected by AMD, has average pH values of 7.7, EC of 125 µS/cm, and low alkalinity (36 mg/L $CaCO_3$). In contrast, the Sancho reservoir exhibits acidic conditions (average pH of 3.6) and elevated concentrations of sulfate (184 mg/L; Fig. 5.5) and toxic metals (835 µg/L Fe, 3064 µg/L Zn, 6.6 µg/L Cd, etc.). The Andévalo and Olivargas reservoirs have neutral pH values, low alkalinity (around 25 mg/L $CaCO_3$), and sulfate concentrations close to 60 mg/L (Fig. 5.5), due to a lower impact from acidic waters compared to the Sancho reservoir.

The sulfate concentration in surface waters of the IPB is a good indicator of AMD contamination and allows quantifying the acidity load reaching each reservoir. In areas not affected by AMD, dissolved sulfate in water is primarily originated from atmospheric aerosols. Considering that sulfate concentrations in the Jarrama and Corumbel reservoirs (average of 11.5 mg/L) as background values in non AMD-affected IPB reservoirs, the difference between the sulfate concentration in each reservoir and this background value would represent the contribution associated to mining contamination. Therefore, in the Sancho reservoir, the contribution of mining-derived sulfate would be 172.5 mg/L (184 mg/L minus 11.5 mg/L), while in the Olivargas and Andévalo reservoirs, it would be 51.5 and 45.5 mg/L, respectively. Multiplying these values by the average contribution to each reservoir allows estimating the acidity they receive, as for every mole of sulfates, the reservoir would receive one mole of H_2SO_4. Thus, it is calculated that the Olivargas reservoir receives approximately 2700 tons of H_2SO_4 per year, while the Andévalo and Sancho reservoirs would receive values close to 5600 tons. However, it is important to consider that the water contribution to the Andévalo reservoir is much greater than that to the Sancho reservoir, making the impact of the acidity load much higher in the latter case. Calculating the acidity load received per hm^3 of water contribution, it is found that the Sancho reservoir receives a contaminant load of 176 tons of H_2SO_4/hm^3, about 3.8 times more than the Andévalo (46 tons of H_2SO_4/hm^3) and 3.3 times more than the Olivargas (53 tons of H_2SO_4/hm^3).

Despite the acidity received, the pH values of Olivargas and Andévalo are only slightly lower than those of unaffected reservoirs (Jarrama and Corumbel) because the pH is buffered by the alkalinity contained in the reservoir waters. However, if this alkalinity were depleted, the pH would decrease abruptly. This buffering plays a critical role in water quality, as with neutral pH values, most toxic metals (such as Al, Fe, Cu, and Pb) precipitate or coprecipitate and accumulate in the reservoir bottom sediments. On the contrary, in the Sancho reservoir, alkalinity is not sufficient to neutralize the significant acidity input, explaining its acidic pH and consequently, very high concentrations of toxic elements.

The maximum sulfate concentration at which a reservoir located in the IPB would have a neutral pH

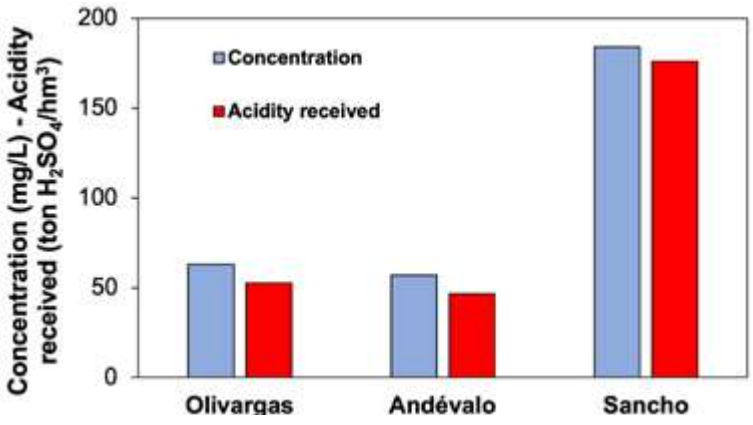

Figure 5.10: Sulfate concentration (mg/L) and acidity received by hm3 of water in main AMD-affected reservoirs in the IPB.

can be estimated using a mixing model, considering the Sancho reservoir water and runoff waters unaffected by AMD (represented by the Jarrama reservoir) as extreme endmembers (Olías et al., 2022). In this model, reactions involving the precipitation of Fe and Al mineral phases were considered, as the formation of these minerals produces acidity (see reactions 2.4 and 2.16 in Chapter 2). As seen in figure 5.11, up to a concentration of approximately 80 mg/L of sulfates, water alkalinity maintains pH values above 7. However, above these sulfate concentrations, pH decreases rapidly to 5.2 due to the depletion of alkalinity. At pH values below 5, corresponding to a sulfate concentration close to 120 mg/L, the buffering capacity of Al is depleted, and pH would rapidly decrease again to a value close to 3.5, where the precipitation of Fe would buffer the water pH.

The sulfate concentrations estimated for the Alcolea reservoir in the available previous reports vary between 157 mg/L and 292 mg/L (DOGHCA, 1996; Olías et al., 2007; ACUAES, 2010; AYESA, 2012; CEDEX, 2011, and 2022). With these values, it is evident that its waters would have acidic conditions, similar to or even worse than those of the Sancho reservoir, requiring a costly water treatment through neutralization before use. Consequently, achieving a good water quality in the Alcolea reservoir would require reducing the acidic discharges in the Odiel watershed by 45% to 70% (Olías et al., 2022).

Several recent studies have been conducted to evaluate the type of restoration measures needed in the Odiel River basin to eliminate acidic discharges and, consequently, improve the water quality stored in the future Alcolea Reservoir. An initial study, with a very limited scope as it has relied exclusively on previously published historical data, has been funded by the Huelva Provincial Council, with the participation of irrigation communities and other associations. The goal of this study is to establish the baseline situation and, based on that, secure funds for the restoration of areas affected by sulfide mining in the Odiel basin. In a preliminary estimate, it is considered that approximately 270 million euros would be needed to carry out these actions. It is important to note that, in addition to improving the state of the Odiel River basin for the Alcolea reservoir to achieve a good water quality status, the elimination of mining discharges is necessary to enjoy a river with good ecological quality, as mandated by the Water Framework Directive. For this reason, commissioned by the General Directorate of Water Resources, the Environmental and Water Agency of Andalusia has conducted a much more comprehensive study called the “Odiel River Basin Restoration Strategy.” In this case, a study focused on characterizing mining residues, affected soils, and acidic waters contained in the mining areas, along with detailed monitoring of surface waters throughout the hydrological year 2020/2021 across the entire basin. With this information, a predictive model of the hydrochemical behavior of the Odiel River has been developed, allowing simulation of the effects of various remediation actions on the final water quality in the reservoir. The main conclusion of this predictive model is that, if the corrective measures outlined in the Strategy are implemented, a reasonably ecologically good status of the Odiel River would be achieved, enabling various uses (agricultural, industrial, etc.) for the water stored in the future Alcolea dam.

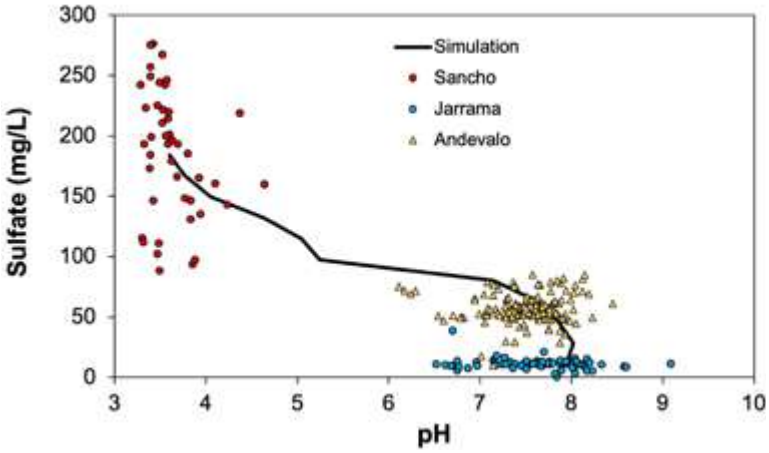

Figure 5.11: Comparison of modelled values of sulfate and pH using a 2-endmember mixing model (solid line) with those reported in studied reservoirs of the IPB (modified from Olías et al., 2022).

5.2 MINING PIT LAKES

5.2.1 Introduction

During open-pit mining operations, large pits are created where, to facilitate ore extraction, the water table must be depressed through pumping. Once mining activity ceases, along with the pumping, there is a gradual recovery of the water table, leading to the formation of anthropogenic lakes. Water inflows to these lakes occur through: 1) Direct precipitation onto the pit, 2) Surface runoff generated in the watershed draining into the pit, and 3) Contributions from groundwater. Outflows occur through: 1) Evaporation from the inundated surface and 2) In some cases, surface overflows or unnoticed underground outlets. Groundwater contributions are higher initially due to the significant water table difference between the pit and the surrounding area, decreasing as the water level rises in the pit. Conversely, evaporation outflows increase as the flooded surface area increases. The volume of water stored in the pit will progressively increase until a balance between water inputs and outputs is reached.

In the case of sulfide mining, the progressive flooding leads to wash out of the oxidation products of pyrite and other sulfides (e.g., chalcopyrite, sphalerite, arsenopyrite, etc.) present in the pit walls. Additionally, the pits are often connected to underground galleries where the oxidation of these sulfides also occurs. The acidity released during these reactions also results in the dissolution of other gangue minerals, causing the waters of these mining lakes to have high acidity and content of sulfate and metals.

There are currently 22 pit lakes in the IPB with acidic waters due to the abandonment of numerous mines, especially from the 1960s until the late 20th century (Sánchez-España et al., 2008a). Among them, Atalaya, Aznalcóllar, Los Frailes, San Telmo, and Filón Norte from Tharsis stand out for their dimensions (Table 5.1). In some of these pit lakes, such as Filón Norte and Sierra Bullones in Tharsis, equilibrium between inputs and outputs has not yeet been reached, and the water level continues to rise year after year, despite mining having ceased decades ago.

These lakes disappear if a mine is reopened, as in the case of Cerro Colorado (Fig. 5.12), since a necessary first step before exploitation is the dewatering of flooded pits and galleries below the pit. In the IPB, acidic waters must be treated before being discharged into the river network, as the stored waters contain high concentrations of toxic metals. Once the new exploitation phase ceases, the pit will be flooded again, after the water table is restored in the area.

Similar to the water level, which takes years to reach hydrological equilibrium, long periods of time are also required for hydrochemical equilibrium to be attained in the water column of a pit lake. For example, the metal concentration measured by Moreno-González et al. (2018) in Filón Centro (Tharsis) was similar to that obtained by Sánchez-España et al. (2008a) a few years earlier. However, in the Filón Norte and Filón Sur pit lakes, also in Tharsis, a significant decrease in metal concentration over time was observed. The concentration of Fe, for instance, decreased from 4620 to 2053 mg/L in Filón Norte and from 1922 to 774 mg/L in Filón Sur between both periods. This is because Filón Centro has been a stable lake since at least 1977, while Filón Sur and Filón Norte are more recent and have not yet achieved hydrochemical equilibrium conditions. Conversely, in the San Telmo pit lake, an increase in the dissolved concentration of As, Cr, Cu, Fe, and Pb was observed in recent years (Sánchez-España et al., 2008a; Cánovas et al., 2015; Fuentes-López et al., 2022).

Similar to reservoirs, mining lakes can undergo hydrochemical changes in the water column associated with thermal stratification (density differences caused by temperature) or chemical stratification (density differences due to water salinity). Lakes with relatively shallow depths that typically experience a seasonal process of stratification and water turnover are known as holomictic (Wetzel, 2001), where complete mixing of the water column occurs

	Watershed	Area ha	Depth m	Averag. radio m	Volume hm^3
Angostura[1]	Odiel	1.0	>40	55	-
Atalaya[2]	Odiel	12.3	99	198	5.4
Aznacóllar[1]	Guadiamar	28.5	38	301	6.0
Aznalcóllar-Los Frailes[1]	Guadiamar	13.3	105	206	6.3
Concepción[1]	Odiel	1.2	15	62	0.4
Confesionarios[1]	Odiel	2.5	80	89	1.0
Cueva de la Mora[1]	Odiel	1.8	39	76	0.3
Lagunazo[1]	Chanza	2.6	-	91	-
Fronteriza[1]	Chanza	0.1	-	18	-
Herrerías-Guadiana[3]	Chanza	1,8	68	75	-
Herrerías-Santa Bárbara[1]	Chanza	1.4	15	67	0.1
La Condesa[1]	Chanza	0.1	-	20	-
La Joya[1]	Odiel	0.7	-	47	-
La Zarza[4]	Odiel	8.0	80	160	1.9
Ntra. Sra. del Carmen[1]	Chanza	0.7	32	47	0.1
Peña del Hierro[1]	Tinto	1.9	-	77	-
San Telmo[5]	Odiel	18.0	>130	239	8.0
Tharsis Filón Sur[6]	Odiel	0.6	5	44	0.02
Tharsis Filón Centro[6]	Odiel	4.0	45	113	1.1
Tharsis Filón Norte[6]	Odiel	13.0	63	203	3.6
Tharsis Filón Sierra Bullones[6]	Odiel	2.0	39	80	0.5
Tinto Santa Rosa[1]	Odiel	1.1	23	59	0.1

Table 5.1: Sizes of the IPB mining lakes. (1) López Pamo et al., 2008; (2) Data from Atalaya Mining in March 2023, (3) Boehrer et al., 2016, (4) Olías et al., 2019, (5) Fuentes-López et al., 2022, (6) Moreno González et al., 2018.

at least once a year. In contrast, meromictic lakes do not undergo this mixing process due to hydrochemical differences associated with the significant depth of the water column or the input of deep, more mineralized waters (Sánchez-España et al., 2008b). In these lakes, a permanent chemical stratification occurs, featuring an upper layer or mixolimnion charac-

Figure 5.12: Left: Cerro Colorado pit lake in 2015, before the reopening of the Riotinto mine. Right: Cerro Colorado pit lake in 2017 after the pit lake water withdrawal.

terized by oxygenated waters and seasonal water mixing, and a lower layer called monimolimnion characterized by anoxic or suboxic conditions, where Fe(II) predominates in solution (Wetzel, 2001). The layer separating both is known as the chemocline. During periods of thermal stratification in the mixolimnion, the epilimnion, thermocline, and hypolimnion are clearly differentiated.

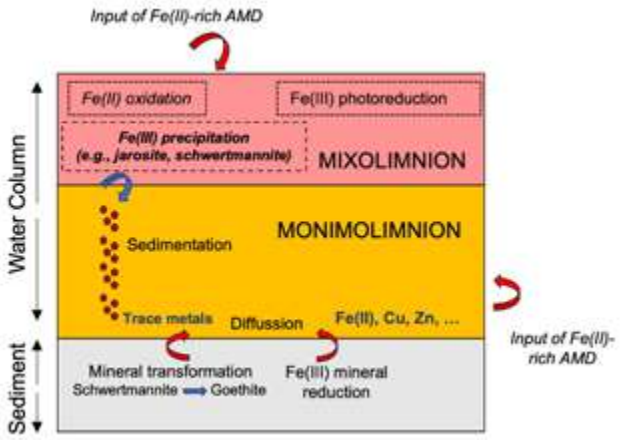

Figure 5.13: Conceptual model of main processes controlling the mobility of metals in meromictic mining pit lakes (modified from Cánovas et al., 2015).

Bacterial oxidation of Fe(II) in mixolimnetic waters typically competes with photoreduction processes of dissolved Fe(III) (Fig. 5.13), resulting in daily cycles of oxidation-reduction where the Fe(II)/Fe(III) ratio changes throughout the day (Herzsprung et al., 1998). However, bacterial oxidation processes of Fe(II) tend to predominate over photoreduction processes (Cánovas et al., 2015), leading to an enrichment in Fe(III) in this layer, resulting in the precipitation of Fe mineral phases such as schwertmannite or jarosite, buffering the pH in an approximate range of 2.5 to 3.5. These precipitates contain other trace elements, which are incorporated through adsorption or coprecipitation processes. The settle down of these particles causes an enrichment in Fe and other metals in the bottom sediments.

On the other hand, the monimolimnion is typically characterized by a scarcity or even absence of dissolved oxygen, with low redox potential values, where bacterial reduction processes of Fe(III) usually predominate. Thus, Fe(II) and other metals are released into the monimolimnion or undergo mineral transformation processes, once buried in the sediment, towards more stable mineral phases such as goethite (Cánovas et al., 2015), also leading to the release of trace metals into the water column (Fig. 5.8). Unlike reservoirs affected by AMD, where the presence of high sulfate concentrations and reducing conditions favor sulfate reduction processes, in acidic meromictic lakes, these processes are limited by the predominance of Fe(III) reduction processes over sulfate reduction, due to thermodynamic constraints upon acidic conditions (Cánovas et al., 2015).

As mentioned earlier, in the IPB most mining lakes have pH values between 2.2 and 3.6, with high sulfate and metal contents (Sánchez-España et al., 2008a). The accumulation of these acidic, metal-rich waters can pose an environmental risk. For example, in the Tharsis pit lakes, it is estimated that at least approximately 32,000 tons of acidity (as $CaCO_3$ equivalent), 9,000 tons of dissolved Fe, 1,000 tons of dissolved Al and Zn, and 47 tons of dissolved As are stored (Moreno-González et al., 2018). If these quantities are extrapolated to the total of 21 pit lakes in the IPB, the volume of acidity and metals/metalloids stored in these lakes is enormous. This could pose an environmental risk in the event of an accidental discharge, considering the uncertainty about the state of mining infrastructure in the abandoned mines of the IPB. An example of such accidental discharges occurred in May 2017 from the Zarza pit lake, detailed in section 5.2.3, with its consequences deeply discussed in section 4.2.3.

Such accidents, in addition to the sharp environmental impact, could have catastrophic consequences on the quality of reservoirs in those areas draining mine sites, leading to the acidification of reservoirs that currently have neutral pH values and good water quality. Below, the main characteristics of some of the most significant pit lakes are described, but for others, there is scarce data regarding their hydrological context. All of this highlights

the need to assess the condition of mining pit lakes in the IPB and implement restoration measures in the area.

5.2.2 Pit lakes in Tharsis

The mining activities carried out from the mid-19th to the late 20th century have left five large open-pit mines in the Tharsis area (Fig. 5.14 and Table 5.1), four of which are currently flooded with acidic waters (Filón Centro, Filón Sur, Sierra Bullones, and Filón Norte), and a large area occupied by tailings and soils affected by mining activities (Moreno-González et al., 2020).

In Filón Centro, the volume of acidic waters stored is close to 1.1 hm^3 (Fig. 5.15; Table 5.1). The water level has remained relatively constant for about 50 years since the exploitation of this open-pit mine concluded. However, there are slight fluctuations between rainy and dry periods. A water balance of the inputs and outputs to the open-pit mine has revealed that during dry years, there are no water outflows from the pit lake, that is, evaporation counterbalances inputs from direct precipitation and contributions from surface and groundwater (Fig. 5.16). In contrast, during wet years, the inputs exceed the outputs, causing a slight rise in water level and leading to outflows towards an acidic spring to the west, located at the foot of waste heaps in contact with the pit lake (Moreno González et al., 2018).

In Filón Sur (Fig. 5.17), the water level is stabilized since the cease of mining activities in 2001, with a small volume of accumulated acidic waters (barely about 20,000 m^3). However, the surface area of the open-pit mine, along with its drainage basin, is high, significantly larger than that of Filón Centro (Table 1). The water balance between inputs and outputs reveals that inputs from precipitation and surface runoff are much higher than outputs from evaporation. This implies that there may be unnoticed outflows from the pit lake. It was believed that these

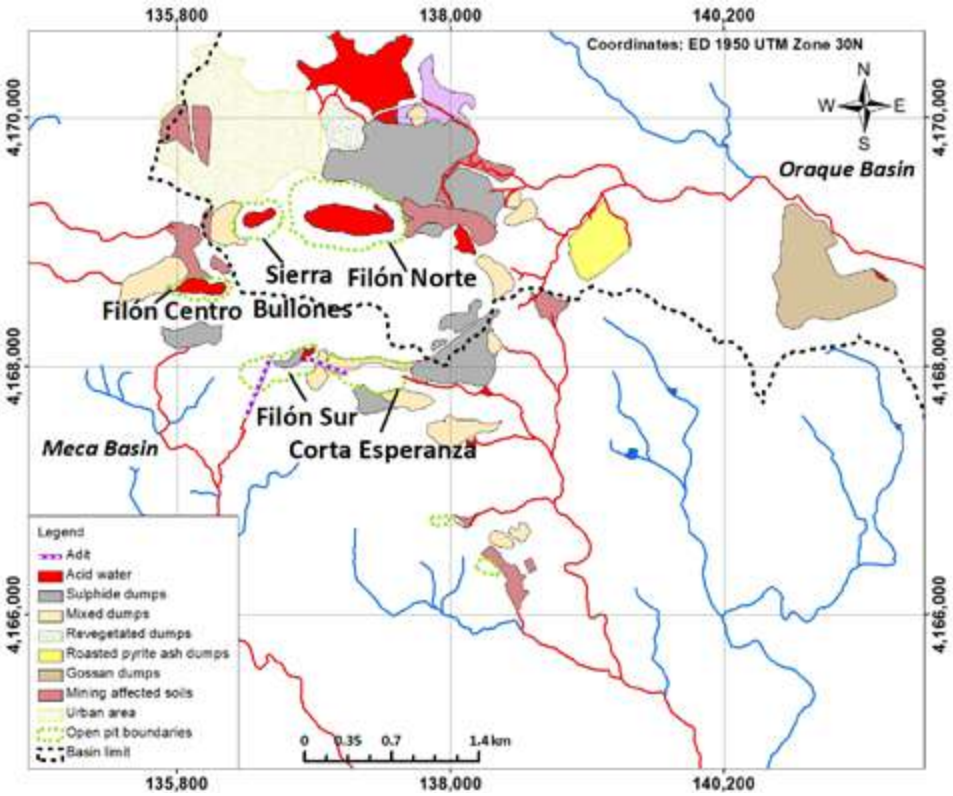

Figure 5.14: Location map of Tharsis mines, showing the occurrence of pit lakes and watercourses affected by AMD (in red).

Figure 5.15: Photo of Filón Centro pit lake in Tharsis

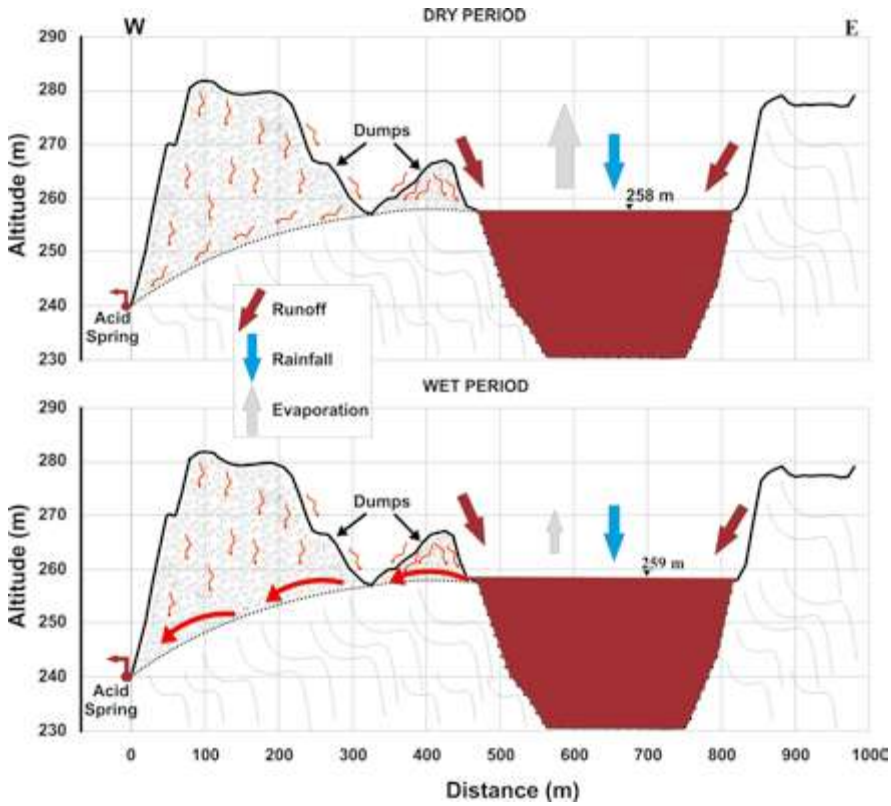

Figure 5.16: W-E schematic profile of Filón Centro pit lake, showing the inputs and outputs of waters during dry and rainy periods (Moreno González et al., 2018).

Figure 5.17: Photo of Filón Sur pit lake (Tharsis), the flooded surface and the stored acidic water volume are small despite the large pit lake surface.

outflows occurred through the La Sabina gallery, located southwest of Filón Sur (Figs. 4.34 and 5.14). However, the flow rates from this gallery are constant and much lower than what, based on its surface area, should be generated in Filón Sur. The outflow may occur through another old gallery located to the east, in Corta Esperanza (Fig. 5.18). This gallery was drilled in the late 19th century (Gonzalo y Tarín, 1888), and its outlet is currently hidden, buried under the materials filling Corta Esperanza.

Finally, the water level in Sierra Bullones and Filón Norte pit lakes (Fig. 5.19 and 5.20) has been rising since the cessation of mining activities. From historical aerial orthophotos, it is observed that both open-pits were dry in 1998 (Fig. 5.21). By 2002, Filón Norte, deeper than Sierra Bullones, started to store water. In 2004, water is observed in both open-pits, and since then, the flooded surface has been increasing, and therefore, the volume of stored acidic waters as well.

The volume of acidic waters stored in Filón Norte is much higher than that of the other open-pits in Tharsis (in 2016, it was around 3.6 hm^3; Table 5.1). Using historical orthophotos and a digital terrain model (DTM), the evolution of the flooding has been reconstructed, showing an increase of 40 meters from 2002 to 2016 (Fig. 5.22). Sierra Bullones follows the same evolution as it is connected through underground galleries to Filón Norte (Fig. 5.23). If the water level continues to rise, there could be a moment when acidic waters overflow from both open-pits, increasing the load of contaminants reaching the Oraque River through the Aguas Agrias stream (Fig. 4.26) and subsequently flowing into the Odiel River and the Huelva estuary. The overflow level is determined by an inclined plane for mineral extraction located to the east of Filón Norte at an elevation of 235 m (Fig. 5.23). A polynomial fit of the level data indicates that the water level would reach this elevation in the year 2051; however, preliminary results from a water balance analysis indicate that evaporation would offset the inputs when the level reaches 228 m, preventing the overflow from these open-pits (Fig. 5.23; Moreno González et al., 2018). It is also worth noting that Sierra Bullones receives a large volume of surface runoff due to its extensive drainage basin.

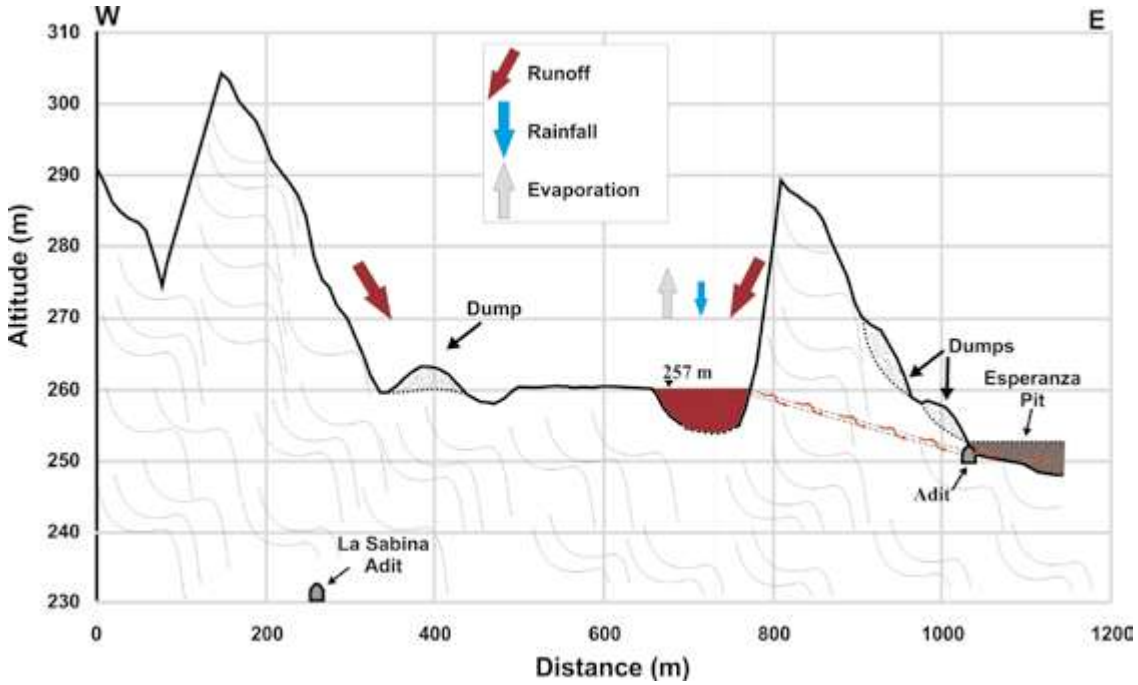

Figure 5.18: W-E schematic profile of Filón Sur pit lake, showing the inputs and outputs of waters (Moreno González et al., 2018).

Figure 5.19: Photo of Sierra Bullones pit lake in 2020, the water level is still rising.

Figure 5.20: Photo of Filón Norte pit lake in 2020, the water level is still rising like in Sierra Bullones, as both pit lakes are hydraulically connected.

Figure 5.21: Historical orthophotographs showing the progressive flooding of Filón Norte and Sierra Bullones pit lakes (Moreno González et al., 2018).

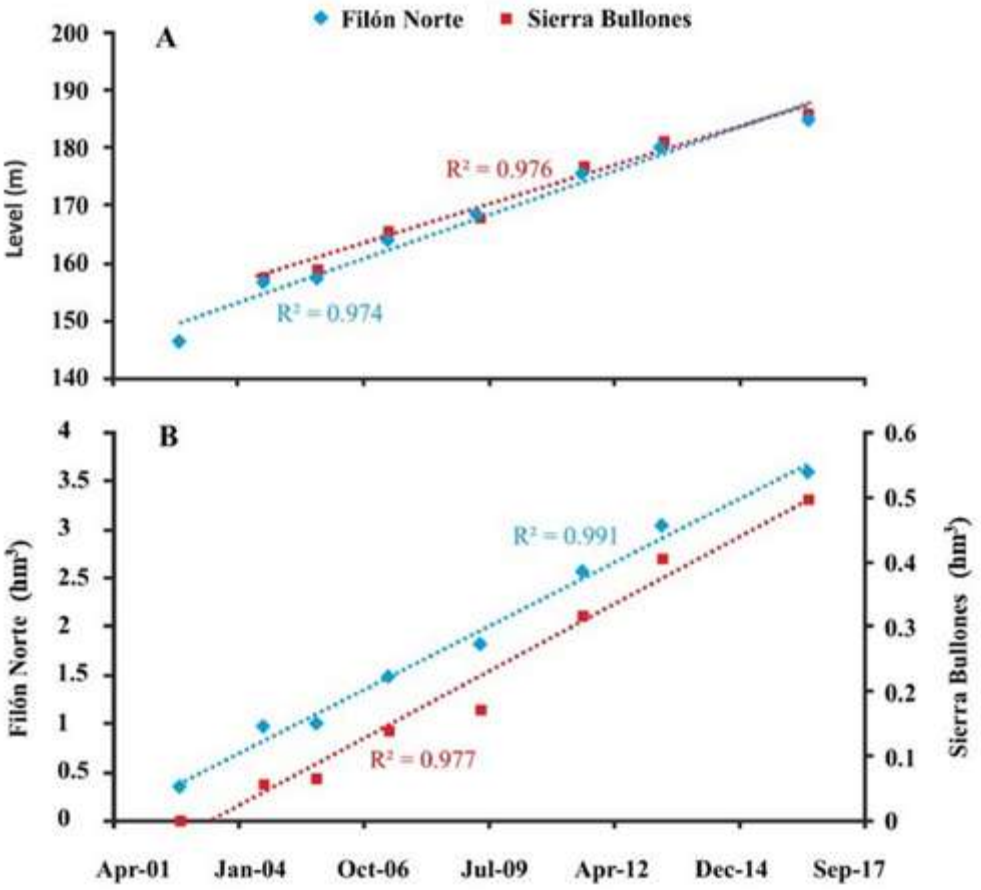

Figure 5.22: Evolution of the water level (A) and the volume of acidic waters (B) stored in Filón Norte and Sierra Bullones pit lakes (Moreno González et al., 2018)

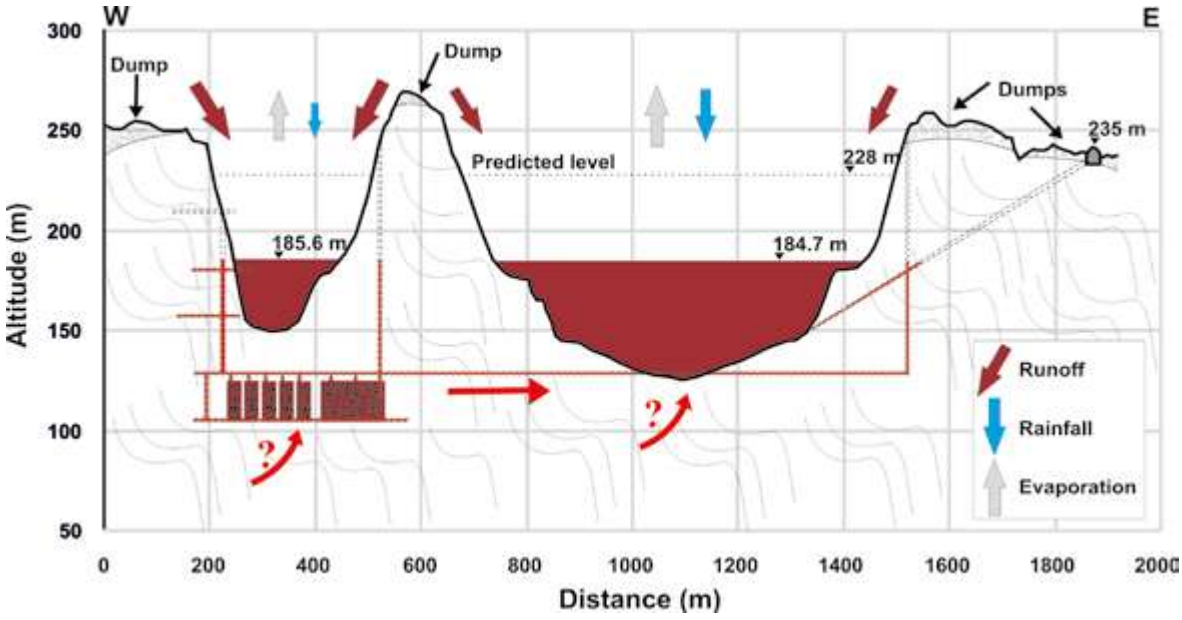

Figure 5.23: W-E schematic profile of Filón Norte and Sierra Bullones pit lakes, showing the inputs and outputs of waters (Moreno González et al., 2018). The equilibrium level estimated, when evaporation would equal to inputs, at 228 m is also indicated.

5.2.3 La Zarza pit lake

Like many other mines in the IPB, La Zarza was exploited during pre-Roman and Roman times, as evidenced by the presence of around 800 Roman wells in the area (Pinedo Vara, 1963; Checkland, 1967; Gonzalo y Tarín, 1888) and several drainage galleries, among which the most important were La Algaida, Los Cepos, and Perrunal (Fig. 5.24). Modern exploitation began in 1853. One of the first tasks carried out was the enlargement and rehabilitation of the Los Cepos gallery for mine drainage and mineral transportation. The exploitation was done using the room and pillar method until the beginning of the excavation of the open-pit in 1888, which allowed for a significant increase in production. Around 1920, once the open-pit reached a depth of about 130 m, surface exploitation was abandoned, and underground mining continued using the method of large ascending chambers (Pinedo Vara, 1963). Due to the crisis caused by the decline in commodity prices, extraction activities in La Zarza ceased in 1991, although drainage pumping in the galleries continued until 1995 (Olías et al., 2019). The La Zarza open-pit has very steep walls, with intensely red-colored waters (Fig. 5.25)

Using a digital terrain model (DTM) and available orthophotos, the evolution of the water level in the open-pit has been reconstructed. In 1998, the pit was without water (Fig. 5.26). The flooding of the pit began in 2002 and, from that date, there was a significant rise in the water level until 2016 (52.5 m), with the greatest increases coinciding with periods of heavy rainfall (Fig. 5.26). From 2011, there is a slowdown in the increase of the water level, and a trend towards stabilization is observed. After the release of acidic waters in 2017 through the Los Cepos gallery (see section 4.2.3), the water level dropped approximately 3.5 m to 210.6 m, just slightly below the gallery level. In the years following the accidental discharge,

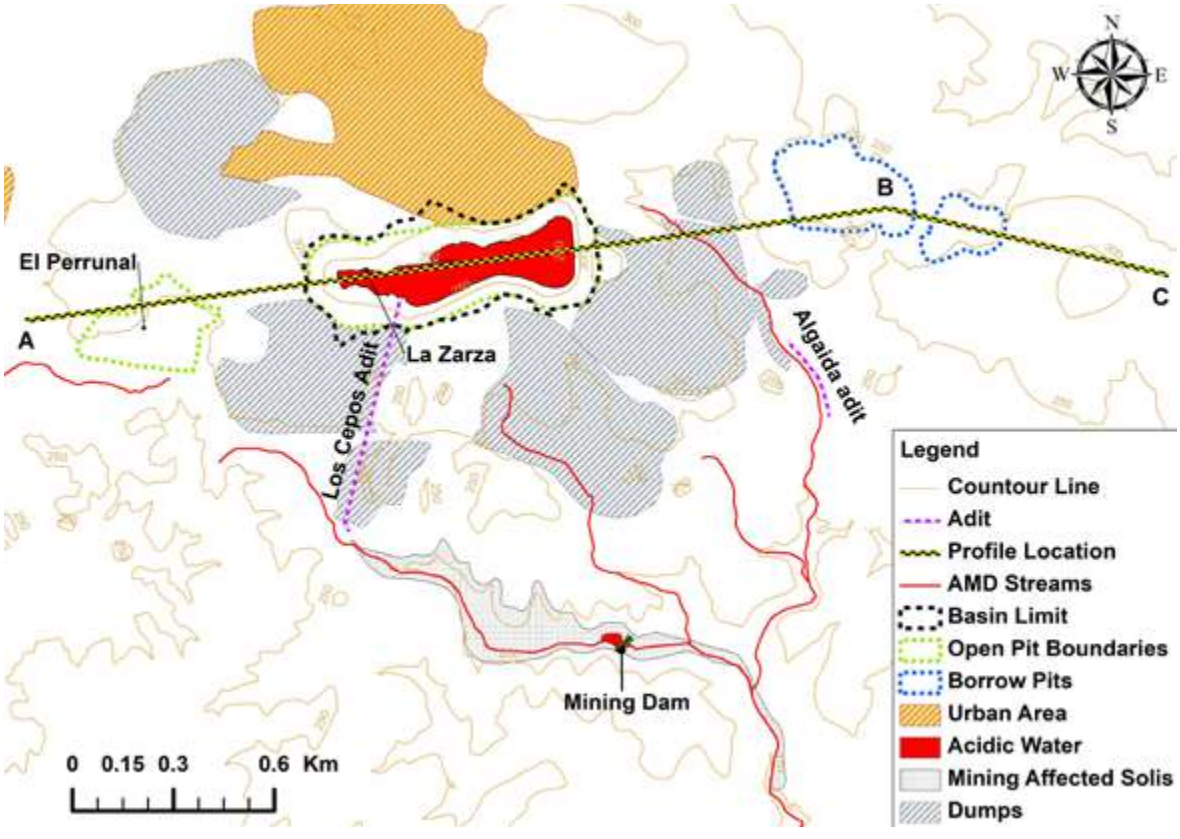

Figure 5.24: Location map of La Zarza mine, showing the occurrence of the pit lake and main old galleries.

Figure 5.25: Photo of La Zarza pit lake (October 2017), with La Zarza town in the background and some old mine works observed in the pit walls.

the water level stored in the pit rose slightly again, stabilizing near an elevation of 213 m since 2019. However, calculations of the water balance in the pit (Moreno González et al., 2023) indicate that the stabilization of the water level is not definitive but it is due to the present drought, with precipitation below average over the last 9 years. Under normal rainfall conditions, the water level in the pit will continue to rise. In this regard, the current volume of stored water would be close to 2 hm^3, in addition to the water accumulated in the underground workings.

In addition, from the water balance of inputs and outputs in the pit lake, it was concluded that the increase in the volume of stored water in the pit cannot be solely justified by precipitation over its drainage basin. Thus, there may be other hidden contributions that may come from: 1) the infiltration of precipitation and surface runoff in the quarries for backfill located east of the pit, or 2) underground discharges from the Perrunal mine (Fig. 5.24). Taking into account the calculated average inputs (from precipitation in the drainage basin and unnoticed underground contributions) as well as the average annual evaporation in the area, the water equilibrium level would be at an elevation of 245 m. In other words, it would rise about 30 m above the observed level in 2022 (Fig. 5.28). However, before reaching the equilibrium between inputs and outputs in the pit, water discharge

Figure 5.26: Orthophotographs showing the progressive fllooding of La Zarza pit lake.

could occur through the Roman gallery of La Algaida. Nowadays, the exit of this gallery is unknown, and it is likely to have collapsed. Still, according to its location on late 19th-century maps (Gonzalo y Tarín, 1888; Checkland, 1967), it would be at an elevation between 210 and 220 m. If, as it is probable, this gallery connects with modern underground workings, the maximum water level in the pit would be determined by this elevation. It could happen that this gallery is blocked by collapses, acting as a plug until the water pressure causes a rapid release. All of this underscores the need for detailed monitoring of the water level in the pit, as well as in the underground workings, and a more thorough investigation

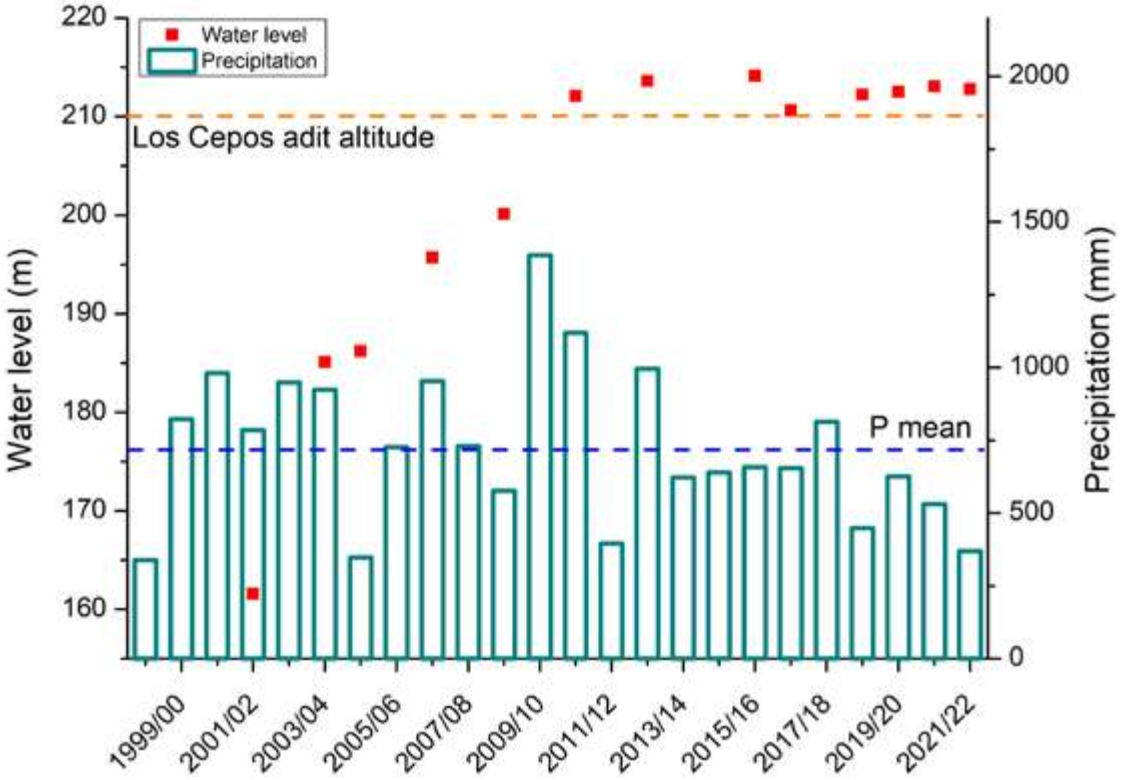

Figure 5.27: Annual evolution of rainfalls and water level in La Zarza pit lake

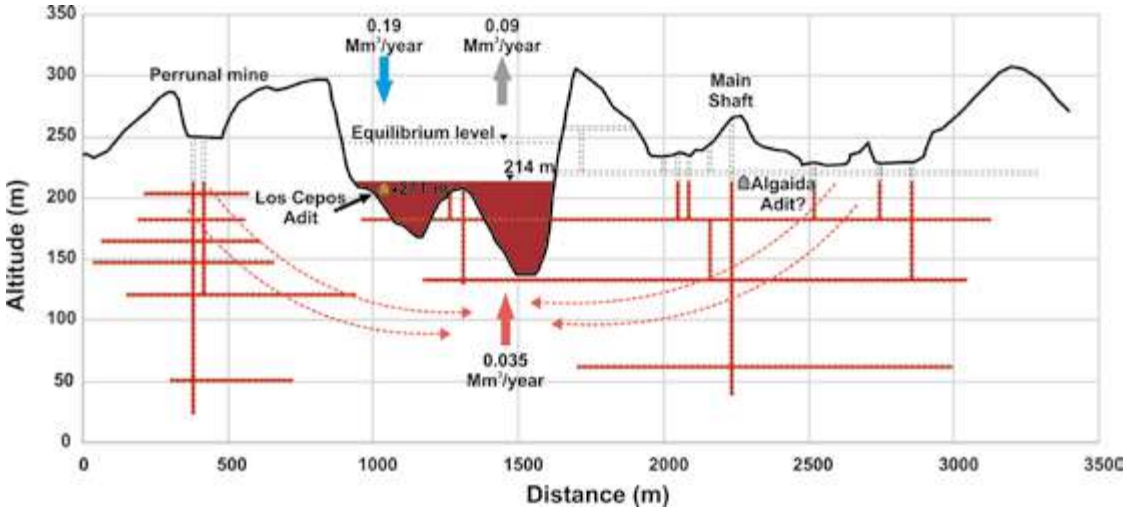

Figure 5.28: W-E schematic profile of Perrunal and La Zarza mines showing the figures of water balance in the pit lake (Olías et al., 2019).

of the area around the La Algaida gallery to prevent another possible discharge, as occurred in May 2017.

On the other hand, small seepages of acidic waters are currently observed in the surroundings of Los Cepos gallery. However, their chemical composition suggests that these waters does not come from the pit lake but from another source similar to that originating leachates from the gallery before the 2017 spill (Moreno González et al., 2023).

5.2.4 San Telmo pit lake

The San Telmo mine was primarily exploited through underground mining until the 1970s, when the excavation of a large open-pit mine began. Mining operations ceased entirely in 1989, leading to the flooding of the open-pit within just about 10 years. Since around 2001, the pit lake has frequently overflowed from its western part, receiving surface contributions from the eastern zone as well (Figs. 5.29 and 5.30). The flooded surface has an approximately circular shape, with a diameter ranging from 380 to 510 m and a depth of 130 m, constituting the largest accumulation of acidic waters in the IPB (around 8 hm^3, Table 5.1).

This mining lake is of meromictic nature, with a chemocline approximately at a depth of 29 m that separates an oxygenated and less mineralized upper mixolimnion from an anoxic and more mineralized monimolimnion (López Pamo et al., 2009; Sánchez España et al., 2008b and 2009; Cánovas et al., 2015). In Figure 5.31, it is observed that the pH is close to 2.8 throughout the water column, while EC is lower in the mixolimnion (around 5.3 mS/cm), clearly different from that of the monimolimnion (about 6.5 mS/cm). Conversely, the redox potential is lower in the mixolimnion.

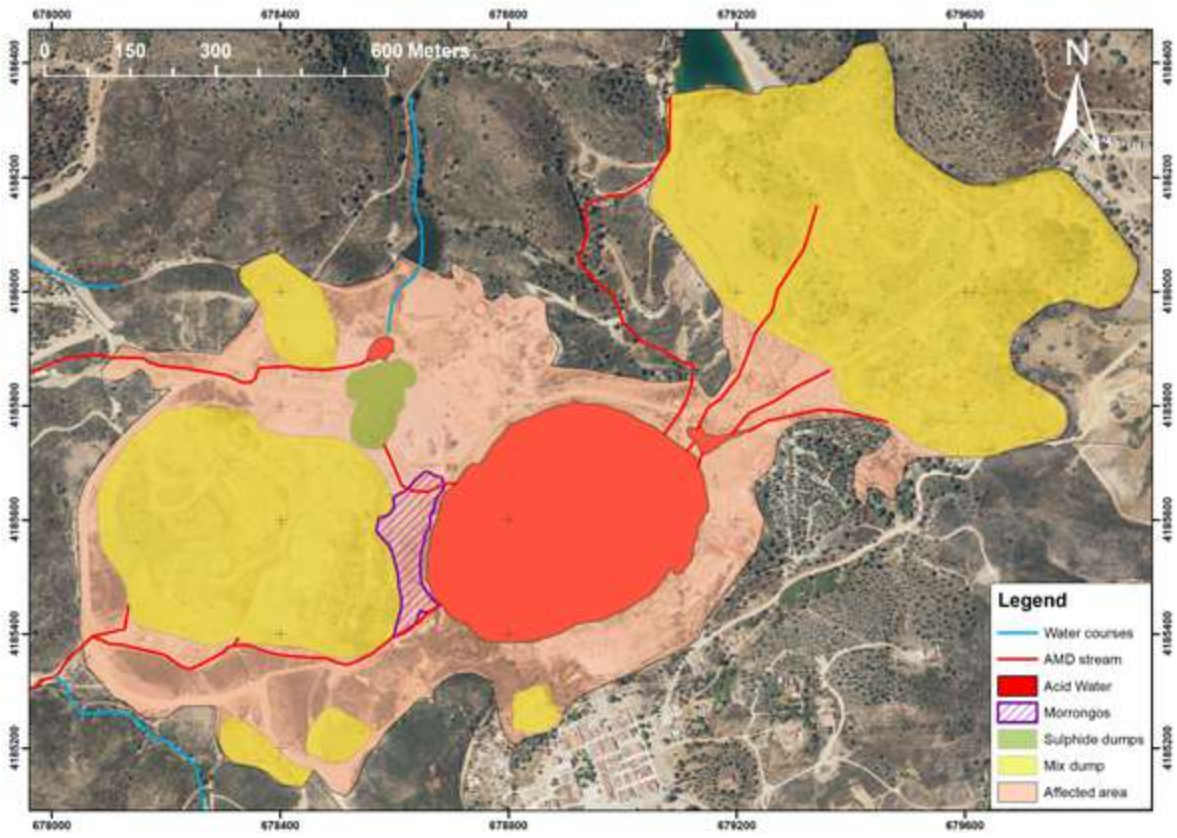

Figure 5.29: Location map of San Telmo mine, showing the the pit lake and other mining affected areas.

Figure 5.30: Photo of San Telmo pit lake towards the west.

There are two large spoil heap areas, one located northeast of the pit lake and the other to the west (Fig. 5.29). Some of these spoil heaps consist exclusively of sulfides, being the San Telmo mine the most significant pollutant source in the northern part of the Oraque river basin.

The occurrence of acidic outflows from the western part of the pit lake depend on the differences between surface and groundwater inputs, on one hand, and evaporation outputs, on the other. Thus, there are continuous discharges in rainy years, while in dry years, evaporation surpasses inputs, and the water level slightly drops below the overflow level, ceasing water outflow from the lake.

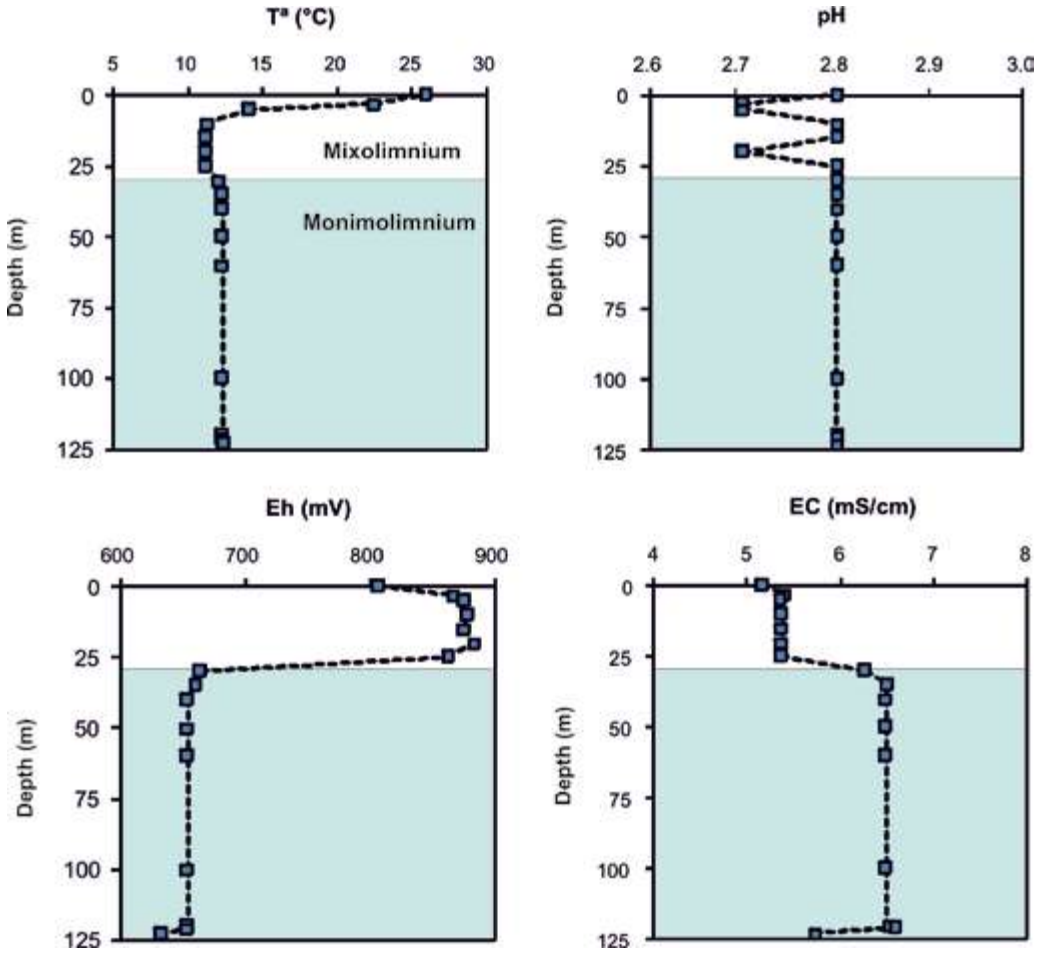

Figure 5.31: Vertical evolution of some physico-chemical parameters in San Telmo pit lake (May 2006). The blue zone indicates the monimolimnion.

The hydrochemical conditions of the lake have remained relatively constant for at least the past 15 years, although there are slight oscillations due to dilution during rainy periods and concentration increases through evaporation during summer. The hydrochemistry of the waters in the upper mixolimnion is primarily influenced by surface water inputs from the eastern part. Additionally, there are underground contributions of acidic waters towards the pit lake, which are enriched in As, Cr, Cu, Fe, and Pb. However, the most significant pollutant contributions in San Telmo come from the spoil heaps located to the west of the mine (Fuentes-López et al., 2022).

5.2.5. Pit lakes in Herrerías. The "killer" lake.

There are two relatively small pit lakes at Herrerías mine, Guadiana and Santa Bárbara (Figs. 5.32 and 5.33), very close each other (the distance between them is less than 300 m) but with completely different colors and characteristics. Mining in the Santa Bárbara open-pit concluded in 1930, and it has been flooded since then. On the other hand, in the Guadiana open-pit, the last phase of exploitation was underground and ended in 1988, subsequently leading to its flooding (López Pamo et al., 2008). However, the distinct conditions of both open-pits are attributed to the extracted minerals. While the target mineral in the Guadiana open-pit was pyrite for sulfuric acid production, in the Santa Bárbara open-pit, copper-bearing shales were extracted for obtaining Cu. The amount of sulfides in the copper-bearing shales of Santa Bárbara is low compared to the pyritic material extracted in the Guadiana open-pit, resulting in greater acidification capacity in the latter. As a consequence, the pH values in both open-pits greatly differ. In the Guadiana open-pit the pH in the surface layer is around 2.5, buffered by Fe. In the Santa Bárbara open-pit the pH ranges between 4.5 and 5, controlled by Al, preventing the presence of dissolved Fe(III) and giving it a bluish-green color. Another open-pit in the IPB that shares similar conditions with Santa Bárbara is that of Los Frailes, in the Aznalcóllar mine.

Another difference between both pit lakes is the water depth and limnological functioning. The Santa Bárbara pit lake has a shallow depth (15 m) and behaves holomictically,

Figure 5.32: Aerial Photo of Santa Bárbara (left) and Guadiana (right) pit lakes in Herrerías mine (Google Earth).

Figure 5.33: Photo of Guadiana pit lake at Herrerías mine in July 2016, including the release of CO_2-rich waters through the pipe installed in the middle of the lake.

while in the Guadiana pit lake the water depth is greater (60 m) and it is meromictic, with a chemocline differentiated at around 15 m depth (López Pamo et al., 2008).

The Guadiana pit lake raised significant concerns in the area after the publication of a news article in El País, one of the most read Spanish newspaper, that warned of a 'killer lake' (El País, July 24, 2016) based on the findings of Boehrer et al. (2016). These researchers found that the water in the monimolimnion of the Guadiana open-pit had a high content of dissolved CO_2, likely due to the dissolution reactions of subsurface carbonate rocks in contact with AMD. The mixolimnion above this layer prevents the CO_2 from escaping into the atmosphere. However, continuous inputs of CO_2 progressively raise the pressure in the monimolimnion. If this pressure would exceed that exerted by the water column in the mixolimnion, a sudden release of all the accumulated CO_2 at the monimonilimnion of the pit lake could occur, a process known as a limnic eruption. This event could pose a threat to the lives of people and animals in the vicinity, as CO_2 is heavier than air and would displace it, leaving the area near the pit lake without oxygen. A similar incident occurred at Lake Nyos in Cameroon in 1986, causing over 1,700 deaths among the local population (Kling et al., 1990), although the dimensions of that lake and the amount of accumulated CO_2 were not comparable at all to the Guadiana open-pit.

To alleviate the CO_2 pressure, a vertical pipe was installed in a pilot experiment, connecting the surface to the monimolimnion, facilitating the exit of water and gas to the surface due to its high pressure (Boehrer et al., 2016; Figure 5.33). In September 2017, a new larger pipe was installed, significantly increasing the release of CO_2, so that by 2018, the pressure of this gas in the monimolimnion had noticeably decreased (Sánchez España et al., 2021).

5.2.6. Corta Atalaya pit lake

Corta Atalaya is the most emblematic open-pit in the IPB, once being the largest in Europe and employing up to 12,000 miners. It has a maximum diameter of 1,200 m and a minimum of 700 m, with a depth of approximately 250 m from its southern edge and 310 m in the northern part. Its excavation began in 1907, simultaneously with underground mining beneath Corta Atalaya through the Alfredo shaft, which reached a depth of about 600 meters. The ore was transported through Tunnel 16 to the Zarandas-Naya area, next to the Tinto River (see Fig. 4.8), where it underwent processing and was loaded onto railways and transported to the Huelva port (Fig. 4.9).

Mining activities in this area ceased in 1992, initiating the flooding of the galleries and underground chambers of the Alfredo shaft. The records show that the flooding of Corta

Atalaya did not begin until 2003, with the water level rising by 115 m between 2003 and 2016 (Fig. 5.34), equivalent to 8.8 m/year. The most significant increase in water occurred between 2009 and 2011, as a result of heavy rainfalls in 2010. Figure 5.35 illustrates the rapid filling of the open-pit based on two photographs taken in 2001 and 2014. The volume of acidic water stored in 2016 was 7.6 hm^3 (Bono and Olías, 2018).

There are two tunnels connecting Corta Atalaya underground galleries with the surface, located at an elevation of around 260 m. Tunnel 5, which was sealed in 2015, heads west towards the Agrio River in the Odiel River basin. On the other hand, Tunnel 16 heads east, connecting Corta Atalaya underground galleries with Cerro Colorado and reaching the Zarandas-Naya area next to the Tinto River. The water inputs into Corta Atalaya are significantly higher than the outputs through evaporation. As a result, the water level would

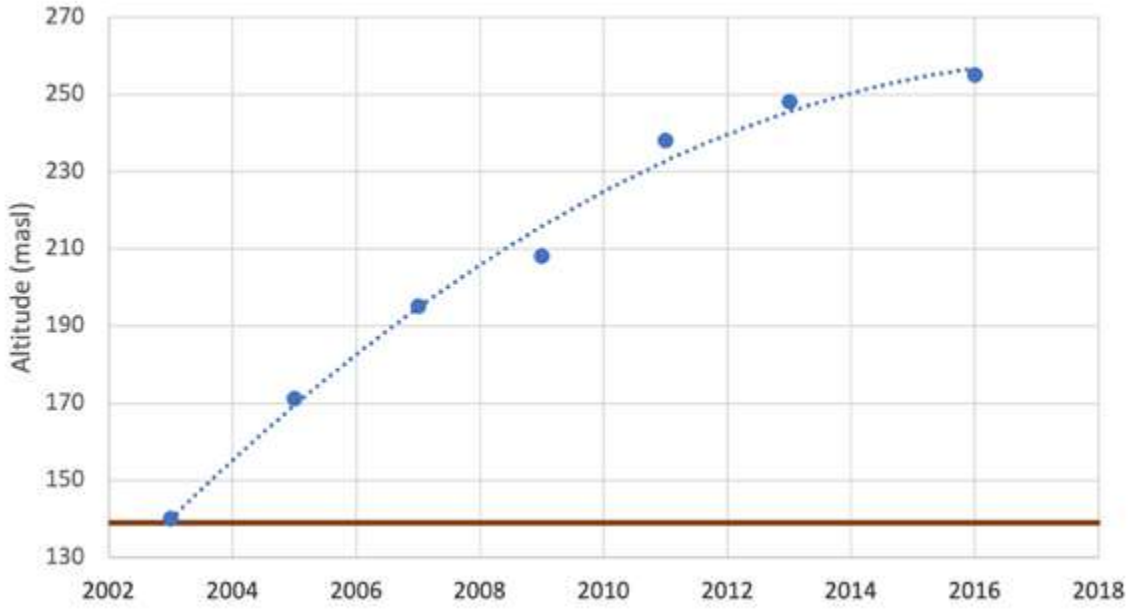

Figure 5.34: Evolution of water level in Corta Atalaya pit lake, obtained from historical ortophotographs and a digital terrain model (DTM) (Bono and Olías, 2018). The discontinuous line indicates a polynomial fitting for collected data, while the brown solid line represents the pit lake bottom (masl: meters above sea level).

Figure 5.35: Photos of Corta Atalaya pit lake in 2001, before flooding (right), and in 2014 (left, the current level is similar to that of 2014).

tend to rise up to the elevation of Tunnel 16, potentially overflowing into the Tinto River and increasing its pollutant load, leading to environmental issues in the Ría de Huelva (Bono and Olías, 2018).

However, Atalaya Mining, the company responsible for the ongoing mining operations in the Cerro Colorado area, regularly monitors the water level in Corta Atalaya to maintain safety levels. Additionally, in the event of a water deficit in the supply to the mining facilities, water stored in Corta Atalaya is used, after treatment, for the ore beneficiation process. Consequently, the water level and volume stored in this pit lake have decreased and are currently at 238.5 m and 5.4 hm^3, respectively (Table 5.1). In the future, there are plans to seal Tunnel 16 to prevent the discharge of mine waters from Corta Atalaya towards Cerro Colorado and from Cerro Colorado towards the Tinto River.

5.3 MAIN CONCLUSIONS

In the Spanish part of the IPB, there are five large reservoirs that receive acidic mine leachates: Andévalo and Chanza in the Chanza river basin, Olivargas and Sancho in the Odiel river basin, and Agrio in the Guadiamar river basin. The Chanza and Agrio reservoirs have not been considered in this chapter due to issues with available analytical data.

On the other hand, the water composition of the Jarrama reservoir is considered representative of AMD non-affected surface waters in the IPB. This reservoir has average pH values of 7.7 and low concentrations of sulfates (11 mg/L) and alkalinity (36 mg/L of $CaCO_3$), reflecting the high vulnerability of IPB surface waters to acidic discharges. Concentrations of dissolved metals (Fe, Cd, Cu, Mn, Pb, or Zn) in this reservoir water are low and pose no significant issues. The Corumbel reservoir is neither affected by AMD but differs in conditions as it receives inputs from areas draining carbonate materials, resulting in higher alkalinity waters.

Of the three studied reservoirs receiving AMD, the Sancho Reservoir has an average pH of 3.6 and elevated concentrations of sulfate (average of 184 mg/L) and toxic metals (averages of 835 µg/L of Fe, 3064 µg/L of Zn, 6.6 µg/L of Cd, etc.). In contrast, the Andévalo and Olivargas reservoirs have neutral pH values, low alkalinity (around 25 mg/L of $CaCO_3$), and sulfate concentrations near 60 mg/L, indicating a lower impact compared to Sancho. In Andévalo and Olivargas reservoirs, due to their neutral pH, most of the toxic metals from mining precipitate and accumulate in the bottom sediments, resulting in dissolved iron concentrations similar to that of unaffected reservoirs. However, some divalent metals with higher solubility in neutral conditions, coupled with their high concentrations in the Monte Romero mine, lead to relatively elevated Cd (0.5 µg/L) and Zn (411 µg/L) concentrations in the Olivargas Reservoir, causing it to be classified as having poor water quality according to the Hydrological Plan of the Tinto, Odiel, and Piedras Watershed.

Metal concentrations in sediments of reservoirs receiving AMD are very high and can redissolve under changing redox conditions. Throughout the year, a cycle of metal precipitation/redissolution occurs depending on thermal stratification processes in the water column. This implies that these elements may return to the water column if physicochemical conditions change.

Historical data for the Sancho Reservoir indicates fluctuations in certain parameters, overlaid with a clear trend of worsening conditions. This trend is more evident from 2007 onwards, with a decrease in pH values from approximately 4.5 to 3.5 and a notable increase in electrical conductivity and concentrations of Fe, Zn, and other mining-related elements. This change is attributed to the closure of Tharsis mines at the end of the 1990s and the cease of pumping and environmental control activities, which caused a rebound effect.

Based on sulfate concentrations, it is inferred that the Sancho Reservoir receives acidity from sulfide mining at a rate of 176 tons of H_2SO_4 per hm^3. In contrast, Andévalo and

Olivargas reservoirs have approximately 3.5 times lower values. In the Sancho Reservoir, alkalinity is not sufficient to neutralize the substantial acidity input, explaining its acidic pH. Consequently, some toxic elements remain dissolved. A hydrogeochemical model suggests that to ensure a neutral pH in a reservoir located in the IPB, sulfate concentrations should be below 80 mg/L. Studies on the future Alcolea Reservoir estimate sulfate concentrations to be between 157 and 292 mg/L, indicating that, under current conditions, its pH would be lower than 4. Achieving good water quality (pH>7) in Alcolea Reservoir would require eliminating approximately 70% of AMD inputs to the Odiel River basin, as outlined in the remediation strategy discussed in section 5.1.5.

Regarding the mining pit lakes of the IPB, they contain acidic waters with extremely high dissolved concentrations of sulfate, metals, and metalloids. Thermal stratification processes also occur in these mining lakes. Additionally, the presence of deeper waters with higher dissolved concentrations, and hence greater density, can cause permanent chemical stratification, forming meromictic lakes with two significant vertical layers: the mixolimnion in the upper part (which can further be divided into epilimnion, thermocline, and hypolimnion) and the monimolimnion in the deeper zone, typically with more reducing conditions than the mixolimnion.

In the mixolimnion, the precipitation of iron mineral phases like schwertmannite or jarosite occurs, buffering the pH between 2.5 and 3.5. These precipitates can incorporate other trace elements through adsorption or co-precipitation. The settling of these precipitates leads to an enrichment in Fe and other metals in the bottom sediments, where they may undergo redox changes, releasing Fe(II) and other metals into the monimolimnion, or undergo mineral transformation processes, causing the release of trace metals into the water column.

The accidental release of these acidic waters into the aquatic environment, as occurred in La Zarza mine in May 2017 due to the rise in water level in the open-pit and poor sealing performed in the past, can cause severe environmental damages or even acidify reservoirs located downstream these AMD sources. In the La Zarza pit lake, there appears to be a stabilization of the water level in recent years, but this is attributed to a long dry period. During rainy years, the water level is likely to rise, leading to the potential release of acidic waters through old galleries.

In Tharsis, there are four mining pit lakes with different characteristics. In Filón Centro, the water level has been stable for about 50 years, although with slight fluctuations. In Filón Sur, the level is also constant, and volume of acidic waters accumulated is relatively small, suggesting the existence of unnoticed underground outlets through an old gallery. Sierra Bullones and Filón Norte show a similar evolution as they are hydraulically connected by underground galleries, and the water level continues to rise year after year. It is estimated that evaporation losses will compensate the overall inputs before overflow occurs in both pit lakes.

The San Telmo pit lake is very deep (about 130 m), constituting the largest accumulation of AMD in the IPB. The water level is more or less stable and, under normal conditions, there are surface inputs from the eastern edge and overflow outputs from the western part of the pit lake. However, there are also underground inputs enriched in As, Cr, Cu, Fe, and Pb. In dry years, evaporation surpasses inputs, causing a slight decrease in water level, and overflows from pit lakes are therefore interrupted.

In the Herrerías mine, there are two closely located pit lakes with clearly distinct characteristics. The Santa Bárbara pit lake has a pH close to 4.5 and greenish colors due to the predominance of aluminum precipitation, while the Guadiana pit lake has a pH below 3 and intense red color due to high dissolved iron concentrations in the water column. The Guadiana pit lake is meromictic, with a high concentration of dissolved CO_2 in the monimolimnion, causing significant alarm in 2016 due to the potential occurrence of a limnic eruption and

sudden release of CO_2. Currently, the concentration of dissolved CO_2 has significantly decreased due to mitigation measures.

Another significant mining lake in the IPB is formed by the rapid flooding of the Atalaya open-pit in the Riotinto mines. Between 2003 and 2016, the water level rose by 115 m, but subsequently, it has decreased because Atalaya Mining company uses this water in situations of water scarcity and maintains the level within a safety range to prevent its discharge into the Tinto River.

In the IPB, there are other mining pit lakes that have been scarcely studied and are poorly understood, so further research is needed to properly understand their characteristics and prevent potential future problems.

6

POLLUTION IN THE RIA OF HUELVA ESTUARY

6.1. INTRODUCTION

The coastal seawater of the Gulf of Cadiz is enriched in metals, mainly zinc, cadmium, arsenic, and copper, compared to other coastal waters worldwide (Fig. 6.1). These high concentrations were first observed during the 1980s through an oceanographic expedition organized by the *Woods Hole Oceanographic Institution* in Massachusetts (Spivack et al., 1983; Boyle et al., 1985; Sherrell and Boyle, 1988). In fact, the pollution plume circulates and dominates the chemical composition until it enters the Mediterranean Sea through the Strait of Gibraltar (van Geen et al., 1988). Initially, after analyzing the main Iberian rivers that flow into this area (mainly the Guadalquivir River), these authors ruled out the riverine input of metals and explained this enrichment by an upwelling process of water from deep ocean and trapping of metals in the Gulf of Cadiz (van Geen et al., 1991). Later, Elbaz-Poulichet and Leblanc (1996) were the first authors to focus on the source of metals in two small river systems that are relatively minor compared to the Guadalquivir River: the Tinto and Odiel Rivers, which was confirmed a year later by the same authors who detected the anomaly in the ocean (van Geen et al., 1997).

The confluence of the Tinto and Odiel river mouths defines an estuarine system known as the Ria of Huelva estuary. The estuary associated with each river converges into a common channel, known as the Padre Santo channel, which extends from the convergence of both estuaries to the Atlantic Ocean (Fig. 6.2). The transfer of acidity and toxic metals to the Huelva estuary has been the focus of numerous research studies (e.g., Elbaz-Poulichet et al., 2001; Borrego et al., 2002; Olías et al., 2006; Nieto et al., 2013). Pollution levels are so extreme that both rivers and the estuary are considered one of the most contaminated aquatic systems in the world. As mentioned in previous chapters, the riverine contribution of metals to the Huelva estuary under different climatic conditions is well-known. Therefore, there is currently no scientific debate about the fact that the metals circulating through the Gulf of Cadiz are discharged by the Tinto and Odiel Rivers.

The Huelva estuary represents a transitional environment between riverine discharges and marine conditions. The mixing of waters in estuaries implies the existence of a salt wedge and a progressive decrease in salinity inland. However, in the Ria of Huelva estuary, in addition to the salt wedge, there are processes associated with the acid neutralization of waters affected by AMD, as the pH values range from 2.5 to 3.5 in the upper areas of the estuary to

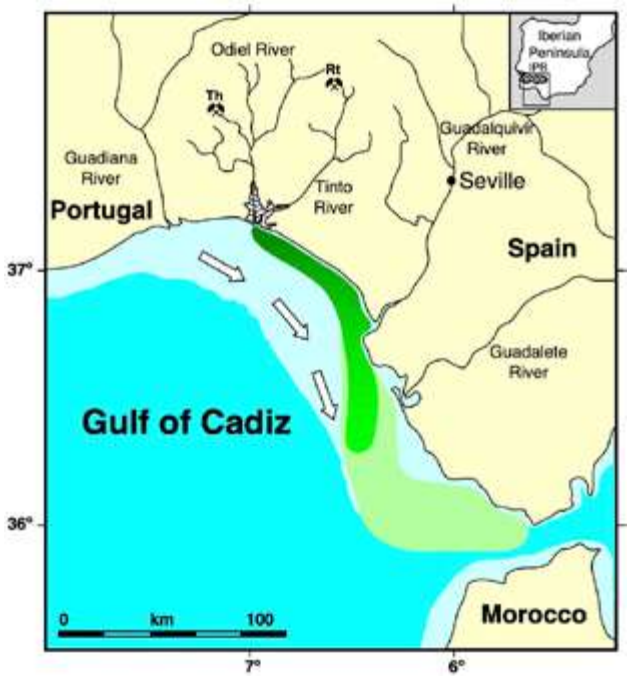

Figure 6.1: Map of the Gulf of Cadiz, Strait of Gibraltar and Mediterranean Sea showing the pollutant plume coming from the Tinto and Odiel Rivers across oceanic waters.

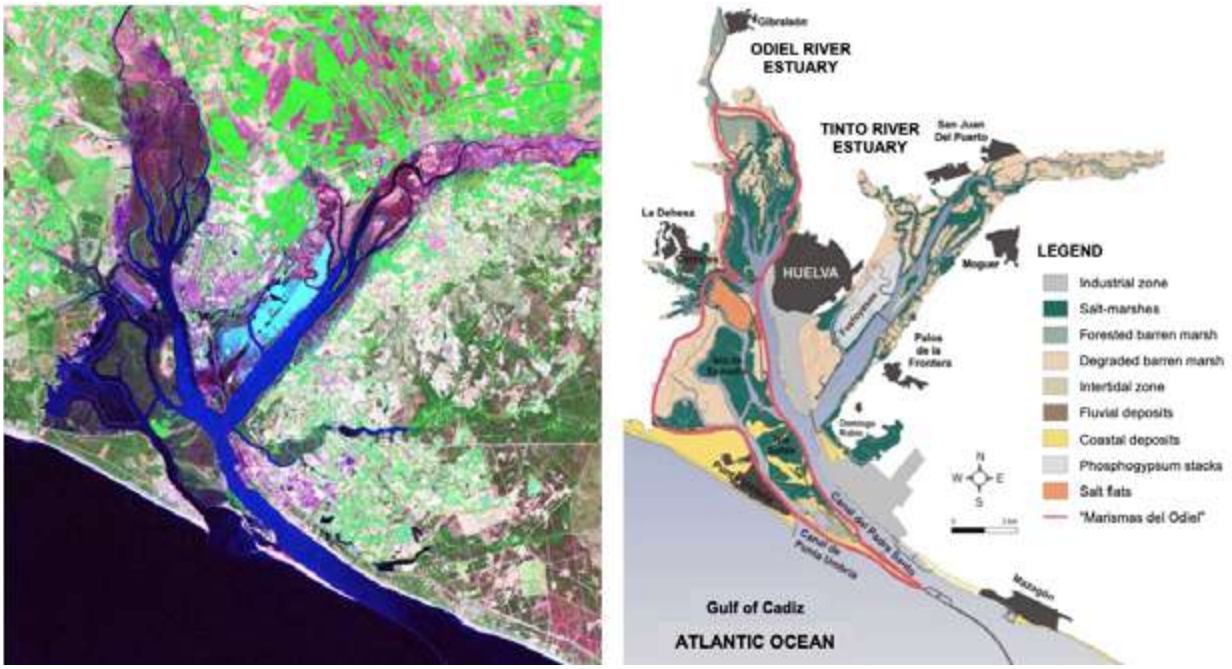

Figure 6.2: Tinto-Odiel estuarine system (Ria of Huelva estuary). Taken from Carro et al. (2018).

values close to 8 in a very short distance (Fig. 6.3). The neutralization of acidity triggers a series of geochemical processes that determine which pollutants subsequently reach the Gulf of Cadiz and in what quantity. These processes are detailed in the following sections.

In addition to the mining-related pollution carried by the Tinto and Odiel Rivers, the waters and sediments of the Huelva estuary receive industrial-related contaminants from the Huelva Industrial Estate. In the 1960s, there was encouragement for companies to establish in this industrial area, and one of the advantages offered was that, due to the estuary being contaminated by AMD, no treatment of wastewater discharges from industries was deemed necessary. This led to significant degradation of the Ria of Huelva estuary. Besides being enriched in metals and metalloids, the waters and sediments of the Tinto and Odiel estuaries are also enriched in nutrients (N and P), suspended particles, and even radionuclides (Borrego et al., 2002; Hierro et al., 2012).

This situation persisted until the late 1980s when, as a consencuence of the environmental degradation, plans were initiated to correct industrial discharges. Furthermore, in 1997, direct discharges of acidic waters and phosphogypsum from fertilizer manufacturing industries into the estuary ceased. These measures contributed significantly to improve the environmental conditions in the estuary concerning industrial discharges. Currently, mining pollution continues to transport large quantities of contaminants to the estuary every year, alongside contributions of acidic leachates, albeit of lesser magnitude, from the phosphogypsum stacks located in the salt marshes on the right bank of the Tinto estuary (Fig. 6.2; Pérez-López et al., 2016).

6.2. WATER POLLUTION

The behavior of metals during the mixing of the Tinto and Odiel Rivers, affected by AMD, and seawater in the estuary has been assessed through sample collection by boat across the Ria of Huelva estuary (Fig. 6.4). In 2018, three samplings were conducted under different hydrological conditions: during a rainfall-induced flooding event (March), before the summer period (May), and after the summer period (November). To prevent potential

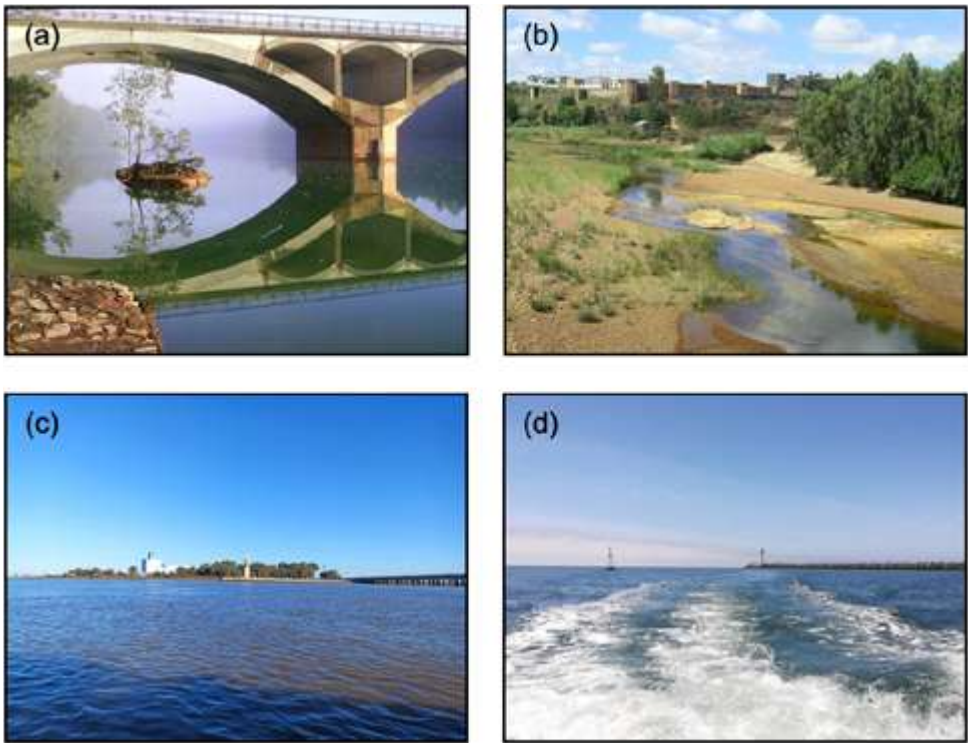

Figure 6.3: Photos corresponding to the lower reaches of the (a) Odiel River (pH ~3.5) and (b) Tinto River (pH ~2.5) before the tidal influence, (c) Christopher Columbus monument nearby Huelva city, where both estuaries join in thePadre Santo channel (pH ~7.5), and (d) outlet of Padre Santo channel towards the Atlantic Ocean (pH ~8.0).

contamination from the boat, samples were taken at 10 m depth with a Van Dorn bottle, except for shallow water areas where the sampling depth was 5 m. In-situ measurements of physical-chemical parameters (pH, electrical conductivity, redox potential, and temperature) were recorded. Onboard, each sample was divided into two aliquots: one filtered at 0.45 µm for the study of dissolved contaminants and another unfiltered for the study of total contaminants after acid digestion.

In the Ria of Huelva estuary, there is an increase in the pH of the water from acidic river values (approximately 2.5 and 3.5 in the Tinto and Odiel Rivers, respectively) to alkaline values typical of the sea (approximately 8). Associated with this pH increase, the behavior of the main mining-related metals can be explained according to the conceptual model shown in Figure 6.5.

On the left side of Figure 6.5 during the riverine discharge of mining-related contaminants, both major (such as iron, aluminum, copper, and zinc) and trace elements (such as arsenic, manganese, nickel, and cobalt) arrive to the estuary. During the transit through the estuary until reaching the Atlantic Ocean on the right side of the conceptual model, contaminants exhibit a behavior that can be grouped into three categories: non-conservative elements, conservative elements, and elements with an ON-OFF behavior. Non-conservative elements, mainly iron, aluminum, and copper, are those removed from the water by mineral precipitation during AMD neutralization; in other words, they tend to become part of the particulate matter that later are deposited in the bottom sediment. On the other hand, conservative elements, mainly zinc, manganese, nickel, and cobalt, remain in solution throughout the estuarine transit, thus reaching the Atlantic Ocean. Finally, elements with an ON-OFF behavior, primarily arsenic, are initially retained through mineral adsorption or coprecipi-

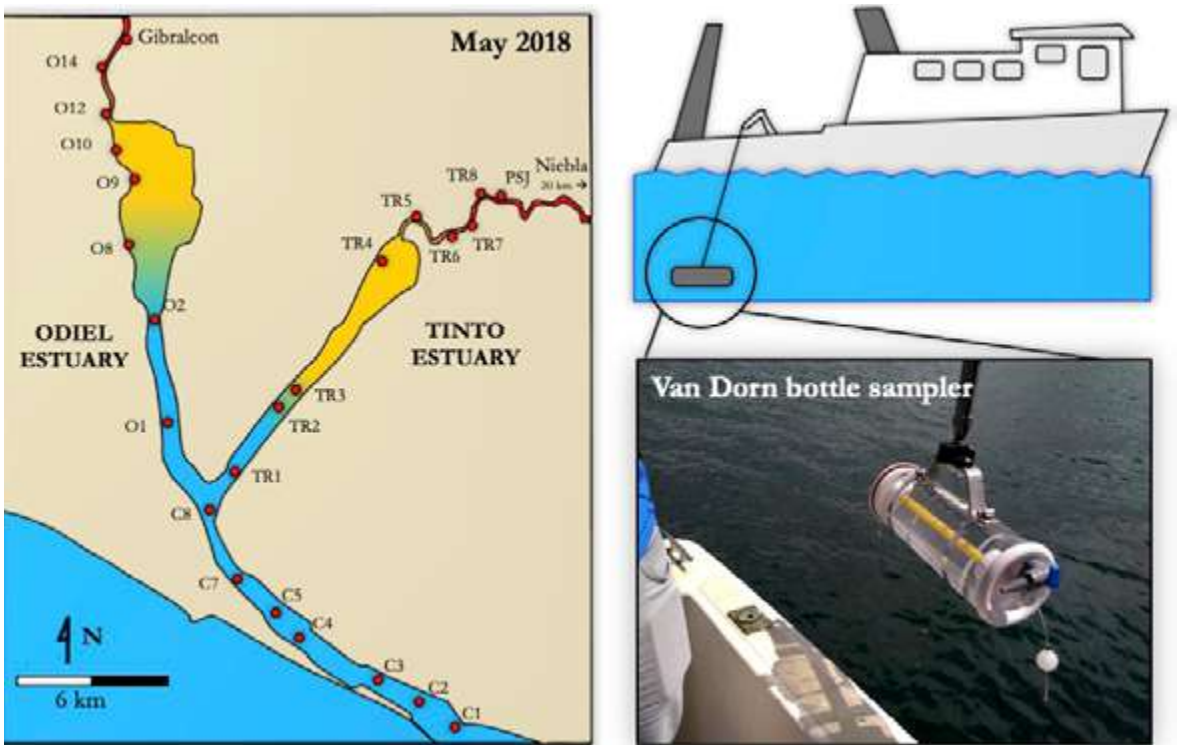

Figure 6.4: Location of sampling points across the Ria of Huelva estuary: O refers to points belonging to the Odiel estuary, TR for Tinto estuary and C those inside the common estuary (Padre Santo channel) which enters the ocean.

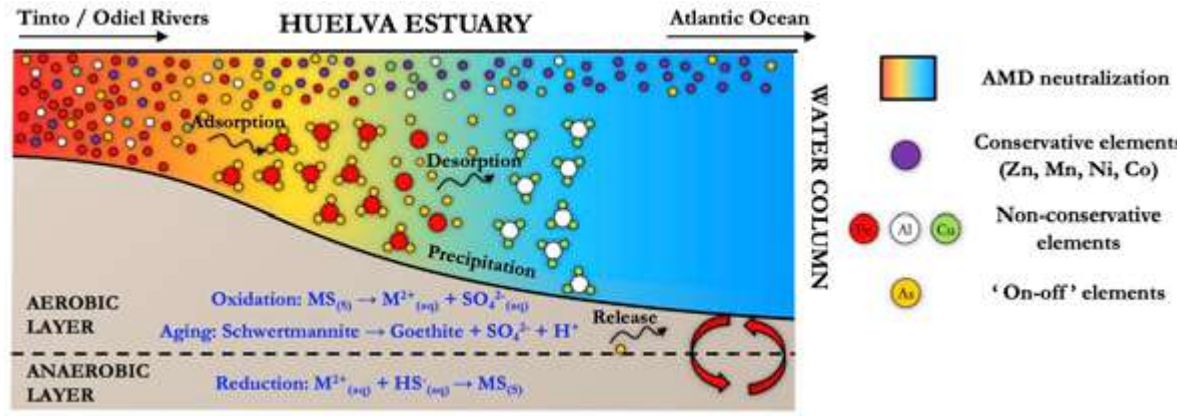

Figure 6.5: Conceptual model of geochemical processes affecting the particulate matter mobiliy across the estuary; from flocculation processes to its settlement in the estuarine sediments.

tation (OFF) and then released back to the water column (ON), also reaching the ocean alongside conservative elements.

Next, the geochemical processes conditioning the different behaviors observed in mining-related metals will be explained in more detail. In the mixing zone (Figure 6.6; orange band), the pH increase is accompanied by a drastic decrease in the concentration of dissolved iron due to mineral precipitation processes. The behavior of iron is noteworthy as it is one of the main mining-related metals, although its concentration in the Odiel River is significantly lower than in the Tinto (see Chapter 4). Arsenic, a trace but potentially toxic element, is firstly retained due to iron precipitation; however, at pH values close to neutrality (vertical

red dashed line; Figure 6.6), arsenic concentrations increase again in solution, suggesting instability of the iron precipitates and a release of previously retained arsenic.

The total retention of iron during the water mixing occurs through the precipitation of schwertmannite ($Fe_8O_8(OH)_6SO_4 \cdot nH_2O$), characterized by an ochre color. In fact, the iron concentration is so high in the Tinto River that the mixing zone of its estuary is tinted with ochre colors due to the abundant presence of this mineral as suspended material (Fig. 6.7).

Under the microscope, schwertmannite exhibits a spherical morphology resembling a "hedgehog" or "pin cushion" due to the presence of acicular crystals on its surface (Fig. 6.8a). The surface of schwertmannite, during its formation at acidic pH, is positively charged, giving it a high potential for "electrostatic attraction" to negatively charged anions such as arsenic, which is predominantly in the form of $H_2AsO_4^-$. This leads to its retention (Courtin-Nomade et al., 2003; Fukushi et al., 2003; Acero et al., 2006). However, when the pH approaches neutral values, the surface polarity of schwertmannite inverts, becoming negatively charged. This reversal causes a repulsion of previously retained anions, including arsenic, leading to its release (Fig. 6.8b). The point of zero charge (PZC) of the mineral surface is reached between these two situations. This explains why arsenic is initially retained during iron precipitation and released at higher pH levels. This retention-release behavior affects not only arsenic but also other elements existing as anionic species, such as chromium, vanadium, molybdenum, or antimony.

These results are observed under different seasonal conditions, for example, before and after summer, and especially during flood events. During a river flood caused by heavy rainfall, the contribution of both rivers increases significantly due to surface runoff. Consequently, the pH values of both rivers upon arrival at the estuary are relatively higher, causing a significant amount of iron to be already precipitated as schwertmannite. At those pH values, arsenic is also retained along with schwertmannite upon arrival at the estuary;

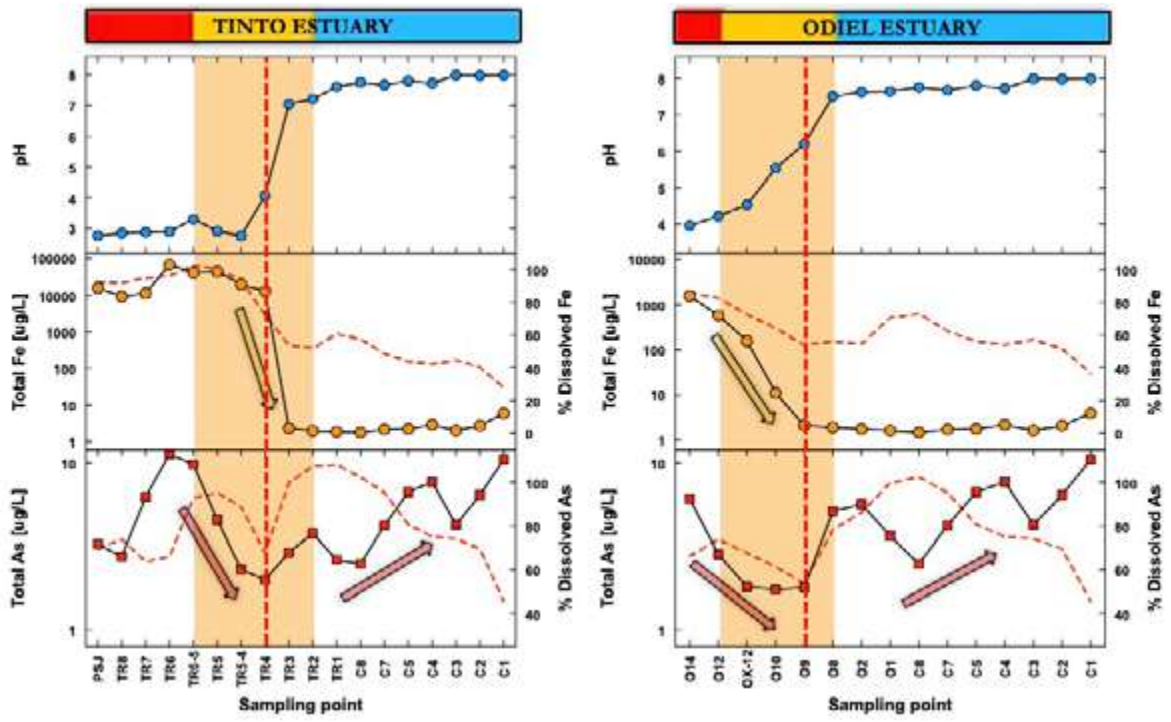

Figure 6.6: Evolution of pH and total concentrations (dashed lines) and percentage in dissolved fraction of Fe and As (symbol lines) across the Ria of Huelva estuary during the sampling of May 2018. Sampling points location can be seen in Fig. 6.4

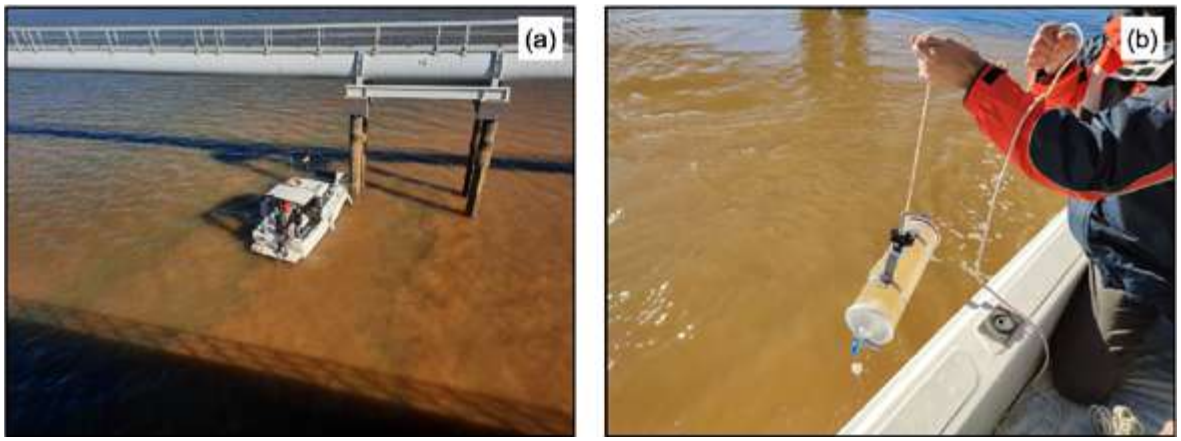

Figure 6.7: General photo (a) and (b) detail of the mixing zone of the Tinto estuary where abundant ochre-colored particulate matter is observed due to intense precipitation of schwertmannite.

however, a gradual release of arsenic is observed as the schwertmannite particles transit along the estuary and the pH gradually rises to values above neutrality (Fig. 6.9).

Other metals of mining origin such as aluminum, copper, zinc, cadmium, cobalt, or nickel are found in solution as cations with a positive charge and, therefore, undergo a process of electrostatic repulsion with the surface of schwertmannite, also positively charged. This fact explain why the precipitation of this mineral can not control the mobility of these metals. Among these metals, some like aluminum and, to a lesser extent, copper exhibit a non-conservative behavior in the estuary, similar to iron. In other words, their total concentrations (dashed lines; Fig. 6.10) tend to decrease in estuarine waters, not only due to a dilution effect when mixing with seawater but also due to mineral precipitation processes. Consequently, the percentage associated with the dissolved fraction relative to the total (gray bars; Fig. 6.10) decreases during the mixing of waters.

Aluminum usually precipitates as a mineral known as basaluminite ($Al_4SO_4OH_{10}\cdot 4\text{-}5H_2O$). Along with this mineral, the coprecipitation of copper also seems to occur through mechanisms of structural retention (Fig. 6.11; Lozano et al., 2020).

Surprisingly, other mining-related metals such as zinc, cadmium, cobalt, and nickel exhibit a conservative behavior in the estuary. The decrease in the total concentrations of these elements (dashed lines; Fig. 6.12) is exclusively due to a dilution effect by seawater. No precipitation occurs during estuarine mixing since the majority of the total concentration of these elements throughout the estuary is constituted by the dissolved fraction (Fig. 6.12).

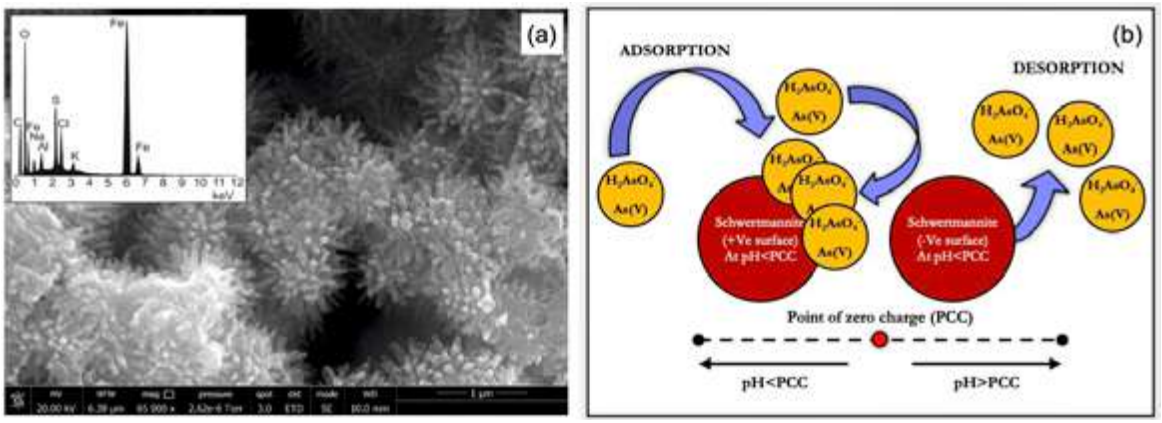

Figure 6.8: (a) Image of scanning electron microscope (SEM) and X-ray dispersive analysis (EDS) of schwertmannite found in particulate matter suspended in the water column of Ria of Huelva estuary. (b) Scheme showing the adsoprtion/desorption processes of arsenic on/from this mineral.

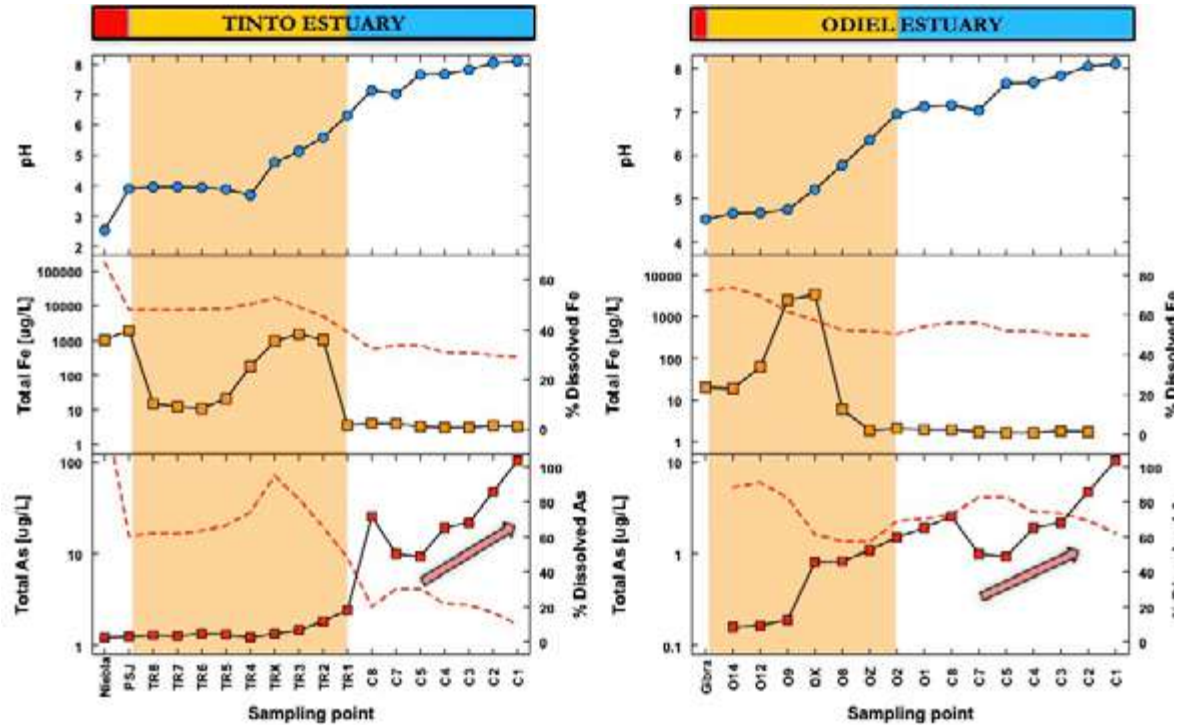

Figure 6.9: Evolution of pH and total concentrations (dashed lines) and percentage in dissolved fraction of Fe and As (symbol lines) across the Ria of Huelva estuary during the sampling of March 2018, coinciding with an intense rainy event. Sampling points location can be seen in Fig. 6.4.

These metals, along with a part of arsenic, would reach the Gulf of Cádiz without obstacles and become part of the contaminant dynamics controlled by ocean currents as discussed in the introduction of this chapter.

As a consequence, the dissolved concentrations of As, Cd, Cu, Zn, and other mining-related metals in the Ria of Huelva estuary exceed the environmental quality standards established in legislation for surface waters (Table 6.1).

6.3. SEDIMENT POLLUTION

The analyzed samples of surface sediments throughout the estuary, as expected from the hydrochemical behavior of metals explained previously, show that iron and aluminum are the main mining-related metals. The general trend observed is that higher fluvial influence corresponds to higher concentrations of these metals; the maximum concentrations are found in estuarine areas where the precipitation and sedimentation of newly formed minerals occur during acid neutralization. The concentration of most trace elements (e.g., Co, Cu, Cr, Ni, Cd, or Pb) shows a positive correlation with both the degree of fluvial influence and the increase in the percentage of silt and clay in sediments. This is because fine grains, probably neoformed minerals, have a very small size and a high surface area. Conversely, the increasing of the sand percentage reduces the pollutant load, and increases the presence of Ca due to the influence of the marine environment on sediments, probably associated with the presence of carbonates. The observed concentrations of these elements in surface sediments (Fig. 6.13) exceed the reference values for sediment quality, reflecting concentrations of probable effect (Table 6.1). In other words, concentrations at which negative effects on exposed organisms would be expected, such as mortality, effects on species diversity, liver or histopathological damages, reduction in burial processes, and decreased respiration ratios. (Long et al., 1995). For instance, concentrations of Cu up to 3000 mg/kg have been found in the estuarine sediments, significantly exceeding values that would

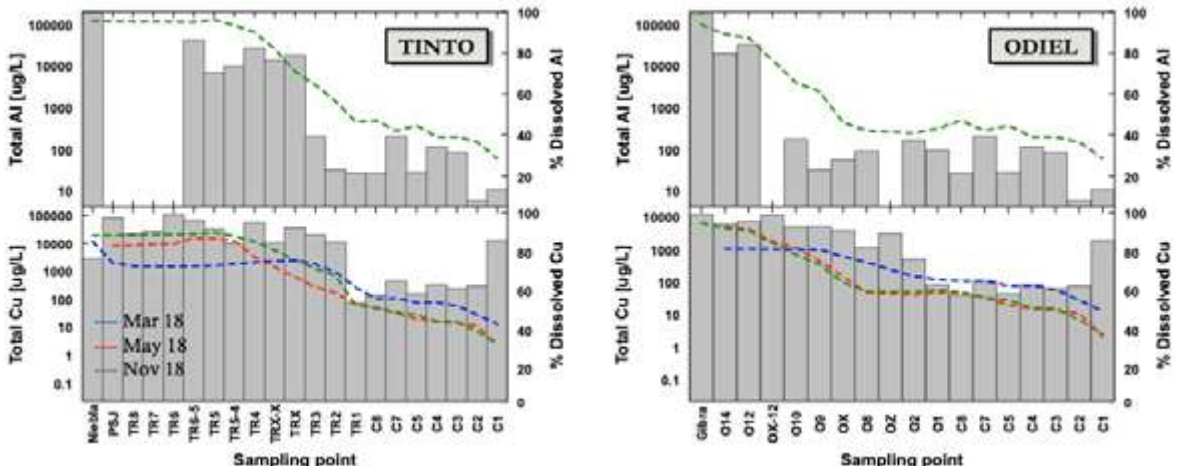

Figura 6.10: Evolution of total concentrations (dashed lines) and percentage in dissolved fraction (grey bars) of Al and Cu across the estuary during the samplings. Data of Al is only available for the sampling in November 2018.

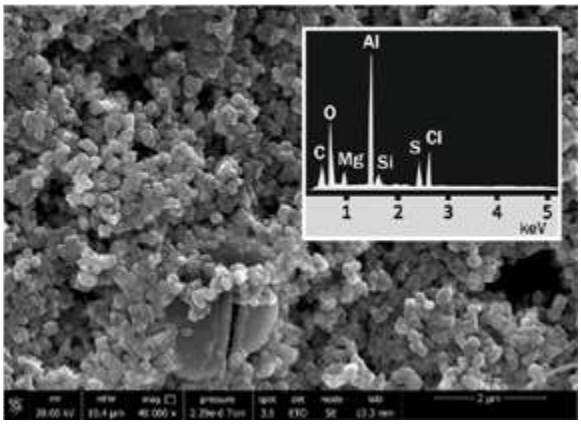

Figure 6.11: SEM image and EDS analysis of basaluminite found as suspended material in the water column of the Ria of Huelva estuary.

be expected to have a toxic effect on exposed biota. In addition, according to Spanish guidelines for dredged material characterization (CEDEX, 2021), these concentrations would be above the threshold for considering sediment as non-hazardous.

Regarding the conditions in deeper sediments, small manual drillings have been carried out to collect short cores in the estuarine channels of the Odiel and Tinto Rivers. The Fe concentration in sediments does not seem to show a clearly defined pattern with depth. In areas closer to the fluvial domain, these concentrations decrease with sediment depth, but this situation is even reversed in the rest of the sampling points. In the case of Al, concentrations at all points decrease with depth. The highest concentrations of other metals associated with Fe and Al oxyhydroxysulfates are observed in the first few centimeters of sediments (< 5 cm). However, at depth, especially in marshland areas, a positive correlation between Cu, Zn, Cd, and S, is observed, which may indicate the precipitation of these elements as metal sulfides in more anoxic zones (Fig. 6.5). In this context, reductive dissolution processes of oxihydroxides to sulfides seem to lead to an increase in the mobility and bioavailability of oxyanions in solution, such as As.

The precipitation of dissolved metals and subsequent sedimentation of particulate matter within the estuary is also affected by natural processes such as tidal cycles and variations in river discharges. Tidal cycles occurring approximately every 6 hours subject the system to strong daily pH variations (from 4 to 7 in some areas), while the variations in river discharges cause the displacement of mixing zones along the estuary, and therefore, the zones of precipitation and sedimentation (Fig. 6.5). During flooding conditions (due to strong rainy events), river flows are so high that the processes of floculation and settling of contaminants shift towards the open sea. For that reason, it is extremely challenging to relate metal concentration in the water column and sediment in such a dynamic environment as the Ria of Huelva estuary.

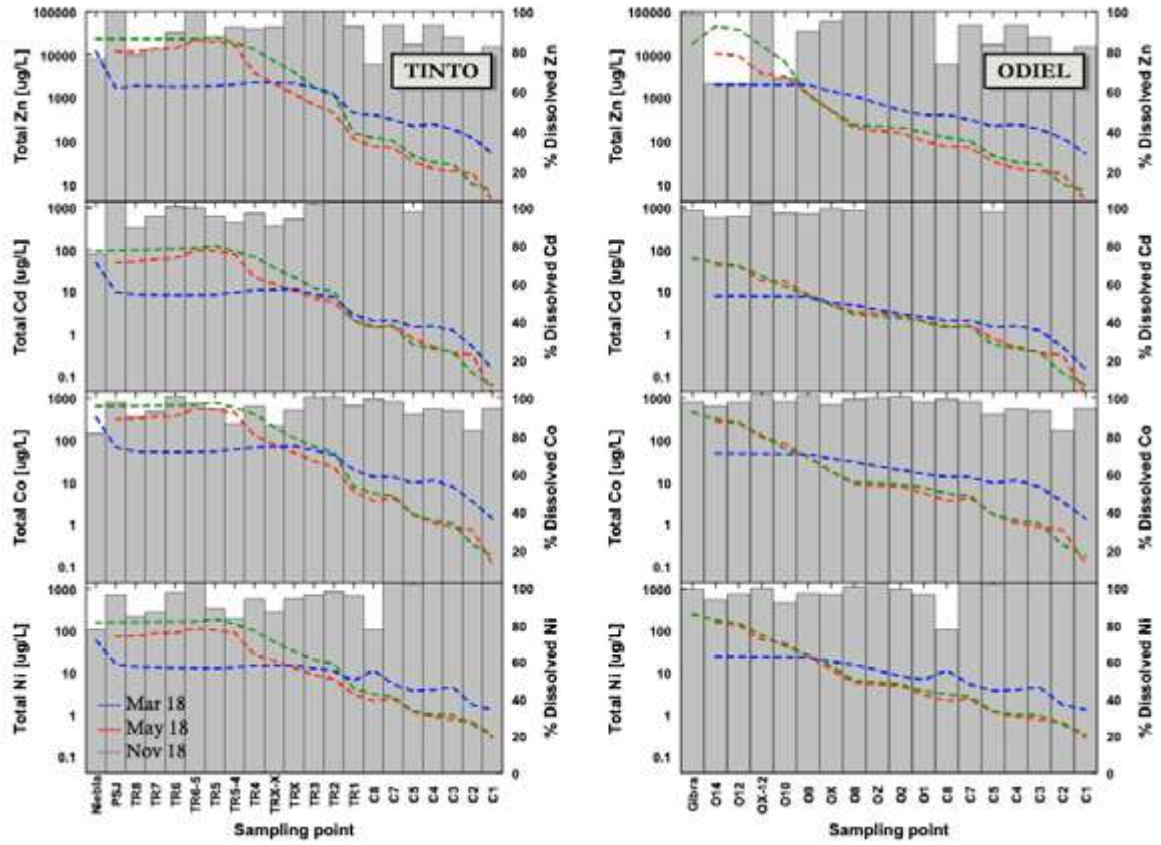

Figure 6.12: Evolution of total concentrations (dashed lines) and percentage in dissolved fraction (grey bars) of Zn, Cd, Co and Ni across the estuary during the samplings.

On the other hand, anthropogenic activities also induce changes in the patterns of metal concentration in the estuary. For instance, periodic dredging activities for maintaining the depth of the navigation channel by the Port of Huelva result in the removal of approximately 280,000 m^3 of sediments annually from the so-called inner channel of the estuary. This activity disrupts sediments, leading to the incorporation of suspended solids and contaminants into the water column, which increases the mobility and bioavailability of metals, as well as their redistribution along the estuary and coastal waters. Potential mining spills, which occur relatively frequently in the IPB (Olías et al., 2019), can also cause changes in the distribution of metals in the estuarine sediments.

All the factors explained above demonstrate that the estuarine sediments act as sinks (temporary or permanent) or sources of metals in the estuary under changing environmental conditions. In this regard, sediments in the Ria of Huelva have been classified as highly toxic according to the guidelines for the characterization of dredged material developed by the Spanish Center for Studies and Experimentation of Public Works (CEDEX; Table 6.1) due to their excessive metal concentrations.

6.4. AFFECTION TO LIVING ORGANISMS

There are several protected areas in the Ria dof Huelva estuary. On one hand, in the Odiel estuary (Fig. 6.14), the Marismas del Odiel (Odiel Marshlands) is found, declared a Natural Site in 1984, which is part of the Natura 2000 Network. These natural coastal wetlands, known for hosting a vast number of migratory birds, are also designated as a Biosphere Reserve by UNESCO since 1983, being included in the RAMSAR Convention

	(*) Surface waters (µg/L)	Sediments (mg/kg)			
		ERL[a]	ERM[b]	Background concentration **	Non-hazardous sediment ***
As	25	8.2	70	10	1000
Cd	0.2	1.2	9.6	0.18	72
Cr	5 (Cr(V))	81	370	30	1000 (Cr(VI))
Cu	25	34	270	14	2500
Ni	20	20.9	51.6	19	1000
Pb	7.2	46.7	218	23	1000
Zn	60	150	410	60	2500

(*) Environmental quality standards expressed as annual average values (NCA-MA) published in Spain's national legislation (Real Decreto 60/2011, of January 21, on environmental quality standards in the field of water policy (BOE, 2015)). The limits are applicable to all surface waters (continental, coastal, transitional waters)

(**) Ranges of heavy metal concentrations in marine sediments along the coastline free from anthropogenic influence (CEDEX 2021).

(***) Threshold values for the classification as non-hazardous sediment according to the guidelines for the characterization of dredged material and its relocation from the maritime-terrestrial public domain (CEDEX 2021).

[a]ERL (effects range-low): threshold values below which biological effects are expected to be rare (Long et al. (1995))

[b]ERM (effects range-median): threshold values above which biological effects are expected to occur frequently (Long et al. (1995))

Table 6.1: Metals and metalloid concentrations of reference for water and sediments.

on Wetlands of International Importance since 1989. It covers an area of over 7,400 ha, with a rich variety of habitats, contributing to significant ecological diversity (Castellanos and Luque, 2022).

On the other hand, the estuary of the Tinto River (Fig. 6.15) is found on the eastern margin of the Ria of Huelva, which extends from San Juan del Puerto to its confluence with the Odiel River at the Padre Santo channel. The Marismas y Riberas del Tinto (Tinto marshlands and riversides) (3,017 ha) and the estuary of the Tinto River (1,167 ha) are located here, both declared Special Conservation Areas and protected since 2015 within the Natura 2000. Both, the Odiel and Tinto estuaries are included in this network as Special Protection Areas (SPA), Sites of Community Importance (SCI), and Special Conservation Areas (SAC).

In addition, on the left bank of the confluence of the Tinto River with the Odiel, the Natural Site of Estero Domingo Rubio is also located, which is fed by waters from the Atlantic Ocean and the confluence of several streams. Because of these special characteristics, it is considered an important continental wetland in its headwaters and middle stretch, with high environmental value as it contains significant biodiversity and serves as a habitat for birds. Finally, about 5,000 ha of the Huelva estuarine-associated shoreline belongs to the SPA Marine Area of the Tinto and Odiel.

A significant part of these protected areas has sediments with high concentrations of potentially toxic elements that, as explained earlier, are transported in the dissolved phase by the Tinto and Odiel rivers and precipitate in the Ria of Huelva estuary (Fig. 6.15).

6.4.1 Affection to vegetation

In the tidal zones of the estuary, both in the northwest area (Odiel estuary, from Gibraleón to Huelva) and in the northeastern marshes (Tinto estuary, from Niebla to the confluence with the Odiel), halophytic plants such as *Salicornia, Sarcocornia, Anthrocnemun*, and grasses like *Spartina* are common (Fig. 6.16). Studies conducted over 20 years ago have demonstrated that these plants take up potentially toxic elements (e.g., As, Cu, Cd, Pb, Zn)

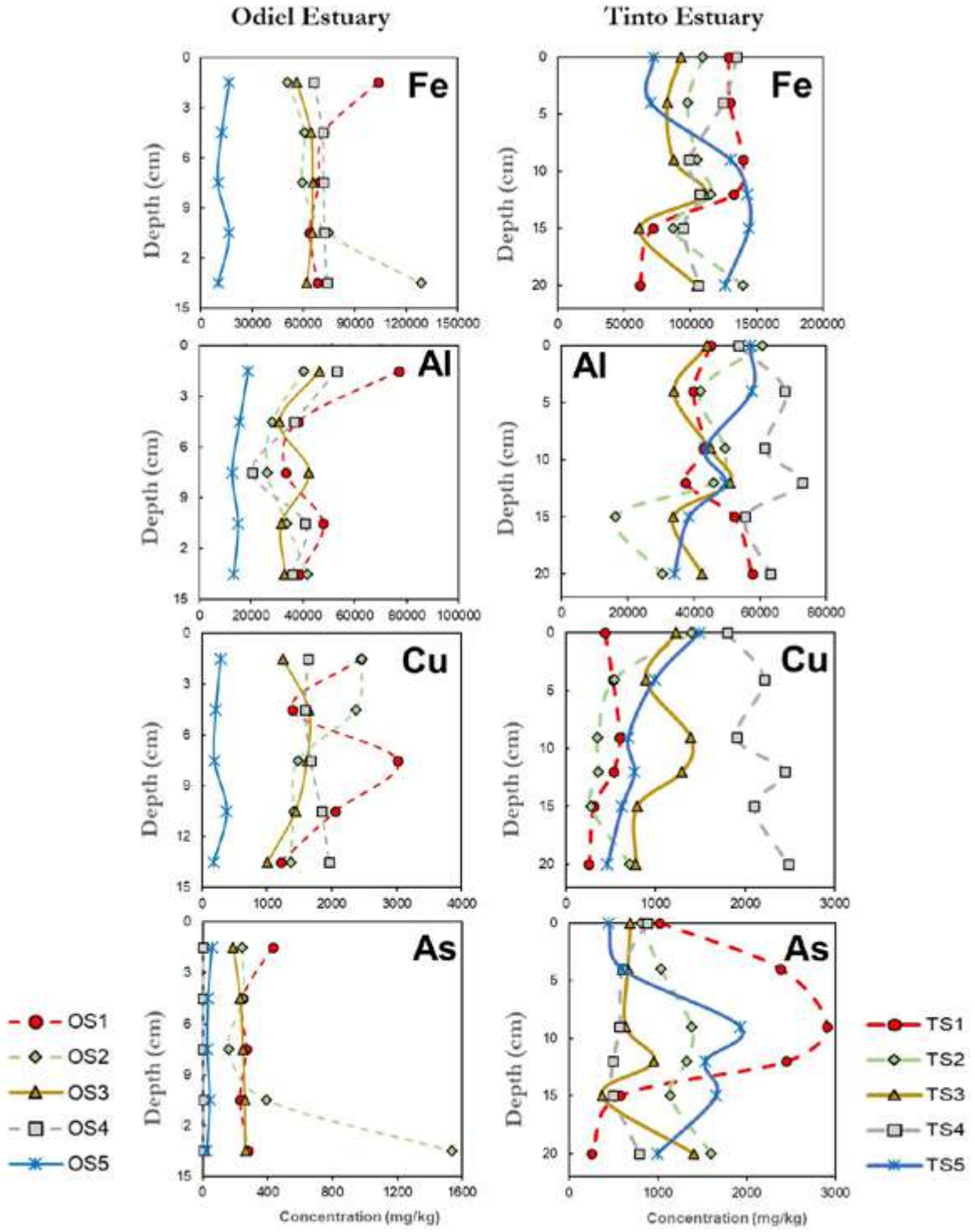

Figure 6.13: Concentration of Fe, Al, Cu and As in surface sediments (0-15 cm) of the Tinto and Odiel estuaries.

accumulated in the sediments without showing acute toxic effects (Luque et al., 1999). For example, *Spartina maritima* showed concentrations of 61 mg/kg (dry weight) of As, 128 mg/kg of Cu, 45.9 mg/kg of Pb, and 297 mg/kg of Zn in young leaves. Similarly, *Zostera noltii*, a protected aquatic plant inhabiting the tidal creeks bottoms and air exposed during the most

Figure 6.14: Aerial photo of Marismas del Odiel (Odiel Marshlands), to the north of the bridge connecting Huelva with Corrales town.

intense low tides (Muñoz-Rodríguez et al., 2022), exhibited the highest concentrations, with 109 mg/kg of As, 878 mg/kg of Cu, 190 mg/kg of Pb, and 2440 mg/kg of Zn.

The concentrations of As, Cu, Pb, and Zn in the tissues of *Spartina densiflora* (an invasive species) and *Spartina maritima* present in the marshlands of the Odiel and Tinto estuaries have also been analyzed (Cambrollé et al., 2008). Elevated average concentrations were observed for both species, with higher levels in the roots than in the aerial tissues. The As content ranged from 1.5 to 450 mg/kg and from 1.5 to 364 mg/kg for *S. densiflora* and *S. maritima*, respectively. Despite the high concentrations of As, no toxicity was observed. This can be explained because, although As is known as a potent metabolic inhibitor, it is less

Figure 6.15: Aerial Photo of the Tinto estuary between San Juan del Puerto and Moguer towns. The ochre/orangish colors are caused by the great amount of Fe minerals contained in sediments.

toxic when the plant is well supplied with phosphorus, which is detected in the Odiel and Tinto marshes at high levels (Martin et al., 1997; Rufo et al., 2007). The Cu concentration varied between 22 and 2546 mg/kg and 27 to 4933 mg/kg for *S. densiflora* and *S. maritima*, respectively, with mean values of 2027 ± 183 and 4405 ± 276 mg/kg, correspondingly. Regarding Pb, its content ranged from 0.1 to 217 mg/kg for *S. densiflora* and from 0.1 to 292 mg/kg for *S. maritima* (mean values of 148 ± 8 and 168 ± 41 mg/kg, respectively). It is well known that low pH values promote the translocation (transport of substances from the roots to the aerial parts of plants) of Pb in plants (Kabata-Pendias and Pendias, 2001), which may explain the high levels of Pb observed in this study, as the sedimentary environments of the Huelva estuary are characterized by low pH values. The Zn content in tissues ranged from 27 to 1249 mg/kg and from 42 to 2326 mg/kg for *S. densiflora* and *S. maritima*, respectively, with mean values of 975 ± 83 and 1258 ± 262 mg/kg, respectively. It was also observed that, at high levels of Zn in sediments, these species are capable of transporting it from the roots and accumulating it in the upper parts of the plant (Cambrollé et al., 2008; Mateos-Naranjo et al., 2008).

There is a recent interest in consuming plant products from the sea, leading to the establishment of companies that market these products. For example, *Salicornia* is already marketed in the province of Cádiz, Portugal, Huelva, and other countries in northern Europe. This has led to the need for new studies to assess the potential of species present in the Huelva estuary (Sanjosé et al., 2022) for commercialization. A recent study on the species *Salicornia ramosissima* in Marismas del Odiel demonstrates a high capacity of these hal-

Figure 6.16: Different landscapes showing the halophytic vegetation that commonly thrive in the Ria of Huelva estuary.

ophytes to absorb metals, with concentrations exceeding the limits established by regulations for consumption. In this regard, the marketing and consumption of species growing in the Huelva estuary are discouraged.

In summary, all studies carried out highlight that the vegetation present in the estuaries of the Tinto and Odiel rivers has adapted to conditions of exposure to high concentrations of metals and, in many cases, acts bioaccumulating these metals. Although no toxic effects are detected for the plants, this bioaccumulation promotes the transfer of these contaminants from sediments and water to the food chain.

6.4.2. Affection to macrobenthos and fishes

In the Huelva estuary, the invertebrate macrobiota in the tidal marshlands and salt flats is highly relevant, featuring populations of microcrustaceans such as copepods and artemia. Polychaetes, like *Hediste diversicolor* (ragworm, sandworm), and crustaceans, with large populations of fiddler crabs (*Uca tangerii*) and green crab (*Carcinus maenas*), are also abundant. These are often captured for artisanal purposes and used as bait for sports fishing and local consumption, respectively (Castellanos and Luque, 2022). The estuary is also rich in bivalve mollusk species, such as the fine clam (*Venerupis decussata*) and wedge clams (*Donax trunculus*).

Studies on macrobenthic structure have demonstrated a lower number of families in areas with greater disturbance, such as the the Tinto and Odiel estuaries, associated with higher pollution levels, which affects the normal development of the benthic community. These effects are also observed in terms of diversity and uniformity of populations (Usero et al., 2008). Other studies have shown that the lower areas of the estuary (closer to the mouth) exhibit greater macrobenthic diversity compared to areas with higher river influence. These results can be explained by the fact that waters in the upper areas, with a lower pH, contain a high concentration of bioavailable metals (e.g., dissolved or in their free form) as well as lower salinity than marine waters, allowing only species adapted to these extreme conditions to thrive (Rosado et al., 2015).

Bivalve mollusks (e.g., clams, mussels, and oysters) are among the organisms most used for biomonitoring metal pollution (Morillo et al., 2005). The striped venus clam (*Chamelea gallina*), a common edible bivalve mollusk on the Atlantic coast of southern Spain, has been employed as a model organism to establish contaminant concentrations on the Huelva coast (Usero et al., 2005 and 2008). In a study covering the entire western coast of the Gulf of Cadiz, where individuals of this clam were sampled, it was observed that the Pb concentration in the striped venus clam, at points near the mouth of the Huelva Estuary, exceeded the maximum limits set by the European Union for bivalve mollusks intended for human consumption (Pb 1.5 mg/kg wet weight) (EEC, 2001; 2002), rendering the species caught in this area unsuitable for consumption. On the other hand, studies conducted at the Tinto and Odiel estuaries and the Padre Santo channel confirm that the metal content of the species *Balanus amphitrite* (filter-feeding organism typically present in relatively disturbed areas where other species are absent), which live attached to surfaces such as rocks, piles, and seawalls in the intertidal zone, clearly correlates with high concentrations of potentially toxic elements in the estuarine waters, especially Cu, Zn, and Mn (Morillo and Usero, 2008). The results have been compared with other areas in the Gulf of Cadiz, showing that the Huelva Estuary contains much higher levels of metals in both water and *Balanus amphitrite* than those found in the Bay of Algeciras, another important industrial area in the south of Spain.

Other organisms known as good biomonitors of metal pollution include polychaetes, crustaceans, micro- and macroalgae (Rainbow and White, 1989), and so they have also been studied in the Ria of Huelva. For example, a study characterizing the environmental

quality of the Odiel-Tinto system based on the spatial and temporal variation of crustacean communities demonstrated a clear relationship between a lower number of species and the abundance and concentration of metals and metalloids in the innermost areas of both estuaries (Sánchez-Moyano and García-Asencio, 2010).

Fish constitute an important part of the human diet, and thus, many studies have focused on the effects of pollutants such as metals, which are highly persistent, non-biodegradable, and potentially toxic, in edible species (Usero et al., 2004). An analysis of metal bioaccumulation in common sole (*Solea vulgaris*), European eel (*Anguilla anguilla*), and golden grey mullet (*Liza aurata*) from marshlands in the Odiel Estuary showed higher metal concentrations compared to fish from marshlands with similar characteristics located on the coast of Cadiz. From a legal standpoint, the muscle tissue of all captured fish was deemed suitable for human consumption; however, concentrations in the liver exceeded legal limits for some metals, such as Cu. Nevertheless, these organs are usually considered viscera without interest for consumption. Another study examined the effect of metal pollution on sole fish (*Solea senegalensis*), which are benthic fish in direct contact with sediments and also feed on invertebrates that can accumulate metals (Oliva et al., 2012). This species is economically and commercially important and is one of the most abundant and representative species in the Atlantic and Mediterranean coasts. The metal concentration in the liver of specimens caught at the mouths of the Tinto and Odiel estuaries and near the industrial zone of Palos reached up to 1148 mg/kg of Cu (dry weight) and 143 mg/kg of Zn. The highest levels were observed in areas with higher metal concentrations, both in water and sediment.

Studies exposing different organisms to sediments from the Ria of Huelva have shown negative acute (mortality) and/or subacute (e.g., histopathological damage) toxic effects. Riba et al. (2004), based on experiments with various organisms (i.e., amphipods, bivalves, fish, and rotifers), concluded that the Ria of Huelva undergoes significant environmental degradation related to high concentrations of metals and hydrocarbons in its sediments. In this regard, the confluence zone of the Tinto and Odiel rivers exhibited severe environmental degradation, while the area near the Padre Santo channel and its mouth had a lesser impact.

A different study evaluating the toxicity of estuarine sediments, based on bioaccumulation data and histopathological damage in bivalves (*Ruditapes philippinarum*) and crabs (*Carcinus maenas*), demonstrated that metal and metalloid concentrations (As, Zn, Cd, Ni, Hg, Cu, and Cr) are very concerning in the area of the Port of Huelva (Martín-Díaz et al., 2008). These sediments are characterized by producing adverse effects (often mortality) in exposed organisms due to the high concentration of potentially toxic elements. Similar results have been observed in other marine organisms, including amphipods (i.e., *Ampelisca brevicornis, Corophium voluntator*; Basallote et al., 2014; Cesar et al., 2007), copepods (*Tisbe battagliai*), microalgae (*Cylindrotheca closterium*; Araújo et al., 2010), the Japanese clam *R. philippinarum* (Rodríguez-Romero et al., 2014; Basallote et al., 2015), oysters (*Crassostrea angulata*; Riba et al., 2005), and even sea urchin larvae (*Paracentrotus lividus*; Basallote et al., 2018).

6.4.3. Affection to birds

This estuary is considered one of the most important coastal wetlands in the Iberian Peninsula, especially due to the multitude of birds inhabiting it, including shorebirds such as the sanderling (*Calidris alba*) or the Kentish plover (*Charadrius alexandrinus*) (Castellanos and Luque, 2022). This significance is confirmed by the declaration of Special Protection Areas for Birds (SPA). These birds feed on invertebrates and microcrustaceans that are exposed to metal pollution in these marshlands. Therefore, there are processes of bioaccumulation and metal transfer through the food chains, which, in turn, could pose a risk of toxicity to wild populations. However, there are few studies evaluating metal toxicity in birds in the Ria

of Huelva. An exception is the study of Rodríguez-Estival et al. (2019) to assess the risk of metal exposure in the black-necked grebe (*Podiceps nigricollis*), categorized as "near threatened" by the International Union for Conservation of Nature. The results showed that black-necked grebes had elevated concentrations of As and Zn in their blood compared to toxicity thresholds determined for birds. These high metal concentrations in grebes were associated with transfer through the food chain via the most important dietary component, which is the brine shrimp (*Artemia parthenogenetica*), inhabiting the Odiel marshes. It was observed that brine shrimp accumulate concentrations of As, Pb, Cu, and Zn between 3 and 12 times higher than brine shrimp inhabiting uncontaminated waters. In this context, brine shrimp are the main food source for many birds inhabiting these marshlands, so it can be affirmed that both grebes and other species are exposed to high concentrations of metals, and there is a high potential for trophic transfer of contaminants.

6.5. MAIN CONCLUSIONS

The Ria of Huelva serves as a transition zone between riverine and marine conditions. The mixing of waters in estuaries results in the presence of a salt wedge and a progressive decrease in salinity inland. Additionally, the Ria of Huelva experiences a pH gradient in the water, ranging from acidic values (approximately 2.5 to 3.5 in the Tinto and Odiel rivers) to alkaline values typical of the sea (approximately 8).

Contaminants transported from mining areas exhibit different behaviors in the estuary: non-conservative elements, mainly iron, aluminum, and copper, are removed from the water through mineral precipitation during the neutralization of AMD. In other words, they tend to become part of the particulate matter that deposits in the bottom sediments. On the other hand, conservative elements like zinc, manganese, nickel, and cobalt remain in solution throughout the estuary, reaching the Atlantic Ocean. Finally, elements with an ON-OFF behavior, mainly arsenic, are initially retained through processes of adsorption or mineral coprecipitation (OFF) and later released back to the water column (ON), also reaching the ocean along with conservative elements.

The precipitation of dissolved metals and subsequent sedimentation of particulate matter within the estuary are influenced by natural processes such as tidal cycles and variations in river discharges. Under conditions of heavy floods, river flows are so high that the flocculation and settling processes of contaminants shift towards the open sea.

Moreover, anthropogenic activities, such as dredging for the maintenance of the navigational channel in the Port of Huelva, also induce changes in metal concentration patterns in the estuary. This activity disrupts sediments, leading to the incorporation of suspended solids and contaminants into the water column, increasing the mobility and bioavailability of metals, as well as their redistribution along the estuary and coastal waters. Due to all these factors, establishing a relationship between metal concentration in the water column and sediment in such a dynamic environment as the Huelva estuary is extremely challenging.

All the factors mentioned above explain why estuarine sediments act as temporary or permanent sinks under changing environmental conditions. In this context, the sediments of the Ria of Huelva have been classified as highly toxic according to numerous scientific studies assessing the concentrations of certain metals and metalloids and their effects on exposed organisms (e.g., plants, crustaceans, bivalves, fish, and even birds). Furthermore, following the guidelines for dredged material characterization developed by the Spanish Center for Studies and Experimentation of Public Works (CEDEX), they are frequently classified as contaminated sediments.

Currently, mining pollution continues to transport annually large amounts of contaminants to the estuary, in addition to the contributions of acidic leachates, of lesser magnitude,

from the phosphogypsum stacks located in the salt marshes on the right bank of the Tinto River estuary.

Despite restoration measures carried out in the estuary, especially since the change in industrial discharge management strategy from 1997, numerous studies confirm that the contamination level by metals and metalloids in the Huelva estuary is very high compared to other estuaries, such as Guadiana, Piedras, or even the Guadalquivir River estuary, and even on a global scale.

The high levels of metals in the water and sediments in the estuary transfer to vegetation, penetrating the food chain and affecting many other organisms inhabiting this environment, including crustaceans, fish, and even birds, posing a severe environmental problem.

7

PREVENTION AND REMEDIATION MEASURES OF ACID MINE DRAINAGE

7.1 INTRODUCTION

The water pollution by AMD in sulfide and coal mining is a serious issue for the mining industry (Öhlander et al., 2012; Hudson-Edwards, 2016). The costs associated with treatment measures in mines generating AMD with high concentrations of contaminants can be very high in the long term, potentially reducing economic benefits and, in some cases, the feasibility of a mining project (Öhlander et al., 2012; Pozo et al., 2017). Therefore, the International Network for Acid Prevention (INAP), a consortium formed by major mining companies worldwide, has developed a guide with best practices to prevent and mitigate the formation of AMD (INAP, 2014).

The primary strategy to prevent and mitigate the formation of acid leachates is to minimize the availability of primary reagents that cause sulfide oxidation, i.e., reduce the availability of oxygen and water, and add neutralizing reagents to prevent the formation of these waters. Additionally, minimizing the generation of residual materials rich in sulfides during the mining process is another important prevention strategy. In current mines, preventing AMD formation is mainly planned during the project development phases and is subsequently implemented during the operational phase of the mine. The prevention process aims to quantify the long-term impacts of different alternatives to select the option with the least impact (Öhlander et al., 2012). Mitigation measures implemented as part of an effective control strategy should require minimal intervention and active management.

In general, before the start of mining activity, there are numerous effective options at a relatively low cost to prevent AMD generation. However, during mine exploitation, these prevention options will decrease, and their costs will increase simultaneously (Fig. 7.1). For a reliable prediction of AMD formation and the effectiveness of possible mitigation measures, a specific study for each mining project must be carried out based on comprehensive characterization of geology, geochemistry, mineralogy, physical properties of the ore (e.g., grain size, porosity, etc.), local hydrology and hydrogeology, and the characteristics of different types of waste that may be generated. Various tests, such as those based on acid-base accounting (ABA), batch or kinetic leaching tests, are crucial in this regard.

The best practices should always focus on preventive measures that mitigate or minimize the formation of AMD. Figure 7.2 illustrates the main preventive measures and general aspects to consider during different stages of the life cycle of a mining project.

Finally, it should be noted that for a successful AMD prevention or mitigation plan, all stakeholders (e.g., regulators, community leaders, environmental groups, NGOs, government agencies, as well as mine managers) must be involved in the decision-making process, reaching a consensus on objectives and the strategy to be followed (Ohlander et al., 2012).

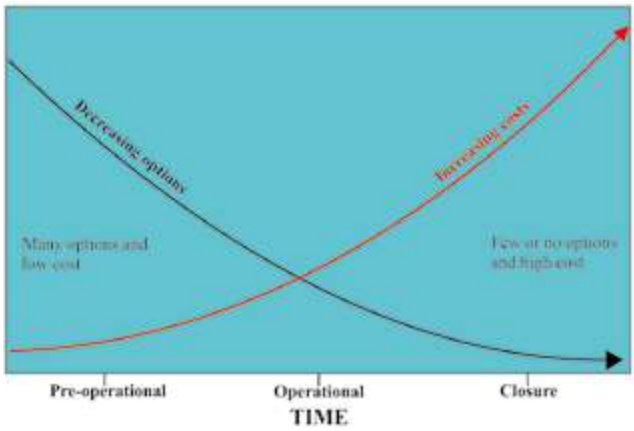

Figure 7.1: Options and costs associated to AMD prevention measures during different phases of a mining project (modified from INAP, 2014).

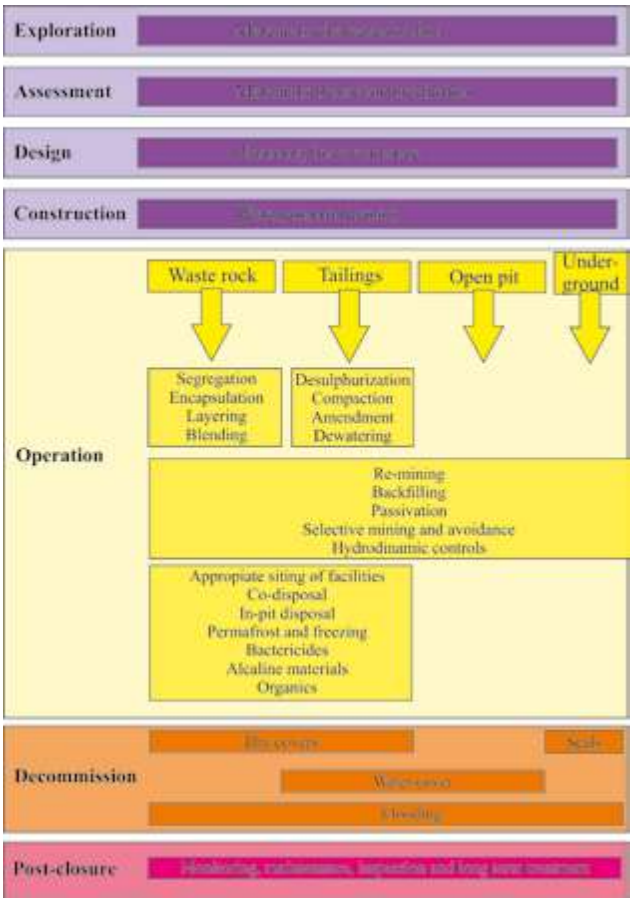

Figure 7.2: General perspective of prevention methods for AMD generation during different phases of a mining project life-cycle (modified from INAP, 2014).

Unfortunately, in the IPB, particularly in the basins of the Odiel and Tinto rivers, the problem is due to leachates generated in dozens of abandoned mines, where there is a vast variety of wastes generated during almost 200 years of intense mining activity (Roman and pre-Roman exploitation is of much lesser extent). Therefore, potential actions are technically challenging and economically very costly, as preventive methods were not used (Fig. 7.1). In each particular case, the best techniques to employ will need to be decided based on a detailed characterization of the area. The following sections will present the most commonly used preventive measures to reduce the production of acid leachates and the methods or technologies for treating affected waters.

7.2 METHODS TO PREVENT AMD GENERATION

The selection of the preventive method or methods to avoid the formation of AMD is typically done in the design phase of the mining project (Fig. 7.2). The following sections summarize these preventive measures using examples applied or investigated in the IPB.

7.2.1 Diversion of surface waters

The objective of this measure is to reduce the volume of AMD and the pollutant load generated by mining operations. Generally, it is much more effective to treat a smaller volume of water with high concentrations of metals and acidity than a larger volume of water with low concentrations.

This measure typically involves the construction of impermeable channels around the operational area (perimeter channels) to prevent the entry of uncontaminated runoff water and its contact with materials containing sulfides. The dimensions of the channels should be designed based on expected precipitation and the hydrology of the area. They usually require maintenance to prevent the accumulation of sediments or other materials, ensuring their effectiveness. In some cases, diverting the flow of groundwater to prevent contact with sulfides may also be advisable.

This measure is relatively cost-effective, even when applied during the project closure stage or in already abandoned mining areas, while the benefit of its use can be very high. A clear example is described by Cánovas et al. (2018b) at the abandoned facilities of Mina Poderosa located in the upper part of the Odiel River sub-basin (Fig. 4.14). In this mine, there is a main discharge with maximum flows of up to 11 L/s and very high concentrations of metals. AMD arises from an old gallery used for transporting the extracted mineral during the underground mining phase of the mine; previously, the activity was carried out in open-pit mining through two open pits (Fig. 7.3). Currently, the recharge of the anthropogenic aquifer generated by mining activity is the direct precipitation on the two abandoned pits and the surface runoff generated towards them (Fig. 7.3). The construction of perimeter channels around both

pits would prevent the entry of surface runoff into the pits, resulting in a reduction of approximately 50% in the discharge volume and pollutant load (Cánovas et al., 2018b).

Another example of the use of perimeter channels to divert surface waters, in this case as a method to mitigate inherited pollution, is found in the reopening of the Riotinto mines by Atalaya Mining. After the reopening, the previous channels were rehabilitated, and new ones were constructed to minimize the access of surface water to materials susceptible to generating acidity (Fig. 7.4). As a result of these actions, a significant part of surface runoff no longer reaches the abandoned sulfide-rich dumps, resulting in a decrease in the flow and pollutant load of the leachates generated in these dumps (Fig. 7.5).

Figure 7.3: Aerial images and photo of Poderosa mine outflows, showing the drainage basin of open pits and the potential location of perimeter channels to reduce the AMD generation (aerial images from Google Earth).

7.2.2 Sealing of mining galleries and shafts

In underground mines, concrete plugs can be used to seal galleries and/or shafts with two fundamental objectives: 1) prevent or limit the entry of water and oxygen into the system, and 2) prevent the release of leachates from these points. For greater safety, it is advisable to inject cements into the areas around the plug, increase the length of the sealed zone, and install secondary plugs (INAP, 2014).

Sealing galleries can also lead to the flooding of areas with reactive minerals, limiting the amount of oxygen available for oxidation. However, flooding can also result in washing away oxidation products accumulated in the unsaturated zone, worsening the contaminant concentration levels of the accumulated water. Therefore, this measure must be accompanied by a detailed hydrogeological study and a good understanding of old mining works, as sealing one outlet often leads to the groundwater level rising until it exits through other points.

Other aspects to consider are the potential catastrophic effects in the event of a seal failure, making monitoring of seal stability over time necessary, which is usually not done in abandoned mine areas. Unfortunately, such accidental discharges are common in the con-

Figure 7.4: Photo of perimeter channel in the Riotinto mines.

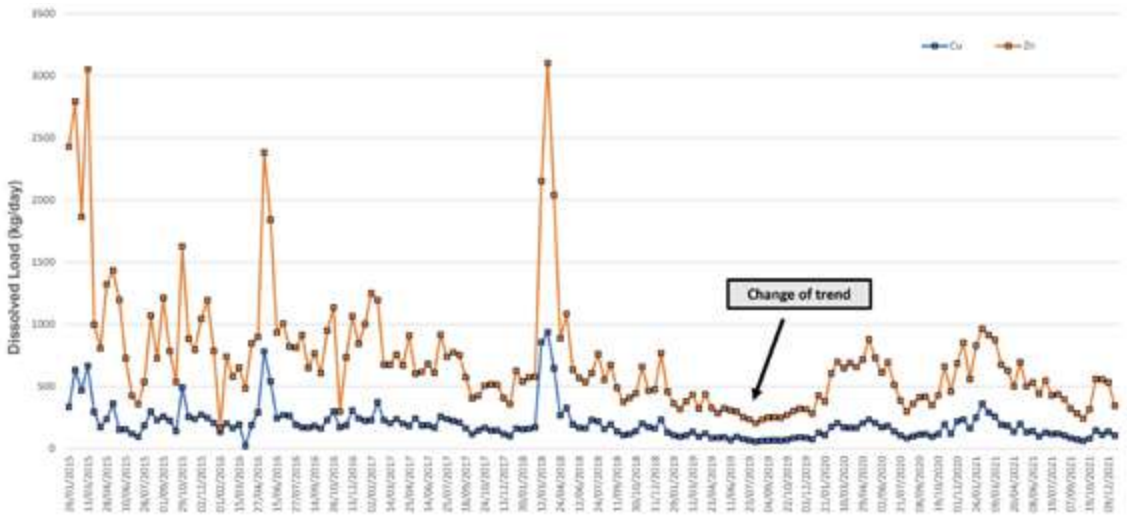

Figure 7.5: Evolution of the pollutant load of Cu and Zn delivered from an AMD source in Riotinto mines. It can be noted a decreasing trend after the water diversion (León et al., 2023).

text of abandoned mining worldwide (e.g., Bureau of Reclamation, 2015; Mayes and Jarvis, 2016; Walton-Day and Mills, 2015; Younger, 2002). This occurred on May 17th 2017 in the IPB, when the concrete seal of the Los Cepos gallery in the La Zarza Mine failed (Fig. 7.6), causing the sudden discharge of approximately 270,000 m^3 of extremely contaminating AMD, which quickly reached the Odiel River and the estuary of the Ria of Huelva (Olías et al., 2019). The description of the consequences and causes of this discharge is presented in sections 4.2.3 and 5.2.3.

Another example in the IPB is the concrete plug at the Tinto Santa Rosa mine, located next to the Villar River. This seal is partially perforated, allowing the discharge of acid mine water at two points (Fig. 7.7).

Figure 7.6: Photo of Los Cepos galleries before (left) and during (right) the mining spill from La Zarza pit lake.

Figure 7.7: Photo of the concrete plug at the Tinto Santa Rosa mine gallery showing the leakage of highly-pressure AMD. General view (right) and detailed view (left).

7.2.3 Dry covers

The covering of mining residues that are susceptible to generating AMD with materials is referred to as dry covers. Such covering can be also possible following flooding strategies, known as wet covers, which are described in the next section. Dry covers involve coating tailings, pyritic sludges, or other sulfide-rich materials with various types of materials to restrict the development of conditions required for sulfide oxidation reactions (i.e., access to oxygen and/or water) and limit the transport of the products of these reactions (acidity and toxic metals) to the environment. Additionally, these coverings can be designed to promote revegetation in the area and reduce problems of fine particle mobilization by the wind, allowing them to be implemented simultaneously with landscape restoration.

There are various possibilities; the coverings can be simple or complex, ranging from a single layer of soil available in the area to multiple layers of different types of materials, including local soils, mining overburden, geosynthetic materials, clays, draining materials to facilitate lateral water flow, and organic-rich materials to reduce oxygen concentrations.

Reducing water infiltration can be achieved by two methods: 1) The cover can be constructed with materials of low hydraulic conductivity, forming a barrier that limits the percolation of rainfall, and 2) Infiltration water is stored in the cover near the surface to be subsequently removed by vegetation evapotranspiration. Obviously, the local climate plays a fundamental role in the type of strategy used (MEND, 2004), so the design will be directly related to the hydro-climatic characteristics of the specific area.

The first step in designing the cover involves detailed characterization of the area and the residues to be covered (e.g., size and geometry of the tailings and their hydrological characteristics, mineralogy of the residues, climatic conditions, etc.). In a second stage, a preliminary design is made with the most appropriate type of cover based on material availability, climate, and expected results of the covering. Numerical modeling is usually performed to explore different possibilities and select cover parameters that achieve the highest efficiency. The final design stage involves field tests to verify the performance. Finally, long-term efficiency control of the cover is necessary (MEND, 2004; 2007).

Figure 7.8: Aerial images of tailings dams in Monte Romero mine, previously to the installation. (above, June 2009) and after the implementation of a dry cover (below, July 2013).

Dry covers are typically applied during the mine closure stages (Fig. 7.2), although they are also used in abandoned mining areas. An example in the IPB of the latter situation can be seen in Figure 7.8, with images of the pyritic sludge ponds at the Monte Romero mine before and after the installation of the cover. Such measures have also been adopted in the IPB at the Concepción mine (Martín Crespo et al., 2010), in the Almagrera mining-industrial complex, or on accumulated residues in the Las Viñas area, north of Sotiel.

7.2.4 Wet covers

The accumulation of acidity-generating materials beneath a layer of water restricts the generation of AMD since the concentration of

dissolved oxygen in water is 30 times lower than in the atmosphere, and its transport in water through advection and diffusion is much slower than in air (INAP, 2014). Other processes that can occur under these saturation conditions include sulfate reduction and the precipitation of metals in the form of sulfides if reductive conditions are found, the formation of layers through sedimentation that inhibits the interaction between reactive materials and water, etc. The flooding must be permanent, as seasonal water level fluctuations that expose materials to atmospheric oxygen can lead to the release of acidity and metals.

These methods are commonly used for covering fine materials, pyritic sludges, or tailings from metallurgical operations. There are different arrangements for the installation of wet covers (INAP, 2014), such as constructing dams to enclose an inner space for depositing sludges, a single linear dam that takes advantage of the terrain slope, etc. In the basins of the Odiel and Tinto rivers, an interesting option that needs further investigation would be the disposal of highly reactive residues in flooded open-pit mines.

However, a fundamental aspect, unfortunately not always addressed, is the physical stability of containment dams over time. From proper design to monitoring stability, these are crucial aspects that must be considered to prevent environmental catastrophes. A clear global example was the Aznalcollar spill on April 25th 1998, where around 2 hm^3 of pyritic sludges and 4 hm^3 of acidic waters were released, causing a massive environmental disaster, affecting 60 km of the Guadiamar River, reaching the boundaries of Doñana National Park. Today, 25 years after the spill, residual contamination still exists in the soils and groundwater around the Aznalcóllar pond (Olías et al., 2021).

7.2.5 Microencapsulation

Microencapsulation involves treating the reactive surfaces of minerals to limit the release of contaminants by creating a chemically inert layer that encapsulates them, thus restricting the access of oxygen and water to the mineral surface. This prevention method has been investigated at the micrometer level in laboratory tests (batch experiments), and various types of reagents have been used to achieve this effect: potassium permanganate (Kang et al., 2015), phosphates or phosphates combined with thiocyanates (Evangelou, 2001), aluminum hydroxide (Zhou et al., 2018), etc. Recent studies have shown promising results in the encapsulation of pyrite by adding a silica-rich solution, along with other substances (Fan et al., 2017).

While these studies show promising results, the laboratory-scale results from Cuenca (2019) using samples from pyrite dumps in the Tharsis mining complex (Fig. 7.9) indicate

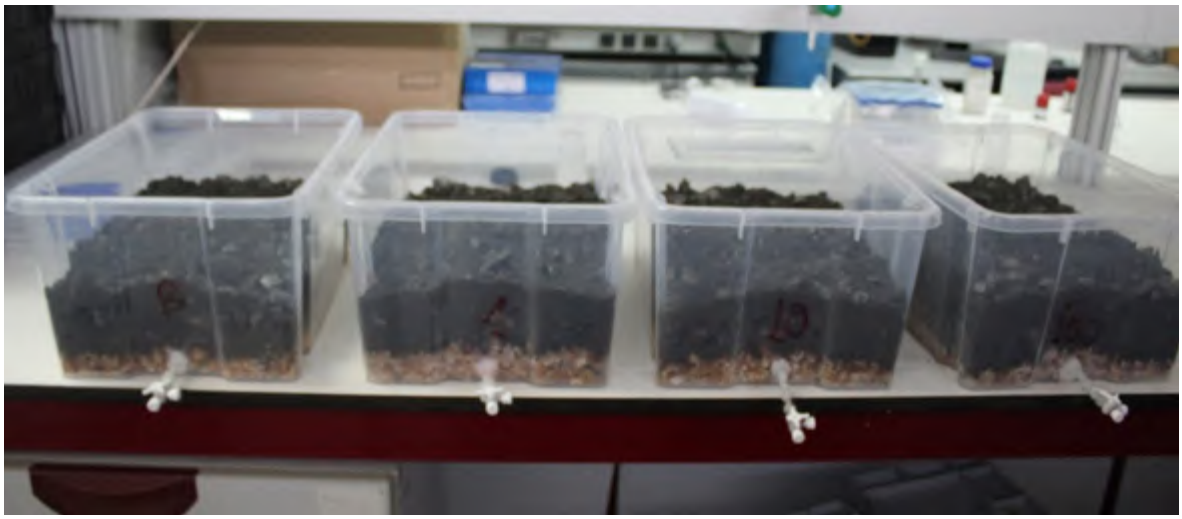

Figure 7.9: Microencapsulation experiments of pyrite-rich wastes at lab scale.

that the temporal effectiveness of encapsulation seems limited. Field-scale experiments are needed to verify the long-term effectiveness of this technology.

In general, it has been observed that treating recently extracted materials is easier and more effective than treating materials that have been exposed to oxidizing conditions for a long time. Furthermore, applying this technology is easier before material disposal in dumps and tailings ponds. Its application to already formed dumps is more complicated due to the difficulty of the agent coming into contact with all surfaces of reactive materials and the existence of preferential flows.

7.2.6 Addition of alkaline materials

One common way to reduce AMD generation is by controlling the pH in acid materials through the addition of alkaline substances. There are various application possibilities, including mixing the alkaline reagent with the materials to be treated or placing it in layers above or below the waste.

Regarding the mixed application of the reagent with the waste, in the case of existing dumps, it would only be usable for a superficial layer with limited sulfide concentrations, which would favor revegetation. When the sulfide concentration is high, periodic addition of alkaline material would be needed, making this measure seemingly unviable. It is necessary to strike a balance between the potential acidification of sulfides and the neutralization effect of the alkaline substance. Additionally, achieving a homogeneous mixture is important to avoid zones with higher sulfide concentrations where acidic conditions may arise.

Another example of this methodology is the experience conducted at the Monte Romero mine in the Olivargas reservoir basin. A layer of fly ash, an alkaline residue obtained from coal-fired power plants, was used to cover an experimental plot on a pyritic sludge pond (Fig. 7.10). When rainwater infiltrates through the ashes and comes into contact with sulfides, due to the intense precipitation of iron and other elements, a hardened layer (hardpan) is formed that prevents the entry of water and oxygen inside the waste dump, thereby reducing the generation of acidic leachates (Pérez-López et al., 2007a and b). This method has the advantage of long-term functionality, as any cracks in this layer would self-repair through the formation of new precipitates.

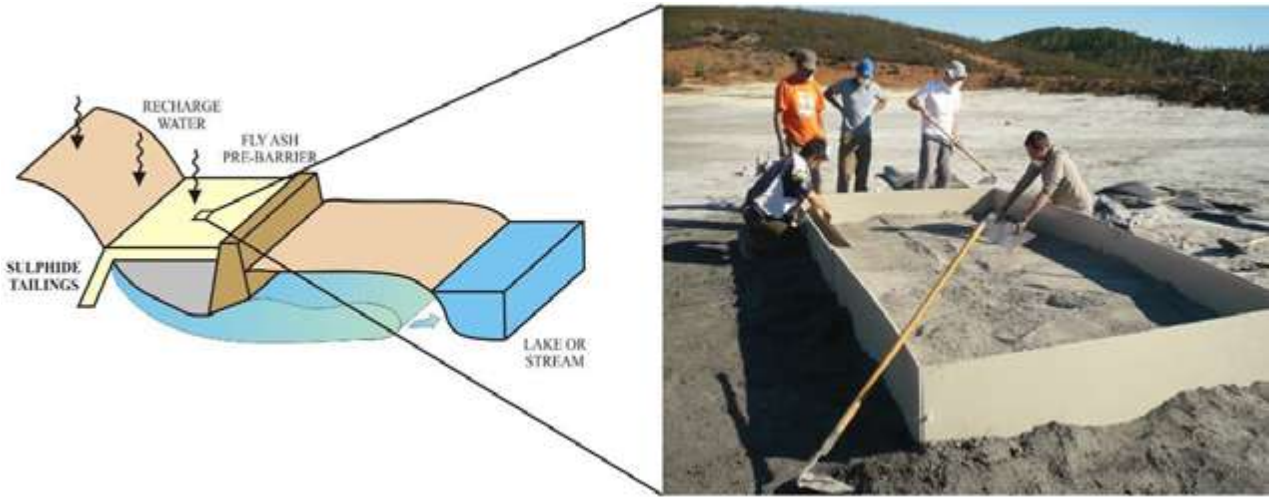

Figure 7.10: Experimental plot for fly ash addition over a pyritic tailing dam at Monte Romero mine.

7.3 TREATMENT METHODS FOR ACIDIC LEACHATES

During the design and development phases of a mining project, treatment methods should always be considered as a secondary option after preventive methods. Figure 7.11 schematically illustrates the preventive methods and controls that should be implemented before considering the treatment of AMD. Avoiding and minimizing the formation of AMD should be the primary objective. When these approaches fail, prove insufficient, or have not been considered, treatment becomes then the only option. This latter situation is common in areas with abandoned mining, as seen in the IPB.

In general, the treatment of AMD will depend on the characteristics of the water to be treated, the required final quality, and economic considerations. Key factors influencing this treatment can be summarized as follows:

- Chemical components, contaminant load, and flow to be treated.
- The origin of the water to be treated, i.e., its source (surface, groundwater, drainages from waste piles or tailing ponds, etc.).
- The expected duration of the treatment.
- Hydrological and climatic conditions.
- The necessary area for the construction of the infrastructure.
- Concentration limits of the discharge permit.

The objectives of mine water treatment (independently of legal compliance) can be diverse and not mutually exclusive:

- Recovery and reuse of AMD in mining operations for mineral processing. The water balance of a mine requires comprehensive management of different volume and water quality demands. In this case, the treatment of acid mine waters aims to modify water quality so that the treated effluent is suitable for the intended use in the mining area.
- Environmental protection, especially concerning the impacts of AMD on surface and groundwater. AMD can act as a transport medium for a wide range of contaminants, often having a high impact when interacting with the environment. The treatment of these waters aims to remove these contaminants to prevent or mitigate their environmental impacts.

Figure 7.11: Scheme of priority methods and preventive controls before proceeding to treat AMD in a mine site (from INAP, 2014).

- Recovery of potentially marketable products from AMD. Although the installation of a water treatment plant to recover some of the compounds transported in solution by acid leachates is unlikely, the recovery of these byproducts improves the economic viability of treatment systems.

On the other hand, there are two basic models of AMD treatment: active and passive. Active treatment seeks to improve water quality using methods that require continuous energy and reagent consumption. Passive treatment achieves water quality improvement using natural processes in systems that do not require energy or significant reagents consumption, only infrequent maintenance.

7.3.1 Active Treatment

Active treatment technologies encompass various methods, including oxidation processes (either through aeration or chemical methods), neutralization and metal precipitation, sedimentation, concentration of obtained sludge, membrane processes, ion exchange, evaporation, biological or chemical sulfate removal, etc. Active treatment methods involve high costs due to the necessary investment for construction (CAPEX), energy and reagent consumption (OPEX), and the need for maintenance personnel. They are frequently employed in active mines, where these costs are already factored into the operating plan. There is a wide variety of active treatment schemes that may involve several of the aforementioned treatment stages; generally, the use or not of these stages depends on the specific characteristics of each mining operation.

However, the processes leading to AMD formation can persist for hundreds or thousands of years after mining activity ceases (Younger et al., 2002). In this context, the costs of active treatments are often impractical. Thus, alternative treatment methods must be considered once mining activity ceases. Nevertheless, in some abandoned mines where acid leachates with high flow rates and contaminant concentrations are produced, and passive methods cannot be applied, active treatment is also employed. Examples include Iron Mountain (California), Wheal Jane (Southwest England), Britannia Mine (Vancouver, Canada), etc. In the IPB, a conventional active treatment plant (oxidation, neutralization, and sedimentation) has been used for many years to treat discharges from the Almagrera mining-industrial complex (Figure 7.12).

Figure 7.12: Active treatment plant at Almagrera mine (currently non-operational). From Francisco Javier Rodríguez Gallardo.

Below, basic processes commonly used in active treatment plants (i.e., oxidation, neutralization and sedimentation) are described.

Oxidation

Dissolved iron (Fe) in AMD (which is generally the predominant metal) can exist in its oxidized form (ferric iron, Fe(III)) or its reduced form (ferrous iron, Fe(II)). Fe(III) is only soluble at acidic pH, precipitating at values above approximately 3. In contrast, Fe(II) is water-soluble even at neutral pH. A key aspect of active treatment is oxidation to ensure that all iron is in the ferric form, allowing it to precipitate during subsequent neutralization treatment. To a lesser extent, this also applies to manganese (Mn).

Oxidation is typically achieved through two different mechanisms: (1) mechanical aeration, increasing the amount of dissolved oxygen and thereby promoting the oxidation of iron and manganese, and/or (2) addition of strongly oxidizing chemical reagents, such as hydrogen peroxide, hypochlorite, or similar substances. Aeration also facilitates the removal of dissolved CO_2, which is commonly present in waters from underground mines, promoting an increase in pH and potentially reducing the significant use of chemical reagents.

Neutralization

Neutralization involves the controlled addition of alkaline substances to neutralize the acidity of water (raising the pH) and to induce the hydrolysis and precipitation of dissolved metals. As a result of increasing the solution pH, the precipitation of trivalent dissolved metals occurs. This precipitation usually takes place as metallic hydroxides and depends on the pH value reached. The precipitation of Fe and Al, which are typically the most abundant metals in AMD, promotes the adsorption and co-precipitation of many other divalent metals. Compounds commonly used for the neutralization of AMD include calcium oxide (CaO), calcium hydroxide ($Ca(OH)_2$), and sodium hydroxide (NaOH; caustic soda). Occasionally, magnesium hydroxide ($Mg(OH)_2$), limestone ($CaCO_3$), and sodium carbonate ($NaCO_3$), among others, are also used (INAP, 2014; Skousen, 2014). The choice of alkaline reagent to use usually depends on economic criteria, as there is a significant cost difference between them, but it also depends on the expected performance of the treatment plant to meet discharge limits.

Calcium hydroxide or hydrated lime ($Ca(OH)_2$) is typically added as a controlled dust dispersion in water or as a lime slurry. Neutralization with calcium hydroxide in the form of a high-density sludge is the most commonly used process today by mining companies for the active AMD treatment, given its relatively low cost, high efficiency, and low volume of generated waste.

Calcium carbonate ($CaCO_3$), usually in the form of limestone, is less expensive than lime and poses little or no handling risk. Its use is recommended when the contaminants to be removed in AMD are primarily Fe and Al. When directly discharged onto the drainage to be treated, it must have a grain size small enough to dissolve before particles can become encapsulated by precipitates on its surface. Both reagents can also be sequentially used in the same treatment system to improve efficiency and reduce costs.

Sedimentation

After neutralization to the required pH value, depending on the metal content of the solution to be treated, the water is typically directed to settling ponds or mechanical thickeners so that the precipitated metals suspended in the water can settle.

Metals often precipitate as a loosely dense matter of flocs that gradually compacts and settles as an orange or red-colored sludge. This sludge must be periodically removed from the settling ponds to prevent clogging and to maintain the residence time of the already treated water in the pond. Another crucial aspect of these systems is the management and treatment of the generated sludge.

The stages described earlier can be considered "conventional" within active technologies. However, there are various technologies known as "emerging" that are either used as independent steps for the removal of specific contaminants or serve as comprehensive active treatments. Some of these technologies are already being used by mining companies on an industrial scale, while others are still in the technological development stage. Noteworthy technologies include those based on ettringite precipitation ($Ca_6Al_2(SO_4)_3(OH)_{12}\cdot 26H_2O$) or biological treatments for sulfate removal, electrocoagulation, closed-loop or high-pressure reverse osmosis, among others (INAP, 2014).

7.3.2 Passive treatment

These treatments involve improving water quality using natural processes without regular human intervention or energy consumption. Only infrequent maintenance is needed for the removal of precipitates and occasional replacement of reagents. The entire process derives its energy from available natural sources, such as topographic gradients that enable water flow from one part of the system to another, as well as microbial metabolic energy, photosynthesis, etc., facilitating the necessary reactions for water treatment. In general, this is a process where sequential removal of acidity and metals occurs in an artificial system that mimics natural systems, such as wetlands.

In these types of treatments, various types of organic (e.g., plant residues, manure, etc.) and inorganic wastes (e.g., slag, alkaline waste, soils, etc.) are commonly used to promote vegetation or bacterial growth. Crucial reactions include the reduction of iron and sulfates, favoring the precipitation of metal sulfides and acidity removal. Additionally, a material that consumes acidity and adds alkalinity to the environment is often used; limestone is the most common material for this purpose.

The effectiveness of these systems is limited to treating moderate AMD flows, typically no more than a few liters per second, and relatively low metal concentrations (tens of mg/L). Often, multiple technologies are applied to treat acidic discharge, with some of them used in series. Table 7.1 and Figure 7.13 summarize different conventional passive treatments and the type of AMD they could treat. The acronyms for various technologies are AeW (Aerobic Wetlands), AnW (Anaerobic Wetlands), BCR (Biochemical Reactors), SRB (Sulfate Reducing Bioreactors), RAPS (Reducing and Alkalinity-producing Systems), VFW (Vertical Flow Wetlands), ALD (Anoxic Limestone Drains), OLD (Open/Oxic Limestone Drains), OLC (Open/Oxic Limestone Channels), MOB (Manganese Oxidation Beds), and MRB (Manganese Removal Beds). The following are descriptions of the most widely used methodologies globally, and finally, the one developed (DAS, Dispersed Alkaline Substrate) at the University of Huelva for highly metal rich AMDs typical of the IPB.

Passive Treatment Systems	Type of Water
Aerobic wetlands (AeW)	Alkaline water; polluted by N
Anaerobic wetlands (AnW)	Acid water; high metal contents
Biochemical reactors (BCR) or Sulfate Reducing Bioreactors (SRB)	Acid or neutral water; high metal contents, selenium, sulfate, etc.
Reducing and Alkalinity-producing Systems (RAPS) or Vertical Flow Wetlands (VFW)	Acid water; high metal content
Anoxic Limestone Drain (ALD)	Acid water; low content in Al, Fe and dissolved oxygen
Open/Oxic Limestone Drains or Channels (OLD, OLC)	Acid water; high metal content, low sulfate content
Natural Fe Oxidation Lagoons (NFOL)	Acid water; high Fe(II) content
Manganese Oxidation/removal Beds (MOB or MRB)	Neutral; high Mn concentration

Table 7.1: Types of conventional passive treatment methods and characteristics of waters subject to be treated.

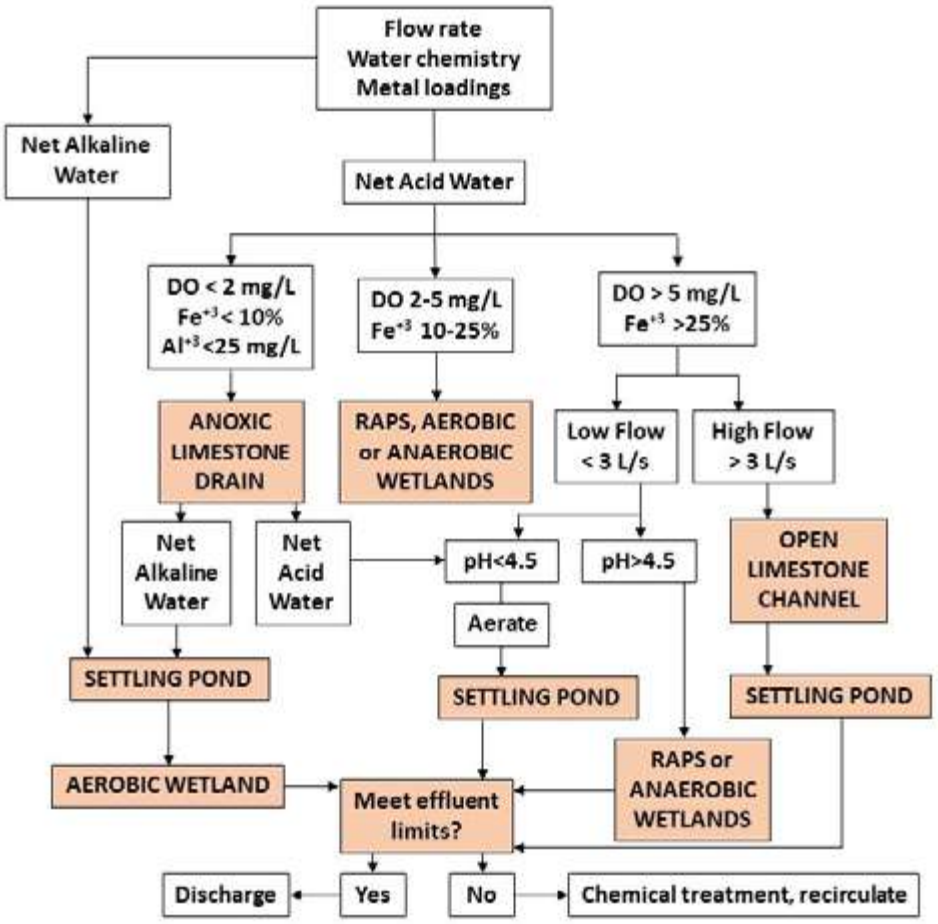

Figure 7.13: Flow diagram for choosing the suitable passive treatment system (modified from Ford, 2003).

7.3.2.1 Constructed wetlands

In natural wetlands, a series of metal retention processes occur, promoting their removal from water (Fig. 7.14). These processes include, among others, the oxidation of Fe and precipitation of Fe and Al hydroxysulfates in the oxic zone, the reduction of Fe and sulfates in deeper zones, the bioabsorption of metals in plants, the fixation of metals to the soil through ion exchange processes with clay minerals or interaction with organic matter, etc. Artificial wetlands based on these processes are designed to mimic biogeochemical reactions and physical mechanisms that naturally occur in these environments. They constitute the most widely used passive treatment option in different climates (Wu et al., 2023).

These wetlands are divided into two groups, depending on whether the contaminant retention processes occur primarily under oxidizing conditions (**aerobic wetlands**) or under reducing conditions (**anaerobic wetlands**). The choice between them depends on the characteristics of the water to be treated (Table 7.1).

Aerobic wetlands (**AeW**) are used for treating waters that have a net alkalinity capable of neutralizing the acidity generated in the hydrolysis of dissolved metals. Therefore, for these wetlands to be effective, the water to be treated must have low concentrations of Fe and Al. These systems consist of one or more interconnected basins through which water flows by gravity. The depth should be shallow (usually less than 30 cm) to ensure oxygenation. They may also include cascades to promote aeration. Under these conditions, the

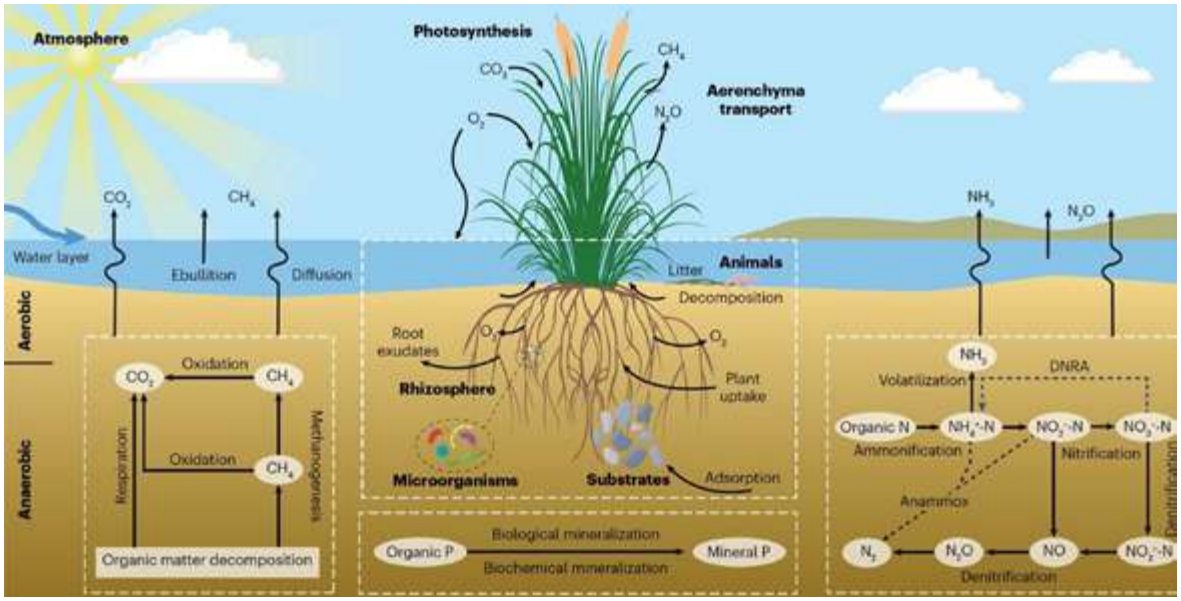

Figure 7.14: Natural processes of metal retention in natural wetlands (Wu et al., 2023).

precipitation of Fe and Al hydroxides, the filtration and deposition of formed colloids and precipitates, metal adsorption, and ion exchange with substrate materials occur.

These wetlands are widely used in the treatment of discharges generated in coal mining, where metal concentrations are low. However, when this technology is applied to strongly acidic waters with high metal concentrations, such as the typical waters in the metallic mining of the IPB, the metal retention processes become ineffective. This is the case with the aerobic wetland at the Lousal mine in the Portuguese part of the IPB (Fig. 7.15).

Anaerobic wetlands (AnW) have a larger water depth (usually between 30-60 cm) to favor the anoxic conditions they require. The substrate consists of a layer of organic matter and limestone. The purpose of the organic substrate is to eliminate dissolved oxygen, to reduce Fe(III) to Fe(II), and to generate alkalinity by reducing sulfates. The performance strongly depends on temperature since the activity of sulfate-reducing bacteria decreases as the temperature drops. Additionally, these systems require long water residence times with reactive substrate for optimal bacterial activity; this implies the need for large land areas to achieve these residence times.

7.3.2.2 Anoxic limestone drains (ALD)

This treatment aims to increase pH through the dissolution of carbonate minerals, mainly calcite. The environment must be anoxic because if iron is in the ferric form, it precipitates on the surface of carbonate minerals, forming a coat that inhibits the subsequent dissolution of the mineral (passivation process). Additionally, the solubility of carbonates depends on the partial pressure of CO_2, which is higher in anoxic environments, thus favoring carbonate dissolution.

Typically, these systems consist of a trench filled with limestone fragments upon which an impermeable cover is deposited to isolate it from the atmosphere (Fig. 7.16). At the outlet of the drainage, a pond is arranged for iron oxidation and settling of the precipitates produced. They are not treatment systems usually used on their own but rather as a pre-treatment or complementary treatment with some other systems. The water should not have a high concentration of Fe(III), Al, and dissolved oxygen; otherwise, the drain becomes clogged with Fe and Al hydroxides.

Figure 7.15: Photo and aerial image of an aerobic wetland constructed in Lousal mine (Portugal), with working problems due to the high metal contents of AMD.

In the IPB, a pilot test was conducted based on this treatment system to check its applicability in waters with high metal concentrations (Rotting et al., 2007). It was used at the Monte Romero mine (Cueva de la Mora, Almonaster la Real) to treat discharge with an acidity of 2300 mg/L of $CaCO_3$, 400 mg/L of Zn, 350 mg/L of Fe, and 130 mg/L of Al. During its operation, pH values did not exceed 5, and it showed irregular performance, clogging after a few months.

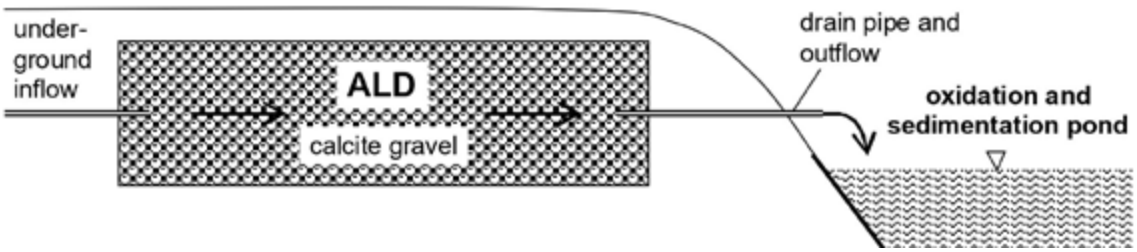

Figure 7.16: General scheme of an anoxic limestone drain (Rotting, 2007)

7.3.2.3 Reducing and Alkalinity-Producing Systems (RAPS)

Also known as Sequential Alkalinity Producing Systems (SAPS) or Vertical Flow Wetlands (VFW). They are based on the same processes involved in an anaerobic wetland but require a much smaller surface area. It consists of a reservoir or pond in which two substrates are deposited: an organic layer and, below it, an anoxic limestone drain (ALD) (Fig. 7.17). The flow is downward. In the organic layer, Fe(III) is reduced to Fe(II) to prevent precipitation in the limestone layer. Additionally, sulfate reduction can occur through the action of suitable bacteria, producing additional alkalinity and decreasing sulfate concentration in water. At the outlet, a pond is located for the oxidation of Fe and settling of the precipitates produced.

This method has been tested in the IPB, specifically for treating the waters of Esperanza Mine with around 600 mg/L of Fe and 125 mg/L of Al. The system consisted of a rectangular tank with an area of 120 m^2. The reactive material comprised calcarenite and horse manure. The treated flow rate was 0.2 L/s, but after two months of operation, it became clogged, highlighting the challenges of its application in waters with high metal concentrations.

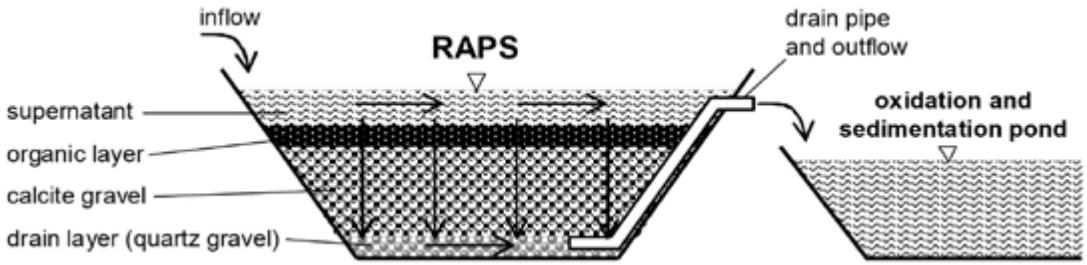

Figure 7.17: General scheme of a RASP treatment (Rotting, 2007)

7.3.2.4 Sulfate Reducing Bioreactors (SRB)

This treatment has some similarity to RAPS as they use an organic substrate, but unlike RAPS, metal removal in these systems is exclusively due to sulfate reduction carried out by bacteria and not the dissolution of limestone (Gusek, 2002). The total metal load that these systems can support is very low because it cannot exceed the sulfate reduction rate caused by bacteria. Therefore, to treat waters with high metal concentrations, the surface area required for these systems is very high. Additionally, elevated concentrations of Zn, Cu, Ni, and other metals are toxic to most bacteria (Cabrera et al., 2006; Utgikar et al., 2003), making these passive systems generally not applicable in the IPB neither in other mining sites with highly metal rich AMDs.

7.3.2.5 Open Limestone Channels (OLC)

Also known as Oxic Limestone Drains (OLD), this system consists of channels with coarse limestone fragments located in steep stream segments (preferably >20%) that perform well in waters with pH values < 3 and high net acidity (500-2600 mg/L of $CaCO_3$ equivalents, Skousen et al. 2017). Leachates are neutralized and oxidized, causing the precipitation of metal hydroxides (Cravotta and Trahan, 1999). The precipitates cover the surface of the limestone edges, but it has been proven that, albeit at a slower rate, their dissolution continues. Additionally, many of the generated precipitates are eroded and carried away during floods (Skousen et al., 2017). However, if Fe concentrations are very high, they are not applicable because the spaces between limestone fragments become completely cemented. This is the case with the use of this technology in the IPB, as demonstrated in the urgently constructed OLC after the spill in La Zarza on May 17th 2017 (Fig. 7.18). pH values never exceeded 3 during its operation.

Figure 7.18: Construction of an Open Limestone Channel (OLC) after the accidental mining spill of La Zarza (June 2017) due to the break of a concrete plug (left). This system failed to treat the spilled AMD due to limestone grains coating due to intense Fe precipitation. It can be seen the coating of the channel and a limestone block totally coated by Fe precipitates (right).

7.3.2.6 Disperse Alkaline Substrate (DAS)

The passive methods previously mentioned are not suitable for treating leachates with high acidity and contaminant concentrations, such as those found in most discharges in the IPB. The reason for this ineffectiveness is due to two fundamental problems: (1) **passivation** - the concentration of Fe and Al is so high that precipitate layers quickly form around

reactive grains, preventing contact with AMD, making them insoluble, and therefore not generating alkalinity to remove contamination; and (2) **clogging** - the concentration of Fe and Al is so high that massive precipitation inside the reactors quickly clogs the substrate pores, preventing water flow.

To address these issues, the research group in Geochemistry and Environmental Mineralogy belonging to the Department of Earth Sciences and the Center for Research in Natural Resources, Health, and the Environment (RENSMA) at the Faculty of Experimental Sciences of the University of Huelva, in collaboration with researchers from the Spanish National Research Council (CSIC) (IDAEA-CSIC), has developed the technology called Dispersed Alkaline Substrate (DAS). This technology was developed during the execution of three doctoral theses (Rötting, 2007; Caraballo, 2011; and Macías, 2012 a,b,c) and is protected under patent (Patent No: ES2534806) from the University of Huelva.

Lab scale experiments

To design this technology, laboratory tests were initially conducted using columns filled with sand and limestone gravel to provide alkalinity, along with an inert material to achieve high porosity and permeability in the system (Fig. 7.19). The acidic water was circulated in a downward direction, leading to the precipitation of Fe first, and further down with higher pH values, the precipitation of Al occurred. In these two zones, the coprecipitation of many other toxic elements takes place (Ayora et al., 2013).

Figure 7.19: Column filled with reactive materials for the design of AMD treatment based on DAS technology. The flow is from top to bottom. Precipitates formed at the contact of the reactive material with AMD are visible.

Pilot scale experiments

Once the effectiveness of different mixtures of reactive material (for water treatment) and inert material (for maintaining system permeability) was demonstrated in laboratory tests, in 2005 a pilot plant was constructed to treat AMD from the Monte Romero mine (Fig. 7.20). The leachates had an average pH of 3.4, 370 mg/L of Zn, 300 mg/L of Fe, 90 mg/L of Al, etc. The inert material used was wood shavings mixed with limestone sand. Wood shavings provide high permeability due to the large pore size, reducing clogging issues caused by precipitates. On the other hand, the small size of the limestone grains provides a large specific surface area, reducing material passivation and increasing reactivity. The treatment pilot plant consisted of a reactive tank with a capacity of 3 m^3 followed by several interconnected settling ponds with aeration cascades. The treated flow rate was approximately 1 L/min (Rotting et al., 2008). Although a significant portion of Fe and all dissolved Al were retained, high concentrations of Zn and other divalent metals could not be completely eliminated. Therefore, a tank filled with caustic magnesia (MgO) and wood shavings was added at the end of the system, achieving an outlet pH above 10 and total removal of con-

Figure 7.20: Pilot plant for AMD treatment based on DAS technology in Monte Romero mine.

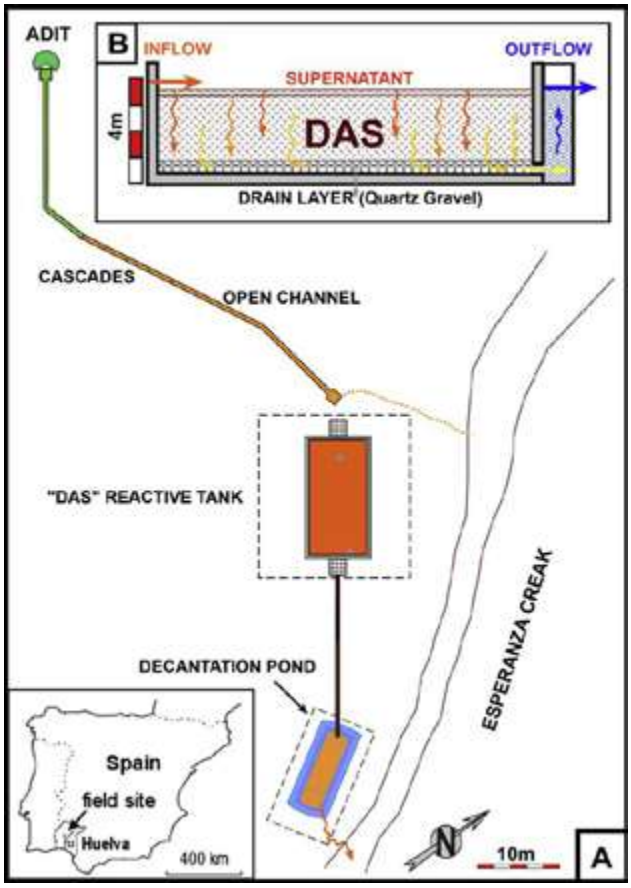

Figure 7.21: A) Distribution and dimensions of different components forming the pilot scale treatment of Esperanza Mine. B) Profile of the reactive tank.

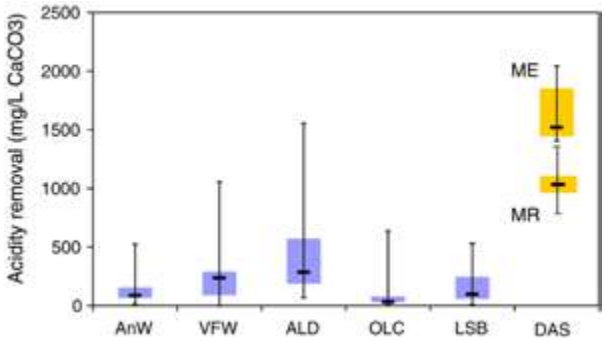

Figure 7.22: Comparison of acidity removal (median, 25th, and 75th percentiles) from AMD treated using conventional treatment systems (80 samples) and two pilot plants in the Odiel River basin (ME: Esperanza Mine, MR: Monte Romero). AnW: Anaerobic Wetlands, VFW: Vertical Flow Wetlands (RAPS), ALD: Anoxic Limestone Drains, OLC: Open/Oxic Limestone Channels, LSB: Limestone leaching beds, DAS: Dispersed Alkaline Substrate system (Ziemkiewicz et al., 2003).

taminants. The high outlet pH, due to atmospheric CO_2 reequilibration, quickly stabilized to values around 8, within the pH range of natural waters (6.5-8.5).

Finally, with all the knowledge gained both at the laboratory and pilot scales at the Monte Romero plant, a larger-scale pilot treatment plant was built at Esperanza Mine, in the upper part of the Odiel River basin. Esperanza Mine is an old mine located in the municipality of Almonaster la Real that was in operation from 1906 to 1931 and is currently abandoned. However, acidic waters continue to flow from the mine entrance with a fairly constant flow, averaging 0.8 ± 0.2 L/s, with peaks of up to 4 L/s after very occasional intense rainfall events. Figure 7.21 shows the schematic of the pilot passive treatment system built at Mina Esperanza.

During the nearly 20 months of continuous operation of the Esperanza mine pilot passive treatment (from 03/24/2007 to 10/15/2008), biweekly sampling was carried out at different parts of the system, with more than 400 samples taken. This allowed for a very detailed study of its operation and effectiveness. Figure 7.22 shows the acidity removal effectiveness of the pilot treatment plants installed at Monte Romero and Esperanza compared to other conventional passive treatment systems (Ziemkiewicz et al., 2003). In both cases, more than half of the initial reactive substrate was consumed without any significant encapsulation issues of the carbonate grains, resulting in a much higher removal of total acidity from the influent water than in other passive treatment systems reported in literature.

Once demonstrated the effectiveness of the DAS system for treating AMD with high metal contents at the pilot scale, two full-scale treatment plants (Esperanza Mine and Concepción Mine) have been constructed in the upper Odiel River basin, and they are currently in operation.

Esperanza Mine full scale plant

At the end of 2014, a treatment plant was constructed to comprehensively treat AMD from the Esperanza mine adit as part of the TAAM project (Research and Development of New Treatments to Improve the Quality of Acid Mine Waters, Ref. ITC-20111083). The project was funded by the Center for Technological and Industrial Development (CDTI) under the FEDER-INNTERCONECTA program. In this case, the treatment plant was not designed as a pilot plant but rather sized for medium to long-term operation with the goal of permanently eliminating the discharge to the river.

The treatment system consists of a pre-treatment (PN) with a surface area of 100 m^2, connected to the AMD discharge from the old gallery through an open and stepped channel. The purpose is to achieve complete oxidation of Fe(II) from the adit to Fe(III) before entering the system. The effluent from this pre-treatment is directed to a first reactive tank (TR-1) with a volume of 960 m^3 (divided into 2 tanks) filled with DAS-limestone reactive material. This reactive tank is connected in series with 100 m^2 surface area settling ponds (D-1 and D-2) and an intermediate second reactive tank (TR-2) with a volume of 720 m^3 using the same reactive fill as the first tank. An aerial image of the final plant configuration is shown in Figure 7.23.

The AMD outflowing from the Esperanza Mine adit exhibits an average pH value of 2.7, with electrical conductivity ranging between 2.03 and 3.13 mS/cm, and approximately 10% dissolved oxygen. It has an average net acidity of 2003 mg/L of $CaCO_3$ equivalent and contains mean values of 683 mg/L of Fe, 117 mg/L of Al, 16 mg/L of Cu, 15 mg/L of Zn, between 0.1-3 mg/L of As, Cr, Cd, Co, Ni, and an average of 726 µg/L of REY (Rare Earth Elements and Yttrium). The discharge has an average flow rate of 0.8 ± 0.2 L/s, with recorded minimum and maximum values during the monitoring period of 0.48 and 2.01 L/s, respectively.

The treatment plant was commissioned in December 2014 and is currently operational. However, the alkalinity in the first tank has been depleted, requiring the replenishment of reactive tank fill during maintenance activities. During the initial 4 years of operation, no permeability loss was detected within the tanks. However, a gradual decline in the reactivity of the fill material was observed, with average alkalinity generation values of 300 mg/L during the first year of operation and 190 mg/L during the last.

Figure 7.23: Aerial image of the passive treatment system at Esperanza Mine; water flows from upper left side of the figure and outflows from the lower left side.

Figure 7.24 illustrates the pH evolution and concentration of main metals throughout the treatment plant over the first 30 months of operation. After passing through the first reactive tank, there is intense limestone dissolution, leading to alkalinity generation and a rise in pH. From this point onwards, pH values remain above 6 until the final discharge. These sharp hydrochemical changes result in significant metal retention at various stages of the process. In fact, the Esperanza Mine DAS plant is capable of retaining 100% of Al, Cu, Zn, REY, As, Co, Ni, Cr, and Cd, along with 90% of Fe. In the initial stage of the process (PN), only Fe, As, and Cr are partially retained, with average retention values of 17%, 60%, and 12%, respectively.

Inside the TR-1 tank the primary metal retention occurs, with removal values exceeding 99% for Al, Cu, Zn, REY, and Cd. The amount of As and Cr not previously retained in the PN is completely eliminated in this TR-1. The retention of Fe after this tank reaches 67%. Regarding Co and Ni, while their main removal occurs in TR-1, they are gradually retained in the settlers and TR-2, with values exceeding 99% of retention at the outlet of D-2. At this point, 90% of Fe has already been eliminated.

The significant efficiency in metal removal achieved in different parts of the plant can be quantified. This provides a clear understanding of the magnitude of metal retention that the system is capable of achieving. Table 7.2 presents the amounts of accumulated metals in PN and TR-1 after the first 30 months of system operation.

	Al	Cu	Fe	Zn	REY	Co	As
				kg			
PN	0	0	6191	0	0	0	10
TR-1	5148	655	16018	563	33	11	6

Table 7.2: Metal loads accumulated in the pretreatment (PN) and the first reactive tank (TR-1) after 30 months operation of the Esperanza Mine DAS treatment plant (REY: Rare Earth Elements and Yttrium)

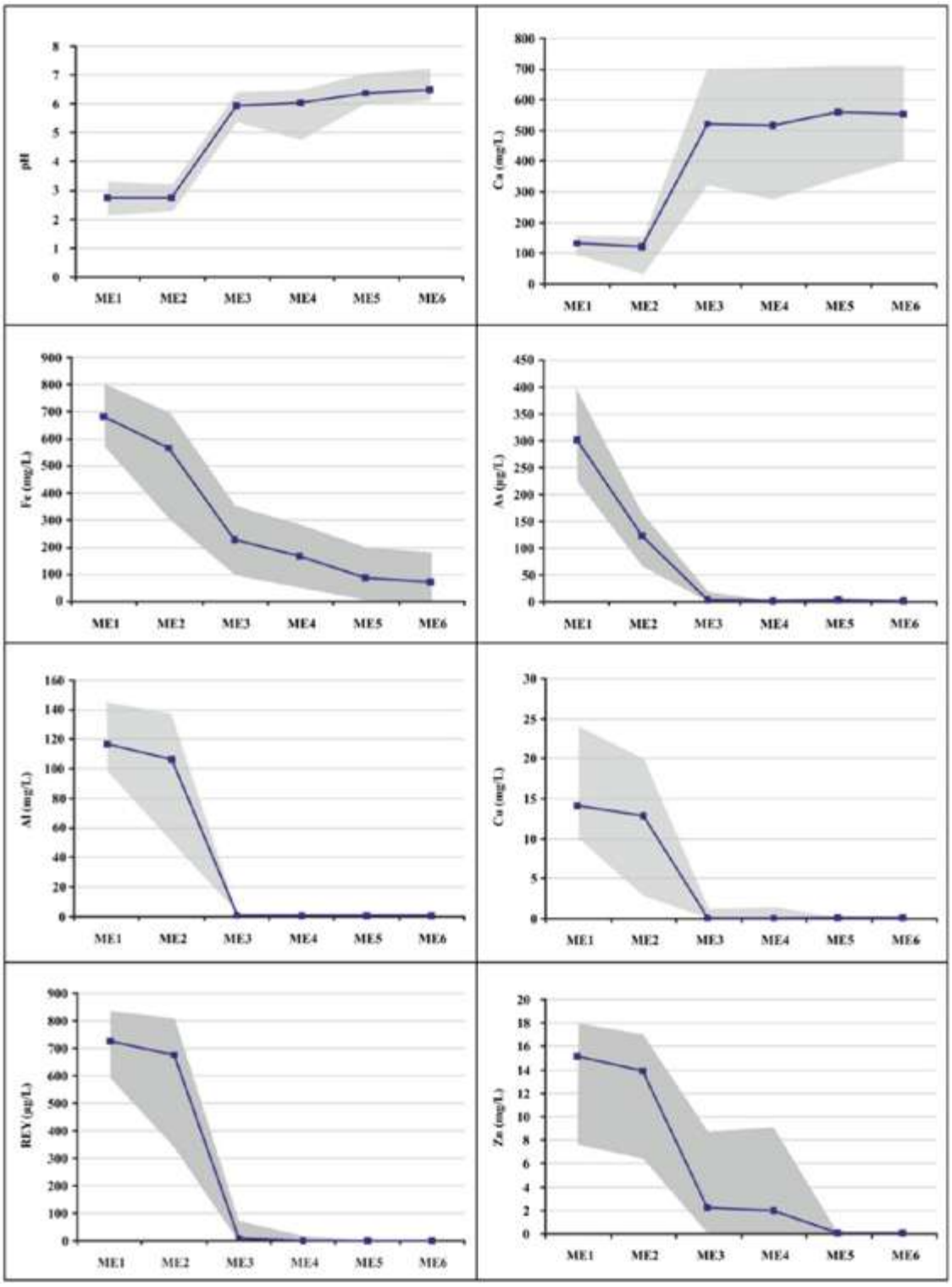

Figure 7.24: Evolution of pH and the concentration of selected representative elements along the Esperanza Mine plant. The blue line represents the average values, and the shaded area depicts the extreme values during the first 30 months of plant operation.

During this period, around 54,381 m^3 of AMD have been treated in the plant, with an average of 0.8 L/s, although with some fluctuations associated to rainfalls. The metal retention rates per surface obtained have been very high (Orden et al., 2021). Only the pretreatment

has retained 6.2 tons of Fe and 10.5 kg of As during this period, averaging 7 kg/day of Fe and 12 g/day of As retained. According to the previously discussed hydrochemical data, the amounts of metals accumulated in TR-1 are orders of magnitude higher than those accumulated in PN (Table 7.2). It is worth noting the accumulation of Al (5 tons), Fe (16 tons), Cu (655 kg), Zn (563 kg), and REY (33 kg) in this reactive tank.

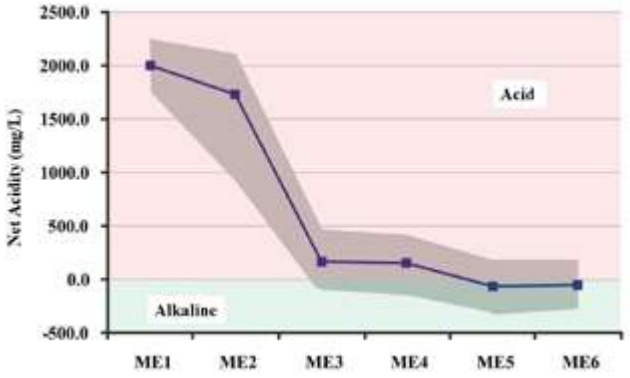

Figure 7.25: Evolution of net acidity throughout the different components of Esperanza Mine treatment plant. The blue line represents the mean value, while the shaded area represents the extreme values during the first 30 months of operation of the plant.

The evolution of net acidity throughout the different components of the plant (Fig. 7.25) confirms the substantial improvement in water quality of outflows. This parameter not only takes into account the solution pH but also includes alkalinity and the concentrations of the main hydrolysable metals contained in the discharge that are susceptible to generating acidity after their precipitation. The net acidity (2003 mg/L of average) of AMD entering the system is substantially reduced (down to 165 mg/L) at the outlet of TR-1 (Fig. 7.25), accounting for around 92% acidity removal. At the outlet of D-2, the average net acidity is -50 mg/L, indicating this negative value that the final result of the treatment is a net alkaline water.

Mina Concepción Mine full scale plant

The treatment plant built at Concepción Mine (Almonaster la Real, Huelva) is somewhat more complex than the Mina Esperanza plant discussed in the previous section. In this case, the objective of the plant is to treat AMD from the Concepción Mine pit lake, along with discharges coming from an old waste dump located next to the plant. Both discharges are collected in respective pretreatment ponds with the aim of oxidizing Fe(II) and allowing a significant fraction to precipitate before entering the first reactive tank (Fig. 7.26). The plant was built in 2016 under the project "Ecological Treatment of Acid Drainage" (LIFE-ETAD, Ref. LIFE12 ENV/ES/000250), funded by the EU under the LIFE+ Environment & Climate program.

From the pretreatment ponds, the acidic water flows through a system of reactive tanks and settling ponds connected in series (Fig. 7.26). Reactors TR-1 and TR-2 are based on the DAS technology, using limestone sand to react with the acidic water. One of the TR-3 reactors is based on magnesium DAS, where limestone is replaced by MgO, while the remaining was filled with witherite ($BaCO_3$). The dissolution of limestone raises the solution's pH to around 6, generating alkalinity. Under these conditions, trivalent metals become insoluble and precipitate. In the case of MgO, its dissolution raises the pH to values close to 9, causing the precipitation of divalent metals. The aim of using witherite was to analyze its effectiveness in removing sulfate, in addition to divalent ions. In the intermediate settlers (D-1 and D-2), the residence time of the water is increased so that the alkalinity generated in the reactive tanks is consumed by the precipitation of metals that were not retained in the previous reactors.

The AMD treatment plant at Concepción Mine started working in April 2016 and is currently operational. In the case of this plant, due to the seasonal nature of the discharges entering the plant, its operation is interrupted during summer when AMD discharges dry up (Fig. 7.27). During the first year of operation, 20,225 m^3 of AMD were treated, with an average flow rate of 1.1 L/s, excluding the summer period. However, the plant is designed to treat a flow rate of up to 5 L/s.

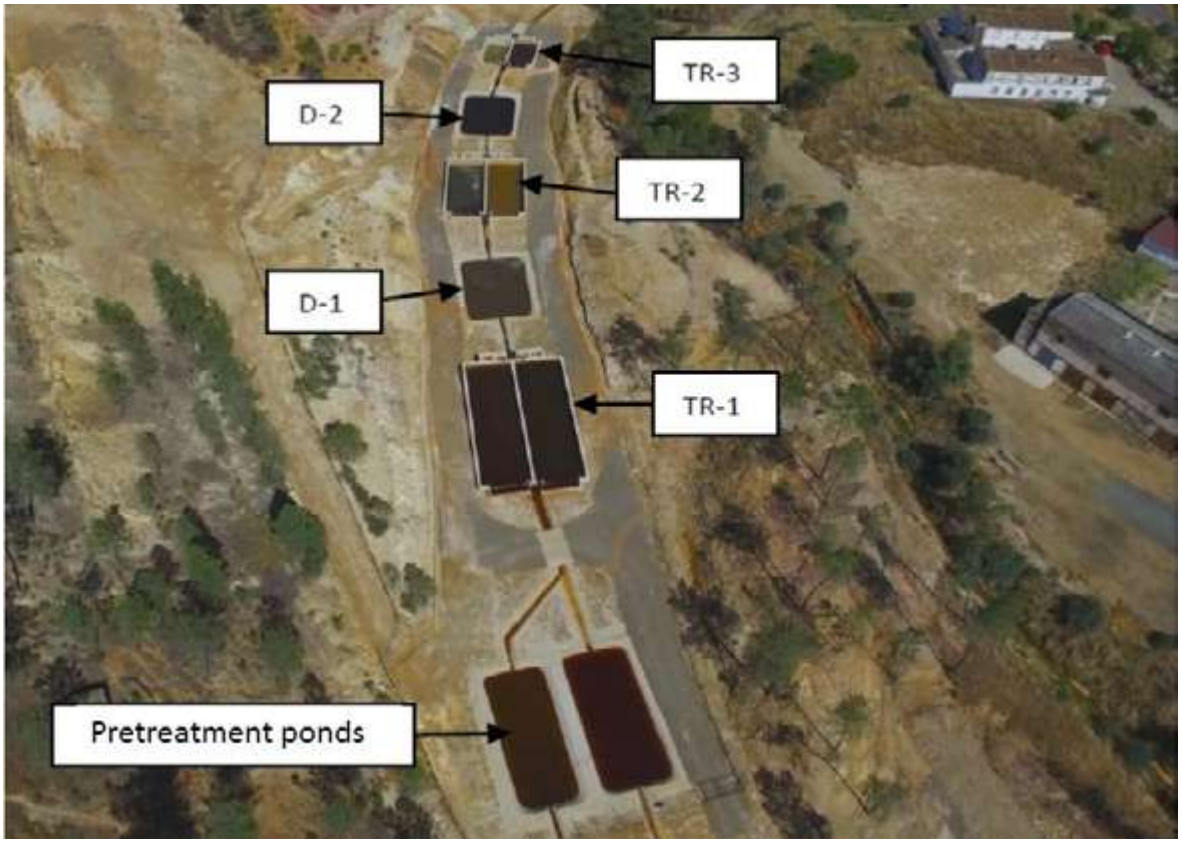

Figure 7.26: Aerial image of the different components forming the Concepción Mine (TR: reactive tanks; D: settling ponds).

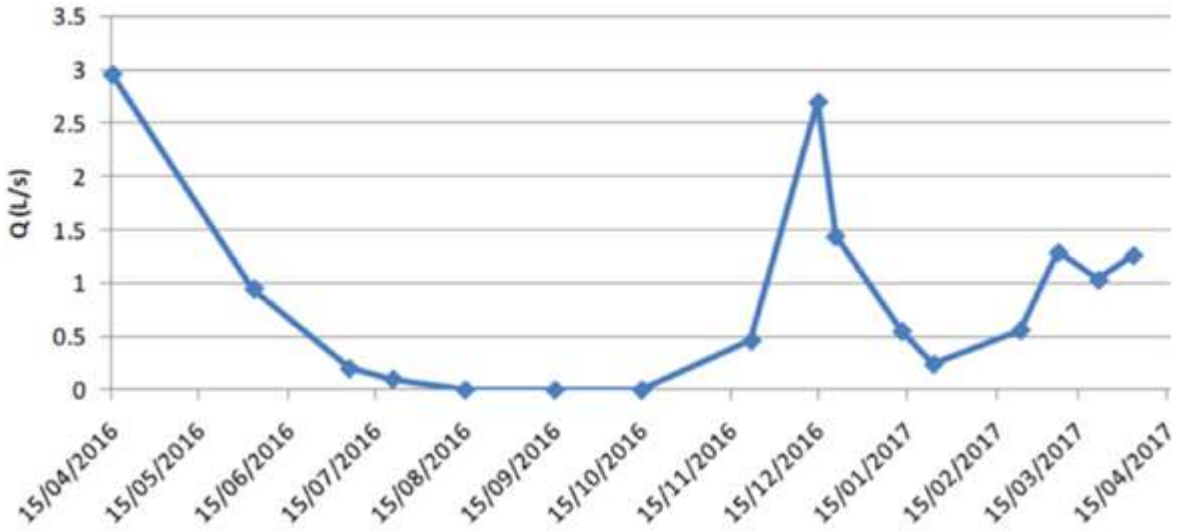

Figure 7.27: Seasonal variations in the inflow rate at the DAS plant of Concepción Mine during the first year of operation.

Both discharges treated at the Concepción Mine plant, one coming from the pit lake (MC1) and the other from a nearby pyritic waste dumps (MC2), exhibit high net acidity. The MC1 discharge has an average of 1451 mg/L of $CaCO_3$ equivalent, while the MC2 has 1283 mg/L. Table 7.3 shows the chemical composition (mean, maximum, and minimum values) for the most representative elements of both discharges for the first year of plant operation.

	pH	EC mS/cm	Al mg/L	Ca mg/L	Cu mg/L	Fe mg/L	Mg mg/L	Mn mg/L	SO_4 mg/L	Zn mg/L
					MC1					
Mean	2.66	2.21	85	72	11	446	103	16	2177	26
Minimum	2.47	2.04	84	64	8	308	97	11	1815	19
Maximum	2.83	2.39	86	79	14	584	109	21	2538	32
					MC2					
Mean	2.76	1.45	198	72	7	48	117	3	2097	2
Minimum	2.17	0.61	193	65	7	35	115	3	1974	2
Maximum	3.18	2.36	204	85	7	60	120	3	2175	3

Table 7.3: Basic statistical values for pH, electrical conductivity (EC, mS/cm), and the concentration of main elements in MC1 and MC2.

The discharge from the pit lake (MC1) is characterized by high concentrations of Fe (mean value of 446 mg/L) and moderate concentrations of Cu, Mn, and Zn, with 11, 16, and 26 mg/L respectively. Regarding trace elements, it is worth noting the high concentrations of REY (sum of yttrium and rare earth elements) and Co, with averages of 1200 and 1426 µg/L, respectively. In the case of MC2, which originates from the waste dump, it can be considered an atypical acid drainage compared to common AMD discharges from metal mining. It has very low concentrations of Fe (men value of 48 mg/L) and very high concentrations of Al, with maximum values exceeding 200 mg/L. The high concentration of Co (mean value of 815 µg/L) is also remarkable in this water.

The results and effectiveness of the plant operation (Fig. 7.28) are quite similar to those previously shown for Esperanza. During the first year of operation, the Concepción Mine plant achieved the removal of 100% of Fe, As, Cr, Al, Cu, REY, Pb, Zn, Cd, and Mn from the incoming leachates; more than 95% of Co and Ni, and up to 68% of sulfate. During this period, the outflowing waters had a pH above 7, generating net alkaline water (Fig. 7.29), similar to the values shown for Esperanza plant. The improvement in water quality is also reflected in the natural and spontaneous appearance of *Typha domingensis* (cattail) in the settling ponds (Fig. 7.30).

Although most contaminants are retained in reactors 1 and 2 with limestone-based DAS, there are some divalent metals that are not completely removed. Therefore, in reactors 3, caustic magnesia (MgO) and witherite ($BaCO_3$) are used to increase the pH above 7-9, leading to the total elimination of divalent metals and Fe(II). In the case of witherite, it also aims to reduce sulfate concentration, which although less harmful than Fe, Al, and other metals, can cause problems by increasing the salinity of the receiving environment due to its high concentrations in AMD. Figure 7.31 shows how the reactor tank filled with witherite raises the pH and reduces Fe and Co concentrations to below the detection limit. At the same time, there is a significant reduction in sulfate concentration (76% across the system) due to the precipitation of $BaSO_4$ (Guerrrero et al., 2024).

On the other hand, as previously mentioned, the AMD from the IPB have high concentrations of REY (rare earth elements and yttrium). These elements are increasingly important raw materials for modern technologies, and new supply sources are currently needed. Hence, they are considered critical raw materials in the European Union, with significant strategic and economic importance. These elements precipitate in specific zones of the reactive tanks, concentrating and facilitating their subsequent extraction. Therefore, initial studies conducted in the IPB indicate that the precipitates from DAS systems could represent a modest but significant source of REY. In this context, the IPB could function as a

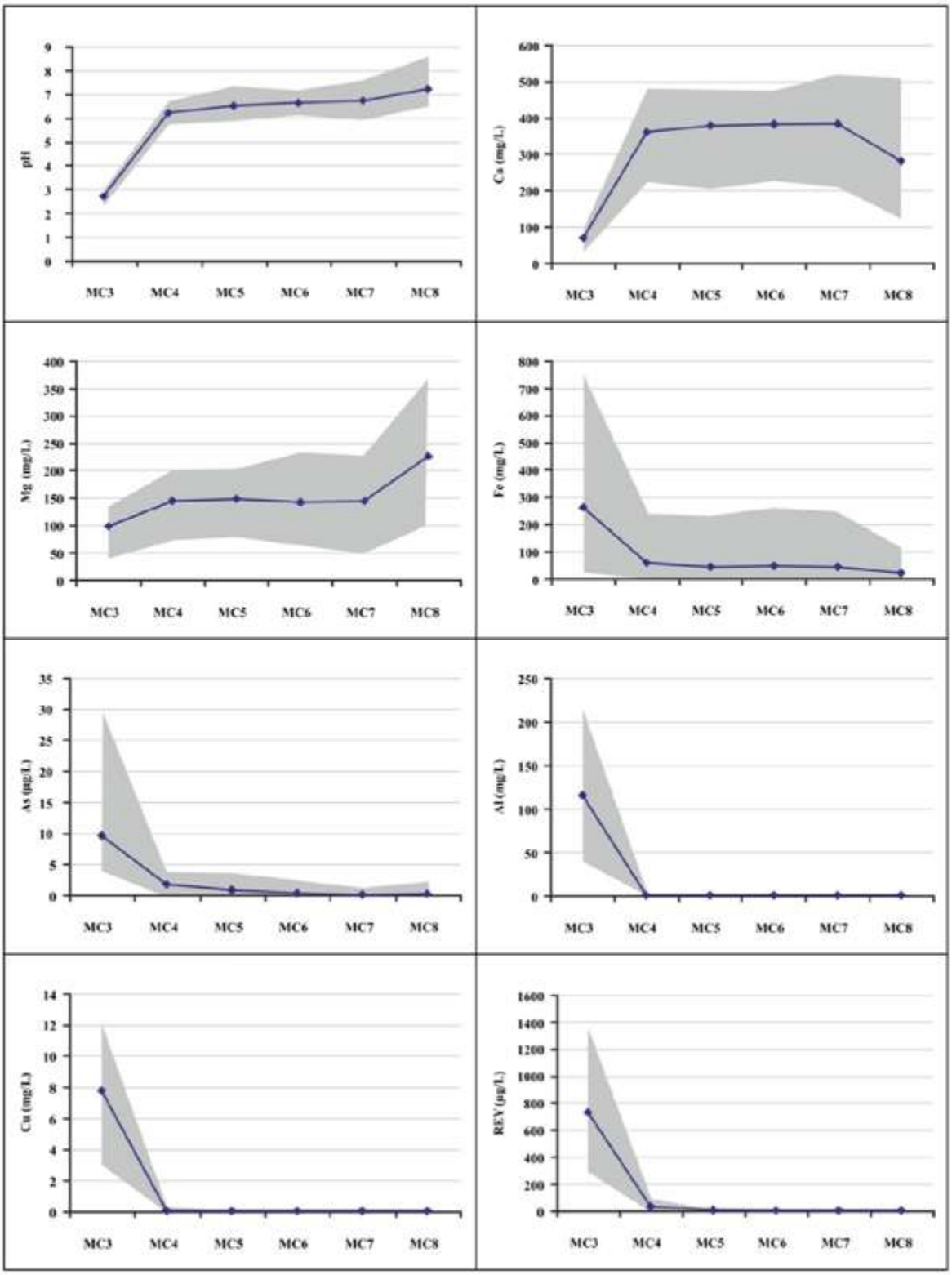

Figure 7.28: Evolution of pH and the concentration of some representative elements along the DAS plant at Concepción Mine. The blue line represents the mean values, and the shaded area represents the extreme values during the first year of plant operation. MC3 to MC8 are sampling points located before and after each reactive tank or settling pond, see Figure 7.24.

gigantic leaching process on a regional scale, where rain and oxygen act as natural drivers without energy investment. In addition to the environmental benefits of its treatment, it is expected that AMD will last for hundreds of years, and therefore, the reserves are practically unlimited (Ayora et al., 2016; León et al., 2021).

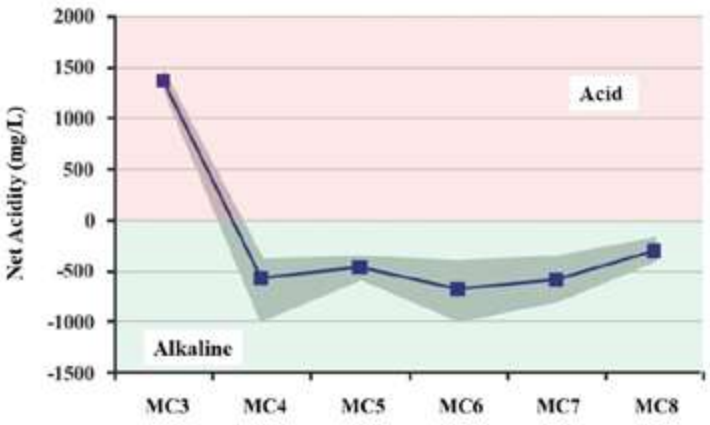

Figure 7.29: Evolution of net acidity throughout the different components of the Concepción treatment plant. The blue line represents the mean value, and the shaded area represents the extreme values during the first year of plant operation.

Figure 7.30: Spontaneous appearance of *Typha domingensis* (cattail) in settling pond 1, demonstrating the significant improvement in the water quality.

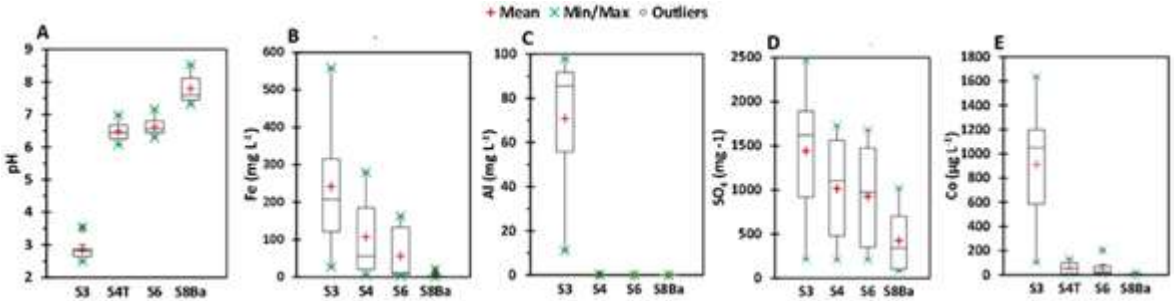

Figure 7.31: Box plots of pH values and some elements along different points of the Concepción Mine plant. S3: Input waters (mixing of discharges MC1 and MC2), S4: after TR1, S6: after TR2 with limestone, S8Ba: after TR3 containing witherite (Guerrrero et al., 2024).

7.4. MAIN CONCLUSIONS

The costs associated with the generation of AMD in sulfide and coal mines can be very high and jeopardize the economic viability of operations. These costs are much lower if mitigation measures are properly planned before mining begins. Conversely, abandoned mines require very high investments.

The main methods to prevent the generation of AMD are:

- Diverting surface (and/or groundwater) to prevent contact with sulfide-containing materials.
- Sealing mine shafts and galleries to prevent water from entering the mined area and/or the release of AMD. This measure must be studied in detail in each case to ensure its effectiveness and to avoid potential catastrophic releases of AMD.
- Covering mine wastes with various types of impermeable materials to prevent contact with water and atmospheric oxygen ('dry covers'). In fine tailings ponds, they can also be covered with water ('wet covers') to limit the amount of oxygen and oxidation reactions.
- Adding alkaline materials to control pH and, primarily, to prevent the development of acidophilic bacteria that catalyze oxidation reactions.
- Another technique currently being tested is the microencapsulation of sulfide grains to form a chemically inert layer around them, preventing their oxidation.

Treating acid leachates should be a subsequent option to preventive methods in mine planning. However, once acid waters are formed, there are two main groups of options: active treatment and passive treatment. Active treatment requires continuous energy and reagent consumption and exhaustive process control, while passive treatment rely on natural processes, requiring no energy consumption and only infrequent maintenance. The chosen methodology will depend on the flow rate, the characteristics of the water to be treated, the required final quality, and economic aspects. The unit cost per cubic meter is usually much higher in active treatment, but it is the only option when high flow rates need to be treated. Generally, active treatment is used during the operational phase, while passive treatments are used after mine closure, when small flows of acid waters can be generated for many years.

Active treatment typically involves three stages: oxidation (either by mechanical or chemical aeration), neutralization, and metal precipitation and sedimentation. Membrane processes, ion exchange, evaporation, biological or chemical sulfate removal, etc., can also be employed.

For passive treatment, various types of organic (plant residues, manure, etc.) and inorganic (slags, alkaline residues, soils, etc.) wastes are used to promote vegetation growth or bacterial activity. The key reactions pursued include: 1) the reduction of iron and sulfates, favoring the precipitation of metal sulfides and the elimination of acidity, and 2) the neutralization of acidity by adding an alkaline material, typically limestone.

Different types of passive systems are applicable depending on the concentration of metals in the inlet water (especially Fe and Al), dissolved oxygen concentration, and flow rate: aerobic and anaerobic wetlands, limestone anoxic drains, limestone oxic channels, oxidation ponds or cascades, sulfide-reducing reactors, systems producing alkalinity, etc.

Generally, these passive methods are not suitable for treating leachates with high acidity and contaminant concentrations, such as those found in most discharges of the Iberian Pyrite Belt (IPB), because 1) high concentrations of Fe and Al precipitate around the alkaline material and passivate it (only the surface layer is dissolved), and 2) the precipitates cause clogging and coating problems. The passive treatment system based on DAS (Dispersed Alkaline Substrate) technology, developed at the University of Huelva (Spain), solves these problems by using a fine-grained alkaline material mixed with wood chips to provide high porosity to the system. Currently, there are two full-scale plants using this technology in the abandoned mines Esperanza and Concepción, with high efficiency in metal and acidity removal.

8

BIBLIOGRAPHY

Acero P., Ayora C., Torrento C. Nieto J.M. (2006). The behavior of trace elements during schwertmannite precipitation and subsequent transformation into goethite and jarosite. *Geochimica et Cosmochimica Acta* 70: 4130-4139.

ACUAES (2010). Modificación nº 1 del proyecto de ejecución de las obras de la presa de Alcolea. Anejo nº 18. Calidad de Aguas. Informe Técnico, Aguas de las Cuencas de España, Ministerio de Medio Ambiente y Medio Rural y Marino, 149 p + Anexos.

Achterberg, E.P., Herzl, V.M.C., Braundgardt, C.B., Millward, C.E. (2003). Metal behaviour in an estuary polluted by acid mine drainage: the role of particulate matter. *Environmental Pollution* 121: 283-292.

Adánez Sanjuán, P., Llamas Borrajo, J. F., Locutura Rupérez, J., Garcia Cortes, A. (2014). Estudio geoquímico de los sedimentos de llanura de inundación en la cuenca de los ríos Tinto y Odiel (Huelva). Boletin Geologico y Minero, 125(4), 585–599.

Allman, C.J., Gómez-Ortiz, D., Burke, A., Amils, R., Rodriguez, N., Fernández-Remolar, D. (2021). Hydrogeochemical variability of the acidic springs in the Rio Tinto headwaters (2021). *Water* 13: 2861.

Almodóvar, G.R., Yesares, L., Sáez, R, Toscano, M., González, F., Pons, J.M. (2019). Massive Sulfide Ores in the Iberian Pyrite Belt: Mineralogical and Textural Evolution. *Minerals* 9: 653.

Alpers, C.N., Nordstrom, D.K. y Thompson, J.M. (1994). Seasonal variations of Zn/Cu ratios in acid mine water from Iron Mountain, California. In: Alpers, C. N. and Blowes, D. W. (Eds.), *Environmental Geochemistry of Sulfide Oxidation*. American Chemical Society.

Alpers C.N. and Nordstrom D.K (1999). Geochemical modeling of water-rock interactions in mining environments. En: Plumlee GS, Logsdon MS (eds) *The environmental geochemistry of mineral deposits*. Part A: Processes, techniques and health issues. Society of Economic Geologists, Littleton, Reviews in economic geology, vol 6A, 289–323.

Alvarez-Campana JM, Ramos Martínez A (2009). Impacto ambiental del drenaje ácido en obras de ingeniería: el caso de la autovía del Cantábrico y el río Eume (N Galicia). *V Congreso Nacional de Evaluación de Impacto Ambiental, Cooperación, Desarrollo y Sostenibilidad*, Córdoba, 6 p.

Alvarez Valero, A., Sáez, R., Pérez-López, R., Delgado, J., Nieto, J.M. (2009). Evaluation of heavy metal bio-availability from Almagrera pyrite-rich tailings dam (Iberian Pyrite Belt, SW Spain) based on a sequential extraction procedure. *Journal of Geochemical Exploration* 102:87-94.

Amaral Zettler, L.A., Gomez, F., Zettler, E., Keenan, G., Amils, R. Sogin, M.L. (2002). Eukaryotic diversity in Spain's River of Fire. *Nature* 417: 137.

Amils, R., González-Toril, E., Fernández-Remolar, D., Gómez, F., Aguilera, A., Rodríguez, N., Malki, M., García-Moyano, A., Fairen, A.G., de la Fuente, V., y Sanz, J.L. (2007). Extreme environments as Mars terrestrial analagogs: The Río Tinto case. *Planetary and Space Science* 55: 370-381.

Amils, R., Fernández-Remolar, D., et al. (2014). Río Tinto: A geochemical and mineralogical terrestrial analogue of Mars. *Life*: 4, 511–534.

Anciola, A.L and Cossio, E. (1856). Memoria sobre las minas de Río-Tinto. Madrid, 166 p.

Araújo, C.V., Diz, F.R., Tornero, V., Lubián, L.M., Blasco, J., Moreno-Garrido, I. (2010). Ranking sediment samples from three Spanish estuaries in relation to its toxicity for two benthic species:

The microalga Cylindrotheca closterium and the copepod Tisbe battagliai. *Environmental Toxicology and Chemistry* 29(2): 393-400.

Arenas Posadas, C. (2017). Riotinto: el declive de un mito minero (1954-2003). *Revista de Historia Industrial* 69: 109-141

Arroyo, M., Ruiz, F., González-Regalado, M.L., Rodríguez-Vidal, J., Cáceres, L., Olías, M., Campos, J.M. et al. (2021). Late Holocene evolution of the Tinto River estuary (SW Spain). *Scientia Marina* 85: 113-123.

AYESA (2012). Informe sobre la calidad del agua prevista en el embalse de Alcolea. Informe Técnico, 71 p.

Ayora, C., Caraballo M.A., Macías F., Rötting T., Carrera J., Nieto J.M. (2013). Acid mine drainage in the Iberian Pyrite Belt: 2. Lessons learned from recent passive remediation experiences. *Environmental Science and Pollution Research* 20: 7837-7853.

Ayora, C., Macías, F., Torres, E., Lozano, A., Carrero, S., Nieto, J.M., Pérez-López, R., Fernández-Martinez, A., Castillo-Michel, H. (2016). Recovery of Rare Earth Elements and Yttrium from Passive-Remediation Systems of Acid Mine Drainage. *Environmental Science & Technology* 50: 8255-8262.

Baceta J.I. and Pendón J.G. (1999). Estratigrafía y arquitectura de facies de la Formación Niebla. Neógeno Superior, sector occidental de la Cuenca del Guadalquivir. *Revista de la Sociedad Geológica de España* 12: 419-438.

Basallote, M.D., De Orte, M.R., DelValls, T.Á., Riba, I. (2014). Studying the Effect of CO2-Induced Acidification on Sediment Toxicity Using Acute Amphipod Toxicity Test. *Environmental Science & Technology*, 48(15): 8864-8872.

Basallote, M.D., Rodríguez-Romero, A., De Orte, M.R., Del Valls, T.Á., Riba, I. (2015). Evaluation of the threat of marine CO_2 leakage-associated acidification on the toxicity of sediment metals to juvenile bivalves. *Aquatic Toxicology*, 166: 63-71.

Basallote, M.D., Rodríguez-Romero, A., De Orte, M.R., DelValls, T.Á., Riba, I. (2018). CO_2 leakage simulation: effects of the pH decrease on fertilisation and larval development of Paracentrotus lividus and sediment metals toxicity. *Chemistry and Ecology*, 34(1): 1-21.

Bayless E. R. and Olyphant G. A. (1993). Acid-generating salts and their relationship to the chemistry of groundwater and storm runoff at an abandoned mine site in southwestern Indiana, U.S.A. *Journal of Contaminant Hydrology* 12: 313-328.

Berger A.C., Bethke C.M., Krumhansl M.L. (2000). A process model of natural attenuation in drainage from a historic mining district. *Applied Geochemistry* 15: 655-666.

Besada, V., Bellas J., Sánchez-Marín, P., Bernardez, P., Schultze F. (2021). Metal and metalloid pollution in shelf sediments 1 from the Gulf of Cádiz (Southwest Spain): long-lasting effects of a historical mining area. *Environmental Pollution* 295: 118675.

Bigham J.M., Schwertmann U., Traina S. J., Winland R. L. Wolf M. (1996). Schwertmannite and the chemical modeling of iron in acid sulfate waters. *Geochimica et Cosmochimica Acta* 60: 2111-2121.

Bigham, J.M. and Nordstrom, D.K. (2000). Iron- and Aluminium-Hydroxysulfate Minerals. In: Alpers, C. N., Jambor, J. L., y Nordstrom, D. K. (Eds.), Sulfate Minerals - Crystallography, Geochemistry and Environmental Significance. *Reviews in Mineralogy and Geochemistry*, v.40, Mineralogical Society of America, Washington D.C.

Blodau, C. (2006). A review of acidity generation and consumption in acidic coal mine lakes and their watersheds. *Science of the Total Environment* 369, 307-332

Blowes D.W., Ptacek C.J., Jambor J.L. Weisener C.G. (2004). The geochemistry of acid mine drainage. In: Treatise on geochemistry. Environmental geochemistry, 9, Elsevier. Ed. Lollar, B. S., 149-204.

Boehrer, B., Yusta, I., Magin, K., y Sánchez España, J., (2016). Quantifying, assessing and removing the extreme gas load from meromictic Guadiana pit lake, Southwest Spain. Science of the Total Environment 563–564: 468–477.

Bono, J., y Olías, M., (2018). Análisis de la evolucion del volumen de agua en corta Atalaya, Minas de Riotinto (Huelva). En: X Simposio del Agua en Andalucía, Club del Agua Subterránea, vol. II: 1171-1179.

Borrego J., Morales J. A., de la Torre M. L. Grande J. A. (2002). Geochemical characteristics of heavy metal pollution in surface sediments of the Tinto and Odiel river estuary (southwestern Spain). *Environmental Geology* 41: 785-796.

Boyle, E.A., Chapnick, S.D., Bai, X.X., Spivack, A., (1985). Trace metal enrichments in the Mediterranean Sea. *Earth and Planetary Science Letters*, 74(4): 405-419.

Buckby T., Black S., Coleman M.L., Hodson, M.E. (2003). Fe-sulphate rich evaporative mineral precipitates from the río Tinto, southwest Spain. *Mineralogical Magazine* 67: 263-278.

Bureau of Reclamation (2015). Technical evaluation of the Gold King mine incident.Denver, CO, U.S. Department of the Interior, Bureau of Reclamation, Technical Service Center.

Cabrera, G., Pérez, R., Gómez, J.M., Ábalos, A., Cantero, D. (2006). Toxic effects of dissolved heavy metals on Desulfovibrio vulgaris and Desulfovibrio sp. strains. *Journal of Hazardous Materials* 135(1-3): 40-46.

Cambrollé, J., Redondo-Gómez, S., Mateos-Naranjo, E., Figueroa, M.E., (2008). Comparison of the role of two Spartina species in terms of phytostabilization and bioaccumulation of metals in the estuarine sediment. *Marine Pollution Bulletin*, 56(12): 2037-2042.

Cánovas C.R., Olias M., Nieto J.M., Sarmiento A.M. Cerón J.C (2007). Hydrogeochemical characteristics of the Odiel and Tinto rivers (SW Spain). Factors controlling metal contents. *Science of the Total Environment* 373: 363-382.

Cánovas, C.R. (2008). La calidad del agua de los ríos Tinto y Odiel. Evolución temporal y factores condicionantes de la movilidad de los metales. Tesis Doctoral. Universidad de Huelva. 354 p.

Cánovas, C.R., Olias, M., Nieto, J.M. Galvan, L. (2010). Wash out processes of evaporitic sulfate salts in the Tinto river: Hydrochemical evolution and environmental impact. *Applied Geochemistry* 25: 288-301.

Cánovas, C.R., Olías, M., Sarmiento, A.M., Nieto, J.M., Galván, L., 2012. Pollutant transport processes in the Odiel River (SW Spain) during rain events. *Water Resources Research* 48, W06508.

Cánovas, C.R., Peiffer, S., Macías, F., Olías, M., Nieto, J.M. (2015.) Geochemical processes in a highly acidic pit lake of the Iberian Pyrite Belt (SW Spain). *Chemical Geology* 395, 144–153..

Cánovas C.R., Olías M., Macías F., Torres E., San Miguel E.G., Galván L., Ayora C. Nieto J.M. (2016). Water acidification trends in a reservoir of the Iberian Pyrite Belt (SW Spain). *Science of the Total Environment* 541: 400-411.

Cánovas, C.R., Macías, F., Olías, M., Pérez López, R., Nieto, J.M., (2017). Metal-fluxes characterization at a catchment scale: study of mixing processes and end-member analysis in the Meca River watershed (SW Spain). *Journal of Hydrology* 550, 590–602.

Cánovas, C.R., Macías, F., Olías, M. (2018a). Hydrogeochemical behavior of an anthropogenic mine aquifer: Implications for potential remediation measures. *Science of the Total Environment* 636: 85-93.

Cánovas, C.R, Riera, J., Carrero, S. Olías, M (2018b). Dissolved and particulate metal fluxes in an AMD affected stream under different hydrological conditions: The Odiel River (SW Spain). *Catena* 165: 414-424.

Caraballo, M.A., Macías, F., Rötting, T.S., Nieto, J.M., Ayora, C. (2011). Long term remediation of highly polluted acid mine drainage: A sustainable approach to restore the environmental quality of the Odiel river basin. *Environmental Pollution* 159: 3613-3619.

Caro, R. (1634). Antigüedades y Principado de la ilustrísima ciudad de Sevilla y Chorographia de su Convento Jurídico, o antigua Chancillería".

Carro, B., Borrego, J., Morales, J.A., (2018). Estuaries of the Huelva Coast: Odiel and Tinto Estuaries (SW Spain). En: Morales, J. (Ed.), The Spanish Coastal Systems. Springer, Cham. Springer Nature Switzerland.

Carrasco Martiañez, I. (2000). Historia en la Faja Pirítica. *Bocamina* 5: 8-49.

Casiot C., Leblanc M., Bruneel O., Personne J. C., Koffi K. y Elbaz-Poulichet F. (2003). Geochemical processes controlling the formation of As-rich waters within a tailings impoundment (Canoulès, France). *Aquatic Geochemistry* 9: 273-290.

Castellanos, E.M., and Luque, C.J., (2022). Ecología del litoral onubense (I): marismas mareales, En: Biología de Huelva: Naturaleza, Biodiversidad, Bioindicadores y Biomarcadores (Ed. R.Torronteras). Servicio de Publicaciones de la Universidad de Huelva, pp. 379-416.

CEDEX (2011). Estudio preliminar sobre el proyecto del embalse de Alcolea en el río Odiel: Calidad del agua y medidas para su utilización. Informe Técnico, Centro de Estudios y Experimentación de Obras Públicas, Madrid, 72 p + 2 Anejos.

CEDEX (2021). Directrices para la caracterización del material dragado y su reubicación en aguas del dominio público marítimo-terrestre. Comisión Interministerial de Estrategias Marinas, 2021.

CEDEX (2022). Estudio sobre la calidad del agua de la cuenca del Odiel en relación con el proyecto del embalse de Alcolea. Informe Técnico, Centro de Estudios y Experimentación de Obras Públicas, Madrid, 92 p + 2 Anejos

Cesar, A., Choueri, R., Riba, I., Morales-Caselles, C., Pereira, C., Santos, A., Abessa, D., DelValls, T.A (2007). Comparative sediment quality assessment in different littoral ecosystems from Spain (Gulf of Cadiz) and Brazil (Santos and São Vicente estuarine system). *Environment International*, 33(4): 429-435.

Checkland S.G. (1967). *The mines of Tharsis: Roman, French and British enterprise in Spain*. George Allen & Unwin Ltd. 288 pp.

Córdoba, F. (2022). Las bacterias extremófilas de los ríos ácidos de Huelva. En: Biología de Huelva. Naturaleza, Biodiversidad, Bioindicadores y Biomarcadores (Ed. Rafael Torronteras Santiago). Servicio de Publicaciones de la Universidad de Huelva, 17-50.

Cortina, J.L., Lagreca, I., De Pablo, J., Cama, J. Ayora, C. (2003). Passive in situ remediation of metal-polluted water with caustic magnesia: Evidence form columna experiments. Environmental Science and Technology 37: 1971-1977.

Corzo, A., Jiménez-Arias, J.L., Torres, E., García-Robledo, E., Lara, M., Papaspyrou, S., (2018). Biogeochemical changes at the sediment- water interface during redox transitions in an acidic reservoir: exchange of protons, acidity and electron donors and acceptors. *Biogeochemistry* 139 (3): 241−260.

Courtin-Nomade, A., Bril, H., Neel, C., Lenain, J.F., 2003. Arsenic in iron cements developed within tailings of a former metalliferous mine—Enguialès, Aveyron, France. *Applied Geochemistry*, 18(3): 395-408.

Cravotta C., (1994). Secondary iron-sulfate minerals as sources of sulfate and acidity. En: Alpers, C. N. and Blowes, D. W. (Eds.), *Environmental Geochemistry of Sulfide Oxidation*. American Chemical Society.

Cravotta, C.A., and Trahan, M. (1999). Limestone drains to increase pH and remove dissolved metals from acidic mine drainage. *Applied Geochemistry* 14, 581-606

Cuenca C. (2019). Encapsulación in situ de sulfuros en residuos mineros para la remediación del drenaje ácido de minas. Trabajo Fin de Máster Geología y gestión ambiental de los recursos minerales. Universidad de Huelva, 61 pp.

Davis R. A., Welty A. T., Borrego J., Morales J. A., Pendon J. G. Ryan J. G. (2000). Rio Tinto estuary (Spain): 5000 years of pollution. *Environmental Geology* 39: 1107-1116.

Delgado, J., Boski, T., Nieto, J.M., Pereira, L., Moura, D., Gomes, A., Sousa, C. García-Tenorio, R. (2012). Sea-level rise and anthropogenic activities recorded in the late Pleistocene/Holocene sedimentary infill of the Guadiana Estuary (SW Iberia). *Quaternary Science Reviews*, 33: 121-141.

De Prado C. (1851). Minas de Riotinto. De sus circunstancias e importancia. De su enagenacion. *Revista Minera* II: 97-112.

DGOHCA (1996). Estudio de la calidad del agua almacenada en la presa de Alcolea. Anejo nº 5 del Proyecto de la Presa de Alcolea, Dirección General de Obras Hidráulicas y Calidad del Agua, 91 p

Dionisio Pires, M. (2021a). Síntesis sobre los posibles impactos en la calidad del agua de la futura presa de Alcolea. Informe Técnico, Deltares, Paises Bajos, 42 p.

Dionisio Pires, M. (2021b). Addendum synthesis report possible impacts on water quality by future Alcolea dam. Informe Técnico, Deltares, Países Bajos, 4 p..

Dzombak, D.A. and Morel, F.M. (1990). *Surface Complexation Modelling: Hydrous Ferric Oxide*. John Wiley, New York.

EEC (2001). Commission regulation (EC) No. 466/2001 of 8 March 2001 setting maximum levels for certain contaminants in foodstuffs. Official Journal of the European Communities. L77, pp 1–13.

EEC (2002). Commission regulation (EC) No. 221/2002 of 6 February 2002 amending regulation n 466/2001 setting maximum levels for certain contaminants in foodstuffs. Official Journal of the European Communities. L37, pp 4–6.

Elbaz-Poulichet, F., and Leblanc, M., (1996). Transfert de métaux d'une province minière à l'océan par des fleuves acides (Rio Tinto, Espagne).

Elbaz-Poulichet F., Morley N. H., Cruzado A., Velasquez Z., Achterberg E. P. Braungardt, C. B. (1999). Trace metal and nutrient distribution in an extremely low pH (2.5) river estuarine system, the Ria of Huelva (South-West Spain). *The Science of the Total Environment* 227: 73-83.

Elbaz-Poulichet, F., Braungardt, C., Achterberg, E., Morley, N., Cossa, D., Beckers, J., Nomérange, P., Cruzado, A., Leblanc, M., (2001). Metal biogeochemistry in the Tinto–Odiel rivers (Southern Spain) and in the Gulf of Cadiz: a synthesis of the results of TOROS project. *Continental Shelf Research* 21(18): 1961-1973.

Elbaz-Poulichet F., Morley N. H., Beckers J. M. Nomerange P. (2001). Metal fluxes through the Strait of Gibraltar: the influence of the Tinto and Odiel rivers (SW Spain). *Marine Chemistry* 73: 193-213.

Essalhi, M., Sizaret, S., Barbanson, L., Chen, Y., Lagroix, F., Demory, F., Nieto, J.M., Sáez, R. Capitán, M.A. (2011): A case study of the internal structures of gossans and weathering processes in the Iberian Pyrite Belt using magnetic frabrics and paleomagnetic dating. *Mineralium Deposita*, 46: 981-999.

Evangelou, V.P. (1995). Pirite Chemistry: The key for abatement of acid mine drainage. In: *Acid Mining Lakes. Acid Mine Drainage, Limnology and Reclamation* (Ed: W. Geller, H. Klapper, W. Salomons). Springer, 197-222.

Evangelou V.P. (2001). Pyrite microencapsulation technologies: Principles and potential field application. *Ecological Engineering* 17,165–178.

Fan, R., Short, M.D., Zeng, S.J., Qian, G., Li, J., Schumann, R.C., Kawashima, N., Smart, R.S.C., Gerson, A.R. (2017). The formation of silicate-stabilized passivating layers on pyrite for reduced acid rock drainage. *Environmental Science and Technology* 51: 11317-11325.

Fernandez-Caliani, J.C. (2008). Una aproximación al conocimiento del impacto ambiental de la minería en la Faja Pirítica Ibérica. Macla, 10: 24-28.

Fernández-Remolar, D.C., Rodríguez, N., Gómez, F. Amils, R. (2003). Geological record of an acidic environment driven by iron hydrochemistry: the Tinto River system. *Journal of Geophysical Research* 108, 5080.

Fernández Rodríguez, C., and Diaz Azpiroz, M. (2008). Geología de la zona de Ossa Morena (Sierra de Aracena). En: *Geología de Huelva. Lugares de interés geológico*. Servicio de Publicaciones de la Universidad de Huelva, 8-13.

Ferrero Blanco, M.D. (1999). Capitalismo minero y resistencia rural en el suroeste andaluza. Rio Tinto, 1873-1900. Servicio de Publicaciones de la Universidad de Huelva, 240 p.

Flores Caballero M. (1983). La rehabilitación Borbónica de las minas de Riotinto (1725-1810). *Instituto de Estudios Onubenses "Padre Marchena"*.

Ford, K.L. (2003). Passive treatment systems for acid mine drainage. Technical Note 409, Bureau of Land Management, National Science and Technology Center, 13 p.

Fortes-Garrido, J.C., Rodríguez-Pérez, A.M., Hernández-Torres, J.A., Caparrós-Mancera, J.J., Dávila-Martí, J.M., Castilla-Gutiérrez, J. (2023). Comparative analysis of water extraction mechanism in Roman mines. *Foundations of Science*,

Fuentes-López, J.M., Olías, M., León, R., Basallote, M.D., Macías, F., Moreno-González, R., Cánovas, C.R., (2022). Stream-pit lake interactions in an abandoned mining area affected by acid drainage (Iberian Pyrite Belt). *Science of the Total Environment* 833: 155224.

Fukushi, K., Sasaki, M., Sato, T., Yanase, N., Amano, H., Ikeda, H., 2003. A natural attenuation of arsenic in drainage from an abandoned arsenic mine dump. *Applied Geochemistry*, 18(8): 1267-1278.

Galván, L., Olías, M., Villarán San Juan, R., Domingo-Santos, J.M., Nieto, J.M. Cánovas, C.R. (2009). Application of the SWAT model to an AMD-affected river (Meca River, SW Spain). Estimation of transported pollutant load. *Journal of Hydrology* 377: 445-454.

Galván, L. (2011). Modelización hidrológica del río Odiel: aplicación al estudio de la contaminación por drenaje ácido de minas. Tesis Doctoral. Universidad de Huelva. 394 p.

Galván, L., Olías, M., Cánovas, C.R., Sarmiento, A.M., Nieto, J.M. (2016): Hydrological modeling of a watershed affected by acid mine drainage (Odiel River, SW Spain). Assessment of the pollutant contributing areas. *Journal of Hydrology* 540: 196-206.

Galván, L., Olías, M., Cerón, J.C., Fernández de Villarán, R. (2021). Inputs and fate of contaminants in a reservoir with circumneutral water affected by acid mine drainage. *Science of the Total Environment* 762: 143614.

García del Hoyo, J.J. (2010). El impacto económico de la expansión minera del siglo XIX: efectos inducidos en el tejido productivo de la provincia de Huelva. In: Patrimonio Geológico y Minero. Una apuesta por el desarrollo local sostenible. (Coord. E.M. Romero Macías). Servicio de Publicaciones Universidad de Huelva, 57-70.

García Palomero, F. (2004). Yacimientos de la Faja Pirítica Ibérica. In: Metallum. La minería suribérica (E. Romero and J.A. Pérez Macías, Eds.), 13-29.

GESAMP, 1987. *Land/sea boundary flux of contaminants: contributions from rivers*. Reports and Studies No. 32. IM0/FAO/UNESCO/WMO/WHO/IAEA/UN/UNEP Group of Experts on the Scientific Aspects of Marine Pollution. Paris.

Gómez-Ortiz, D., Fernández-Remolar, D.C., Granda, A., Quesada, C., Granda, T., Prieto-Ballesteros, O., Molina, A., Amils, R. (2014). Identification of the subsurface sulfide bodies responsible for acidity in Río Tinto source water, Spain. *Earth Planet. Sci. Lett.*, 391, 36–41.

Gómez Ruiz R. (2003). Molinos en el Río Odiel. Un estudio de arqueología Industrial en los límites del Andévalo. Junta de Andalucía. Consejería de Medio Ambiente. 138 pp.

Gonzalo y Tarín, J. (1888). Descripción física, geológica y minera de la provincia de Huelva. Primera parte: Descripción física. Memorias de la Comisión del Mapa Geológico de España, Madrid, 274 p.

Grande J.A., Borrego J. y Morales J.A. (1999). A study of heavy metal pollution in the Tinto-Odiel estuary in southwestern Spain using factor analysis. *Environmental Geology* 39: 1095-1101.

Grande J.A., Borrego J., De La Torre M.L. Sainz A. (2003). Application of cluster analysis to the geochemistry zonation of the estuary waters in the Tinto and Odiel Rivers. (Huelva, Spain). *Environmental Geochemistry and Health* 25: 233-246.

Grande, J.A. (ed.) (2016). Drenaje ácido de mina en la Faja Pirítica Ibérica. Técnicas de estudio e inventario de explotaciones. Servicio de Publicaciones de la Universidad de Huelva, 345 p.

Gray N.F (1998) Acid mine drainage composition and the implications for its impact on lotic systems. *Water Research* 32: 2122–2134.

Guerrero, J.L., Macías, F., León, R., Pérez-López, R., Nieto, J.M. (2024). First time full-scale of Ba-CO_3-DAS to remove sulphate from acid mine drainage. Macla.

Gusek, J.J. (2002). Sulfate-Reducing Bioreactor Design and Operating Issues: Is this the Passive Treatment Technology for your Mine Drainage? 2002 NAAMLP 24th Annual Conference Proceedings, Park City, Utah.

Hammarstrom J.M., Seal II R.R., Meier A.L. Kornfeld J.M. (2005). Secondary sulfate minerals associated with acid drainage in the eastern US: recycling of metals and acidity in surficial environments. *Chemical Geology* 215: 407-431.

Herzsprung, P., Friese, K., Packroff, G., Schimmele, M., Wendt-Potthoff, K., Winkler, M. (1998). Vertical and annual distribution of ferric and ferrous iron in acidic mining lakes. *Acta Hydrochimica et Hydrobiologica* 26(5): 253–62.

Hierro, A., Bolivar, J.P., Vaca, F., Borrego, J., (2012). Behavior of natural radionuclides in surficial sediments from an estuary impacted by acid mine discharge and industrial effluents in Southwest Spain. *Journal of Environmental Radioactivity*, 110: 13-23.

Hierro, A., Olías, M., Ketterer, M.E., Vaca, F., Borrego, J., Cánovas, C.R., Bolívar, J.P., (2014). Geochemical behavior of metals and metalloids in an estuary affected by acid mine drainage (AMD). *Environmental Science and Pollution Research* 21 (4): 2611–2627.

Hong, S., Candelone, J.P., Patterson, C.C. Boutron, C.F. (1996). History of ancient copper smelting pollution during roman and medieval times recorded in Greenland ice. *Science* 272: 246-249.

Hudson-Edwads, K.A. (2016). Tackling mine wastes. *Science* 352: 288-290.

Hubbard, C.G. (2007). *Acid mine drainage generation and transport processes in the Tinto River, SW Spain*. Tesis Doctoral. Universidad de Reading.

Igarashi, T. and Oyama, T. (1999). Deterioration of water quality in a reservoir receiving pyrite bearing rock drainage and its geochemical modeling. *Engineering Geology* 55: 45–55.

INAP (2014). The Global Acid Rock Drainage Guide. International Network for Acid Prevention.

Jambor J.L., Nordstrom D.K. Alpers C.N. (2000). Metal-sulphide salts from sulfide mineral oxidation. *Reviews in Mineralogy and Geochemistry*, 40. Mineralogical Society of America. Geochemical Society. Washington D.C. 305-340.

Jofre-Meléndez, R., Torres, E., Ramos-Arroyo, Y.R., Galván, L., Ruiz-Cánovas, C., Ayora, C. (2017). Reconstruction of an acid water spill in a mountain reservoir. Water 9: 613.

Kabata-Pendias, A., and Pendias, H. (2001). Trace elements in soils and plants CRC Press Inc. Boca Raton, FL, USA.

Kang C.U., Jeon B.H., Park S.S., Kang J.S., Kim K.O., Kim D.K., Choi U.K. Kim S.J. (2015). Inhibition of pyrite oxidation by surface coating: a long-term field study. *Environmental Geochemistry & Health* 38: 1137–1146

Keith C.N and Vaughan D.J (2000). Mechanisms and rates of sulphide oxidation in relation to the problems of acid rock (mine) drainage. In: Cotter-Howells JD, Campbell LS, Valsami-Jones E, Batchelder M (eds). *Environmental mineralogy: microbial interactions, anthropogenic influences, contaminated land and waste management*. Mineralogical Society, London, Mineralogical Society Series no 9, pp 117–139.

Keith D.C., Runnells D.D., Esposito K.J., Chermak J.A., Levy D.B., Hannula S.R., Watts M. Hall L. (2001). Geochemical models of the impact of acidic groundwater and evaporative sulfate salts on Boulder Creek at Iron Mountain, California. *Applied Geochemistry* 16: 947-961.

Kirby C.S and Cravotta C.A (2005). Net alkalinity and net acidity 1: theoretical considerations. *Applied Geochemistry* 20: 1920–1940.

Kling, G.W., Kusakabe, M., Maley, J., Tchoua, F.M., Tietze, K., (1990). Conclusions from Lake Nyos disaster. *Nature* 348, 201.

Langmuir D. (1997). *Aqueous environmental geochemistry*. Prentice Hall, Upper Saddle River

Leblanc M., Morales J. A., Borrego J. Elbaz-Poulichet F. (2000). 4,500-Year-old mining pollution in southwestern Spain: Long-term implications for modern mining pollution. *Economic Geology* 95: 655-661.

Lee G., Bigham J.M. Faure, G. (2002) . Removal of trace metals by coprecipitation with Fe, Al and Mn from natural waters contaminated with acid mine drainage in the Ducktown Mining District, Tennessee. *Applied Geochemistry* 17: 569-581.

León R., Macías F., Cánovas C.R., Pérez-López R., Ayora C., Nieto J.M., Olias M. (2021). Mine waters as a secondary source of rare earth elements worldwide: The case of the Iberian Pyrite Belt. *Journal of Geochemical Exploration* 224: 106742.

León R., Romero-Matos J., Macías F., Sanjuan E., Nieto J.M (2023). Actuaciones encaminadas a la reducción de los aportes difusos de Drenaje Ácido de Mina de la Mina de Riotinto a las cuencas de los ríos Odiel y Tinto (Huelva). *Geogaceta*, 2023.

Long, E.R., MacDonald, D.D., Smith, S.L., Calder, F.D., (1995). Incidence of adverse biological effects within ranges of chemical concentrations in marine and estuarine sediments. *Environmental Management* 19: 81-97.

López-Archilla, A.I. and Amils, R. (1999). A comparative ecological study of two acidic rivers in southwestern Spain. Microbial Ecology 38: 146-156.

López-González N., Borrego J., Morales J. A., Carro B. Lozano-Soria O. (2006). Metal fractionation in oxic sediments of an estuary affected by acid mine drainage (SW Spain). *Estuarine Coastal and Shelf Science* 68: 297-304.

López Pamo, E., Sánchez España, J., Diez Ercilla, M., Santofimia Pastor, E., Reyes Andrés, J. (2008). Cortas mineras inundadas de la Faja Pirítica: inventario e hidroquímica. IGME, Serie: Medio Ambiente nº 13, 265 p.

Lottermoser B.G (2003). *Mine Wastes. Characterization, Treatment, Environmental Impacts*. Springer-Verlag, Berlin Heidelberg, 304 pp.

Lozano, A., Ayora, C., Macías, F., León, R., Gimeno, M.J., Auqué, L., (2020). Geochemical behavior of rare earth elements in acid drainages: Modeling achievements and limitations. *Journal of Geochemical Exploration*, 216: 106577.

Luque, C.J., Castellanos, E.M., Castillo, J.M., Gonzalez, M., Gonzalez-Vilches, M.C., Figueroa, M.E, (1999). Metals in halophytes of a contaminated estuary (Odiel Saltmarshes, SW Spain). *Marine Pollution Bulletin*, 38(1): 49-51.

Macías F., Caraballo M.A., Rötting T., Pérez-López R., Nieto J.M., Ayora C. (2012a). From highly polluted Zn-rich acid mine drainage to non-metallic waters: Implementation of a multi-step alkaline passive treatment system to remediate metal pollution. *Science of the Total Environment* 433: 323-330.

Macías F., Caraballo M.A., Nieto J.M., Rötting T., Ayora C. (2012b). Natural pretreatment and passive remediation of highly polluted acid mine drainage. *Journal of Environmental Management* 104: 93-100.

Macías F., Caraballo M.A., Nieto J.M. (2012c). Environmental assessment and management of metal-rich wastes generated in acid mine drainage passive remediation systems. *Journal of Hazardous Materials* 229-230: 107-114.

Madejon, P., Burgos, P., Murillo, J,M., Cabrera, F. Madejón, E. (2009). Bioavailability and accumulation of trace elements in soils and plants of a highly contaminated estuary (Domingo Rubio tidal channel, SW Spain). *Environmental Geochemistry and Health* 31: 629:642

Madoz, P. (1845 a 1850): Diccionario Geográfico-Estadístico-Histórico de España y sus posesiones de ultramar. Madrid, 16 tomos.

Martin, J., Martínez-Aguirre, A., Respaldiza, M., Da Silva, M., (1997). Anthropogenic contamination analyzed by TTPIXE in samples from the Odiel salt marsh at the SW Spain. *Journal of Radioanalytical and Nuclear Chemistry* 223: 33-40.

Martín Crespo, T., De Ignacio-San José, C., Gómez-Ortiz, D., Martín-Velázquez, S., Lillo-Ramos, J. (2010). Monitoring study of the mine pond reclamation of Mina Concepción, Iberian Pyrite Belt (Spain). *Environmental Earth Science* 59: 1275-1284.

Martín-Díaz, M.L., Jiménez-Tenorio, N., Sales, D., DelValls, T.A. (2008). Accumulation and histopathological damage in the clam Ruditapes philippinarum and the crab Carcinus maenas to assess sediment toxicity in Spanish ports. *Chemosphere* 71(10): 1916-1927.

Mateos-Naranjo, E., Redondo-Gómez, S., Cambrollé, J., Luque, T., Figueroa, M. (2008). Growth and photosynthetic responses to zinc stress of an invasive cordgrass, Spartina densiflora. *Plant Biology* 10(6): 754-762.

Mayes W.M, and Jarvis A.P (2016). Mine water outbreak and stability risks: examples and challenges from England and Wales. In: Proceedings IMWA 2016, Freiberg, Germany, 1078-1083.

Mayoral E. (2008). Geología de la cuenca del Guadalquivir. En: *Geología de Huelva. Lugares de Interés Geológico*. Servicio de Publicaciones de la Universidad de Huelva, 20-27.

MEND (2004). Design, construction and perfomance monitoring of cover systems for waste rock and tailings. Mine Environment Neutral Drainage progam, Report 2.21.4 vol. 1, Canadá.

MEND (2007). Macro-scale cover design and perfomance monitoring manual. Mine Environment Neutral Drainage progam, Report 2.21.5, Canadá.

Moreno, C., Capitán, M.A., Doyle, M., Nieto, J.M., Ruiz, F. Sáez, R. (2003): Edad mínima del gossan de las Cruces: implicaciones sobre la edad del inicio de los ecosistemas extremos en la Faja Pirítica Ibérica. Geogaceta, 33: 67-70.

Moreno, C. and González F. (2004): Estratigrafía, capítulo: Zona Sudportuguesa. In: Vera, J. A. (Ed.). *Geología de España*. SGE-IGME, Madrid. 199-222.

Moreno Bolaños, A. (2011). Mineral extraído en minas de Riotinto (1725-2002). In: Río Tinto. Historia, Patrimonio Minero y Turismo Cultural (Eds: Pérez Macías, J.A., Delgado Domínguez, A., Pérez López, J.M., García Delgado, F.J.). Servicio de Publicaciones: Universidad de Huelva, 761–770.

Moreno-González, R., Olías, M., Macías, F., Cánovas, C.R., Fernández de Villarán, R. (2018). Hydrological characterization and prediction of flood levels of acidic pit lakes in the Tharsis mines, Iberian Pyrite Belt. *Journal of Hydrology* 566: 807-817.

Moreno González, R., Cánovas, C.R., Olías, M., Macías, F. (2020). Seasonal variability of extremely metal rich acid mine drainages from the Tharsis mines (SW Spain). *Environmental Pollution* 259: 113829.

Moreno-González, R., Olías, M., Cánovas, C.R., Basallote, M.D., Rodrigo García, A., (2023). Evolución del nivel del agua en una corta inundada de la Faja Pirítica Ibérica: Implicaciones ambientales. Geogaceta 73, 55-58.

Morillo, J. Usero, J. Gracia, I. (2004). Heavy metal distribution in marine sediments from the southwest coast of Spain. *Chemosphere* 55: 431-442-

Morillo J., Usero J., Gracia I. (2005). Biomonitoring of trace metals in a mine polluted estuarine system (Spain). *Chemosphere* 58: 1421-1430.

Muñoz-Rodríguez, A.F., Izquierdo-Infante, M.D., Gullón, E.S. (2022). Síntesis de la flora de la provincia de Huelva, Biología de Huelva: Naturaleza, Biodiversidad, Bioindicadores y Biomarcadores. Universidad de Huelva, pp. 77-114.

Nieto J.M., Sarmiento A.M., Olías M., Cánovas C.R., Riba I., Kalman J. Delvalls T.A. (2007). Acid mine drainage pollution in the Tinto and Odiel rivers (Iberian Pyrite Belt, SW Spain) and bioavailability of the transported metals to the Huelva estuary. *Environment International* 33: 445-455.

Nieto, J.M., Sarmiento, A.M., Canovas, C.R., Olias, M., Ayora, C., (2013). Acid mine drainage in the Iberian Pyrite Belt: 1. Hydrochemical characteristics and pollutant load of the Tinto and Odiel rivers. *Environmental Science and Pollution Research*, 20(11): 7509-7519.

Nocete, F. (2004). Odiel: Proyecto de investigación arqueológica para el análisis del origen de la desigualdad social en el suroeste de la Península Ibérica. Monografías Arqueología nº 19. Consejería de Cultura de la Junta de Andalucía, 409 pp.

Nocete F., Alex E., Nieto J.M., Sáez R. Bayona, M.R. (2005). An archaelogical approach to regional environmental pollution in the south-western Iberian Peninsula related to Third Millenium B.C mining and metallurgy. *Journal of Archaeological Science* 32: 1566-1576.

Nocete, F. (2006). The first specialised copper industry in the Iberian Peninsula: Cabezo Juré (2900-2200 BC). *Antiquity*, 80: 646-654.

Nocete, F., Queipo, G., Sáez, R., Nieto, J.M., Inacio, N., Bayona, M.R., Peramo, A. Cruz-Auñón, R. (2008). Specialised copper industry in the political centres of the Guadalquivir Valley during the Third Millennium BC: The smelting quarter of Valencina de la Concepción, Sevilla, Spain (2750-2500 BC). *Journal of Archaeological Sciences*, 35: 717-732.

Nordstrom, D.K. (1982a). Aqueous pyrite oxidation adn the consequent formation of secondary iron minerals. En: *Acid sulfate weathering: pedogeochemistry and relationship to manipulation of soils minerals*. Hossner, L.R., Kittrick, J.A. Fanning, D.F (Eds.). Soil Science Society of America Press, 46: 37-56.

Nordstrom D.K. (1982b). The effect of sulfate on aluminum concentrations in natural waters: some stability relations in the system Al_2O_3-SO_3-H_2O at 298 K. *Geochimica et Cosmochimica Acta* 46: 681-692.

Nordstrom D.K. and Ball, J.W. (1986). The geochemical behaviour of aluminium in acificied surface waters. *Science* 232: 54-56.

Nordstrom D.K. and Alpers C.N. (1999a). Geochemistry of acid mine waters. In: *The environmental geochemistry of mine waters*. Rev econ geol., 6A, 133-160.

Nordstrom, D.K. and Alpers, C.N., (1999b). Negative pH, efflorescent mineralogy, and consequences for environmental restoration at the Iron Mountain Superfund site, California. *Proceedings of the National Academy of Sciences* 96: 3455-3462.

Nordstrom, D.K. (2015). Baseline and premining geochemical characterization of mined sites. *Applied Geochemistry* 57: 17-34.

Öhlander, B., Chatwin, T., Alakangas, L. (2012). Management of Sulfide-Bearing Waste, a Challenge for the Mining Industry. *Minerals 2*: 1-10.

Olías M., Nieto J. M., Sarmiento A. M., Cerón J. C. Canovas C. R. (2004). Seasonal water quality variations in a river affected by acid mine drainage: The Odiel river (south west Spain). *Science of the Total Environment* 333: 267-281.

Olías M., Cánovas C., Nieto J. M. Sarmiento A. M. (2006). Evaluation of the dissolved contaminant load transported by the Tinto and Odiel rivers (South West Spain). *Applied Geochemistry* 21: 1733-1749.

Olías M., Nieto J.M, Galvan L., Sarmiento A.M. Canovas, C.R. (2007). Sobre la calidad del agua del futuro embalse de Alcolea (Cuenca del río Odiel, Huelva) *Geogaceta* 42: 59-62

Olías, M., Nieto, J.M., Sarmiento, A.M., Cánovas, C.R. (2010). La contaminación minera de los ríos Tinto y Odiel. Informe Técnico. Facultad de Ciencias Experimentales de la Universidad de Huelva. 166 p.

Olías, M., Nieto, J.M., Sarmiento, A.M., Cánovas, C.R., Galván, L., (2011). Water Quality in the Future Alcolea Reservoir (Odiel River, SW Spain): A Clear Example of the Inappropriate Management of Water Resources in Spain. Water Resour Manage 25, 201–215.

Olías, M. and Nieto J.M. (2012). El impacto de la minería en los ríos Tinto y Odiel a lo largo de la Historia. Revista de la Sociedad Geológica de España 25: 177-192.

Olías, M. and Nieto J.M. (2015). Background Conditions and Mining Pollution throughout History in the Río Tinto (SW Spain). Environments 2: 295-316.

Olías, M., Nieto, J.M, Macías, F. (2018). Propuesta para el plan de restauración de la contaminación minera de la cuenca del rio Odiel. Informe Técnico. 118 p.

Olías, M., Cánovas, C.R., Basallote, M.D., Macías, F., Pérez-López, R., Moreno-González, R., Millán-Becerro, R., Nieto, J.M. (2019). Causes and impacts of a mine water spill from an acidic pit lake (Iberian Pyrite Belt). *Environmental Pollution* 250: 127-136.

Olías, M., Cánovas, C.R., Macías, F., Basallote, M.D., Nieto, J.M. (2020). The Evolution of Pollutant Concentrations in a River Severely Affected by Acid Mine Drainage: Río Tinto (SW Spain). *Minerals* 10: 598.

Olías, M., Cánovas, C.R., Basallote, M.D. (2021). Surface and Groundwater Quality Evolution in the Agrio and Guadiamar Rivers After the Aznalcollar Mine Spill (SW Spain): Lessons Learned. *Mine Water and the Environment* 40: 235-249.

Olías, M., Cánovas, C.R, Moreno González, R., Macías, F., Nieto, J.M. (2022). Factores condicionantes de la acidificación de embalses por lixiviados mineros en la Faja Pirítica Ibérica. *Revista De La Sociedad Geológica De España*, 35(2), 28–40.

Oliva, M., José Vicente, J., Gravato, C., Guilhermino, L., Galindo-Riaño, M.D (2012). Oxidative stress biomarkers in Senegal sole, Solea senegalensis, to assess the impact of heavy metal pollution in a Huelva estuary (SW Spain): Seasonal and spatial variation. *Ecotoxicology and Environmental Safety* 75: 151-162.

Orden S., Macías F., Cánovas, C.R., Nieto, J.M. Pérez-López, R. Ayora C. (2021). Eco-sustainable passive treatment for mine waters: Full-scale and long-term demonstration. *Journal of Environmental Management* 280: 111699.

Ortiz Mateo, M. (2004). Las escorias de Riotinto. *De Re Metallica* 2: 9–22.

Ortiz Mateo, M. and Romero Macías, E. (2004). La metalurgia de las minas de Riotinto, desde su rehabilitación hasta su alquiler al Marqués de Remisa (1725-1849) y obtención de indicadores ambientales del consumo de combustible en los procesos metalúrgicos. *Boletín Geológico y Minero*, 115: 103-114.

Palanques A., Diaz J. I. and Farran M. (1995). Contamination of heavy metals in the suspended and surface sediment of the Gulf of Cadiz (Spain): The role of sources, currents, pathways and sinks. *Oceanologica Acta* 18: 469-477.

Pérez-López R., Nieto, J.M. Almodóvar, G.R. (2007a). Utilization of fly ash to improve the quality of the acid mine drainage generated by oxidation of a sulphide- rich mining waste: column experiments. *Chemosphere* 67: 1637-1646.

Pérez-López R., Cama, J., Nieto, J.M. y Ayora, C. (2007b). The Iron-coating role on the oxidations kinetics of a pyrite sludge doped with fly ash. *Geochimica et Cosmochimica Acta* 71: 1921-1934.

Pérez-López, R., Macías, F., Cánovas, C.R., Sarmiento, A.M., Pérez-Moreno, S.M., (2016). Pollutant flows from a phosphogypsum disposal area to an estuarine environment: An insight from geochemical signatures. *Science of the Total Environment*, 553: 42-51.

Pérez Macías J.A. (1996). Metalurgia extractiva prerromana en Huelva. Servicio de publicaciones de la Universidad de Huelva.

Pérez Macías, J.A. and Delgado Domínguez, A. (2011). Ingeniería minera antigua y medieval en el suroeste ibérico. Boletín Geológico Ibérico 122: 3-16

Pinedo Vara I. (1963). *Piritas de Huelva. Su historia, minería y aprovechamiento*. Summa. Madrid, Spain. 1003 pp.

Pozo, G., Pongy, S., Keller, J., Ledezma, P., y Freguia, S., (2017). A novel bioelectrochemical system for chemical-free permanent treatment of acid mine drainage. *Water Research* 126: 411–420.

Prenda, J. (2022). Ictiofauna continental onubense. En: Biología de Huelva (Ed. Torronteras Santiago, R.), Servicio de Publicaciones de la Universidad de Huelva, 295-334.

Preston, S.D, Bierman, V.J, y Silliman, S.E (1989). An evaluation of methods for the estimation of tributary mass loads. *Water Resources Research* 25:1379–89.

Quilbé, R., Rosseau, A.N., Duchemin, M., Pouling, A., Gangbazo, G., Villeneuve, J.P. (2006). Selecting a calculation method to estimate sediment and nutrient loads in streams: application to the Beaurivage River (Québec, Canada). *Journal of Hydrology* 326, 295–310.

Rainbow, P.S. and White, S.L. (1989). Comparative strategies of heavy metal accumulation by crustaceans: zinc, copper and cadmium in a decapod, an amphipod and a barnacle. *Hydrobiologia* 174: 245-262.

Raiswell, R.R and Canfield, D.E., (2012). The iron biogeochemical cycle, past and present. *Geochemical Perspectives* 1: 1–220.

Regenspurg S. and Pfeiffer S. (2005). Arsenate and chromate incorporation in schwertmannite. *Applied Geochemistry* 20: 1226–1239.

Riba, I., Casado-Martínez, C., Forja, J.M., y DelValls, A. (2004). Sediment quality in the Atlantic coast of Spain. *Environmental Toxicology Chemistry* 23(2): 271-82.

Riba, I., Blasco, J., Jiménez-Tenorio, N., DelValls, T.Á., (2005). Heavy metal bioavailability and effects: I. Bioaccumulation caused by mining activities in the Gulf of Cádiz (SW, Spain). *Chemosphere* 58(5): 659-669.

Rimstidt J.D. and Vaughan D.J. (2003). Pyrite oxidation: A state-of-the-art assessment of the reaction mechanism. *Geochimica et Cosmochimica Acta* 65: 873-880.

Ritchie A.I.M. (1994). Rates of mechanisms that govern pollutant generation from pyritic wastes. En: Alpers,C.N, Blowes D.W (eds) *Environmental geochemistry of sulfide oxidation*. American Chemical Society, Washington DC (Symposium Series 550, pp 108–122).

Rodríguez-Estival, J., Sánchez, M.I., Ramo, C., Varo, N., Amat, J.A., Garrido-Fernández, J., Hornero-Méndez, D., Ortiz-Santaliestra, M.E., Taggart, M.A., Martinez-Haro, M., Green, A.J., Mateo, R., (2019). Exposure of black-necked grebes (Podiceps nigricollis) to metal pollution during the moulting period in the Odiel Marshes, Southwest Spain. *Chemosphere* 216: 774-784.

Rodríguez-Romero, A., Jiménez-Tenorio, N., Basallote, M.D., De Orte, M., Blasco, J., Riba, I. (2014). Predicting the Impacts of CO_2 Leakage from Subseabed Storage: Effects of Metal Accumu-

lation and Toxicity on the Model Benthic Organism Ruditapes philippinarum. *Environmental Science & Technology*, 48(20): 12292-12301.

Romero, A., González, I. Galán, E. (2003). Estimation of potential pollution of waste mining dumps at Peña del Hierro (Pyrite Belt, SW Spain). As a base for future mitigations actions. *Applied Geochemistry* 21: 1093-1108.

Romero, V., Ruiz, F., Prudencio, M.I., Muñoz, J.M., Rodriguez-Vidal, J., Gómez, P. et al. (2023). Rare earth elements as statistical sentinels of pollution and paleoenvironments?: Application to a highly polluted estuary in southwestern Spain. *Marine Pollution Bulletin* 186: 114419.

Rosado, D., Usero, J., y Morillo, J., (2015). Application of a new integrated sediment quality assessment method to Huelva estuary and its littoral of influence (Southwestern Spain). *Marine Pollution Bulletin*, 98(1): 106-114.

Rosman K., Chisholm W., Hong S., Candelone J.P. Boutron C.F. (1997). Lead from Carthaginian and Roman Spanish mines isotopically identified in Greenland ice dated from 600 B.C. to 300 A.D. *Environmental Science and Technology* 31: 3413-3421.

Rothenberg, B., and García Palomero, F. (1986). The Rio Tinto enigma-no more. Institute for Archaeo-Metallurgical Studies Newsletter 8: 3–5.

Rötting, T.S. (2007). Dispersed Alkaline Substrate (DAS): A novel option for the passive treatment of waters with high metal concentrations. Tesis Doctoral, Instituto de Ciencias de la Tierra “Jaume Almera”, CSIC, pp. 136.

Rötting T.S., Caraballo M.A., Serrano J.A., Ayora C., Carrera J. (2008) Field application of calcite Dispersed Alkaline Substrate (calcite-DAS) for passive treatment of acid mine drainage with high Al and metal concentrations. *Applied Geochemistry* 23: 1660-1674.

Rufo, L., Rodríguez, N., Amils, R., de la Fuente, V., Jiménez-Ballesta, R., (2007). Surface geochemistry of soils associated to the Tinto River (Huelva, Spain). *Science of the Total Environment* 378(1-2): 223-227.

Ruiz F., González-Regalado M.L, Borrego J., Morales J. A., Pendón J.G Muñoz J.M. (1998). Stratigraphic sequence, elemental concentrations and heavy metal pollution in Holocene sediments from the Tinto-Odiel Estuary, southwestern Spain. *Environmental Geology* 34: 270-278.

Ruiz F., (2001). Trace Metals in Estuarine Sediments from the Southwestern Spanish *Coastal Marine Pollution Bulletin* 42: 481-489.

Ruiz, F., Borrego, J., Gonzalez-Regalado, M.L., López-González, N., Carro, B. Abad, M. (2009). Interaction between sedimentary processes, historical pollution and microfauna in the Tinto Estuary (SW Spain). *Environmental Geology* 58: 779-783.

Ruiz, F, Rodríguez Vidal, J., Cáceres, L.M., Olías, M., González-Regalado M.L., Campos, J.M. et al. (2020). Silver and copper as pollution tracers in Neogene to Holocene estuarine sediments from southwestern Spain. *Marine Pollution Bulletin* 150: 110704.

Sainz, A., Grande, J.A., de la Torre, M.L. (2003). Odiel River, acid mine drainage and current characterisation by means of univariate analysis. *Environment International* 29: 51-59.

Sainz, A. and Ruiz, F. (2006). Influence of the very polluted inputs of the Tinto-Odiel system on the adjacent litoral sediments of southwestern Spain: A statistical approach. *Chemosphere* 62: 1612-1622-

Salkield, L.U., (1987). *A technical history of the Rio Tinto mines: some notes on exploitation from pre-Phoenician times to the 1950s*. The Institute of Mining and Metallurgy, London.

Sánchez España J., Lopez Pamo E., Santofimia E., Aduvire O., Reyes J. Barettino, D. (2005). Acid mine drainage in the Iberian Pyrite Belt (Odiel river watershed, Huelva, SW Spain): Geochemistry, mineralogy and environmental implications. *Applied Geochemistry* 20: 1320-1356.

Sánchez España J., Lopez Pamo E. Santofimia Pastor E. (2007). The oxidation of ferrous iron in acidic mine effluents from the Iberian Pyrite Belt (Odiel Basin, Huelva, Spain): Field and laboratory rates. *Journal of Geochemical Exploration* 92: 120-132.

Sánchez España, J., López Pamo, E., Santofimia Pastor, E. Diez Ercilla, M. (2008a). The acídic pit lakes of the Iberian Pyrite Belt: An approach to their physical limnology and hydrogeochemistry. *Applied Goechemistry* 23: 1260-1287.

Sánchez España, J., González-Toril, E.G., Lopez Pamo, E., Amils, R., Diez Ercilla, M., Santofimia Pastor, E. San Martín_Úriz, P. (2008b). Biogeochemistry of a hyperacidic and ultraconcentrated pyrite leachate in San Telmo mine (Iberian Pyrite Belt, Spain). *Water, Air and Soil Pollution* 194: 243-257.

Sánchez España, J., Pamo, E.L., Diez, M., Santofimia, E., (2009). Physico-chemical gradients and meromictic stratification in Cueva de la Mora and other acidic pit lakes of the Iberian Pyrite Belt. *Mine Water and the Environment* 28, 15–29.

Sánchez España, J., Yusta Arnal, I., Boehrer, B., (2021). Monitorización y análisis de la desgasificación del lago de la Corta Guadiana (minas de Herrerías, Huelva). Informe Final. Instituto Geológico y Minero de España, Madrid, Informes Técnicos, nº 13, 104 p.

Sánchez-Moyano, J.E., and García-Asencio, I. (2010). Crustacean assemblages in a polluted estuary from South-Western Spain. *Marine Pollution Bulletin* 60(10): 1890-1897.

Sanjosé, I., Navarro-Roldán, F., Montero, Y., Ramírez-Acosta, S., Jiménez-Nieva, F., Infante-Izquierdo, M.D., Polo-Ávila, A., Muñoz-Rodríguez, A. (2022). The Bioconcentration and the Translocation of Heavy Metals in Recently Consumed Salicornia ramosissima J. Woods in Highly Contaminated Estuary Marshes and Its Food Risk. *Diversity* 14(6): 452.

Sarmiento, A.M. (2007). Study of the pollution by acid mine drainage of the surface waters in the Odiel basin (SW Spain). Ph.D. Thesis. UMI ProQuest, Publ. No.: AAT 3282346. Ann Arbor, USA, 352pp.

Sarmiento, A.M, Olias, M., Nieto J.M, Cánovas C.R. y Delgado J. (2009a). Natural atenuation processes in two reservoirs receiving acid mine drainage. *Science of the Total Environment* 407:2051-2062.

Sarmiento, A.M., Nieto, J.M., Olías, M. y Cánovas, C.R. (2009b). Hydrochemical characteristics and seasonal influence on the pollution by acid mine drainage in the Odiel river basin (SW Spain). *Applied Geochemistry* 24: 697-714.

Schroth A.W. and Parnell J.R.A (2005). Trace metal retention through the schwertmannite to goethite transformation as observed in a field setting, Alta Mine, MT. *Applied Geochemistry* 20: 907-917.

Sherrell, R.M., and Boyle, E.A. (1988). Zinc, chromium, vanadium and iron in the Mediterranean Sea. Deep Sea Research Part A. *Oceanographic Research Papers*, 35(8): 1319-1334.

Singer P.C., and Stumm W. (1970). Acid mine drainage: the rate limiting step. *Science* 167: 1121-1123.

Skousen, J. (2014). Overview of acid mine drainage treatment with chemicals. In: James et al. (eds), Acid mine drainage, rock drainage, and acid sulfate soils. Causes, Assessment, Prediction, Prevention and Remediation. Ed. John Wiley & Sons, USA, 486 p.

Skousen, J., Zipper, C.E., Rose, A, Ziemkiewicz, P.F., Nairn, R., McDonald, M.L., Kleinmann, R.L. (2017). Review of Passive Systems for Acid Mine Drainage Treatment. *Mine Water and the Environment* 36: 133-153

Skousen, J.G., Ziemkiewicz, P.F., McDonald, L.M. (2019). Acid mine drainage formation, control and treatment: Approaches and strategies. *The Extractive Industries and Society* 6: 241–249.

Smith K.S. (1999). Metal sorption on mineral surfaces: an overview with examples relating to mineral deposits. En: *The Environmental Geochemistry of Mineral Deposits*. Reviews in Economic Geology, Vol. 6A, Ed. Plumlee, G. S. y Logsdon, M. J., 161-182.

Spivack, A., Huested, S., Boyle, E., (1983). Copper, nickel and cadmium in the surface waters of the Mediterranean. En: Trace metals in sea water (Ed. C.S. Wong), Springer, New York, pp: 505-512.

Stumm W. and Morgan J. (1996). *Aquatic Chemistry. Chemical Equilibria and Rates in Natural Waters*. Environmental Science and Technology. New York. 1022 pp.

Torres, E., Ayora, C., Cánovas, C.R., García-Robledo, E., Galván, L., Sarmiento, A.M., (2013). Metal cycling during sediment early diagenesis in a water reservoir affected by acid mine drainage. *Science of the Total Environment* 461 (462): 416–429.

Torres, E., Ayora, C., Jiménez-Arias, J.L., García-Robledo, E., Papaspyrou, S., Corzo, A. (2014). Benthic metal fluxes and sediment diagenesis in a water reservoir affected by acid mine drainage: a laboratory experiment and reactive transport modelling. *Geochimica et Cosmochimica Acta* 139, 344–361.

Torres, E., Couture, R.M., Shafei, B., Nardi, A., Ayora, C., Van Cappellen, P., 2015. Reactive transport modelling of early diagenesis in a reservoir lake affected by acid mine drainage: trace metals, lake overturn, benthic fluxes and remediation. *Chemical Geology* 419, 75–91.

Torres, E., Galván, L., Cánovas, C.R., Soria-Piriz, S., Arbat-Bofill, M., Nardi, A., Papaspyrou, S., Ayora, C., 2016. Oxycline formation induced by Fe (II) oxidation in a water reservoir affected by acid mine drainage modeled using a 2D hydrodynamic and water quality model - CE-QUAL-W2. *Science of the Total Environmen*t 562: 1–12.

Usero, J., Izquierdo, C., Morillo, J., Gracia, I. (2004). Heavy metals in fish (Solea vulgaris, Anguilla anguilla and Liza aurata) from salt marshes on the southern Atlantic coast of Spain. *Environment International* 29(7): 949-956.

Usero J., Morillo J., Gracia, I. (2005). Heavy metal concentrations in molluscs from the Atlantic coast of southern Spain. *Chemosphere* 59:1175-1181.

Usero, J., Morillo, J., El Bakouri, H., (2008). A general integrated ecotoxicological method for marine sediment quality assessment: Application to sediments from littoral ecosystems on Southern Spain's Atlantic coast. *Marine Pollution Bulletin*, 56(12): 2027-2036.

Utgikar, V.P., Tabak, H.H., Haines, J.R., Govind, R. (2003). Quantification of toxic and inhibitory impact of copper and zinc on mixed cultures of sulfate-reducing bacteria. *Biotechnology Bioengineering*. 82: 306-312.

Valente, T., Grande, J.A., de la Torre, M.L., Gomes, P., Santisteban, M., Borrego, J., Sequeira Braga, M.A. (2015). Mineralogy and geochemistry of a clogged mining reservoir affected by historical acid mine drainage in an abandoned mining area. *Journal of Geochemical Exploration* 157: 66-76.

van Geen, A., Boyle, E.A. Rosener P. (1988). Entrainment of tracemetal enriched Atlantic shelf water in the inflow to the Mediterranean Sea. *Nature* 331: 423-426.

van Geen, A., Boyle, E.A. Moore, W.S. (1991). Trace metal enrichments in the waters of the Gulf of Cadiz. *Geochimica et Cosmochimica Acta* 55: 2173-2191.

Van Geen, A. Adkins, J.F., Boyle, E.A., Nelson, C.H. Palanques, A. (1997). A 120-year record of widespread contamination from mining of the iberiam pyrite belt. *Geology* 25: 291-294.

Vicente-Martorell, J.J.. Galindo-Riaño, M.D., Garcia-Vargas, M., Granado Castro, M.D. (2009). Bioavailability of heavy metals monitoring water, sediments and fish species from a polluted estuary. *Journal of Hazardous Materials* 162: 823-836.

Walton-Day, K., and Mills, T.J (2015). Hydrogeochemical effects of a bulkhead in the Dinero mine tunnel, Sugar Loaf mining district, near Leadville, Colorado. *Applied Geochemistry 62*: 61-74.

Webster J.G., Swedlund P.J. Webster K.S. (1998). Trace metal adsorption onto an acid mine drainage iron(II) oxyhdroxisulfate. *Environmental Science and Technology* 32: 1361-1368.

Wetzel, D.B., (2001). Limnology, 3rd ed., Lake and river ecosystems. Academic Press, San Diego, California.

Wu, H., Wang, R., Yan, P. et al. (2023). Constructed wetlands for pollution control. *Nature Reviews Earth & Environment* 4: 218–234.

Williams, M. (1999). Arsenic in mine waters: an international study. *Environmental Geology* 40: 267-278.

Younger P.L., Banwart S..A. Hedin R. S. (2002). *Mine water. Hidrology, Pollution, Remediation. Environmental Pollution*. Kluwer Academic Publishers. Dordrecht. Vol. 5, 442 pp.

Zänker H., Moll H., Richter W., Brendler V., Hennih C., Reich T., Kluge A. Huttin G. (2002). The colloid chemistry of acid rock drainage solution from an abandoned Zn-Pb-Ag mine. *Applied Geochemistry* 17: 633-648.

Zhou Y., Fan R., Short M.D., Li J., Schuman R.C., Xu H., Smart R., Gerson A.R Qian G. (2018). Formation of Aluminum Hydroxide-Doped Surface Passivating Layers on Pyrite for Acid Rock Drainage Control. *Environmental Science and Technology* 52, 11786−11795

Ziemkiewicz, P.F., Skousen, J.G. Simmons, J. (2003). Long-term Performance of Passive Acid Mine Drainage Treatment Systems. *Mine Water and the Environment* 22: 118–129.